PH.D THESIS ENTITLED

Assessment of agro-industrial and bacterial surfactant based bio-adsorbent columns for heavy metal removal from industrial wastewater

SUBMITTED TO

BABASAHEB BHIMRAO AMBEDKAR (A CENTRAL) UNIVERSITY, LUCKNOW-226025

FOR THE DEGREE OF

DOCTOR OF PHILOSOPHY

IN THE SUBJECT OF

ENVIRONMENTAL MICROBIOLOGY

Submitted by

Swati Rastogi

(Enrolment no. 1380/16)

Under the supervision of

Dr. Rajesh kumar

Professor

Department of Environmental Microbiology
Babasaheb Bhimrao Ambedkar University
(A Central University, NAAC Accreditation „A" Grade)
Vidya Vihar, Raebareli Road, Lucknow-226 025, Uttar Pradesh, India

2021

CERTIFICATE

This is to certify that work embodied in this thesis entitled, **–Assessment of agro-industrial and bacterial surfactant based bio-adsorbent columns for heavy metal removal from industrial wastewater‖**, being submitted by **Ms. Swati Rastogi** is an original research work and has not been previously submitted in part or full for the award of any degree or diploma to this or any other university. The thesis submitted to Babasaheb Bhimrao Ambedkar (A central) University, Lucknow satisfies all the requirements as stipulated in the Doctor of Philosophy (Ph.D.) regulations- 1999 as amended in 2008/2010/2013/2016 and it is fit for submission and evaluation for the award for the degree of Doctor of Philosophy of the university.

Place: Lucknow **Supervisor**
Date:

Head of Department

DECLARATION

I, **Swati Rastogi,** hereby declare that the work presented in this thesis entitled **"Assessment of agro-industrial and bacterial surfactant based bio-adsorbent columns for heavy metal removal from industrial wastewater"**, is carried out by me under the guidance of **Prof. Rajesh Kumar,** Department of Environmental Microbiology, Babasaheb Bhimrao Ambedkar (A Central) University, Vidya Vihar, Raebareli Road, Lucknow. The work is original and has not been submitted in part or in full to any other university or institute for award of any research degree. The extent of information derived from the existing literature has been indicated in the body of the thesis at appropriate places giving the references.

Place: Lucknow

Date:

Swati Rastogi
Deptt. of Environmental Microbiology
Babasaheb Bhimrao Ambedkar University,
Lucknow

Acknowledgement

It would be wrong to address as myself the only individual who completed this thesis. This thesis is the supreme education of mine, I have earned so far but it was not my journey only, it was the work of my passion, devotion, and trust in the universe and my loved ones that I could make it possible. My loved ones have given me the encouragement and assistance that I am now going to complete this journey and it is my extreme privilege to get this opportunity to express my gratitude towards them.

I express my heartiest veneration and I feel indeed my privilege to work under the talented and inspiring guidance, supervision, conspicuous ability and constructive criticism of my supervisor ***Prof. Rajesh Kumar, Department of Environmental Microbiology, BBAU, Lucknow.*** *As my advisor not merely as traditional formerly but actually am overwhelmed for his talented and inspiring guidance, invaluable suggestion, unending zeal and sympathetic attitude rendering during the study and while writing the thesis.*

Besides my advisor, I would also like to thank the rest of faculty members: ***Prof. Ram Chandra, Dr. Jai Shankar Singh, Dr. Ram Naresh Bhargava, Dr. Pankaj Arora, Dr. Digvijay Verma, and Dr. Ravi Kumar Gupta,*** *for their interminated help, invaluable suggestion and even a healthy criticism.*

I would like to express my sincere regards and special thanks to Post doctorate fellow ***Mr. Aniruddh*** *and all Ph.D. scholars of Rhizospheric Biology Laboratory;* ***Ms. Shweta Ambust, Ms. Shweta Bharti, Ms. Apoorva Dixit, Mr. Sheel Ratna, and Mr. Ajay Prakash here*** *for their kind support, suggestions and for encouraging me during the entire course of Ph.D. work.*

I would also like to give special thanks to ***Mr. Ashok Kumar, Mr. Sumit Kumar, and Mr. Pankaj*** *from chemistry department, for their kind assistance in instrumentation facility and theoretical guidance related to my work.*

I would like to extend my sincere thanks to my dissertation interns ***Mr. Jeetendra Kumar, Ms. Zeba Khan, Ms. Shweta Tiwari, Mr. Sonu, Ms. Aparna, and Ms. Amrita*** *for creating a conducive environment, assistance, kind support and*

respect and exploration of some deep aspects and generating a new perspective related to my work on bio-adsorbents. It was an integrated work where a small objective of their report has extended my knowledge on working with bio-adsorbents for the bioadsorption of heavy metals through literature survey.

I would also like to express my sincere thanks to ***Mrs. Sunita Pal, Mr. Rahul Srivastava, Mr. Avikesh and other official staff of DEM and USIC, BBAU, Lucknow*** *for giving unconditional support and help related to any official and experimental work. I would like to express my sincere thanks to* ***Dr. Nitesh Kumar Verma, Assistant Librarian, BBAU, Lucknow*** *for his cooperation, any attribute will be less for him.*

I would also like to express my gratitude to staff of ***CSIR-Central Institute of medicinal and aromatic plants (CIMAP), Lucknow, Biokart India Pvt. Limited, Bengaluru and Sanjay Gandhi post graduate institute of medical sciences (SGPGIMS), Lucknow*** *for their instrumentation facilities and easy availability for the smooth propagation of this study.*

Words are lacking to express my thanks to my friends ***Mrs. Prema Suman Jose, Mr. Anil Jose, Mr. Prashant Dhanwantri, Rojita Di, Mr. Rahul Singh, Mr. Anilesh Singh, Mr. Shubham, Mrs. Archana, Mrs. Anjali, Ms. Saanchi, and Mr. Ankit Mishra*** *for their endearment, support, cooperation and consolatory behaviour during the whole time period of this study. Any attribute will be less for them. Although I am not in touch with some of my friends anymore, but their continuous support, never changing affection and encouragement directly or indirectly to do better at each and every step in my life when I was with them, had always motivated me to become a better version of myself so that I push myself to do better, and whenever I needed them, they were always beside me and this is heart touching and will be cherished for lifetime.*

I am highly attached to my adopted dog ***Max*** *for coming into my life and making my life more colourful and beautiful which in turn has motivated me to be kind, loving, humble, and being grateful towards God for all the care and affection, I got from my loved ones and making me capable to find goodness in people. Although*

Max *is no more with us but he is alive in my heart and this has helped me to thrive to do better during this Ph.D. journey and many more journeys ahead in this life.*

Finally, I have no words to express about the help, affection and moral support of my mother ***Mrs. K.D. Rastogi****, my father* ***Mr. R.K. Rastogi****, my brother* ***Mr. Prateek Kumar Rastogi*** *and my bhabhi* ***Mrs. Divya Rastogi*** *for their indispensable encouragement, selfless sacrifice, sustained inspiration and valuable assistance throughout my life and support during the completion of this thesis.*

Above all, I would like to thank the ***Almighty*** *for giving me the strength and patience to work through all these years so that today I can stand proudly with my head held high.*

Thanks for all your encouragement!
["Grit leads you to the trail of victory":- ***Swati Rastogi****]*

Place: Lucknow (**Swati Rastogi)**

Contents

List of Tables

List of Figures

Abstract

Industrial wastewater is any wastewater produced from any processing, manufacturing, or agricultural unit/industry or could be generated during an operation other than sanitary or domestic ones. Such wastewaters contain various heavy metal(s), for instance, lead (Pb^{2+}), cadmium (Cd^{2+}), copper (Cu^{2+}), zinc (Zn^{2+}), chromium [Cr(VI)], mercury (Hg^{2+}) etc. causing adverse effects and are mainly discharged from manmade sources such as battery, electroplating industry, smelting process, electronic goods, pulp and paper industry, through mining, metal and alloy fabrication, paint, dyeing, printing, etc. The anarchic discharge of untreated wastewaters with toxic heavy metals into the aqueous systems negatively affects its flora and fauna, causing toxicity in humans. Wastewater treatment thus becomes essential so that water quality of various water bodies can be maintained, hence, all life forms and can also offer the possibility of re-using treated water in other applications that do not require high quality water. Therefore, present study dealt with the preparation of bio-adsorbents, their characterization and their efficacy/screening for removal of Pb^{2+} and Cd^{2+} ions from aqueous solution in a batch adsorption process. The study also involved isolation of Pb^{2+} and Cd^{2+} resistant biosurfactant producing bacteria from hydrocarbon contaminated sites whose metabolite (biosurfactant) would be utilised in heavy metal bioremediation. It includes screening, characterization, and extraction of biosurfactant and amalgamation of extracted biosurfactant with the selected bio-adsorbent for removal of Pb^{2+} and Cd^{2+} ions from industrial effluents in a continuous column process. The bio-adsorbents prepared viz. activated orange peel powder (AcOPP), activated banana peel powder (AcBPP) and biosurfactant modified activated banana peel powder (BSBP) illustrated the presence of microporous particles in their asymmetric structures and pores which contributed towards the affinity for high binding of the pollutants through various characterization techniques. The bioadsorption process was affected by change in pH, contact time, bio-adsorbent dose, and initial metal ion concentration. Bio-adsorbents were best regenerated using 0.1N HNO_3 and were reusable up to 3 times with little loss in the efficiency. The Langmuir adsorption isotherm model showed best fit having maximum bioadsorption capacities (q_m) of 111.11 and 54.05 mg/g, respectively using activated banana peel powder (AcBPP). The pseudo-second-order kinetic model was

found to be in agreement with the bioadsorption process. The biosurfactant producing bacterial strain E1 was reported to yield ~3.7 g/L surfactin biosurfactant that was utilised to modify the activated banana peel powder (AcBPP) to make biosurfactant modified activated banana peel powder (BSBP) giving uptake (bioadsorption) capacity of 130.65 and 130.05 mg/g for Pb^{2+} and Cd^{2+} removal from aqueous solutions and bioadsorption percentage of 92.19 and 92.24 % for Pb^{2+} and Cd^{2+}, respectively from an electroplating effluent in column mode. The continuous column mode study showed better results than the batch process.

This recommends its application at industrial scale as biofilter material for the treatment of effluents and their discharge into natural bodies of water.

Keywords: *Bio-adsorbents; Biosurfactants; Heavy metals; Bioadsorption; Fixed-bed adsorption*

Chapter 1

Introduction

1.0 Background

The sustenance of all life form depends on water which is a precious renewable resource and is renewed naturally via hydrological cycle. But owing to ever increasing exploitation and resulting pollution has raised an alarm towards its scarcity (Vasistha & Ganguly, 2020). This pushes us to work on solutions that can provide access to clean water for human population thus becoming an issue of ultimate significance in the present world. A report by UN (GLAAS, 2012) indicated inaccessibility to the drinking water for nearly one billion people due to enhanced water consumption in other related activities (Tortajada, 2020). The Global Analysis and Assessment of Sanitation and Drinking–Water (GLAAS) is an initiative implemented by WHO (World Health Organization) in UN (United Nation) which in association with OECD (Organisation for Economic Co-operation and Development) and UNDP (United Nations Development programme) focuses on implementing Sustainable Development Goal (SDG) 6 (GLAAS, 2019). The increasing rate of world population is correlated directly with the need for potable water access. Also, the magnitude of pollution due to its utilization directly corresponds to the intentional usage (Immerzeel et al., 2020).

The noteworthy causes of the water crisis are: restricted claim to pollution free safe drinking water, geographical and regional struggle for shared water resources, etc. The contaminated water resources adversely affect aquatic life and biodiversity on the earth making it a key urgency and the reason for fatality and ill health around the world (Pauli, 2020). Several regulations have been made in the developed world for proper disposal of industrial wastewater (IWW) containing toxic heavy metals (HMs) and other chemical entities (Shoushtarian & Negahban-Azar, 2020). However, there is a catastrophic scenario in the developing nations; therefore, there is a need to make people sensible about its sustainable usage. Besides this, suitable measures are also required to be taken towards availability of clean water and treatment of industrial effluents before their discharge into natural water bodies (Santucci & Scully, 2020). Understanding the severity of the problem, government agencies are investing a lot in research on utilization of wastewater after proper treatment as well as disposal into natural bodies of water. Government of India has launched various research schemes in this area of industrial wastewater treatment before disposal in natural bodies of water, i.e. the rivers, which are the lifeline of the country.

1.1. Industrial wastewater, heavy metal pollution in water and health risks

Industrial wastewater is any wastewater produced from any processing, manufacturing, or agricultural unit/industry or could be generated during an operation other than sanitary or domestic ones. Such wastewaters (WWs) contain various heavy metal(s), for instance, lead (Pb^{2+}), cadmium (Cd^{2+}), copper (Cu^{2+}), zinc (Zn^{2+}), chromium [Cr(VI)], mercury (Hg^{2+}) etc. causing adverse effects and are mainly discharged from manmade sources such as battery, electroplating industry, smelting process, electronic goods, pulp and paper industry, through mining, metal and alloy fabrication, paint, dyeing, printing, etc. (Mao et al., 2021). The anarchic discharge of untreated wastewaters with toxic heavy metals into the aqueous systems negatively affects its flora and fauna, causing toxicity in humans (Rao & Yan, 2020). The trace amounts of these metal ions are considered necessary for certain activities and as nutrients for the body but their elevated intake for example, Cu^{2+} can affect gastrointestinal system, Wilson‘s disease, lead to liver and kidney damage, insomnia; while Cd^{2+} can cause birth defects, renal and hepatic failure, red blood cells (RBCs) disruption, Itai-Itai disease, hypertension, high blood pressure, and is carcinogenic in nature (Rastogi & Kumar, 2020). Though Pb^{2+} has no essential purpose in humans but an increased uptake can lead to encephalopathy, seizures, mental retardation, kidney damage, reduced haemoglobin production and disruption of nervous system. It also affects reproductive and immune system and can harm the offspring when accumulated in a pregnant woman (Ram et al., 2021) while Zn^{2+} is used by plants but in humans can cause lethargy, neurological dis-functionality like seizures, dehydration, *etc*. (Souza et al., 2020). Bio-accumulation of these obnoxious elements in aquatic life forms and their bio-magnification through food chain is another source of heavy metal(s) entry in the living organisms where it inhibits their growth and contaminates groundwater ecosystem as well (Rastogi et al., 2021a). The toxic effects of Hg^{2+} includes birth defects, DNA damage, paralysis, blindness, etc. (Ajsuvakova et al., 2020). Wastewater treatment thus becomes essential so that water quality of various water bodies can be maintained, hence, all life forms and can also offer the possibility of re-using treated water in other applications that do not require high quality water (Xiang et al., 2020).

1.2 Removal techniques for heavy metals in water

Several treatment methodologies are available for de-contamination of wastewater *viz.* chemical precipitation, coagulation, flocculation, membrane separation, ion-exchange,

electrochemical methods but all of these techniques are expensive, require high maintenance, generate secondary sludge, and are not sensitive to remove low levels of HMs (Rastogi et al., 2019). Adsorption process on the other hand is gaining momentum and is now widely used for treatment of heavy metals containing wastewater. This technique has proved its usefulness to remove inorganic and organic pollutants from different WWs and is even effective for removal of lower concentrations of heavy metal ions present in the effluent (Rastogi et al., 2021b). The efficiency of adsorption depends on the type of adsorbent used for HM removal process where commercially activated carbons (CACs) are most commonly utilized for this purpose but are not economical and require high preparatory conditions (Zhu et al., 2021). However, the application of non-conventional bio-adsorbents have facilitated the improvement of adsorption process and aroused the demand to look for more alternative adsorbents that can make the process effective as well as economical. In the context of finding alternatives, biosurfactant (BS) modified bio-adsorbents are an emerging fabricated material for enhanced removal of heavy metal ions from wastewater system. Biosurfactants are considered as surface active molecules having both hydrophilic and hydrophobic entities in them, hence amphipathic; are produced by microorganisms that have the capability to reduce the surface and interfacial tension of the surface and interfaces respectively (Rastogi & Kumar, 2021). They have varied structure from glycolipid, lipopeptide, polysaccharide/lipid based to polymeric etc. (Malik & Kerkar, 2021). Biosurfactants, (secreted by microbial surfaces), chelate/adsorb heavy metal(s) from the solid/liquid surface forming a metal-biosurfactant complex and thus assists in bio-adsorption process to ameliorate heavy metal ions from the contaminated systems (Tang et al., 2020).

1.3 Heavy metals and biosurfactant mediated bio-adsorption process

Bio-adsorption (or biosorption) is defined as a fast, non-metabolically physico-chemical process that utilizes biological materials like fruit peel wastes, dead microbial biomass, etc. for decontamination of heavy metal ions containing aqueous solutions. This is generally a reversible process and the materials employed are known as bio-adsorbents (or biosorbents) (Guo et al., 2020). The search of a cost effective, easily available, abundant bio-adsorbent has directed into the investigation of diverse bio-materials, many of which were earlier used to be considered as futile waste material but are now being explored for their potential in heavy metal

remediation and assisting in management of these wastes as well (Ratna et al., 2021a). This is an emerging water decontamination technology and limited literature is available regarding their usage (Srivastava et al., 2021) and several recent studies indicate finding substitutes that can be easily tailored, are economically feasible, highly sensitive, and support enhanced heavy metal remediation process (Ratna et al., 2021b). Evidential amount of attention has been given in the past towards the synthesis, identification, and characterization of surface metabolites i.e., biosurfactant‘s (BS‘s) using microorganisms whose type and magnitude depends on the producing microorganism, trace elements, and the factors such as carbon/nitrogen, temperature, etc. that affects production process significantly (Guez et al., 2021). Biosurfactants are gaining popularity in the remediation of heavy metal ions due to their diverse characteristics for instance; stability towards varied environmental conditions like salinity, temperature, etc; biodegradable nature, less toxicity, chemical diversity, etc (Tang et al., 2020). On the working principle of Le Chatelier‘s , these biosurfactant molecules can precipitate out metal ions from the solution phase in the form of micelles on the solid /solution interface by reducing the surface and interfacial tension which can be easily separated by using micellar enhanced microfiltration (MEMF) or micellar enhanced ultrafiltration (MEUF) (Rastogi & Kumar, 2020). The integration of suitable biosurfactants with biological material leads to enhanced surface chemistry of the bio-adsorbent having varied surface composition with functional groups such as amino, carboxylate, hydroxyl, amides, etc which aids in binding and sequestering of heavy metal(s) from the solution (Malik & Kerkar, 2021). The surface/membrane composition of biosurfactants itself supports complexation of heavy metal(s) that in concurrence with other chemical processes occurring at the surface of bioadsorbent like ion-exchange, electrostatic interactions, precipitation followed by complicated merged mechanism supports biosorption of heavy metal ions (Rastogi & Kumar, 2021). The rate and efficiency of bio-adsorption process is more or less selective and depends on the choice of bio-adsorbent taken and heavy metal ion under study.

1.4 Aims and objectives

The primary aim of this study was to prepare bio-adsorbents, their characterization and their efficacy screening for removal of Pb^{2+} and Cd^{2+} ions from aqueous solution in a batch adsorption process. The study also involved isolation of Pb^{2+} and Cd^{2+}

resistant biosurfactant producing bacteria from hydrocarbon contaminated sites whose metabolite (biosurfactant) would be utilised in heavy metal bioremediation. It includes screening, characterization, and extraction of biosurfactant and amalgamation of extracted biosurfactant with the selected bio-adsorbent for removal of Pb^{2+} and Cd^{2+} ions from industrial effluents in a continuous column process.

The following specific objectives are to be apprehended in order to meet the above goal:

1. Preparation and screening of low cost bio-adsorbents from different organic waste materials.
2. To study and compare the efficacy of selected bio-adsorbents in removal of heavy metals (Cd and Pb) from aqueous solutions using adsorption technology.
3. Isolation and characterization of Cadmium and lead resistant bacterial strains having bio-surfactant production ability.
4. Molecular characterization of selected potent bio-surfactant producing strains to be used in treatment of heavy metals from industrial effluents.
5. Physico-chemical characterization of the industrial effluent before and after the treatment process.
6. Heavy metal (Cd and Pb) remediation from effluent using combination of bio-surfactant and bio-adsorbent material.

1.5 Novelty of the project

The increasing rate of environmental pollution has tended to shift the focus on the development of eco-friendly adaptive remediation strategies that are alternative to traditional approaches, and at the same time are feasible to remediate multiple contaminants when present concomitantly in the test system. In past few years, various literature regarding study of adsorption/bio-adsorption in heavy metal removal from the aqueous system are available (Saini et al., 2020), but scanty information is present in terms of biosurfactant mediated bio-adsorption of heavy metals ions from the wastewater or aqueous system. In one scientific contribution, biosurfactants were extracted from the leaves of *Ziziphus spina-christi* plant to prepare colloidal gas aphrons that were utilised in the removal of Cu^{2+} and Pb^{2+} from aqueous system (Saleem et al., 2019). In a single and multistage cascaded flotation

method, authors have reported low but significantly high i.e. up to 90.7% (Cu^{2+}) and 88.2% (Pb^{2+}) removal efficiency respectively. In another study, rhamnolipid modified ground grass were utilised for the removal of Cd^{2+} ions from aqueous solutions with 85.77% removal efficiency at pH 7 (Ghaith et al., 2019). The effect of rhamnolipid fabricated Na-montmorillonite clay was also investigated in another study for bioadsorption of Cu^{2+} ions from aqueous solutions (Özdemir & Yapar, 2009). Researchers have reported enhanced bioadsorption rate on account of distribution of rhamnolipids onto the positively charged edges of clay platelets and therefore, even distribution of platelets in water inhibiting diffusion resistance. There are some studies available that target integrated biosurfactant/bio-adsorbent material for removal of organic pollutants (Bhosale et al., 2019). However, only few reports have focussed on remediation of heavy metals using this approach (Wang et al., 2020). As a result, the study aims to contribute towards the remediation of toxic heavy metal ions using biosurfactant modified fruit peel residues, which is a growing area of research and by exploring their potential, these can be tailored with other low cost waste materials to understand the adsorption and desorption process for a particular or mixed pollutant in a co-contaminated system.

1.6 Research hypothesis and outline of thesis

In this study, the removal of toxic heavy metal ions, Pb^{2+} and Cd^{2+} from aqueous solutions was done using bio-adsorbents made from orange and banana fruit peel agro/bio materials that are abundant in nature or disposed of as wastes. The other organic waste materials such as rice husks and *Eucalyptus* saw dust were also prepared as bio-adsorbents and characterized for their surface properties to know their application potential. Also, Pb^{2+} and Cd^{2+} resistant biosurfactant producing bacterial strains were isolated from hydrocarbon contaminated soil to be used (their metabolite) along with bio-adsorbents for the removal of Pb^{2+} and Cd^{2+} from wastewater by improving the characteristics of bio-adsorbent, and amplifying the understanding of adsorption and desorption process system.

Entire work of this thesis has been divided into a total of seven chapters, where Chapter 1 gives the background and general introduction to the existing problem of wastewater treatment for disposal into natural bodies of water. It also includes the objectives, hypothesis and outline of the thesis. Chapter 2 reviews the significant

information from the previous studies related to the heavy metal pollution, its impact, removal techniques available, their limitations, bio-adsorption and their affecting factors, its advantages over other conventional methods, about bio-adsorbents and their characteristics, abundance, recent modifications on them, biosurfactants: classification, properties, factors affecting biosurfactant production, their mechanism of action etc. This chapter also engages mathematical isotherm modelling and kinetics of adsorption process and distinction between batch and column models for evaluating the performance of bio-adsorption process. Chapter 3 describes about the experimental investigation done for the fulfilment of the objectives covering materials and methods including the preparation, screening, and characterization of low cost bio-adsorbents from different organic waste materials, comparing the efficacy of selected bio-adsorbents in the removal of HMs (Pb^{2+} and Cd^{2+}) from aqueous solutions using adsorption technology in a batch process via optimization of factors affecting their bio-adsorption. It also explains the enrichment and isolation of biosurfactant producing bacterial strains from hydrocarbon contaminated sites, their screening, and characterization. Also, mass biosurfactant production, its extraction, characterization, and optimization of process parameters for maximum biosurfactant production from the selected strain using fruit peel waste as a low cost substrate along with their potential in biosorption of heavy metals. The physico-chemical characterization of real wastewater, fixed bed column experiments done for the removal of heavy metal ions from real wastewater using biosurfactant modified bio-adsorbent at selected experimental conditions are also mentioned. Chapter 4 covers the evaluation of the prepared bioadsorbents in terms of their characterization and also adsorption of HMs (Pb^{2+} and Cd^{2+}) from aqueous solutions in single metal system using the procedures and conditions mentioned in Chapter 3. Chapter 5 discusses the results obtained during enrichment and isolation of biosurfactant producing bacterial strains from hydrocarbon contaminated sites along with biosurfactant extraction and its characterization. Chapter 6 evaluates the findings of the experiments undertaken for bio-adsorption of Pb^{2+} and Cd^{2+} in a continuous column process under various conditions along with physico-chemical evaluation of wastewater parameters. The procedures for the dynamic column bioadsorption experiments are reported in chapter 3. All the results are explained in relation to the available information for other bio-adsorbents in literature. The last phase of the thesis i.e. Chapter 7 includes conclusion and recommendations based on the results obtained in the study, followed by the references section.

Chapter 2

Literature Review

2.0 Background

Excessive human intervention and industrial set ups has an accelerated strain on the environment that has caused a concern for the safety and availability of contamination free resources for the industrial and developing countries. This is not a present day problem but is century old which has leaded the environment towards a worse state (Song et al., 2020). The ever increasing needs for humans has raised the industrial development including modern agricultural practices and over exploitation of resources and became major sources of environmental pollution in the form of solid, liquid and gaseous contaminants. This raised problem has affected both living and non-living forms atrociously (Khan & Ozturk, 2020).

The release or accumulation of toxic heavy metal (HM) ions into the water streams on account of biological, natural, geological, and/or industrial inputs by humans from the era of _green revolution‘ to till date now has raised an alarming concern for the safety of human health and environment due to their persistent obnoxious nature and bio-accumulation in the food chain (Diarra & Prasad, 2021; Yu et al., 2021). The perils of HM such as lead (Pb), cadmium (Cd), chromium (Cr), copper (Cu), zinc (Zn), mercury (Hg), arsenic (As), etc. is not only limited to humans but greatly affects the other life forms viz., animals, plants and microorganisms via their discharge at concentrations higher than the prescribed standard limits that are set by various regulatory bodies **(Table 2.1)**. Many sources are available for HM pollution but different industrial bodies utilises water in considerate amounts leading to the generation of large amounts of wastewater (WW) consisting of both inorganic and organic contaminants, likewise numerous set ups/ technologies have been suggested or developed for their clean up in today‘s pollution clean-up age, it still remains one of the major problem associated with the technologists from the last 30 years (Chai et al., 2021; Lodhi et al., 2021).

Table 2.1 Heavy metal type, their permissible limits and harmful effect to the living organisms

Heavy metal	Sources	Permissible limit in soils (mg/kg) adapted from Deuel and Holliday, 1994	Permissible limit in drinking water (mg/l) ; WHO standards	Toxic effect	References
Cadmium(Cd)	Electroplating, Pigmented products, mining etc.	0.01-0.7	0.005	Damage to liver, kidneys, hypertension, carcinogenic	(Das & Al-Naemi, 2019; Pavón et al., 2019)
Copper (Cu)	Wood processing industries	2-100	1.0	Dermatitis, chronic asthma, generation of free radicals	(Alak et al., 2019)
Arsenic (As)	Wood processing industries, through herbicides, mining, etc.	1-50	0.05	Visceral cancers, kidney and vascular disease,	(Navasumrit et al., 2019)
Lead (Pb)	Paint and pigment industries, batteries, automobiles, etc.	2-200	0.05	Damage to brain, fetus, liver, kidneys, bones,	(Chung et al., 2019)
Zinc (Zn)	Electrolysis, Galvanization processes, paints, fertilizers, etc.	10-300	5.0	Nervous sytem dysfunction, growth retardation	(Poole et al., 2019)
Mercury (Hg)	Soil leaching, fossil fuel burning, etc.	0.01-0.3	0.001	Circulatory and nervous system disorders,	(Cariccio et al., 2019)
Iron (Fe)	Smelting, fertilizers, mining, etc.	7000-550,000	0.1	Retarted growth, low RBC count	(Hino et al., 2019)

2.1 Sources, toxicity and environmental fates of heavy metals

2.1.1 Sources of heavy metals

Several anthropogenic and natural activities such as weathering of rocks, hydrocarbon burning, metal surface work are primary causes of HM emissions in the atmosphere. Different household wastes, smelting and fertilizer industries releasing HM containing WWs are mainly responsible for the water pollution (Zhou et al., 2020) while combustion of coal and landfilling‘s causes soil contamination with HMs. The four main big sources of HM pollution include industries of acid-mining, electroplating, fossil fuel power generation, and nuclear power generation that involve uranium (U) mining (Xu et al., 2020).

Industrial WW generation and its safe disposal is a worldwide problem. Different industries are responsible for the production of HMs containing WW such as electroplating and surface treatment methods releases hazardous Pb, Cd, Zn, Ni, Cu, Cr, V, Hg and Ti due to multiple processes / applications. Mining, textile, battery, tanneries, petroleum, pigment and paints, pesticides, printing, photographic industries etc. are some major sources of HM pollution (Muhammad et al., 2021). HM pollution is a concern for the nations as unlike organic contaminants; these are non-biodegradable that leads to bioaccumulation and bio magnification problems causing several diseases and disorders in the living forms (Devda et al., 2021). Therefore, it becomes essential to eliminate these noxious forms before their discharge into the natural systems. Other considerable sources of HM pollution includes timber industries where wood treatment generates As, Cr, Cu containing wastes, hydrocarbon sector where petroleum refining using catalysts and its conversion produces Ni, V, Cr, industries dealing with films, and photographs generates silver (Ag), etc. Such industries generate huge amounts of WW in the form of residues, and sludge that requires massive treatment procedures (Lahlou et al., 2020).

Another source of HM contamination is domestic WW that gets affected due to the discharge received from households and industries. For instance, detergents contain trace amounts of Fe, Mg, Cr, Cu, etc. which gets adsorbed on the biological solids (Bakos et al., 2020). Landfills are another important source containing HMs along with solid wastes. Anaerobic environment lowers the pH of the dumping sites over a period of time that leads to the pushing of the HMs (Manasa & Mehta, 2020).

However, the sludge generated is a rich source of nutrients but rich in HM content which when utilised as fertilisers could enter into the ground or surface water and toxic environment for the plants and microorganisms as well.

2.1.2 Toxicity caused by heavy metal pollution

Various oxidation-reductions, precipitation/coagulation/dissolution, adsorption-desorption processes modifies the physical-chemical form and speciation of HM ions in the aqueous environments (Sanaei et al., 2021). For instance Cd is mainly found as associated complexes of hydroxide, sulphates, carbonates, etc above pH 7 and as Cd^{2+} during redox processes (Bernhoft, 2013). Pb as Pb^{2+} is the most stable form naturally but could also exists in 0, +1, +4 oxidation state as well. Between the pH 5 and 7, Pb is mostly found as precipitated form of chlorides, sulphates, hydroxides, phosphates, however, as +2 cation when pH is below 5 (Rana et al., 2018). **Fig. 2.1** illustrated the various sources and toxicity caused by heavy metal ions.

Metals are basically divided into two categories: essential and non-essential. Essential metals are necessary for the survival such as Fe and Ca, but those that are obnoxious for heath such as Pb and Cd are dangerous. Their raised concentrations above the permissible limits poses serious threats to the living forms and contaminates the surface and might even seep into the ground water as well causing contamination of potable water (Niu et al., 2020). The severe toxic effects of these HMs could be seen as mental, central nervous system failure, damage to the lungs, kidneys, heart, liver while their long term exposure can cause malignant tumors/cancers, muscular dystrophy, multiple sclerosis, Parkinson‘s and Alzheimer‘s diseases (Briffa et al., 2020).

The expression and the toxic effect of HMs depend on its form (divalent or higher) and when present in precipitated form might reside in the human body for longer period of time. These get adsorbed on to the organic groups present in the various human tissues that might mimic or causes the biological molecule to leave its site. Also, redox reactions by them might change the chemistry of basic elements such as carbon (C) leading to its oxidation. Generally the higher form of the metal is considered more toxic than its lower oxidation form (Zhang & Wang, 2020).

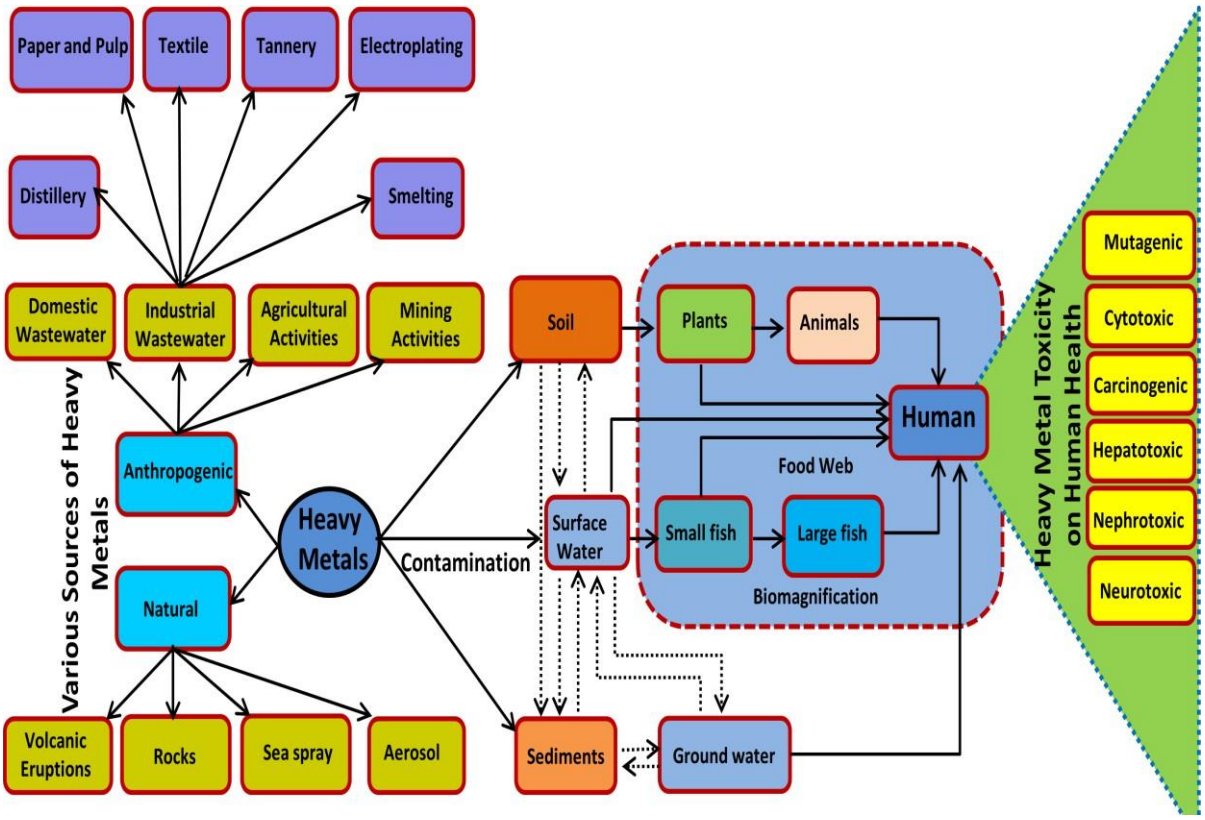

Figure 2.1 Schematic representation of sources and toxic effects of heavy metal ions

2.1.2.1 Effect of lead

Pb is an inhibitory metabolically carcinogenic element for humans. The major accumulation route of Pb in humans is through inhalation, occupational places (hazards/exposure), ingestion, or placenta. The percentage of Pb absorption through ingestion varies from 10% to 40-55% in adult and children respectively (Kumar et al., 2020). Lead poisoning is often seen to be transmitted due to usage of shiny earthenware surfaces or from paint pigments that leads to symptoms such as irritability, unnecessary/abnormal emotional swings, headache, weakness etc (Charkiewicz & Backstrand, 2020). Young ones are often found to suffer from the consequences of Pb poisoning that also cause mental retardation and brain damage (central + peripheral nervous system), replaces Ca from the bones, gets deposited in the bones ultimately bone breakage, neurological disorders, and renal failure is seen (Naranjo et al., 2020). The other routes include entry from corroded water pipes which can cause anaemia, miscarriage, declined fertility in males, behavioural disruption in children, damage to the pregnant woman so foetus as well.

2.1.2.2 Effect of Cadmium

After Pb, Cd and also Hg are considered as major toxic elements among HMs. Acute or lethal dosage of Cd can exert vomiting, diarrhoea, stomach irritation, Gastric irritation, lungs edema, nausea, chills, lethargy, bone damage are some common symptoms and is carcinogenic as well (Tamele & Vázquez Loureiro, 2020). Cd affected people showed spinal pain, fractures, deformation of bones and several diseases and disorders such as Itai-Itai in Japan. Chronic Cd poisoning can cause renal failure, damage to the liver, emphysema, proteinuria, hypertension, prostate and lung cancer, kidney stones are also seen (Pan et al., 2021). The main routes of Cd in humans is through foodstuffs such as mushrooms, mussels, dried seaweed, or for people working near hazardous sites containing toxic wastes etc that could lead to psychological disorders, DNA damage, and affected immune system, reproductive issues, etc. (Yazdi et al., 2021).

Various HMs are being engaged in the industrial sector in assorted ways and play an economical role for nations but simultaneously after release in the environment show deleterious effects on terrestrial and aquatic bodies and human beings due to their toxic, highly persistent, and bio-accumulative properties (Igiri et al., 2018). Industrial WW (tannery, distillery, paper and pulp, pharmaceutical, batteries, mining, electroplating, etc.) is a major source of HM contamination in terrestrial and aquatic ecosystems (Jaiswal et al., 2018a; Vardhan et al., 2019). Researchers reviewed previous literature and reported that increased concentration of HMs affect soil, and plant growth. Srivastava and co-authors concluded that metals like Cu, Mn, Co, Zn, and Cr are essentially required in trace amounts for plants for their metabolic activities, but increased concentration affects the soil microbial diversity and growth and development of plant through altered biochemical, physiological, and metabolic processes and finally enters into the food chain (Srivastava et al., 2017). HMs such as Al, Pb, Cd, Au, and Hg do not have any biological role but causes acute and chronic malicious effects on living organisms (Briffa et al., 2020; Lakherwal, 2014). Most of the HMs shows toxicity on aquatic and terrestrial organisms when present insoluble and available through bioaccumulation in the food chain (Bernhoft, 2013).

Researchers had reviewed the effect of long term usage of HMs on enzyme activity and microbial community in soil and concluded that the release of HMs containing

agricultural and industrial WW severely affects the soil ecosystem (Chetty & Pillay, 2019). One group of researchers had performed a comparative study to evaluate the soil quality and map distribution of HMs under long term irrigation with Nile fresh water and sewage WW (Abd-Elwahed, 2018). He delineated in his report that long sewage WW increased the Cu and negatively affected the soil quality by surging salinity and availability of HMs. In another report, it was assessed the effect of long-term irrigation with industrial WW then rain-fed field on the soil. They find variations in concentration of HMs, Pb > Cu > Ni > Zn > Fe > Cd > Mn and Fe > Zn > Mn > Pb > Cd > Cu > Ni respectively in WW and rain-fed field irrigated soil. Also, they concluded that WW irrigation led to raised levels of pH, EC, and salt accumulation ratio in the soil (Haroon et al., 2019). In another scientific contribution, it was investigated the accumulation, translocation factor, and health risk potential of Cd in a soil wheat system irrigated with a different cone of treated WW and freshwater. All treated WW irrigated soil had higher EC (75-143%) and 2 to 4 times higher availability while concentration of Cd were enhanced up to 2- 4 times compared to freshwater. They concluded that the health risk factor of Cd for different age groups had low non-carcinogenicity after consuming wheat; while Cd carcinogenic health risks (CR) value (1×10^{-5} to 1×10^{-4}) suggested low to moderate potential risks (Rezapour et al., 2019). Recently, James and co-worker assessed the contamination status of HMs containing WW open dumping centres and their vicinity on topsoil. It was found that mean contamination of HMs are lower than the permissible limits according to WHO‘s. However, due to their toxic, highly persistent, and bio-accumulative properties, they recommended periodic monitoring to minimize the inadvertent exposure of humans (James et al., 2020). In one study, it was investigated the concentration and sources of nine HMs (Cd, Pb, Cu, Cr, Fe, Mn, Ni, Co, and Zn) in Bafa lake sediment. Multivariate analysis indicated that anthropogenic activity is also one considerate factor after natural sources of HM contamination. Their study reported that Cd, Cr, and Ni were the most serious hazard for the ecosystem of the Bafa Lake (Algül & Beyhan, 2020).

In one study, the effect of Fe > Mn > Zn > Co > Ni > Cu = Cr loaded WW on histopathology, biochemical and molecular changes in *Channa punctatus* (fish) was reported. They reported that oxidative stress markers such as superoxide dismutase (SOD), catalase (CAT), and lipid peroxidation (LPO), were significantly higher while the reduction in glutathione (GSH) in all its tissues. While, damaged DNA of gill,

liver, and kidney were present at raised levels (Javed et al., 2017). The effects of HMs on the Egyptian aquatic ecosystems was studied and summarised that Cd, Pb, Cu As, Ni and Zn caused toxic, carcinogenic and mutagenic effects at the cellular level of aquatic organisms (Al Naggar et al., 2018). The potential risk of five HMs metals/metalloids on commercial fish (*Anodontostoma chacunda*, *Johnius belangerii*, and *Cynoglossurs arel*) in Persian Gulf was investigated. Out of five HMs, As and Hg were the most hazardous HMs, while the target risk of As indicated that long-term consumption of fish could led to impose carcinogenic effects on human health (Keshavarzi et al., 2018). In another study, the relationship between the WW and its impact on the ecosystem was examined and concluded that As, Cd and Cr are the key water pollutants that causes severe deleterious consequences on human health through carcinogenic effects on the pancreas, brain, and thyroid (Keshavarzi et al., 2018). Recently, the noxious repercussions of HM contamination on the aquatic ecosystem and human health was reviewed (Sonone et al., 2020). HM contagion degrades the aquaculture via physical abnormalities in its flora and fauna by way of diseases. Further, through fish consumption HMs enters into human bodies and poses deleterious effects on health in an indirect manner.

2.2 Treatment technologies for the remediation of heavy metals from wastewater

2.2.1 Chemical precipitation and oxidation

This is the most widely studied process in which heavy metal ions reacts with the appropriate chemical and are precipitated out in the form of their insoluble hydroxides, sulphides, carbonates and phosphates. The major disadvantage associated with this method is generation of large amounts of low density sludge, unsuitable for mixed metal system, formation of colloidal precipitates and their filtration problem, release of toxic hydrogen sulphide gas during sulphide precipitation in acidic medium, etc. (Gautam et al., 2019).

2.2.2 Flotation

Flotation is one such integrated physicochemical separation process which is suitable for removal of less dense smaller particles with low retention time and is efficiently utilized in the paper and pulp industry but it requires high input cost from chemicals used to process maintenance and energy utilisation while its selectivity is highly pH dependent (Azimi et al., 2017).

2.2.3 Coagulation and Flocculation

Coagulation is the process of surface charge neutralization of contaminant using coagulants such as aluminium, ferric chloride, etc. while flocculation results into clumping of contaminants into large particles that then are separated by sedimentation and filtration. Generation of sludge, high operational chemical cost, low efficiency, etc. are major limitations of this process (Patidar et al., 2017).

2.2.4 Ultrafiltration

Ultrafiltration (UF) is a low pressure driven /membrane separation based heavy metal removal technique in which micellar enhanced UF and polymer enhanced UF is widely used that offers high selectivity and high metal concentrates as their prime advantages (Li et al., 2018). Membrane fouling and selectivity/ its design are prime disadvantages of this method that amplifies its investment costs (Maharana et al., 2021).

2.2.5 Ion-exchange

Ion exchange materials of cationic or anionic charge are used for the removal of HMs [Cu^{2+}, Zn^{2+}], nitrate, sulphate, etc. of opposite charge and is a widely used methodology. It is a highly sensitive pH dependent process (Bashir et al., 2019).

2.2.6 Reverse osmosis

Reverse osmosis (RO) is a semipermeable membrane based separation process that restricts the movement of contaminants (solute) to pass through the membrane and allow the passage of solvent (effluent in study) through it. The major drawback is being high power consumption process and membrane reproducibility (Abdullah et al., 2019).

2.2.7 Electrochemical treatment

This method is preferred over coagulation method as it is a fast and efficient separation process involving electrolysis. It is effectively utilized in the elimination of HM ions, oils, and etc. but engages high operational inputs (Rajkumar & Palanivelu, 2004).

2.2.8 Phytoremediation

Phytoremediation is a green technology that utilizes plants to eliminate toxic pollutants from the environment. This is a cost effective treatment methodology where the cost of treatment is directly related with the type of contaminant, its concentration, etc but also suffers from limitations such as hyper-accumulation, a slow seasonal process and accretion of the contaminant in the edible parts of the plant (Farraji et al., 2016).

2.2.9 Electrodialysis

Electrodialysis (ED) is a charged ion-exchange membrane based separation process that involves movement of ions from one liquid to another under the influence of an electric field. The limits of this process are high voltage utilisation and maintenance of temperature that often leads to diminished separation percentage (Bagchi & Behera, 2020).

2.3 Bioadsorption and bioadsorbents

2.3.1 Adsorption

Among all the conventional approaches available for remediation of heavy metals, adsorption is the most appropriate ancient technology as it is simple to perform, requires less operational cost and has design flexibility. C.W. Scheele in 1773 showed first time the uptake of gases onto charcoal and clays (Bhatnagar and Minocha, 2006) but the term ‗Adsorption' was coined by a German physicist Heinrich Kayser in 1881 (Calvert, 1990). It is defined as a surface phenomenon which involves adherence or binding of a chemical species (known as adsorbate) on to the solid or liquid surfaces termed as adsorbent (Crini *et al*., 2019). An adsorbent is selected on the basis of its pore size (surface porosity), high surface area and surface chemistry and the type of pollutant in study (Bhatnagar & Minocha, 2006).

2.3.2 Wastewater treatment by adsorption

In general, an adsorption process constitutes a triad of adsorbent, adsorbate, and the WW that could be either of industrial origin (effluent) or designed aqueous solution/system (Rastogi & Kumar, 2020). An adsorbent is the material that is involved selectively in adhering adsorbate particles on its surface while an adsorbate is generally described as the pollutant in study. The selectivity of the adsorption

process is based on adsorbent-adsorbate‘s thermodynamics and kinetics including their surface interactions, and mass transfer. The maximum uptake of the contaminant by the adsorbent is defined as the adsorption capacity that is largely depended upon these interactions between both adsorbent and adsorbate; adsorbent and water; adsorbate and the solution. Hydrophobicity of the pollutant favours the adsorption process owing to their low solubility in the solution (Bashir et al., 2019).

Researchers are often confused with the term ‗adsorption‘ with ‗sorption‘, ‗bioadsorption‘, ‗biosorption‘ and ‗bioaccumulation‘ (Crini et al., 2019), and are used interchangeably frequently; thereby it becomes imperative to unclutter the disarray caused and define them. The suitability of the term is delineated by the type of adsorbent used in the study.

The physical binding or chemical interaction of a adsorbate from its solution onto the adsorbent surface leading to its diminished concentrations in the solution is termed as adsorption that gives rise to the surface complexes of inner or outer-region within/on the adsorbent (Dąbrowski, 2001) while ‗sorption‘ is the term generally used to describe adsorption and absorption process taking place simultaneously in the system. Biosorption or bioadsorption is the physicochemical process for the removal of diverse contaminants using biological materials that comprises of biopolymers or biosorbents such as agricultural food wastes, dead biomass of plants and microorganisms, clearly excluding live microbial cells (Park et al., 2010). Such biosorbents are high in demand due to their easy availability, low maintenance, selectivity and are economical as well (Gupta & Diwan, 2017). Another confusing terminology is ‗bioaccumulation‘ with ‗biosorption‘ where former includes precipitation, etc; a slow, metabolically activated and irreversible while ‗biosorption‘ is a non-metabolically mediated, rapid and a reversible process (Ayangbenro & Babalola, 2017).

2.3.3 Adsorption contacting system and desorption process

Such adsorption technology can be put into practice using different contact modes existing between adsorbent and adsorbate such as batch process, column or fixed-bed type, fluidized beds, pulsed beds, etc where batch and column mode are the most predominant ones that are discussed ahead in the literature for the removal of HM ions. An efficient adsorption phenomenon depends upon certain factors viz., origin and structural complexity of the adsorbent that includes its particle size, porosity,

specific surface area, surface chemistry i.e., kinds of functional groups present, surface charge (& zero point charge; pZPC), mechanical strength, physical or chemical activation conditions, effect of process variables; the adsorbate (contaminant) itself, and the WW conditions such as its pH, conductivity, level and kinds of impurity present in it, etc. (Crini et al., 2019).

The obstruction that can be stated for this technology is the generation of metal loaded sludge and its disposal that could limits its application, however, fixed-bed studies provides two alternatives i.e., regeneration and replacement. These not only will make the process more economical but also suggests metal recovery from the WW. This is done using desorption studies where loaded metal is desorbed from the adsorbent using molar concentration of mineral acids and the material is regenerated for another round but this aspect of adsorption is needed to be dealt in detail in order to decipher the mechanism of adsorption well (Dotto & McKay, 2020). **Fig. 2.2** representing different adsorbent types and the methods employed for the adsorption process.

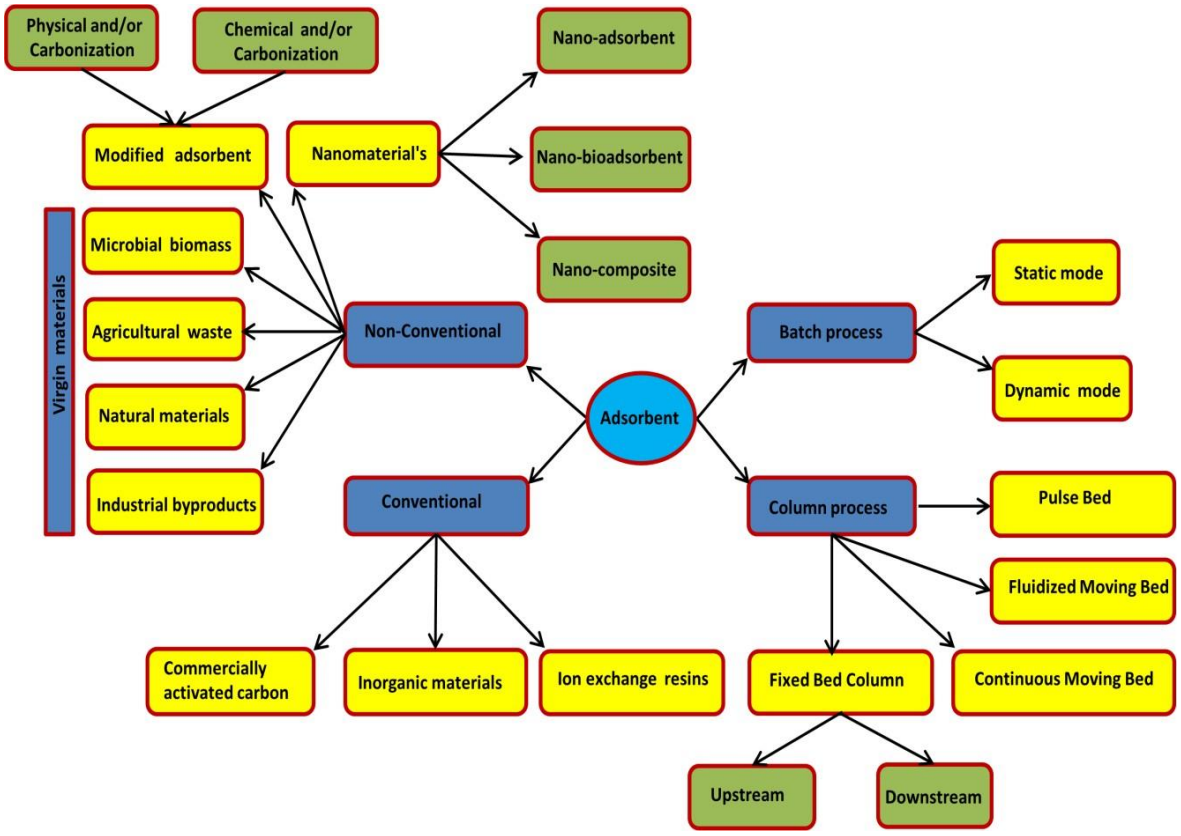

Figure 2.2 Adsorbent types and adsorption methods

2.3.4 Heavy metal remediation using non-conventional bioadsorbents

The usage of commercial activated carbons (CACs) or materials that are being converted into ACs are being restricted due to their expensive operational and manufacturing cost and attention has been shifted towards application of cost effective non-conventional adsorbents (NCAbs). These NCAbs could be of biological origin or from natural materials and can be applied directly in their raw or treated form (Crini *et al*., 2019). Their application has been increased at an alarming rate in the past few years as they are abundant in nature, are economical ready to use (or can be modified) but their usage is still restricted to pilot scale and needs to be explored more in large field applications (Sangeetha et al., 2017) .

2.3.4.1 Agricultural solid wastes as adsorbents/ nonconventional green adsorbents

In recent years, agricultural solid waste (ASW) has been explored at various levels in their natural or modified form using physico-chemical methods for pollutant removal as former mainly composed of lignin, hemicellulose, lipids, hydrocarbons, carbohydrates, proteins, water that contain various functional groups on their surfaces. These functional groups present on their surfaces have charges that can facilitate binding of a particular pollutant by varying pH levels (Rastogi et al., 2019). Rosales and his team investigated the role of untreated lime peel and pineapple core wastes in the removal of Cr (VI) from aqueous solutions with adsorption capacities of 9.20 and 4.99 mg/g respectively at pH 2.01 (Rosales et al., 2019). In an another recent study conducted using peels of *Artocarpus nobilis* for the removal of Ni^{2+} showed enhanced metal removal efficiency from 50 to 71 to 93% through optimization processes having 12,048 mg/kg as maximum adsorption capacity via static and dynamic conditions with Freundlich model as the best fitted adsorption model where regression coefficient has 0.994 value (Priyantha & Kotabewatta, 2019). An efficient adsorption process includes optimization of various factors that can affect an adsorption study such as pH, adsorbent dose, reaction contact time, initial metal concentration, temperature, revolutions per minute (rpm), pressure, etc. which are needed to be identified for the large scale application of adsorption process (Guyo et al., 2017). In one study, scientists employed central composite design (CCD) for adsorption factors optimization using a novel biochar aliginate composite adsorbent in the removal of

Zn^{2+} ions . They reported the initial Zn^{2+} concentration (43.18 ppm) and adsorbent dose (0.062 g) as most effective factors on account of high f-value which explained maximum adsorption capacity of 120 mg/g giving 85% removal efficiency. Though the conversion of agricultural waste residue at nano-scale level provides high surface area but also leads to difficulty in their separation from the study system, therefore, focus has been shifted to utilise them in the dual form where an adsorbent is merged with a suitable membrane (Zeng et al., 2016). In another study, it was explored the efficiency of green ceramic hollow fibre membrane (CHFM) synthesised from rice husk ash (RHA) in removal of Ni^{2+}, Zn^{2+} and Pb^{2+} ions giving 99% removal rate (Hubadillah et al., 2017). The modified CHFM/RHA based dual function material and others might serve as a promising low-cost adsorbent + filtration unit for the removal of noxious heavy metal ions from the aqueous systems.

2.3.4.2 Industrial by-products as low-cost adsorbents

The processing of substances at industrial level generates huge amount of secondary wastes whose disposal is another problem but these can be utilised as adsorbents in their raw or modified form. For instance, the iron industry during smelting of iron in blast furnace produces slag waste whereas coal industry generates fly ash wastes that can be optimized for heavy metal removal from waste streams. Nguyen and his team assessed the removal efficiency of slag and fly ash wastes in the removal of five metals (Pb, Cu, Cd, Cr and Zn) and found the maximum adsorption capacity for Pb and Cd, when used in multiple metal system at an optimum pH 6.5 (Nguyen et al., 2018). Liu and his team employed fly ash based granular adsorbent containing zero valent iron (ZVI-GAM) for the removal of Pb^{2+} and Cr(VI) from the aqueous system with 78.13 and 15.70 mg/g maximum adsorption capacities respectively (Liu et al., 2017). Red mud is another waste by-product that is being exploited as an efficient adsorbent. Hydrazine sulphate mixed red mud when incorporated in calcium alginate beads utilised as an excellent adsorbent for Pb^{2+} ions removal having 138.6 mg/g adsorption capacity (Naga Babu et al., 2017). Tsamo and his team explored the efficiency of low cost raw and hydrocholoric acid treated red mud in the removal of Cr(VI), Cu^{2+} and Pb^{2+} (Tsamo et al., 2018). They reported that acid treated red mud had only little affect in removal of Cr(VI) and Cu^{2+} but had increased removal percentage for Pb^{2+} (79.365 from 52.083 μmol/g adsorption capacity). In the recent years, many researchers have worked with industrial wastes as suitable adsorbents for

the heavy metal removal. For instance, iron ore slime (a mining waste) for Pb^{2+} and Hg^{2+} removal (Sarkar et al., 2017); coal fly ash for Hg^{2+} removal (Attari et al., 2017); magnetic 4A-zeolite from red mud for Al^{3+}, Fe^{2+}, and other metals (Xie et al., 2018). Recently, hollow porous granules (PS-HPGs) were synthesised from industrial wastes of polysulphone hollow fibre membranes when incorporated with nano-range polydopamine (PD) served as efficient adsorbent for the 80% removal of Cu^{2+} ions and for Zn^{2+} and Ni^{2+} ions after certain modifications (Posati et al., 2019).

2.3.4.3 Natural materials

It is usually advocated that mesoporous adsorbents derived from natural materials are good candidates for the heavy metal removal study as these provide large surface activity due to large surface area and uniform large pore size. Mesoporous silica materials (MSMs) derived from MCM41 type was investigated in the removal of Cu^{2+}, Cd^{2+} and Pb^{2+} with adsorption capacities around 36.3,32.3 and 58.5 mg/g in the pH range 5-7 (Zhu et al., 2017). Vojoudi and his team evaluated the efficiency of magnetic mesoporous silica as nanoadsorbent for the removal of Pb^{2+} and Hg^{2+} ions in batch study leading to 303.03 and 256.41 mg/g adsorption capacities respectively (Vojoudi et al., 2017).

2.3.4.4 Microbial bioadsorbents

The utilization of microorganisms in the eradication of toxic pollutants from contaminated environment is known as bioremediation. Their inbuilt biosorptive or bioaccumulative mechanistic ability helps them to tolerate heavy metal toxicity that can be employed in many ways such as absorption, adsorption, oxidation, etc. in pollutant removal or in restoration of original environment (Javanbakht et al., 2014). Also, these microorganisms either bacteria, fungi or alga are being exploited in their live as well as dead form that makes them as potential biosorbing agents for the sequestration of heavy metal ions from the aqueous environments (Ayangbenro & Babalola, 2017). In one study, it was used alginate beads immobilized with fungal biomass as biosorbing material in the removal of As at pH 6 and found the adsorption capacity of about 59.5 mg/g (Jaiswal et al., 2018b). The potential of dried *Gelidium amansii* (marine alga) biomass in free and immobilized form was assessed for the removal of Pb^{2+} leading to 100% removal percentage at pH 4.5 (El-Naggar et al., 2018). In another study, it was investigated the potential of bacterial cellulose

pellicles modified with polyethyleneimine in the removal of Cu^{2+} and Pb^{2+} ions with maximum adsorption capacities to be 148 and 141 mg/g respectively (Jin et al., 2017). Microorganisms are being used not only as whole in live or dead form as adsorbents but their secretions are also explored as suitable adsorbents for the removal of toxic metal ions from waste streams. Castro and his team explored the efficiency of biogenic (bacterial) iron compounds mainly siderite and magnetite as adsorbent in the removal of Cu, Zn, As, and Cr and reported higher removal percentage for As in single and bimetal system (As-Cu) (Castro et al., 2018). Li and Zhou used heavy metal resistant immobilized *Brevibacterium* as bioadsorbent for the removal of Pb and Cd having 114.36 and 82.12 mg/g maximum adsorption capacity (Li & Zhou, 2018).

2.3.4.5 Nanoadsorbents/nanocomposites

The applicability of adsorbents that are carbon-based or metal oxide and metal organic frameworks (MOFs), zeolites in the nano-range has been increased in the recent years due to their large surface area and high surface chemistry (Nasir et al., 2019). Zanin *et al*. assessed the role of natural clinoptilolite zeolite (CL) as adsorbent in the removal of heavy metals from graphic industry with removal efficiency up to 95.4, 96.0 and 85.1% for Fe, Cu and Cr respectively (Zanin et al., 2017). But these nanocomposites tend to agglomerate that results in reduction of surface area, also gives rise to recyclability and environmental issues due to which these are utilized in hybrid composite forms (Bajpai et al., 2019).Shahat *et al.* explored the role of an organic nano-ligand N, N‘-di (3-carboxysalicylidene)-3, 4-diamino-5-hydroxypyrazole that was anchored using building block approach on mesoporous silica and termed as facial adsorbent for the removal of Co^{2+} ions from their aqueous solutions and reported maximum adsorption capacity of 157.73 mg/g at higher pH values (Shahat et al., 2015). In an another similar study conducted by Vafaeifard *et al*. analysed the potential of nanostructured flowerlike $Mg(OH)_2$ that was assembled on granular polyurethane as nanoadsorbent for the removal of Cu^{2+}, Cd^{2+} and Pb^{2+} with astonishing 472, 1050 and 1293 mg/g adsorption capacities respectively in batch processes and up to 184 mg/g adsorption capacity for Cu^{2+} in a continuous-flow column study (Vafaeifard et al., 2019). Bio-nanocomposites are advantageous as they impart biodegradability, biocompatibility and antimicrobial activity (Bajpai *et al.,* 2019). Souza *et al*. investigated the potential of *Malpighia emarginata D.C.* seed fibers microparticles (Me-SFMp) as bioadsorbent and found metal removal

efficiencies up to 81, 84.2, 86.8, and 95.1% for Ni, Cu, Pb and Cr respectively while 100% for both Zn and Cd (Souza et al., 2018). An efficiency of a novel chitosan-iron (oxyhydr) oxide composite known as chitosan goethite bionanocomposite (CGB) in the form of beads was explored and found to remove As(V) more than As^{3+} from aqueous solutions through diffusion-adsorption mechanism (He et al., 2016). Ahmad and Mirza evaluated the role of methionine modified bentonite/alginate (Meth-bent/Alg) in the removal of Pb^{2+} and Cd^{2+} at pH 5 and 4 respectively with 30.86 and 217.39 mg/g adsorption capacities at 303 K respectively (Ahmad & Mirza, 2015).

Polymer-layered silicate nanocomposites (PLSNs) and polymer-functionalized nanocomposites (PFNCs) are emerging as superior nonconventional nanocomposites as these provide stability, better reinforcement rate at less than 10%, resistance against many solvents, temperature, ions and have mechanical strength, diverse functional groups on their surfaces leading to strong specific bindings to metal ions or any other pollutant (Ucankus et al., 2018).

2.4 Bacterial surfactant/ metabolite based heavy metal removal

The unfavourable environment triggers a stress response in microorganisms such as bacteria and fungi to produce various secondary metabolites to cope up with those antagonistic conditions. Bacterial bio-surfactants are one such compound that has proved their existence fruitful for the bioremediation of inorganic contaminants particularly heavy metals (Akbari et al., 2018). Some of the common properties that make a bio-surfactant molecule to be preferred over chemical surfactants are surface and interfacial tension reduction ability, highly tolerant to pH, salinity, temperature moderations, biodegradability and biocompatibility, less toxic, specificity and emulsification capacity (Usman et al., 2016). There has been done much work in the recent years that has proved the role of bio-surfactant producing bacteria in the bioremediation of heavy metal contaminated soils. Chen *et al*. assessed the potential of bio-surfactant rhamnolipid in washing of heavy metal ions from river sediment. A dose of 0.8% rhamnolipid removed Cu (80.21%), Cd (86.87%), Pb (63.54%) and Cr (47.85%) after 12 h at pH 7.0. They emphasised that the efficiency of washing depended on initial heavy metal ion speciation, rhamnolipid concentration, washing time, liquid/solid ratio and pH (Chen et al., 2017). In an another experimental setup, researchers modified the conventional electro-kinetic treatment with biodegradable

rhamnolipid and complexing agent Tetrasodium of N, N-bis (carboxymethyl) glutamic acid (GLDA) in heavy metal removal from sewage sludge and showed significantly higher removal percentages of 70.6 ± 3.41%, 82.2 ± 5.21%, 89.0 ± 3.34%, 60.0 ± 4.67%, 88.4 ± 4.43% and 70.0 ± 3.51% for Cu, Zn, Cr, Pb, Ni and Mn respectively (Tang et al., 2017).Similar studies performed by Yang *et al.*, they proposed an efficient bioleaching technique using bio-surfactants from *Burkholderia* sp. Z-90 in combination with flocculation by poly aluminium chloride (PAC) as a cost effective, environment-friendly remediation model for severely heavy metal contaminated soils. Their results showed removal efficieny of Zn, Pb, Mn, Cd, Cu and As upto 44.0, 32.5, 52.2, 37.7, 24.1 and 31.6% respectively at 1:20 (w/v) soil liquid ratio for 5 days which were found to be more efficient than that by 0.1% of rhamnolipid (Yang et al., 2018). The bioremediation potential of bacterial bio-surfactants pertains to their high biodegradable nature, low toxicity, multi-functionality, environmental compatibility and economical production which make them an excellent alternative over various synthetic surfactants that are available in the market (Akbari *et al.,* 2018).

2.4.1 Biosurfactant mediated methods for the management of heavy metal contaminated soils

There are various methods available for remediation of heavy metal contaminated soils. The different in-situ approaches include surface capping, encapsulation, electro-kinetic extraction, soil flushing, chemical immobilization, bioremediation and phytoremediation and ex-situ methods are landfilling, solidification, soil washing and vitrification (Liu et al., 2018) but bio-surfactant producing bacteria manages this high density metal pollution through soil washing and soil flushing methods (Ayangbenro & Babalola, 2018).

2.4.1.1 Soil flushing: This is an in-situ approach where a small quantity of biopolymer is injected in the contaminated soil in a cement mixer that has drain pipes or trenches for the introduction and collection of biopolymer solution into or out of the soil. This surfactant based flushing technique was first demonstrated by Pankow and Cherry (Pankow & Cherry, 1996) . The complex thus formed due to the strong bonding between anionic bio-surfactants and cationic heavy metal ions is flushed out of the mixer as it easily separates out from soil matrix and soil gets deposited back

into it. The metal-biopolymer complex precipitates out the biopolymer leaving behind the metal ion (Mulligan et al., 2001). Wang and Mulligan did column experiments to assess the potential of rhamnolipid JBR425 and found enhanced removal of As(V), Cu, Zn and Pb using 0.1% rhamnolipid with 70 pore-volumes flushing operation under alkaline conditions (Wang & Mulligan, 2009). The desorption of adsorbed metal ions from the adsorbent matrix can be enhanced by flushing the matrix with bio-surfactant-foam solution as demonstrated by Haryanto and Chang in removal of adsorbed Cu^{2+} ions from sand-packed columns (Haryanto & Chang, 2015).

2.4.1.2 Soil washing: This ex-situ remediation technology eliminates obnoxious heavy metal ions from the soil through washing and scrubbing of the soil with bio-surfactant solution (Sarubbo *et al.,* 2015). Diaz *et al*., (2015) assessed Fe and Zn removal from contaminated soil using alternate cycles of bioleaching with oxidising bacteria (*Acidithiobacillus thiooxidans* and *Acidithiobacillus ferrooxidans)* and washing with rhamnolipid solution and found the combined strategy to enhance removal percentage up to 36% for Fe and 63 % to 70% for Zn than alone treatments. The high percentage of toxic contaminants in the soil and sludge may obstruct nutrient recycling and land usage. The washing of soil sediments with bio-surfactant solution could provide a suitable bioremediation alternative that can enhance mineral availability and land application. Tang *et al*. (2019) showed increased metal mobility, binding ability and removal efficiency of Cu, Zn, Cr, Ni and Mn up to 62 %, 74 %, 60 %, 68 % and 64 % respectively than Pb (only 15 %) using rhamnolipids and saponins in multiple washing steps.

2.4.2 Mechanism of heavy metal removal by bio-surfactants

The working strategy for BS mediated HM remediation is based on Le Chatelier‘s principle either through precipitation or adsorption. BSs are capable of forming complexes with free metal ions present in the solution leading to desorption of metal ions (Wu *et al.,* 2017) from the solution phase. Qi *et al.* (2018) assessed the removal of Pb^{2+} and Cd^{2+} from soil by utilising sophorolipids of *Starmerella bombicola* CGMCC 1576 and reported about 95 and 52% of Cd and Pb removal percentage respectively by complexation mechanism in soil washing system. Secondly, as BSs can reduce the surface and interfacial tension of the medium, these get accumulated in the form of micelles on the solid/solution interface and bind the metal ions on

themselves (Ayangbenro and Babalola, 2018). According to Tortora *et al.* (2016) the metal-BS complex or metal-micelle complex can be taken out from the system using micellar enhanced microfiltration (MEMF) or micellar enhanced ultrafiltration (MEUF). The efficiency of BSs depends on their size, class type, charge and structure that facilitates or determines their interaction with the sorbed metal on the soil (solid) surfaces (Wan *et al.*, 2017), also their translocation through soil pores on to the sorbed metal ions. Alternatively, the type of soil, its structure, contamination level and duration, pH, cation exchange capacity (CEC) and soil particle pore size also affects BS ability to remove metal ion from their surfaces or depth (Xue *et al.*, 2018; Pourfadakari *et al.,* 2019).

2.4.3 Surfactant/bio-surfactant modified low cost bioadsorbents

Chemically originated or biologically secreted surfactants are amphillic molecules having both hydrophilic and hydrophobic ends and are widely used in the HM remediation process where biological surfactants are preferred over chemically synthesised surfactants as the former have low toxicity, specificity, biodegradable nature, etc (Hailu *et al.,* 2018). The natural materials such as zeolites and clays are known to be used as adsorbents in the HM removal process whose efficiency can be intensified by using acids or alkalies (Jimenez-Castaneda and Medina, 2017). In recent years, many studies have been conducted where these amphillic molecules when incorporated on such zeolites or clay materials, has increased the efficiency of the latter in the remediation process through ion exchange mechanism (Jimenez-Castaneda and medina, 2017; Li *et al.,* 2007). Tran *et al.* (2018) explored the efficiency of cationic surfactant ‗hexa-decyl-tri-methyl-ammonium' (HDTMA) modified organo-zeolite (Na-H-zeolite) in the removal of Pb, Cu, Ni and other organic pollutants. In a similar study, cationic surfactant ‗hexa-decyl-tri-methyl-ammonium-bromide' C16 and zwitterionic surfactant ‗hexa-decyl-di-methyl (3-sulphonatopropyl) ammonium' Z16 were applied on organo-montmorillonites for the removal of Cu^{2+} ions from the aqueous system (Ma *et al.,* 2016).

2.5. Factors affecting adsorption activity

2.5.1 Contact time

Song et al., (2011) studied the effect of contact time from 30 min to 12 h for adsorption of Hg^{2+}, Cd^{2+}, Mn^{2+} and Cr^{3+} using 5.0 mg of polyrhodamine-encapsulated

magnetic nanoparticles (PR-MNPs) at pH 4. Liu et al., (2017) assessed the role of magnetic chitosan/anaerobic granular sludge (M-CS-AnGS) composite as an adsorbent for Pb^{2+} and Cu^{2+} ions removal and factors affecting the adsorption process. The batch experiments were conducted in the time range of 5 to 1440 min. The increased initial removal efficiencies within 30 min were attributed to larger available binding sites on the adsorbent than the later equilibrium time. The biosorption process involving activated carbon from *Ulva lactuca* in the removal of Cu^{2+}, Cd^{2+}, Cr^{3+} and Pb^{2+} was studied by Ibrahim et al., (2016). Their study also supported the initial increased in removal percentage of metal ions approximately within 60 min owing to greater fraction of available contact sites onto the adsorbent.

2.5.2 pH

The point of zero charge (pH_{zpc}) is taken into consideration while studying the effect of pH during adsorption process. There is a limit to increase in adsorption process with gradual increase in pH of adsorbate (metal ions) solution. When pH= $pH_{zpc,}$ the surface of the adsorbent carries no charge while above pH_{zpc}, it is negatively charged and below pH_{zpc} , it has positive charge. Generally, it is found that above $pH_{zpc,}$ the rate of adsorption process increases due to strong attraction forces that exists between positively charged metal ion species and negatively charged adsorbent surface (Abbas et al., 2017). Kolodynska et al., (2017) performed adsorption experiment using carbonaceous adsorbents obtained from spent ion exchange resins for the removal of Cu^{2+}, Cd^{2+}, Co^{2+} and Pb^{2+} ions. They reported the interference of hydronium ions with metal ions at low pH whereas hydroxides of metal ions were found at high pH i.e., at pH 8. All the metal ions got precipitated as their metal hydroxides above neutral pH. Hence, the sorption process was performed at pH 5 for all the metal ions. Afolabi et al., 2015 explored the efficiency of phosphoric acid activated carbon from milk bush kernel shell, activated at temperatures 400 and 600 ˚C (MBK400 and MBK600) in the removal of Cd^{2+}, Pb^{2+}, Ni^{2+}, Zn^{2+}, Fe^{2+} and Cu^{2+} ions in dairy industrial WW (DIWW). They reported an important finding from their experiments that initial pH of the adsorbent is not responsible for change in pH pattern of treated effluent as in their case. Along with other adsorption factors, pH of the treated DIWW was found to be increased from pH 6.1 to ranges of 6.7, 6.8, 6.9 but it was in the limits of European ranges set for discharge in aquatic environment. With increasing MKB600 adsorbent doses, the pH was decreased which could state that pH of adsorbent might not be a

contributing factor for bringing about changes in pH of treated DIWW. The surface charge of an adsorbent tends to change above or below their zero point charge (pZPC). In a study involving adsorption of Hg^{2+} ions on magnetic polyrhodanine nanoparticles showed increased adsorption performance at increased pH from 2 to 4 (4 being optimum) and negligible increase from pH 4 to 8 (Song et al., 2011). The low adsorption rate at low pH corresponded to competitive inhibition of Hg^{2+} ions by increased protons (H^{+}) ions in the solution that diminished on increasing pH making available more binding sites for metal ion or deprotonation took place.

2.5.3 Adsorbent dose

Ibrahim et al., 2016 studied the effect of adsorbent dose obtained from algal *Ulva* powder (AP) and its activated carbon (AAC) in various ranges were studied at pH 6 with 10 mg/l initial metal ion concentration of Cr^{3+}, Cu^{2+}, Pb^{2+} and Cd^{2+}. They reported increased adsorption rate and capacity with the increase in algal dose from 0.2 to 0.8 g/l on account of increased metal adsorption active sites on the surface of adsorbent (maximum adsorption at 0.8g/l). The AAC showed better results than AP due to presence of large surface area i.e., availability of more actives sites for adsorption process. Fallah et al., 2017 developed titanium oxide (TiO_2) modified cellulose nanocomposite via click reaction for the uptake of Pb^{2+}, Cd^{2+} and Zn^{2+} ions from aqueous solutions. Their findings also explained similar results as above mentioned i.e., increased amount of adsorbent dose leads to increased rate of adsorption due to free sites of interaction between metal ions and adsorbent. The maximum adsorption rate was obtained with 10 mg adsorbent in their case of study.

2.5.4 Initial metal ion concentration

The enhanced driving force facilitates rise in adsorption capacity when initial metal ion concentrations are increased as it resists the mass transfer between liquid and solid state but it also sometimes leads to decreased adsorption percentage due to increased metal ions competition for the limited set of available active sites of the adsorbent (Ariffin et al., 2017). Fakhre and Ibrahim, (2017) studied effect of initial metal ion concentration on adsorption process by novel supramolecular polysaccharide composite from cellulose (CEL) and dibenzo-18-crown 6 using ceric ammonium nitrate as initiator (CEL+DB18C6). They reported that increased initial concentration of Ni^{2+}, Cu^{2+}, Zn^{2+}, Cd^{2+} and Pb^{2+} ions from 2 to 12 mg/l at particular pH (pH 6)

would increase binding or competition of these metal ions with H^+ ions on adsorbent surface by stronger attractive interactions and thus, leading to increased removal percentage of metal ions from their solutions.

2.5.5 Temperature

Chowdhury et al., (2016) developed mesoporous magnesium oxide (MgO) nanostructures having morphologies in the form of nanoplate, nanosheet and nanoparticle in heavy metal uptake from aqueous solutions and the factors affecting the adsorption process. One of the factor ‗temperature' was studied in the range from 310 -340K for Pb^{2+} and Cd^{2+} ions and found a linear increase in heavy metal adsorption with increase in temperature due to rise in kinetic energy thus movement of metal ions leading to higher adsorption rate on the surface of adsorbent. In another similar study, effect of temperature was studied in the range of 313 to 323K while keeping other factors constant for the adsorption of Pb^{2+} and Cd^{2+} ions on banana peel powder(Ibisi and Asoluka, 2018). Results were found opposite to Chowdhury et al., (2016) where increase in temperature lead to weakening of binding forces between metal ions and the adsorbent in the case of Pb^{2+} ions but increased adsorption percentage for Cd^{2+} ions due to increased diffusion from external surface to internal pores of adsorbent and on the surface as well.

2.5.6 Adsorbent particle size

The different range of particle size of various adsorbents affects the adsorption process in distinguished manner. It is generally found that smaller the particle size, larger is the surface area of adsorbent making available more space for the reaction process leading to enhanced rate of adsorption (Ahmed and Ahmaruzzaman, 2016) but it should also be kept in mind that this is not the only factor that might increase adsorption rate, surface chemistry of the adsorbent also plays an important role in this regard (Duan et al., 2020).

2.6. Mechanism of adsorption

The plausible justification for the mechanism of adsorption can be well understood by studying the interactions taking place at adsorbent and solvent interface. The adsorbent molecule has generally strong affinity for the adsorbate in study (here HM ions) that involves multiple processes taking place at their junction such as

physisorption, chemisorption, surface adsorption, weak Van der waal‘s interaction, complexation, chelation, hydrogen bonding, precipitations (microprecipitation), membrane diffusion, ion exchange, entrapment in fibrils of adsorbent, electrostatic/covalent interactions, acid-base interactions, Yoshida‘s interactions, redox titrations (Sud et al., 2007; Crini et al., 2019) . The adsorption process often includes a set of complex steps that could be an amalgamation of above mentioned mechanisms in combination. It is hard to extract just by looking at the interactions, other factors such as high capacity in terms of q_{max} , surface chemistry and selectivity, their kinetics and thermodynamic parameters, low cost, material composition also plays a significant aspect while selecting the most appropriate adsorbent (Zhu et al., 2019).

Depending on the type of adsorbent/adsorbate under study, the mechanism of adsorption varies accordingly. For instance, it is advocated by many authors that removal of pollutants such as HMs and dyes using non-conventional adsorbents that are mostly composed of lignin, tannins, cellulose, etc. is a result of ion-exchange, hydrogen bonding and adsorption along with other process parameters (Panda et al., 2018; Xu et al., 2018). Ali, (2017) investigated the potential of acrylonitrile polymerized bleached pulp of banana peels in the removal of Mn^{2+} leading to 94% adsorption. The bleaching and co-polymerization of banana peels assisted in exposing more functional groups on cellulosic skeleton of the peels aiding towards efficient binding of metal ions.

The mechanism underlying the usage of commercial activated carbons (CACs) in eliminating toxic pollutants from aqueous systems is highly controversial besides being versatile, surface porosity, high surface area (Burakow et al., 2018). The concentration of carbon/oxygen functional groups on the surface of the adsorbent and the properties (size) of specific HM significantly affects the adsorption chemistry.

Researchers often explain the mechanism of adsorption to be proton (H^+) exchange in oxygen functional group with the metal ion but this could not be enough to justify more or less adsorption of divalent HM ions. Kuroki et al., (2019) investigated the mechanism of adsorption of more Pb^{2+} on six types of activated carbons than Zn^{2+} and Ni^{2+} ions. They explained that Pb^{2+} is considered as a soft metal while Zn^{2+} and Ni^{2+} are border line metals which can behave as soft or hard depending on the pH of the

solution according to the concepts of hard and soft acid and bases (HSAB) theory. In their study with activated carbons, they presented oxygen functional group on the edge of a graphene surface as hard sites while basal planes of surface polyaromatic rings having pi (π) orbitals in graphene as soft sites. This justified more adsorption of soft metal Pb^{2+} on the basal planes of the graphene ultra-micropores as it was a soft site and also comparable size with the micropores whereas Zn^{2+} and Ni^{2+} behaved as hard metals due to pH being 4 and their adsorption on edge sites of graphene.

Biopolymers and their derivative based adsorbents for instance, cyclodextrin, lignin, cellulose, starch, chitosan, etc. are known to involve mainly chelation or complexation (or coordination) and ion-exchange interactions during metal removal that are often found to be more suitable than ancient ion-exchange resins as they are known to have diverse functional groups (Carboxyl, hydroxyls, etc.) on their surfaces which leads to strong affinity between metal ions and the adsorbent involved. Saleh et al., (2016) investigated the adsorption of As^{3+} ions on chitosan modified vermiculite with 72.2 mg/g adsorption capacity. They explained the possibility of chelation or stabilised complex formation between As^{3+} with amino(─NH_2) groups of chitosan or ion- exchange of H^+ of ─NH_2 groups and As^{3+}.

2.6.1 Biosorption mechanism

The adsorption study involving microbial biomass either living or dead is generally categorised into two basic mechanisms that is metabolism dependent and metabolism independent. The location of metal is also an important aspect that is needed to be kept in mind while exploring the mechanism of biosorption using microbial biomass. While using living biomass for biosorption of HM ions, it becomes metabolism dependent where accumulation of metal ions could be intracellular through cell membrane transporters or extracellular via precipitation/complexation/ion-exchange mechanisms. The rapid and generally reversible metabolism independent pathway includes dead biomass where surface biosorption /precipitation take place through adsorption, ion-exchange, or complexation (coordination) mechanism (Papirio et al., 2017). The kind of living microbial cell and their intrinsic metabolic machinery involved in respiration or nutrient uptake can affect the biosorption process either positively or negatively (Ayangbenro and Babalola, 2017). The recovery of metals (desorption) from the microbial adsorbent is also difficult where when metals are

entrapped intracellular as without disruption of the cells, it can‘t be taken out (Yin et al., 2019). The surface adsorption might take place on the cell wall or the products secreted by microorganisms such as exopolysaccharides (EPS) or biosurfactants (BSs) (Gupta and Diwan, 2017). The efficiency of biosorption via EPS or BS is influenced by process parameters such as pH, amount of the metabolite secreted by microorganisms and their type and composition (Rastogi et al., 2021). The stable metal-EPS complex generally formed hinders the metal recovery process but the metal-BS micellar complex could be used for metal recovery by altering the pH.

2.7. Batch vs. Column adsorption process for heavy metal elimination

The removal of non-biodegradable toxic heavy metal ions from the aqueous system is an essential aspect in terms of providing pure form of water. This is done using discontinuous batch mode adsorption study that is quite popular among researchers and sufficient literature is available regarding its application (Deng et al., 2019; Lopez et al., 2018; Gokila et al., 2017; Ali et al., 2016). Such batch processes for the removal of heavy metal ions (adsorbate) provide information in terms of process parameters used in the study, often are optimized for quoting the best operating conditions for the process and researchers are more inclined towards this than dynamic continuous column adsorption study due to minimal requirement of adsorbent, small volumes of solution, takes short span of time, is economical, parameters affecting adsorption process can be manipulated, etc. (Ince and Ince, 2017; Vardhan et al., 2019). Bankole et al., (2019) explored the efficiency of purified and polyhydroxybutyrate functionalized carbon nanotubes to remove HM ions in a batch mode and assessed the effect of contact time, adsorbent dose, and pH on the removal process. But, this batch mode treatment is not convenient for field scale application, for which column or fixed-bed study is preferred as the adsorbent is in continuous contact with the solution, has higher residence time and is a good mass transfer adsorption phenomenon. Batch study helps in assessing the performance of the material and the chemistry of adsorbate-adsorbent system at small scale study and suggests its suitability at large scale (Pyrzynska, 2019). Adsorption isotherm models are available for depicting the maximum equilibrium adsorption capacity for a particular adsorption study as shown by researchers in their study (Mahdi et al., 2018; Papirio et al., 2017; Borna et al., 2016). Fixed bed adsorption study is generally employed at industry level for the removal of variety of contaminants, odour and

color from industrial WW (Ma et al., 2018; Malik et al., 2018). Different mathematical models/equations and the estimation of breakthrough curve assists in analysing the performance of column adsorption, its functionality and regeneration aspect, also the knowledge of its rate kinetics and dynamics that helps in its design architecture (Patel, 2019; Zhou et al., 2018). Rajamani and Rajendrakumar, (2019) investigated the performance of chitosan-boehmite based desiccant nanocomposite to remove Pb^{2+}, Cd^{2+}, and Hg^{2+} in a fixed-bed column study. Their study emphasised on the time and shape of breakthrough curve by employing Thomas and Yoon-Nelson kinetic models in the adsorption process via column mode and suggested initial complete removal of metal ions while the saturation of top adsorbent column zone led to adsorption in the bottom as the duration is increased. The column adsorption parameters such as flow rate, bed height and initial ion concentration have a huge impact in determining the breakthrough point. An increased flow rate explains lower residence time for the heavy metal ions not giving enough time for adsorption reactions and an early saturation point as ascertained in the study of Manirethan et al., (2019). Similarly, increased bed height provides more adsorption sites to the adsorbate (HM ions) and a delay in saturation point leading to better adsorption process (Papirio et al., 2017).

2.8. Selection criteria for biosorbents

2.8.1 Pore size and porosity

A good biosorbent should possess high capacity and fast kinetics which can be improved by using biosorbents having high micropore volume and large pore network for the movement of adsorbate molecules to the interior. Depending upon the pore size of the biosorbent, they are classified as microporous (diameter (d) < 2nm), mesoporous (2<d<50nm), and macroporous (d>50nm). Around 97% surface of any biosorbent is covered by micropores, hence, leading to larger surface area, and more amount of adsorbate would adhere to it. The biosorbent selection should also depend upon the size of the adsorbate. The larger size of the adsorbate should be removed by using mesoporous, and macroporous biosorbents (Samuel PN et al., 2020). Jiang and his team in their study exploited lignosulfonate-lysine hydrogel for the adsorption of Co, and Cu ions with excellent adsorption capacities of 270.4, and 365.1 mg/g , respectively (Jiang et al., 2020).

2.8.2 Surface area

The pore size and surface area of the biosorbent have direct impact on each other. The surface area is the area available on the surface of the biosorbent for the adsorption of targeted pollutant. It is generally expressed as m^2/g. Researchers are often focused on increasing the surface area of the biosorbent so that less amount of biosorbent is utilized for the adsorption of large amount of adsorbate molecules, thus making it an economical process (Samuel PN et al., 2020). Recent technological advances include the utilization of nanobiosorbents/nanocomposites for the removal of HM ions from the aqueous solutions. Parastar and his team explored chitosan cross-linked into graphene oxide/iron^{3+} oxide hydroxide nanocomposites for the adsorption of Pd, and Cd. Their study reported excellent adsorption percentage with 84, and 95% of removal efficiency from aqueous solutions (Parastar et al., 2021).

2.8.3 Surface chemistry

Besides, physical characteristics (pore size, and surface area) of the biosorbent, the chemical characteristics i.e., surface chemistry of the biosorbent also plays a crucial role in the adsorption process. The surface of the biosorbent is made up of diverse functional groups such as hydroxyl (─OH), carbonyl (>C═O), carboxyl (─COOH), amino (─NH_2), amide (─C═ONH_2), etc. that comes from the biomolecules constituting the cell wall. The targeted adsorbate molecule interacts with these functional groups and forms covalent bond (adsorption) with them. Similarly, the cell wall of microorganisms consists of peptidoglycan, etc. having charged ligands on it that assists in adsorption of HM ions (Samuel PN et al., 2020). The surface of the biosorbent is made rich in such functional groups by their fabrication with chemical agents. Hasanin and their team assessed the potential of nano chamomile waste for the adsorption of Pb (621.6 mg/g), Cu (163.9 mg/g), and Fe (522.7 mg/g) (Hasanin et al., 2019).

2.9. Mathematical modelling of biosorption process: kinetics and equilibrium models

2.9.1 Kinetics of biosorption process

The biosorption kinetics explains the process of adsorption with the passage of time and it depends on adsorption parameters such as pH, temperature, initial concentration of adsorbate, etc.

2.9.1.1 Pseudo first order (PFO) model

The PFO reaction model was given by Lagergren (Moussout et al., 2018) which is as follows:

$$\frac{dq_t}{dt} = k_1(q_e - q_t) \quad \text{(2.1)}$$

Here, q_e and q_t are the concentration of the adsorbate per mass of biosorbent at equilibrium and at any time t (min), respectively while k_1 (min^{-1}) is the rate constant of PFO model. The linear and non-linear form of the equation is represented as:

$$\ln(q_e - q_t) = lnq_e - k_1 t \quad \text{(2.2)}$$

$$q_t = q_e(1 - e^{-k1.t}) \quad \text{(2.3)}$$

2.9.1.2 Pseudo second order (PSO) model

The general expression for PSO model (Moussout et al., 2018) is given by:

$$q_t = \frac{q_e^2 k_2 t}{q_e k_2 t + 1} \quad \text{(2.4)}$$

Here, q_e (mg/g) and q_t (mg/g) are amount of adsorbate at equilibrium and at any time t (min), respectively while k_2 (g/mg min) is the PSO rate constant.

The linearized form of the equation is as follows:

$$\frac{t}{q_t} = \frac{1}{k_2 q_e^2} + \frac{1}{q_e} t \quad \text{(2.5)}$$

2.9.1.3 Elovich model

This model is used to describe chemisorption process and is mostly used for adsorption of gases onto solids and contaminants from aqueous solutions. The model is represented as follows:

$$q_t = \frac{1}{\beta}\ln(\acute{\alpha}\beta) + \frac{1}{\beta}\ln t \quad \text{(2.6)}$$

Here, ά is initial adsorption rate (mg/g.min), β is desorption constant combined with the extent of surface coverage and activation energy for chemical adsorption (Ghaneian et al., 2017).

2.9.1.4 Intra-particle (IP) diffusion model

The IP diffusion model is expressed as:

$$q_t = K_{int} t^{1/2} + C \quad \text{..... (2.7)}$$

Here, K_{int} is intra particle diffusion rate constant (mg/g.min$^{1/2}$) and C is the intercept. This model explain about the internal diffusion of the metal ions inside the pores of the biosorbent (Indhumathi et al., 2018).

2.9.2 Isotherm models

2.9.2.1 Langmuir isotherm

Langmuir adsorption isotherm is based on assumptions of monolayer adsorption where adsorption takes place at certain specific sites only (Wang & Guo, 2020). The non-linear form of Langmuir isotherm model is illustrated as:

$$q_e = q_m K_L \frac{C_e}{1 + K_L C_e} \quad \text{..... (2.8)}$$

Here, C_e is the adsorbate concentration at equilibrium (mg/L), q_e is adsorption capacity (mg/g), q_m (mg/g) and K_L (L/mg) are maximum adsorption capacity and enthalpy of adsorption respectively.

The linearized form of this equation is used to predict the value of isotherm parameters which is given as follows:

$$\frac{C_e}{q_e} = \frac{1}{q_m K_L} + \frac{C_e}{q_m} \quad \text{..... (2.9)}$$

2.9.2.2 Freundlich isotherm

This isotherm model explains the multilayer adsorption phenomenon based on assumptions of heterogeneous surfaces (Wang & Guo, 2020). The non-linear and linear forms of this model are presented as:

$$q_e = K_F C_e^{1/n} \quad \text{..... (2.10)}$$

$$\ln q_e = \ln K_F + \frac{1}{n} \ln C_e \quad \text{..... (2.11)}$$

Here, K_F and n are the constants describing the adsorption capacity and intensity of adsorption, respectively.

2.9.2.3 Dubinin-Radushkevich isotherm

The adsorption phenomenon occurring on both homogeneous and heterogeneous surfaces is expressed by this model (Al-Ghouti & Da'ana, 2020). The non-linear and linearized form of this isotherm model is as follows:

$$q_e = q_s \exp(-K_{DR}\varepsilon^2) \quad \text{(2.12)}$$

$$\epsilon = RT ln\left(1 + \frac{1}{C_e}\right) \quad \text{(2.13)}$$

Here, q_s (mg/g) Dubinin-Radushkevich isotherm model adsorption capacity, K_{DR} (mol^2/kJ^2) is mean free energy of adsorption, R (J/molK) is gas constant, and T is absolute temperature in Kelvin (K).

$$lnq_e = lnq_s - K_{DR}\epsilon^2 \quad \text{(2.14)}$$

2.9.2.4 Temkin isotherm

This isotherm model explains the interaction of adsorbent with the adsorbate molecules by ignoring very large and low concentration values. Also, it assumes heat of adsorption as a function of temperature decreases linearly instead of logarithmically (Al-Ghouti & Da'ana, 2020). The non-linear and linear forms of this isotherm model are:

$$q_e = \frac{RT}{b_T} \ln A_T C_e \quad \text{(2.15)}$$

$$q_e = \frac{RT}{b_T} lnA_T + \frac{RT}{b_T} lnC_e \quad \text{(2.16)}$$

2.10 Concept of fixed bed column bioreactor

The dynamic adsorption process is generally conducted using a column filled with a bed of selected adsorbent material where a fresh adsorbate of fixed concentration is fed into the column continuously and a dynamic equilibrium is established. This low energy requiring experimental process can go on for hours in the column and upon

exhaustion of the bed with the pollutant in study, it is regenerated via desorption process.

2.10.1 Breakthrough curve and other analytical concepts

A breakthrough curve is obtained when experimental values are plotted as ratio of effluent and influent concentrations (Ci/C_0) vs time (t). This S-shaped curve corresponds to the process of dynamic adsorption in continuous system, and varies with the design parameters. The curve represents higher concentration of adsorbate in the effluent over a time period meaning high rate of adsorption at the initial phase reaching to the saturation point. A steep breakthrough curve is directly proportional to the increased flow rate, high concentration of adsorbate in the feed solution, and low bed height. The different formulae to calculate adsorption capacity, amount of metal adsorbed, and adsorption percentage is as follows:

Amount of metal adsorbed, ($m_{ad.t}$, mg) at any instant of time by equation:

$$m_{ad.t} = m_{in.t} - m_{out.t} \quad \text{..... (2.17)}$$

Here, $m_{in.t}$ (mg); quantity of metal entering into the column at any time = C_0Qt

$m_{out.t}$ (mg); quantity of unadsorbed metal coming out from the column $= C_0Q \int_0^t \left(\frac{Ci}{C_o}\right) dt$

where, C_0 = influent concentration (ppm); Q = flow rate (mL/min), Ci = effluent concentration (ppm), and t = time (min)

Adsorption capacity of the adsorbent, (q, mg/g) by equation:

$$q = \frac{m_{ad.t}}{m} = \frac{C_oQ \int_o^t \left(1 - \frac{C}{C_o}\right) dt}{M} \quad \text{..... (2.18)}$$

Here, m is mass of the adsorbent (g)

Adsorption percentage, (A %) by equation:

$$Y = \frac{m_{ad.t}}{m_{in.t}} \times 100\ \% \quad \text{..... (2.19)}$$

2.10.2 Kinetic models for adsorption in continuous mode

2.10.2.1 Thomas model

This model explains adsorption-desorption kinetics based on Langmuir assumptions and it also hypothesizes that continuous adsorption is free from axial dispersion as the rate of driving force proceeds via second-order reversible kinetics. The linear form of the Thomas model is represented in equation (4) where a linear plot is drawn between ln [(C_o/C_e) – 1] vs t in order to determine values of model constants k_{th} and q_0.

$$\ln\left[\frac{C_o}{C_e} - 1\right] = \frac{k_{th} q_o M}{Q} - k_{th} C_0 t \ldots\ldots\ldots\ldots \textbf{(2.20)}$$

Here, k_{th}= Thomas model constant (L/mg.min)

q_0= adsorption capacity (mg/g)

M=adsorbent quantity (g)

C_0= concentration of the influent (ppm)

C_e= concentration of the effluent (ppm)

t= time (min)

2.10.2.2 Yoon Nelson model

Yoon-Nelson model highlights the time required for a 50% breakthrough point of the adsorbate. Also, it advocates that the decrease in the rate of adsorption of a particular adsorbate depends upon the adsorbate adsorption and its breakthrough on the adsorbent. The linear plot of ln [(C_t/ (C_o-C_t) vs t gives the values of k_{YN} and τ via equation as given below:

$$\ln\left[\frac{C_t}{C_o - C_t}\right] = k_{YN} t - \tau k_{YN} \ldots\ldots\ldots\ldots\ldots \textbf{(2.21)}$$

Here, k_{YN} = velocity rate constant (per min); τ = time required for 50% adsorbate breakthrough

2.10.2.3 Adams-Bohart model

This model explains the efficiency of the initial breakthrough curve and utility of surface reaction theory along with the relevance of C_t/C_0 and t relationship in

continuous adsorption system. The values of k_{AB} and N_0 are obtained from the linear plot of ln $[C_t/C_0]$ against t from the equation:

$$\ln\left[\frac{C_t}{C_0}\right] = k_{AB} N_0 \frac{Z}{\mu_0} \ldots\ldots\ldots\ldots\ldots\ldots \textbf{(2.22)}$$

Here, k_{AB} = Adams-Bohart rate constant (L/mgmin)

N_0 = equilibrium volumetric sorption capacity (mg/L)

Z = column bed depth (cm)

μ_0 = linear velocity of influent solution (cm/min)

t = time (min)

Co = influent concentration (ppm)

Ct = effluent concentration (ppm)

Chapter 3

Experimental Investigation

3.0 Introduction

This chapter gives the details of the materials, and chemical/reagents and an overview of the methods used for the objectives selected in the study. It discusses about the methods employed for screening and preparation and characterization of bio-adsorbents: activated orange peel powder (AcOPP), activated banana peel powder (AcBPP), and biosurfactant modified activated banana peel powder (BSBP), experimental conditions including procedures (batch and column adsorption process), physico-chemical analysis of industrial wastewater before and after column adsorption. Also, it gives an overview about the isolation, and characterization of lead (Pb^{2+}) and cadmium (Cd^{2+}) resistant biosurfactant producing bacterial strains whose metabolite would be utilised in combination with the selected bio-adsorbent for removal of heavy metals from industrial wastewater in bacterial surfactant based bio-adsorbent column.

3.1 Bio-adsorbent collection, screening and preparation

Different organic waste biomaterials such as fruit peel wastes of orange (*Citrus sinensis*) and banana (*Musa acuminata*), rice husks, *Eucalyptus* saw dust (*E. erythrandra*) were collected from different areas of Lucknow, and Sitapur region, Uttar Pradesh. Initial screening of the organic waste material was based on determination of specific surface area using BET (Brunauer Emmet Teller) analysis (explained in section 3.3.1.1) and then employed for further modification/fabrication.

3.1.1 Orange peel wastes (OPW) and activated orange peel powder (AcOPP)

The raw orange peel wastes (OPW) were collected from the local fruit juice stalls and household in Lucknow, Uttar Pradesh, India. The collected peels were washed several times with distilled water to remove dirt and dust and dried in sunlight for 48 h. The semi-dried peel wastes were subjected to oven drying at 80 ºC for complete evaporation of moisture till 24 h. The completely dried peel waste was grounded into fine powder i.e. orange peel powder (OPP) using mixer grinder and sieved through a 100 mesh siever to get uniform particle size of approximately 150 µm.

The raw orange peel powder was further subjected to acidification using 5% sulphuric acid (H_2SO_4) in a ratio of 3:1 (H_2SO_4: Orange Peel Powder, OPP) and kept for 24 h in an incubating shaker at 303 K (30^0C) for proper mixing. The acidified powder was

dried and then put in muffle furnace for carbonization and activation at 700 ºC for 6 h. The activated carbon of modified orange peel wastes thus obtained was washed with distilled water and dried at 100 ºC for 48 h to get activated orange peel powder (AcOPP) as illustrated in **Fig. 3.1**.

3.1.2 Banana peel wastes (BPW) and activated banana peel powder (AcBPP)

The raw banana peel wastes (BPW) were also gathered from the local fruit juice stalls and household in Lucknow, Uttar Pradesh, India. Collected peel waste was cut into small pieces (< 5 mm) and were subjected to the same process as done in section 3.1.1 to obtain activated banana peel powder (AcBPP) as shown in **Fig. 3.1**.

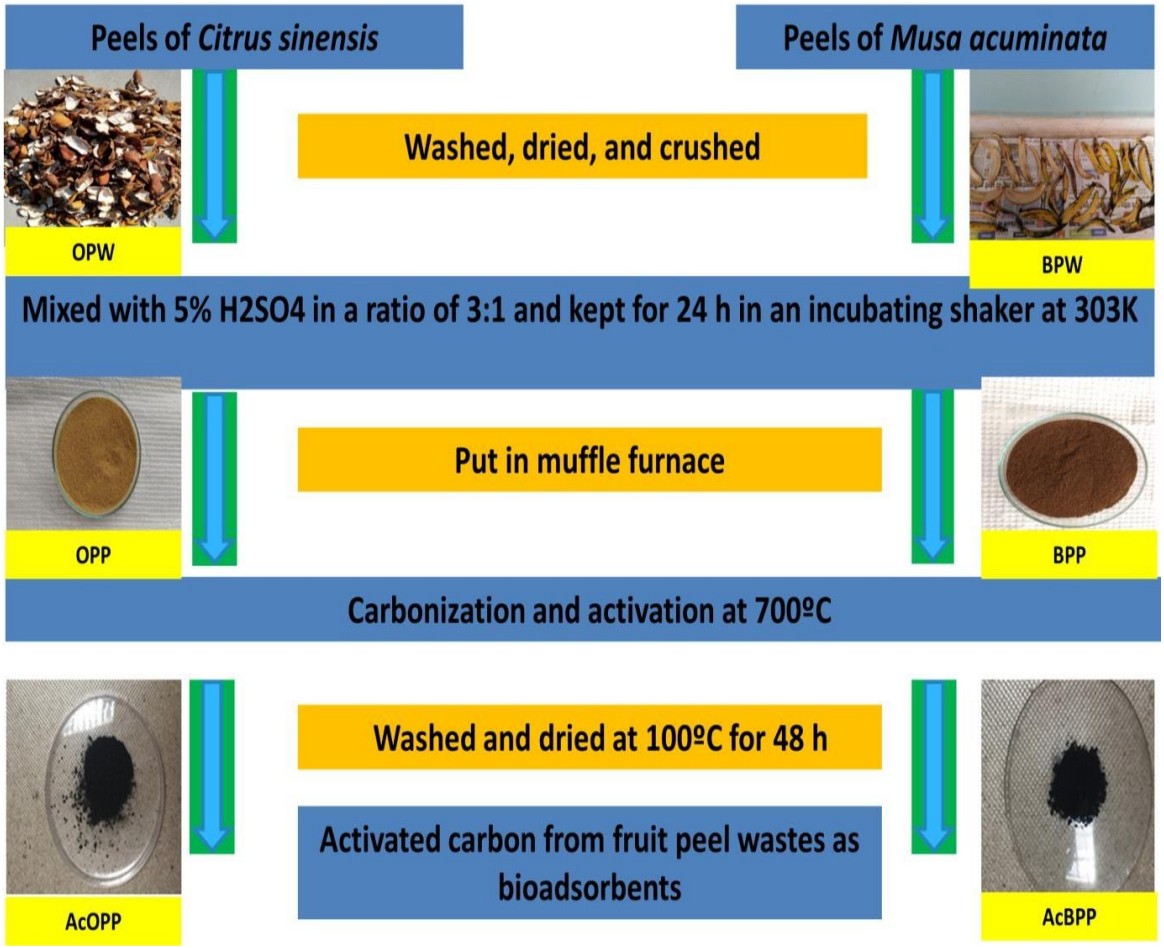

Figure 3.1 Preparation and screening of low cost bio-adsorbents from different organic fruit peel waste materials

(Here, OPW=orange peel waste; OPP= orange peel powder; AcOPP=activated carbon of acidified orange peel powder; BPW= banana peel waste; BPP= banana peel powder, AcBPP= activated carbon of acidified banana peel powder)

3.1.3 Rice husks (RH)

The rice husks (RH) were collected from local area in Lucknow region, Uttar Pradesh, India. The raw RH powder (RHP) was prepared in the same way as described in section 3.1.1(**Fig. 3.2**).

It is to be noted here, the rice husk powder (RHP) thus obtained was not processed further based on the results obtained during initial screening (BET analysis).

3.1.4 Eucalyptus saw dust (SD)

The Eucalyptus saw dust (SD) was gathered from the local timber industry in Sitapur, Uttar Pradesh and was processed according to the method explained in section 3.1.1 to obtain raw saw dust powder (SDP).

It is to be noted here, the saw dust powder (SDP) (**Fig. 3.2**) thus obtained was also not processed further based on the results obtained during initial screening (BET analysis).

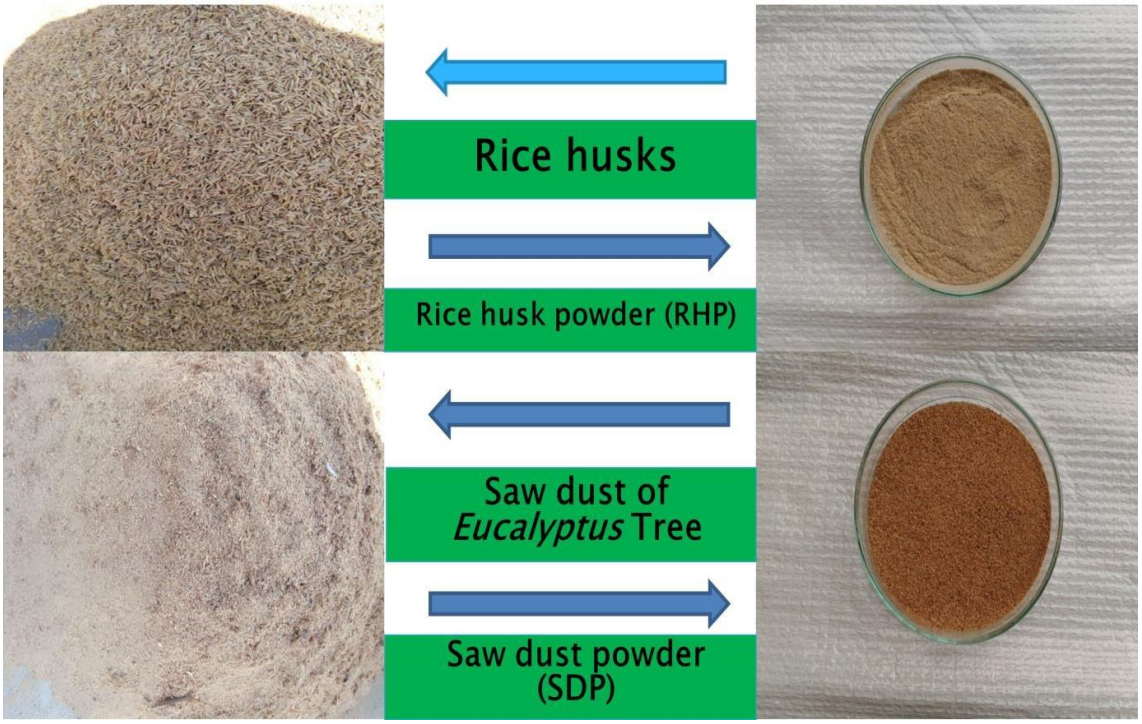

Figure 3.2 Preparation and screening of low cost bio-adsorbents from different organic waste materials

3.1.5 Biosurfactant modified activated banana peel powder (BSBP)

The Activated banana peel powder (AcBPP) obtained in section 3.1.2 was put under fabrication using 2% surfactin biosurfactant to get biosurfactant modified activated banana peel powder (BSBP). For this, 2% of surfactin (w/v) solution was agitated with the significant amount of activated banana peel powder in an incubating shaker for 24 h at 303 K. The surfactin utilised here was initially extracted from the *Bacillus haynesii* strain E1 (process explained in section 3.3.6.3). The mixed product was washed with distilled water to remove unadhered surfactin molecules from the activated banana peel powder. Later on, it was completely dried in an oven at 80 ºC for 48 h and sieved (100 mesh) to get uniform particle size of biosurfactant modified activated banana peel powder (BSBP) as shown in **Fig. 3.3**.

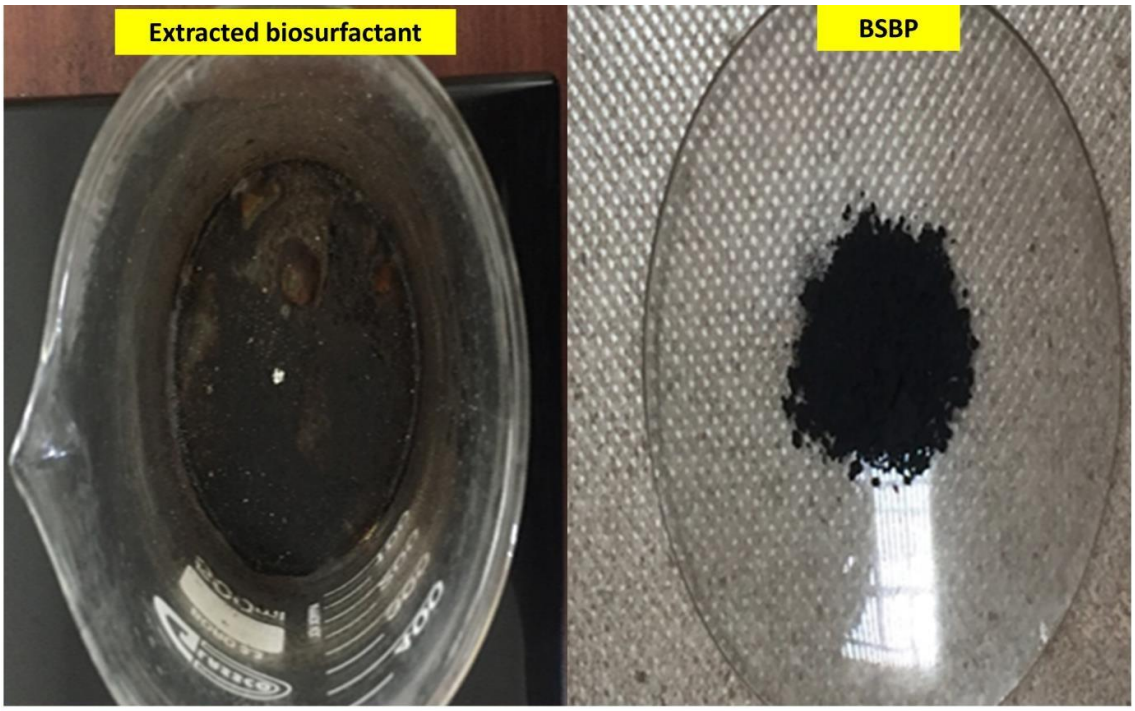

Figure 3.3 Preparation of biosurfactant modified activated banana peel powder (BSBP)

3.2 Stock solution of metals

Stock solutions of metals intended for the experimental work were prepared as given in subsequent sections:

3.2.1 Lead (II) solution

Stock solution of Pb^{2+} was prepared by dissolving 1.598 g of $Pb(NO_3)_2$ (lead nitrate) in 100 mL of distilled water to achieve a concentration of 10,000 ppm. The required standard solutions of Pb^{2+} (as mentioned in section 3.4.2.4) were further prepared by diluting the significant volume of Pb^{2+} stock solution using the **Eq. 3.1**:

$$C1V1 = C2V2 \quad \text{(3.1)}$$

Here, C1 is concentration of stock solution in ppm; V1 is volume of stock solution; C2 is concentration of standard solution in ppm; V2 is volume of standard solution.

3.2.2 Cadmium (II) solution

Stock solution of Cd^{2+} was prepared by dissolving 1.95 g of $CdCl_2.2H_2O$ (cadmium chloride dihydrate) in 100 mL of distilled water to achieve a concentration of 10,000 ppm. The required standard solutions of Cd^{2+} (as mentioned in section 3.3.2.4) were further prepared by diluting the significant volume of Cd^{2+} stock solution using the **Eq. 3.1.**

3.3 Experimental procedures

3.3.1 Characterization of bio-adsorbents

Characterization of selected bio-adsorbents *viz.* orange peel powder (OPP), banana peel powder (BPP), rice husk powder (RHP), saw dust powder (SDP), activated orange peel powder (AcOPP), activated banana peel powder (AcBPP), and biosurfactant modified activated banana peel powder (BSBP) for different properties was carried out as given in subsequent sections below:

3.3.1.1 Brunauer Emmet Teller (BET) analysis

Brunauer Emmet Teller (BET) technique was made in 1938 while working on ammonia catalysts by its inventors S. Brunauer, P.H. Emmet and E. Teller. This technique is devised to measure the specific surface area of finely divided porous materials from adsorbents, pharmaceuticals, filters, catalysts, etc (Brame & Griggs, 2016b) . The working principle of BET analysis involves initially degassing of the material i.e., removal of foreign materials from the surface and adsorption of nitrogen gas on the surface of a particular material at a given pressure for computation of

surface area (Datar et al., 2020). While using BET, controlled dynamics of an inert gas like nitrogen or argon is released and is allowed to be adsorbed and desorbed by observing pressure changes due to the adsorption and desorption (Brame & Griggs, 2016a). By determination of area covered by one adsorbate molecule such as 16.2 $Å^2$ for nitrogen, the total surface area of the material is computed. The initial screening of prepared bio adsorbents (Orange peel powder, Banana peel powder, Rice husk powder and Saw dust powder) were done by determining their specific surface area using BET analyser (BELSORP-max, Japan; **Fig. 3.4**). The materials having low specific surface area were not analysed further and not selected for the study.

Figure 3.4 Brunauer Emmet Teller surface area analyser, Department of Chemistry, Babasaheb Bhimrao Ambedkar University, Lucknow, UP, India

3.3.1.2 Scanning electron microscope-Energy dispersive X-ray (SEM-EDX) analysis

The scanning electron microscope (SEM) utilises a focussed beam of electrons that interacts with the atoms of the sample generating signals and giving rise to the surface topography of the sample, its electrical conductivity, etc (Crockett, 2012). The

imaging of the sample is based on the detection of secondary electrons emitted out of the sample while the elemental mapping of the sample's surface is done through an energy dispersive X-ray spectrometer which is generally attached to the SEM (JEOL JSM6490LV; **Fig. 3.5**). SEM-EDX profile of selected bio-adsorbents: activated orange peel powder (AcOPP), activated banana peel powder (AcBPP), and biosurfactant modified activated banana peel powder (BSBP) was determined for the bioadsorption process.

Figure 3.5 Scanning electron microscope, University Sophisticated Instrumentation Centre, Babasaheb Bhimrao Ambedkar University, Lucknow, UP, India

3.3.1.3 Fourier transform infra-red (FTIR) analysis

Fourier transform infra-red (FTIR) analysis is done to elucidate the structure and determination of organic and inorganic compounds mainly the functional groups present in a given sample. An infrared radiation is passed through a given sample that absorbs and transmits it resulting in a spectrum of absorption and transmission that represents the fingerprint of the sample (Al-Alawi et al., 2004). FTIR spectra of activated orange peel powder (AcOPP), activated banana peel powder (AcBPP), and

biosurfactant modified activated banana peel powder (BSBP) were identified on Nicole™ 6700 FTIR spectrometer as shown in **Fig. 3.6**.

Figure 3.6 Fourier Transform Infra-Red Spectrometer, University Sophisticated Instrumentation Centre, Babasaheb Bhimrao Ambedkar University, Lucknow, UP, India

3.3.1.4 X-ray diffraction (XRD) analysis

The X-ray diffraction analysis is based on the scattering of X-rays from a given sample that has long-range order to determine the nature of material i.e. amorphous or crystalline. A crystalline lattice structure would generate a pattern of peaks of reflections at different angles having different intensities (Sjöström et al., 2019) while amorphous structures will lack sharp peaks. XRD pattern of the prepared activated orange peel powder (AcOPP), activated banana peel powder (AcBPP), and biosurfactant modified activated banana peel powder (BSBP) were identified using D8 Advance Bruker powder diffractometer (**Fig. 3.7**) with a scan rate of 0.02º/s (degree per second).

Figure 3.7 X-ray diffraction instrument, University Sophisticated Instrumentation Centre, Babasaheb Bhimrao Ambedkar University, Lucknow, UP, India

3.3.1.5 Zero point charge (pH_{ZPC}) analysis of bio-adsorbents

The point of zero charge is generally a pH value at which any material's surface has a net charge zero and is determined to know at which pH, material will have a net positive or negative charge. This is determined by solid addition method. 40 mL of 0.1 mol/L KCl (potassium chloride) and 0.002 mol/L citrimide solution was taken in a 100 mL stoppered conical flask (Kutuzova & Dontsova, 2017). The pH of the flasks containing required amount of the bio-adsorbents (0.1 g) were initially adjusted using 0.1N HCl or 0.1N NaOH. The total volume of the solution in each flask was adjusted to 50 mL by adding equal amounts of KCl and citrimide solution. The flasks were kept for 30 min in an incubating shaker at 150 rpm. At the end of 30 min, final pH of the flasks was measured and the flask giving zero value of pH was selected as pH_{ZPC} of selected activated orange peel powder (AcOPP), activated banana peel powder (AcBPP), and biosurfactant modified activated banana peel powder (BSBP) by plotting initial pH against difference in pH (ΔpH).

3.3.2 Experimental conditions to assess adsorption of selected heavy metals by batch process

The batch process was employed to determine the optimum experimental conditions for bioadsorption of Pb^{2+} and Cd^{2+} ions onto activated orange peel powder (AcOPP), activated banana peel powder (AcBPP). A single metal solution study (i.e. one metal at a time, lead and cadmium) was conducted using different parameters as given below to assess the effect of metal and bio-adsorbent itself on the overall bioadsorption process.

3.3.2.1 Effect of pH

A 10 ppm Pb^{2+} and Cd^{2+} standard solutions were prepared in distilled water from the stock solutions using **Eq. 3.1** and 50 mL of this solution was added separately into 06 Erlenmeyer flasks for lead and 06 for cadmium. The initial pH of the samples was adjusted from 2 to 12 with an increment of 2 using 0.1N HCl or 0.1N NaOH solution. To these flasks, 0.1 g of bio-adsorbent (AcOPP and AcBPP) were added separately and allowed to agitate in an incubating shaker for 60 min having 120 rpm. At the end of the contact time, samples were filtered using Whatman^{TM} filter no. 42 (Ashless/125 mm, 100 circles, GE Healthcare, Buckinghamshire, UK) and residual heavy metal (HM) concentrations were determined using Inductively coupled plasma-mass spectroscopy (ICP-MS).

3.3.2.2 Effect of bio-adsorbent dose

The optimum bio-adsorbent dose was determined by taking 50 mL of 10 ppm of Pb^{2+} and Cd^{2+} samples at pH 4-4.5 in 6 Erlenmeyer flasks having AcOPP/AcBPP dose ranging from 0.1 to 2.1 g per 50 mL solution with an increment of 0.4 g. The flasks were put in shaker at 120 rpm for 60 min and were filtered using Whatman^{TM} filter no. 42 (Ashless/125 mm, 100 circles, GE Healthcare, Buckinghamshire, UK) for determination of residual metal ion concentrations using ICP-MS.

3.3.2.3 Effect of contact time

The effect of contact time from 30 min to 180 min with an increment of 30 min was analysed using 10 ppm of Pb^{2+} and Cd^{2+} metal ion solutions at pH 4-4.5 having 0.5 g of bio-adsorbent dose. All the experimental procedures were same except the flasks

were removed at specified time interval from the shaker and analysed for residual metal ion concentrations using ICP-MS.

3.3.2.4 Effect of initial metal ion concentration

The effect of initial Pb^{2+} and Cd^{2+} concentration was assessed in the range 0 to 200 ppm with an increment of 50 ppm in 5 Erlenmeyer flasks having 50 mL of these solutions separately. Since 10 ppm of metal has been used in above three properties as a standard, so 10 ppm was also kept in this part (0, 10, 50, 100, 150, 200 ppm) The optimized conditions obtained from the previous batch experiments were utilised i.e., 4-4.5 pH with bio-adsorbent dose of 0.5 g and agitated for 60 min, filtered and analysed for residual metal ions concentration in the same manner.

3.3.3 Desorption experiments

Desorption of bioadsorbed Pb^{2+} and Cd^{2+} ions from exhausted bio-adsorbents (AcOPP and AcBPP) were studied using 3 types of solvent i.e., 0.1N HNO_3, 0.1N HCl, and 0.1N NaOH. For this, 0.5 g of pre-adsorbed bio-adsorbents (taken after optimization) were put in above mentioned 50 mL of solvents separately and shaken for 60 min at 120 rpm. After mixing, the samples were filtered, and analysed for residual metal ions concentrations by ICP-MS. For regeneration purposes, the eluted bio-adsorbent was washed with distilled water to eliminate any desorbing solution to be used for the next adsorption cycle. The desorption percentage (D %) was measured using **Eq 3.2**.

$$D\% = \frac{C_{desorp}}{C0} \times 100\% \quad \text{..... (3.2)}$$

Here, C_{desorp} is metal ions concentration after desorption in ppm, and C_0 is the initial concentration of metal in ppm.

3.3.4 Adsorption equilibrium studies

For adsorption equilibrium studies, the bio-adsorbent dose from 0.1 to 2.1 g with an increment of 0.4 per 50 mL of 100 ppm of Pb^{2+} and Cd^{2+} solutions (pH 4-4.5) were shaken for 60 min. Respective flasks were filtered after equilibrium is achieved and analysed by ICP-MS. Adsorption capacities (q_e) were calculated as follows;

$$q_e = \frac{(C_0 - C_e)V}{m} \text{.....} \quad \textbf{(3.3)}$$

Here, qe is adsorption capacity in mg/g; C_0 and C_e are initial and final equilibrium metal ion concentrations in ppm; V is volume used in litres, and m is bio-adsorbent dose (g).

3.3.5 Adsorption kinetics

For kinetic studies, the contact time ranging from 30 to 120 min with an increment of 30 min was selected. The bio-adsorbent dose of 0.5 g, pH 4.5 at initial metal concentrations of 50 and 100 ppm for both Pb^{2+} and Cd^{2+} in 50 mL of solution was selected and shaken for 120 min at 120 rpm for kinetic adsorptions, filtered, and later analysed by ICP-MS. The adsorption capacity was calculated according to the **Eq. 3.3** mentioned in section 3.3.4.

3.3.6 Isolation and characterization of biosurfactant producing metal resistant bacterial strains

3.3.6.1 Sampling, enrichment and isolation of biosurfactant producing bacterial strains

Hydrocarbon (Petrol) contaminated soil samples were collected aseptically from different petrol pump sites in Lucknow, Uttar Pradesh **(Table 1)**. The collected soil samples (1 g of each) were first enriched using 100 mL mineral salt medium (MSM) broth with slight modifications having composition(g/l) $NaNO_3$, 2; K_2HPO_4, 1.0; KH_2PO_4, 0.5; $MgSO_4.7H_2O$, 0.5; KCl, 0.1 and $FeSO_4.7H_2O$, 0.01 amended with 1% (v/v) petrol as sole carbon source in a 500 mL Erlenmeyer flask (Sim et al., 1997). The flasks were kept for incubation at 37°C for 7 days at 150 rpm in an incubating shaker. These flasks were checked periodically for growth of culture and foam formation. After a week, 1 mL of the culture inoculum was taken out and transferred into fresh MSM broth with same composition. This enrichment cycle was repeated four times in total and at the end of last enrichment cycle, 100 µl of culture from each flask was poured on nutrient agar (NA) plates from dilutions 10^{-3} to 10^{-6} and spreading was done. The plates were then incubated at 37°C for 24 h for the appearance of single biosurfactant producing colony. The single distinct colonies were picked up carefully and streaked on fresh NA plates to get pure strains. The pure cultures thus obtained were sub cultured periodically and stored at 4°C till further use (Onwosi & Odibo, 2012).

Table 3.1 Details of sampling sites

Sample site	Location	Number of samples
Lucknow, Uttar Pradesh, India	26.8467° N latitude, 80.9462° E longitude	12

3.3.6.2 Selection of potent biosurfactant producing bacteria

The ability of strains to produce biosurfactant was assessed by performing various screening tests. For this, the inoculum was prepared by transferring a loopful of isolated pure bacterial cultures into 25 mL nutrient broth (NB) in a 100 mL Erlenmeyer flask. The NB flasks were incubated at 37°C for 24 h 100 µl of the inoculum was then transferred into separate 100 mL MSM broth having same composition except petrol. Dextrose (15 g/L) was used as the carbon source and inoculated flasks were kept under incubation for 72 h at 37°C with shaking speed 150 rpm. A control flask containing only MSM broth was also kept under same incubation conditions.

3.3.6.2.1 Screening tests

Foaming

The strains showing heavy foam formation in the MSM medium as compared to the control flask were selected and subjected to centrifugation along with the control flask. The centrifugation conditions selected for the separation of bacterial pellets from supernatant were 10,000 rpm for 10 min at 4 °C and this condition is maintained throughout for the collection of supernatant whenever centrifugation was performed wherever explained ahead in the thesis. The collected supernatant containing biosurfactant (crude biosurfactant) was used for the selection of potential biosurfactant producing strain based on biosurfactant properties as assessed further and as given below:

3.3.6.2.1.1 Primary screening

Oil displacement assay: Oil displacement assay (ODA) was performed by the method described by Morikawa, (Morikawa et al., 1993). Approximately 30 ml distilled water was taken in a petri plate and 10 µl of lubricating oil was poured to the

surface of the water to form a thin layer. Afterwards, 10 µl of culture supernatant (crude biosurfactant) was gently added to the centre of the oil film. A clear zone is obtained on displacing the oil layer if biosurfactant is present and is indicative of a positive result.

Drop collapse test: A 96 well microtiter plate and a clean glass slide was taken and 10 µl of lubricating oil was poured into/onto it and was left for setting up to 24 hours (Youssef et al., 2004). To this, a drop of the culture supernatant was placed into the wells and over the oil drop on slide. If it contains biosurfactant, the drop collapses, otherwise remains stable. The presence of significant concentration of biosurfactant in the culture supernatant reduces the surface and interfacial tension between the liquid drop and the hydrophobic surface leading to the destabilization (collapse) of the liquid droplets.

Penetration assay (PA): This is a high throughput screening assay that is based on contact of two insoluble phases leading to colour change as developed by Maczek (Walter et al., 2010), 1 ml of a hydrophobic paste of petrol and silica gel was taken in a 2 ml of centrifuge tube then was covered with 10 µl of petrol. To this, 100 µl of red coloured culture supernatant (10 µl of red safranin stain + 90 µl of the supernatant) was placed. If biosurfactant is present, the hydrophobic petrol phase barrier will be broken by hydrophilic liquid due to the reduction in surface and interfacial tension. This assay describes that silica gel being a dessicant (moisture sensitive) will enter into hydrophilic phase much more quickly from hydrophobic phase if solution has biosurfactant and upper red coloured phase will turn into cloudy white within 10 minutes. Negative results show cloudy upper phase but stays red.

3.3.6.2.1.2 Secondary screening

Emulsification index (E_{24}%): The ability of a culture supernatant to emulsify different hydrocarbon sources was evaluated. 2 ml of culture supernatant was added to 2 ml of hydrocarbons in different test tubes and vortexed for 2 min and then placed for 24 h in dark (Nishanthi et al., 2010).

The emulsification index was determined by the formula:

$$E_{24}\% = \frac{\text{Height of emulsified layer (cm)}}{\text{Total height of liquid column (cm)}} * 100 \quad \text{..... (3.4)}$$

Foaming assay (FA %): According to Abouseoud and his team (Abouseoud et al., 2008), foaming activity was determined by growing the cultures for 96 h at 37°C in 50 ml nutrient broth (NB) in shaking incubator. Foam formation was checked by shaking the flasks gently and then foaming index was measured by adding 10 ml of culture into a graduated cylinder, shaken vigorously for 2 min and percentage was determined by the formula:

$$FA\% = \frac{\text{Height of foam (cm)}}{\text{Total height of foam column(cm)}} * 10 \quad \text{..... (3.5)}$$

Haemolytic assay (HA): 24 h grown fresh cultures in nutrient agar were spot inoculated on sheep blood agar plates containing 5% sheep blood, then incubated for 3-4 days for the formation of halo zone as a type of β-hemolysis as an indicator for positive test for biosurfactant producing isolate (Elazzazy et al., 2015).

Surface tension (ST) reduction: The surface tension of the culture supernatant was measured by drop count method using stalagmometer (Płaza et al., 2006). A stalagmometer is a capillary glass tube with a bulb having markings ‗A' at top end and ‗B' at the other end of the bulb in the middle section of the stalagmometer. The tested liquid is sucked up to the marking ‗A' and is allowed to fall down up to the marking ‗B' under the influence of gravity. The number of drops is counted from A to B and the process is repeated three times to obtain a mean value. The ST of the liquid is calculated using the formula:

$$ST_{Liquid} = \frac{\rho_2 n_1}{\rho_1 n_2} \times ST_{water} \quad \text{..... (3.6)}$$

Where ρ_1 and ρ_2 are density of water and liquid at a particular temperature in g/ml; n_1 and n_2 are number of mean drops of water and liquid from A to B.

If the culture supernatant contains crude biosurfactant, then the measured value of surface tension will be less than that of distilled water and uninoculated MSM broth (whose value is 72 and 67 dynes/cm respectively) that served as control.

3.3.6.2.1.3 Indirect screening method

Bacterial adhesion to hydrocarbon assay (BATH): Rosenberg and his team developed a photometrical assay measuring the hydrophobicity of bacteria based on adherence of bacterial cells to various liquid hydrocarbons (Rosenberg, 1984). For

this, 4 ml of turbid aqueous suspension of phosphate buffer washed bacterial cells were mixed with 4 ml of n-hexane for 2 minutes, and then the two phases were allowed to separate. Biosurfactant containing bacterial cells becomes bound to n-hexane droplets and rises with the hydrocarbon leaving behind less turbid or clear aqueous suspension whose turbidity is measured at 620 nm which is directly proportional to hydrophobicity of the cells. This hydrophobicity (H) is calculated by given formula:

$$H = \left(1 - \frac{A}{A_0}\right) - 100\% \quad \text{..... (3.7)}$$

Where A_0 is the absorbance of the bacterial suspension without hydrophobic phase added and A is the absorbance after mixing with hydrophobic phase measured using UV-Visible spectrophotometer of Thermo scientific EVOLUTION 201. This test finds its usefulness in determining the hydrophobicity of bacterial cells containing emulsifying agents (biosurfactants) and thus, their adherence to various hydrocarbons for emulsification and bioremediation purposes.

3.3.6.2.2 Morphological characterization and scanning electron microscopy (SEM) of bacterial strains

The selected axenic strains were characterized morphologically by careful examination of their colony morphology (cultural characterization) and Gram staining technique.

Gram staining: This is performed by making a smear of a loop full of bacterial culture on a clean glass slide. The smear was heat fixed and was stained with crystal violet (basic dye) for 1 min. After 1 min, the slide was washed under running tap water, and iodine (mordant dye) was added and kept the slide for another 45 sec. The addition of iodine led to the formation of crystal violet-iodine (CVI) complex. This was followed by washing with 95 % ethanol and counter staining with safranin for 30 sec. Then, slides were observed for shape and arrangement of cells under inverted light microscope having oil immersion lens (Claus, 1992).

Scanning electron microscopy (SEM): For SEM analysis, cultures grown in nutrient broth were used. Firstly, the cultures were fixed in 1 mL glutaraldehyde (5 %) in Eppendorf tubes and kept overnight in the refrigerator at 4 ˚C. After fixation, the tubes

were centrifuged at 5000 rpm for 5 min and the pellets were washed with phosphate buffer saline. The washed pellets were then kept in 1 mL of 30 % acetone for 5 min and again centrifuged. This washing step was repeated with different concentrations of acetone (50, 70, 90, and 100 %) with subsequent centrifugation (Fratesi et al., 2004). Further, the tubes containing 100 % acetone were mounted on carbon coated stubs, dried, and observed under the scanning electron microscope (JEOL JSM6490LV).

3.3.6.2.3 Biochemical characterization

As per Bergey‘s manual, Hi-media IMViC biochemical test kit was used for identification of the selected strains having inoculum optical densities up to a minimum of 0.1 at 620 nm (Sneath et al., 1986). Each kit was made ready by peeling off its seal under aseptic conditions in laminar bench while each well of the kit was amended with 50 µL of separate bacterial inoculum and incubated at 37 ºC for 24 to 48 h.

Observations and result: Reagents given with the kit as per the instructions were added and results were interpreted as shown in the **Table 3.2**.

Table 3.2: Result interpretation chart for Hi-media IMViC kit

Well No.	Test	Reagents to be added after incubation	Principle	Original colour of the well (medium)	Positive reaction	Negative reaction
1.	Indole	1-2 drops of Kovac's red reagent	Checks deamination of tryptophan	Colourless	Reddish pink	Colourless
2.	Methyl red	1-2 drops of methyl red reagent	Detects acid production	Colourless	Red	Yellow
3.	Voges Proskauer's	1-2 drops of Baritt's reagent A and B	Checks acetone production	Colourless	Pinkish red	Colourless/slight brown/copper
4.	Citrate utilization	-	Ability of an organism to utilize citrate	Yellowish green	Blue	Yellowish green
5.	Glucose	-	Glucose utilization	Red	Yellow	Red
6.	Adonitol	-	Adonitol utilization	Red	Yellow	Red
7.	Arabinose	-	Arabinose utilization	Red	Yellow	Red
8.	Lactose	-	Lactose utilization	Red	Yellow	Red
9.	Sorbitol	-	Sorbitol utilization	Red	Yellow	Red
10.	Mannitol	-	Mannitol utilization	Red	Yellow	Red
11.	Rhamnose	-	Rhamnose utilization	Red	Yellow	Red
12.	Sucrose	-	Melibiose utilization	Red	Yellow	Red

3.3.6.2.4 Molecular characterization:

For molecular identification of the selected strains, isolated bacterial DNA was electrophoresed in agarose gel followed by PCR amplification of 16S rDNA using universal primers 27'F (AGAGTTTGATCGTGGCTCAG-20) and 1492R (GGTTACCTTGTTACGACTT-20). After the amplification, obtained PCR products were checked on 1% (w/v) agarose gel, and further subjected to sequencing analysis. The evolutionary ancestry of the strain was interpreted using the Neighbour-Joining method (Sakamoto et al., 2006).

The selected bacterial strains were also submitted to the NCBI (National center for Biotechnology Information) database for allotment of the accession numbers.

3.3.6.3 Biosurfactant production and extraction

Selected strains were grown on MSM broth for mass biosurfactant production. For extraction, 72 h grown bacterial MSM broth were subjected to centrifugation and culture supernatant containing the crude biosurfactant were collected and transferred to empty beakers to be acidified with 1M HCl up to pH 2.0. The acidified beakers were kept at 4ºC, overnight.

Liquid-liquid extraction protocol was applied twice using equal amounts of chloroform: methanol in 2:1 ratio and overnight precipitated supernatant by vigorous shaking in a separating funnel. At the end of the separation, an organic layer was collected in separate beakers and was allowed to evaporate for 24 h at room temperature, followed by drying in an oven at 80 ºC for 6 h. The dried biosurfactant was scratched out from the beaker and stored in a desiccator to remove traces of moisture (Sim et al., 1997).

3.3.6.3.1 Chemical analysis of the extracted biosurfactant

Carbohydrate analysis

a) **Anthrone test:** Thin-layer chromatography (TLC) was performed to detect carbohydrate presence in the extracted BS using a 10 × 10 cm pre-coated Silica gel column (silica gel 60 (63-200 mesh), Merck, Germany). For this, 4-5 mg of the extracted BS was completely dissolved in methanol and 5 µl of it was placed on the silica gel plate. The plate was developed using chloroform:

methanol: water (65:15:4, v/v) solvent system. The spots were then identified by spraying fresh anthrone reagent for the appearance of reddish-brown colour (Heyd et al., 2008).

b) **Iodine test:** 1 mL of the freshly prepared iodine solution was added to the small amount of BS in a test tube and shaken properly for observation of colour change (Ishaq et al., 2015).

Lipid analysis

a) **Saponification test:** 2 mL of the 2% NaOH (sodium hydroxide) solution was added to the extracted biosurfactant and mixed well for the formation of foam/soap (Patowary et al., 2015b).
b) **Glycolipid test:** 1 mL of freshly prepared 5% phenol solution was applied to the small amount of BS. To this, 4 mL of the concentrated sulphuric acid (H_2SO_4) was added dropwise and the colour change was detected (Sidkey et al., 2016). Appearance of yellow to orange colour indicated the presence of glycolipids.
c) **Rhamnolipid test:** Cetyltrimethyl ammonium bromide/methylene blue (CTAB/MB) method was used to detect the presence of rhamnolipids in the selected strains (Soltanighias et al., 2019). CTAB/MB based agar plates were prepared according to the composition (g/L) as CTAB: 0.2; MB: 0.005; peptone: 1.5; $MgSO_4$: 0.5; K_2HPO_4: 1.0; $FeCl_3$: 0.1; KH_2PO_4: 1.0; $CaCl_2$: 0.01; $MnSO_4$: 0.005; Agar: 15 and glucose: 15). To the agar plates, the selected strains were spot inoculated and incubated for 7 days at 35ºC.

Peptide analysis

a) **Ninhydrin test:** 0.35% ninhydrin in acetone (w/v) was used to detect free amino groups/peptides by spraying it on the TLC plate for the development of pinkish-violet coloured spots (Dlamini et al., 2020).

3.3.6.3.2 Critical micelle concentration (CMC) and Biosurfactant stability studies

CMC of the extracted biosurfactant was determined by preparing various concentrations of extracted biosurfactant from 10 to 200 mg/l. These concentrations were obtained by diluting a known amount of crude BS obtained after extraction. The surface tension of different concentrations was measured using the drop count method

(Dilmohamud et al., 2005). The concentration, above which surface tension does not further reduce, was taken as its CMC.

A wide range of factors such as pH, temperature, and salinity was applied to check for the stability of the extracted biosurfactant in terms of emulsification index (E_{24}%) and oil displacement assay (ODA). To analyse the effect of pH (2 to 12), temperature (30 to 121 ºC), and salt concentrations (2 to 20 %), equal amounts of kerosene and used mobil oil was mixed with the solution of extracted biosurfactant and kept overnight to observe for the emulsification results while small amount of prepared solution of extracted biosurfactant was poured on the used mobil oil plate for estimation of oil displacement properties at varied factors such as pH, temperature and salinity ((Khopade et al., 2012).

3.3.6.3.3 Characterization of the extracted biosurfactant

Fourier-Transform infrared (FTIR) spectroscopy: The partially purified 4-5 mg of extracted biosurfactant was subjected to FTIR analysis. The respective spectrum was obtained between 400 to 4000 wavenumbers/cm using KBr (potassium bromide) pellet method (Bezza & Chirwa, 2016). The resultant peaks were processed with inbuilt IR analytical software on Nicole^{TM} 6700 FTIR spectrometer (Thermo Scientific, USA).

Proton nuclear magnetic resonance (^{1}H NMR) spectroscopy: The one-dimensional proton nuclear magnetic resonance (1 D ^{1}H NMR) spectra was obtained by dissolving the extracted biosurfactant in deuterated chloroform ($CDCl_3$) and analysed with Bruker 600 MHz spectrometer NMR machine (Pereira et al., 2013).

Liquid chromatography-mass spectrometry- electron spray ionization (LC-MS-ESI): The LC-MS-ESI analysis was done with 50 mg of the crude biosurfactant, dissolved in 5000 µL acetonitrile/ammonium formate buffer (40:60; v/v). The prepared extract was filtered through a 0.20 µm syringe filter and injected into the mass spectrometer via an ESI source pump (Oluwaseun et al., 2017). The mass/charge (m/z) scan range was obtained between 150-2000 with a 10 µL flow rate of sample in both positive and negative mode using Waters ultra-performance liquid chromatography- triple quadrupole photodiode (UPLC-TQD) Mass spectrometer.

3.3.6.3.4 Optimization of Biosurfactant production using biowaste

A statistical approach was used to optimise process parameters for maximum biosurfactant production (Mnif et al., 2012). The central composite design (CCD) was employed using design expert software (Stat-Ease Inc., Minneapolis, MN, US, version 8.0.0) with four variables i.e., biowaste concentration (A), temperature (B), pH (C), and agitation rate (D) giving a maximum of 30 runs where each variable was observed at five levels coded as –ά, -1, 0, +1, + ά.

The CCD methodology evaluates the effect of above mentioned four variables on the measured response that is surface tension reduction and the mathematical quadratic polynomial **Eq. 3.8** as in case of strain E1 and **Eq. 3.9** as in the case of strain F5 obtained was as follows:

$$Y1 = 34.93 - 2.39\,A + 1.85\,B - 1.58\,C - 1.72\,D + 1.13\,AB + 0.8888\,AC - 1.80\,AD + 2.11\,BC - 1.61\,BD - 0.4025\,CD + 1.44\,A^2 + 8.53\,B^2 + 6.92\,C^2 + 6.95\,D^2 \quad \text{..... (3.8)}$$

$$Y2 = 5.77 - 0.22\,A + 0.060\,B - 0.069\,C + 6.244E - 003\,D + 0.045\,AB + 0.12\,AC - 0.082\,AD + 0.14\,BC - 0.026\,BD - 0.071\,CD + 0.17\,A^2 + 0.69\,B^2 + 0.58\,C^2 + 0.48\,D^2 \quad \text{..... (3.9)}$$

Where _Y1‘ and _Y2‘ are the predicted response (surface tension reduction in dyne/cm); A, B, C, and D are the coded factors for biowaste concentration (%), temperature (˚C), pH, and agitation rate (rpm) respectively, followed by verification of experimental design using analysis of variance where the significance of the model was verified by t-test (calculated p-value) and goodness of fit was checked by multiple correlations and determination of regression coefficients (R^2). For statistical validation, the probability value of < 0.05 was set.

The optimization study was conducted in a batch mode using 50 ml of MSM broth in 100 ml Erlenmeyer flasks. The biowaste selected was raw orange peel powder to be utilised as a sole carbon substrate for biosurfactant production. The extract of raw orange peels was prepared (10%; w/v) and it was further diluted to make required levels of 2%, 4%, 6%, 8%, and 10%; v/v for strain E1 and 3 to 7%; v/v for strain F5 to be used in the optimization study. The pH of the medium was maintained using 0.1N HCl and 0.1 M NaOH. Each flask was amended with 100 µL of bacterial inoculum and incubated at respective temperatures with varying agitation rate.

3.3.6.3.5 Biosorption experiments

3.3.6.3.5.1 Growth of isolate on different concentrations of lead

The metal tolerance efficacy of strain E1 and F5 was examined initially to perform the biosorption experiments using separate nutrient agar (NA) media amended with varying concentrations of Pb^{2+} (100, 400, 800, 1200, 1600, 2000 and 2200 mg/L) before solidification. The qualitative minimum inhibitory concentration (MIC) was estimated through ocular surcease of bacterium‘s growth on metal+NA plates.

3.3.6.3.5.2 Simultaneous biosurfactant production and biosorption experiment

A batch study involving synchronic biosurfactant production and metal biosorption was executed. Five 100 mL Erlenmeyer flasks containing 50 mL MSM broth and different concentrations of Pb^{2+} (100, 200, 300, 400, and 500 mg/L) were mixed with 100 µL of culture inoculum (E1 and F5 separately)and incubated at 35 ˚C for 5 days at 150 rpm in an incubating shaker. The growth pattern of the bacterium under different concentrations of Pb^{2+} is ascertained by measuring its optical density at 620 nm while the maximum biosurfactant production under Pb^{2+} stress was estimated in terms of the emulsification index (E_{24}%) measured at 24 h interval up to 5 days. For this, 1 mL of culture supernatant was mixed with an equal amount of mobil oil in a test tube where an increment in E_{24}% value represented enhanced biosurfactant production.

A separate series of experiments was conducted to obtain the optimum parameters for the biosorption study using different experimental conditions such as initial Pb^{2+} concentration, and contact time of 30 to 330 min (with an increment of 30) were studied at pH 7.0 and biomass dosage of 0.05 g. The quantification of residual metal concentration in the supernatant (SN) was done by using ICP-MS after centrifuging the culture broth and flasks at 10000 rpm for 10 min at 4 ˚C. The amount of Pb^{2+} adsorbed on the biomass (qe) was calculated by **Eq. 3.3** as explained in section 3.3.4.

The biosorption capacity of bacterial biomass and its interaction with the Pb^{2+} ions were studied through adsorption isotherm models (Langmuir, Freundlich, and Temkin models explained in chapter 2, section 7)

3.3.7 Lab-scale column experiments

Bio-adsorbents that performed best in batch process were further subjected to column experiments. Only activated banana peel powder (AcBPP) was found to be the best as compared to activated orange peel powder (AcOPP) and continued for column studies after mixing with biosurfactant, giving rise to BSBP i.e. biosurfactant modified activated banana peel powder.

3.3.7.1 Physico-chemical characterization of the wastewater

An electroplating industrial wastewater containing a mixture of other heavy metal ions as well as lead and cadmium was assessed for selective bioadsorption of Pb^{2+} and Cd^{2+} ions. The wastewater was collected three times over a year at an interval of 3 months to examine for changes in the properties for its parameters. Different parameters such as pH, electrical conductivity, temperature, sulphates, phosphates, heavy metal ion concentration were analysed each time, it was collected and its mean ± standard deviation value was represented before the bioadsorption treatment process. The various physico-chemical parameters were also measured after the treatment using APHA protocol (Sankpal & Naikwade, 2012) .

3.3.7.2 Experimental conditions

Fixed bed column experiments were conducted using borosil glass columns of 1.8 cm internal diameter and 50 cm length. The column was packed with the biosurfactant modified activated carbon of banana peel powder (BSBP) where bottom end was packed first with the cotton wool to prevent possible floating of the bio-adsorbent from the outlet. The schematic representation of the column is shown in **Fig. 3.8.** The column bioadsorption study was designed to assess the parameters such as the flow rate (Q in mL/min), the bed height (Z in cm), and the initial or inlet metal ions concentration in case of standard solutions (C_0 in ppm).

An individual study of Pb^{2+} and Cd^{2+} containing standard solution of two concentrations i.e., 50 and 100 ppm was allowed to pass through the fixed bed column separately in the down-flow mode at different volumetric flow rates of 15 and 20 mL/min with bed heights of 2 and 4 cm. For studies with different bed heights, the inlet concentration of metals was selected 50 ppm at 20 mL/min flow rate while for different inlet metal concentrations; the bed height was kept 4 cm at 20 mL/min flow

rate. At different volumetric flow rates, the bed height was 4 cm with 50 ppm of inlet Pb^{2+} and Cd^{2+} concentrations. The metal uptake capacity ($q_{e(exp)}$) which was found higher at selected flow rate and bed height was taken as an optimized value and employed for the selective bioadsorption of Pb^{2+} and Cd^{2+} of particular concentration (present originally in the wastewater) from an electroplating wastewater containing a mixture of heavy metals.

The samples were withdrawn from the fixed bed column at every 15 min until saturation was reached and analysed for residual metal concentrations using ICP-MS and the data was analysed accordingly.

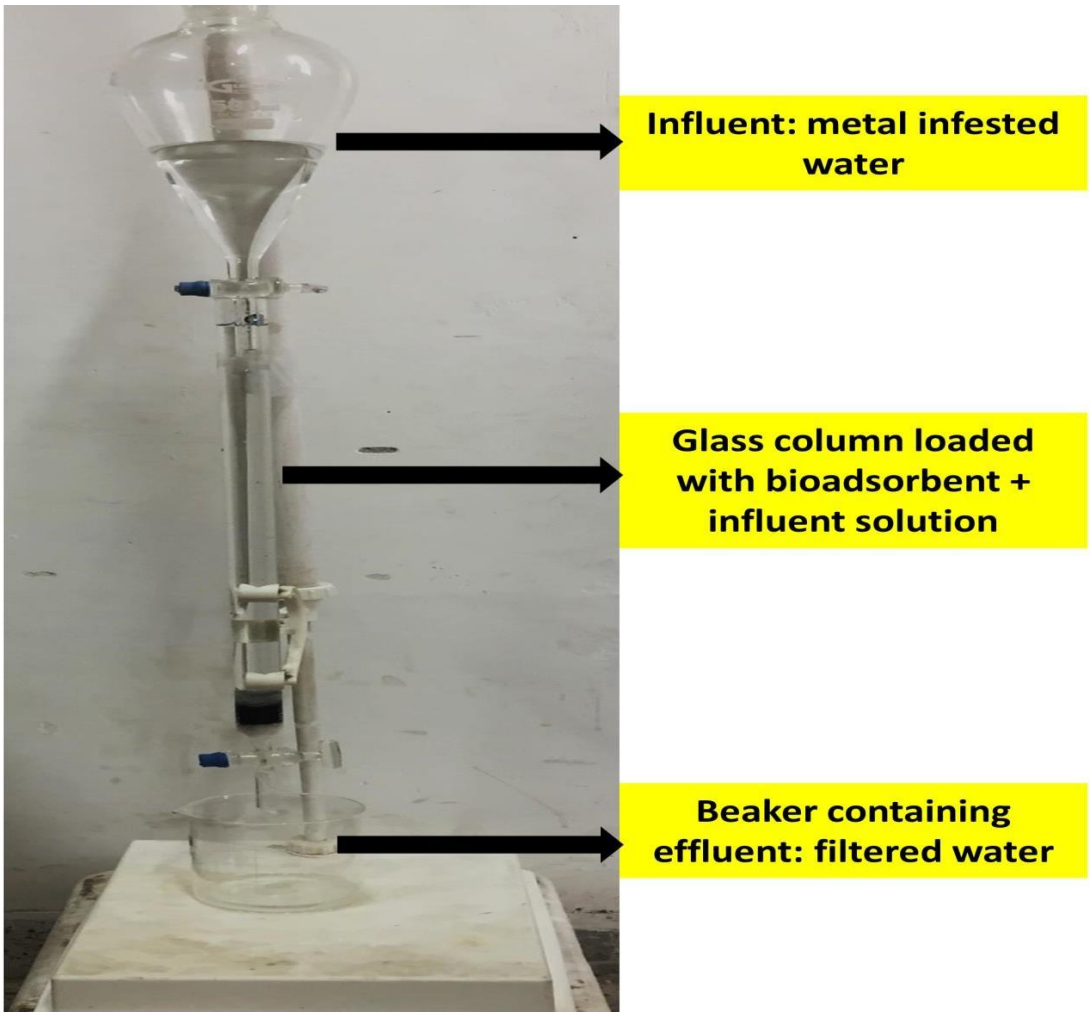

Figure 3.8 Set up of bioadsorption column with BSBP

3.3.7.3 Inductively coupled plasma-mass spectroscopy (ICP-MS) analysis for heavy metal concentration during bioadsorption experiment

The quantitative analysis of HM‘s during bioadsorption experiments were done by ICP-MS. It detects the concentration of elements in a very low range i.e. in parts per billion (ppb) or even parts per trillion (ppt). It involves a plasma source to ionize the elements and then they are separated or analysed on the basis of their masses. Owing to low detection limits with multi-element character, linear range, isotopic composition detection of elements, it is widely accepted instrument for elemental analysis (Vanhaecke & Degryse, 2012). The disadvantages include spectral interferences and high cost of instrumentation. Material should be properly digested with 1% nitric acid and acidified to keep metals in solution (Thomas, 2008).

After end of each bioadsorption experiment, all the samples were tested for residual metal concentration using ICP-MS.

Chapter 4

Screening and Characterization of Low Cost Bio-Adsorbents from Different Organic Waste Material for Heavy Metal Bioadsorption

4.0 Background

In the past few years, agro/fruit waste based bio-adsorbents have been effectively utilized for removal and recovery of heavy metals (HMs) from water and wastewater due to being economical, easy to process, abundant in nature and/or are easily found as by-products or wastes from the agro-industries (Khan et al., 2004). Keeping this background in mind, the activated orange and banana peel powder have been employed in the present study as bio-adsorbents for elimination of Pb^{2+} and Cd^{2+} ions from the aqueous solutions. Such ligno-cellulosic rich fruit peel wastes are readily available, and are regarded as environmental friendly biowastes (Nasim et al., 2004).

The different bio-adsorbents i.e., orange peel powder, banana peel powder, rice husk powder, and *Eucalyptus* saw dust powder (OPP, BPP, RHP, and SDP respectively) prepared in raw form were initially screened for determination of their specific surface area through BET (Brunauer-Emmett-Teller) characterization. Computation of surface area of any bio-adsorbent is essential, as surface acts as the medium for bioadsorption reaction/process and it is composed of varied functional groups that facilitate ion-exchange/ complexation reactions with the heavy metal ions selected in the study (Ibrahim, 2021). Therefore, surface area confers an important role to the bioadsorbing material in the bioadsorption process. The screening of bio-adsorbent to be selected for experimental bioadsorption process and further fabrication was based on this parameter of surface area and the bio-adsorbents having low surface area were not selected for further processing.

The applicability and efficiency of the prepared bio-adsorbents i.e., activated orange peel powder (AcOPP) and activated banana peel powder (AcBPP) in the removal of Pb^{2+} and Cd^{2+} ions was analysed and characterized them after bioadsorption of heavy metal ions and also involves the estimation of maximum bioadsorption capacities of both the bio-adsorbents. The effect of various parameters affecting bioadsorption process has been examined along with their equilibrium and kinetics model studies. Desorption and regeneration aspect of the bio-adsorbents was also evaluated.

4.1 Results and discussion

As mentioned above, orange peel powder, banana peel powder, rice husk powder, and *Eucalyptus* saw dust powder (OPP, BPP, RHP, and SDP respectively) prepared in raw

form were initially screened for determination of their specific surface area through BET characterization and findings are summarized in section 4.1.1 below.

4.1.1 Specific surface area

The surface properties of all four raw bio-adsorbents are tabulated in **Table 4.1**. Orange peel powder (OPP) and Banana peel powder (BPP) were found to have maximum surface area in comparison to the other two bio-adsorbents. Rice husk powder (RHP) was computed to have a surface area 2.4419 m^2/g only and it is the lowest value measured among all the bio-adsorbents. The mean pore diameter of OPP and BPP were found to be 16.416 and 12.432 nm respectively, suggesting these bio-adsorbents are mesoporous based on IUPAC classification (Sotomayor et al., 2018; Zdravkov et al., 2007). The high value of various parameters of OPP and BPP suggested the presence of numerous binding or active sites on their surfaces (Pathak et al., 2015; Stathi et al., 2007).

Table 4.1 Surface parameters of different bio-adsorbents from BET analysis

Parameters of raw bio-adsorbents	**Bio-adsorbents**			
	OPP	**BPP**	**RHP**	**SDP**
BET surface area (m^2/g)	2.1275E+01	1.6576E+01	2.4419E+00	1.0220E+01
Total pore volume (cm^3/g)	8.7309E-02	5.1520E-02	2.0283E-02	7.6847E-02
Mean pore diameter (nm)	16.416	12.432	33.224	30.076

The characterization of a bio-adsorbent before its usage would help in the selection of a suitable bioadsorbent material for removal of heavy metal ions from aqueous solutions and wastewater. **Being low in surface area value and other parameters, rice husk powder (RHP) and saw dust powder (SDP) were not selected for acidification, and carbonization methods.** Orange peel powder (OPP) and banana peel powder (BPP) were subjected to acidification using 5% H_2SO_4 followed by carbonization and activation at 700 ºC for 6 h using muffle furnace (**Fig. 4.1**).

The activated bio-adsorbents (AcOPP, AcBPP, and BSBP; preparation explained in chapter 3, section 3.1.1, 3.1.2 and 3.1.5) were then characterized further to elucidate their surface properties.

Figure 4.1 Muffle furnace for carbonization of bioadsorbents, Department of Chemistry, Babasaheb Bhimrao Ambedkar University, Lucknow, UP, India

Different bio-adsorbent materials *viz.* activated orange peel powder (AcOPP), activated banana peel powder (AcBPP) and biosurfactant modified activated banana peel powder (BSBP) were examined and characterized for different properties further through SEM-EDX, FTIR, and XRD techniques as their principles being explained in chapter 3, section 3.3.1 Findings of the study are discussed below in subsequent sections:

4.1.2 Surface structure and elemental mapping

The surface topography of activated orange peel powder (AcOPP), activated banana peel powder (AcBPP) and biosurfactant modified activated banana peel powder (BSBP) was assessed by scanning electron microscope (SEM) as the procedure explained in Chapter 3, section 3.3.1.2. The micrographs are represented in **Fig.**

4.2(a,b), Fig. 4.3(a,b), and Fig. 4.4(a,b) depicting some significant attributes of their structure.

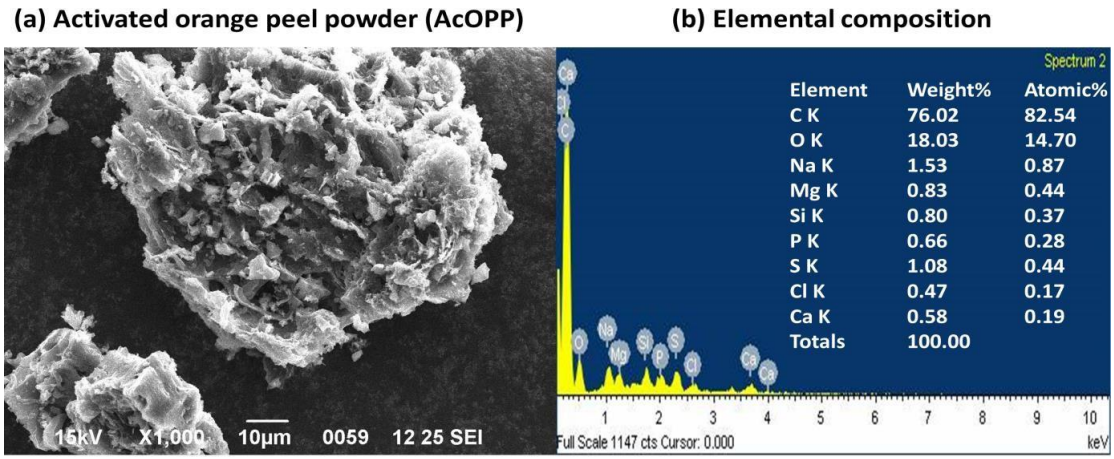

Fig. 4.2 SEM-EDX micrographs of activated orange peel powder (AcOPP)

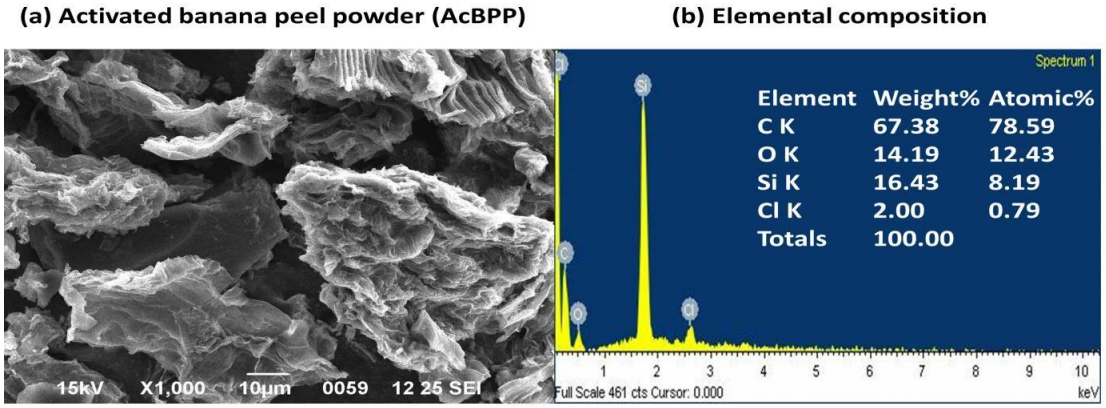

Fig. 4.3 SEM-EDX micrographs of activated banana peel powder (AcBPP)

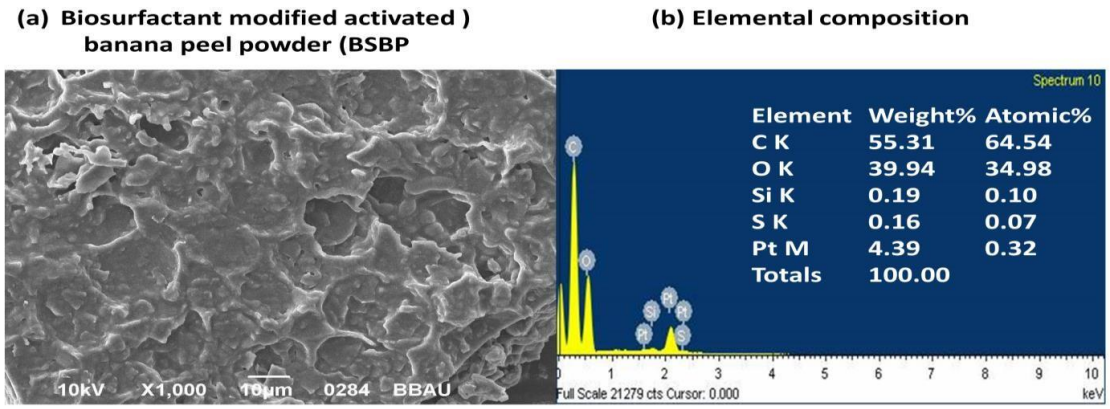

Fig. 4.4 SEM-EDX micrographs of biosurfactant modified activated banana peel powder (BSBP)

The surface morphology of the bio-adsorbents i.e., activated orange peel powder (AcOPP) and activated banana peel powder (AcBPP) depicted the presence of heterogeneous rough porous surface having small and large particles as shown in **Fig 4.2(a)** and **Fig. 4.3(a)**. Similar patterns of topography were reported for other bio-adsorbents prepared from agro-masses (Jawad et al., 2021; Kamsonlian et al., 2011; Selvaraju & Bakar, 2017). Such patterns with large porous texture were expected to facilitate the binding or entrapment and uptake of heavy metal ions (Bediako et al., 2019; Hu et al., 2020; Mondal et al., 2018). To the contrary, the surface characterization of biosurfactant modified activated banana peel powder (BSBP) in **Fig. 4.4(a)** clearly shows the deposition of crystalline structures of surfactin (biosurfactant) molecules that would be suggested to promote better bioadsorption of heavy metal ions as it is rich in ligand binding sites (Ghaith et al., 2019; Perez-Ameneiro et al., 2015; Rastogi & Kumar, 2020).

4.1.3 Functional groups

The Fourier transform infrared spectroscopy (FTIR) was done to elucidate the nature and identification of the functional groups present in activated orange peel powder (AcOPP), activated banana peel powder (AcBPP) and biosurfactant modified activated banana peel powder (BSBP) via the procedure explained in chapter 3, section 3.3.1.3. FTIR spectra of respective bio-adsorbents are presented in **Fig. 4.5 (a,b,c)**. The obtained spectra showed a number of peaks, depicted a complex nature of the bio-adsorbents. As shown in **Fig. 4.5 (a,b,c)**, the bands appearing at 3419.6, between 3087.9-3031.9, 2924.7-2771.9, 2134.9, 1728.8-1511.8, 1439.8-1139.7, and 1036.7-469.9 cm^{-1} were assigned to hydroxyl (─OH) group stretch, alcohol and phenol groups having free ─OH groups, hydrogen bonds (H-bond in alcohols, phenols), ─OH stretch in carboxylic acids (─COOH), alkyne stretch in alkanes, Nitrile stretch (─CN), alkene bond (C═C) stretch in alkanes, primary amine band ($─NH_2$), ─OH band stretch of carboxylic acids and esters respectively. It is pretty evident from the findings that the presence of carboxylic and hydroxyl groups would play a major role in the biaodsorption of heavy metal ions as reported in previous literatures (Bankar et al., 2010; Hashem et al., 2020; Hashemian et al., 2014).

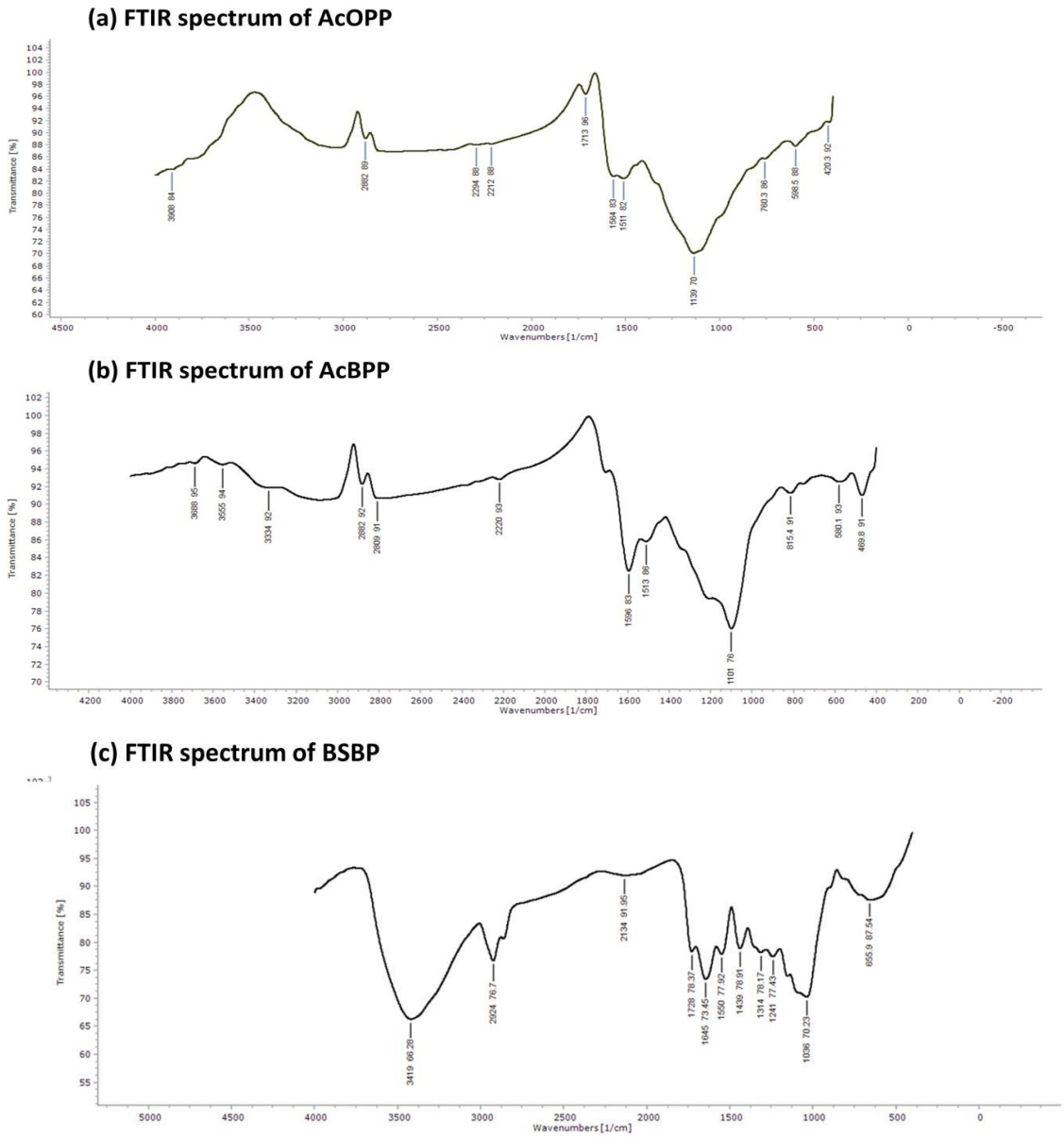

Fig. 4.5 FTIR spectra of different bio-adsorbents

4.1.4 XRD

XRD spectra of the selected bio-adsorbents confirmed the amorphous nature of the prepared bio-adsorbents. An exquisite peak at 2θ= 26.65º in **Fig. 4.6(a)** for activated orange peel powder (AcOPP) represents the characteristic graphite micro crystallite indicating intermediate between amorphous carbon and graphite (Lathiya et al., 2018). The small peak at 2θ= 31.26º as shown in **Fig. 4.6(b)** indicated graphite, moreover, absence of sharp peaks depicted negligible existence of ash residues in the structure as represented in **Fig. 4.6(c)** (Taer et al., 2017).

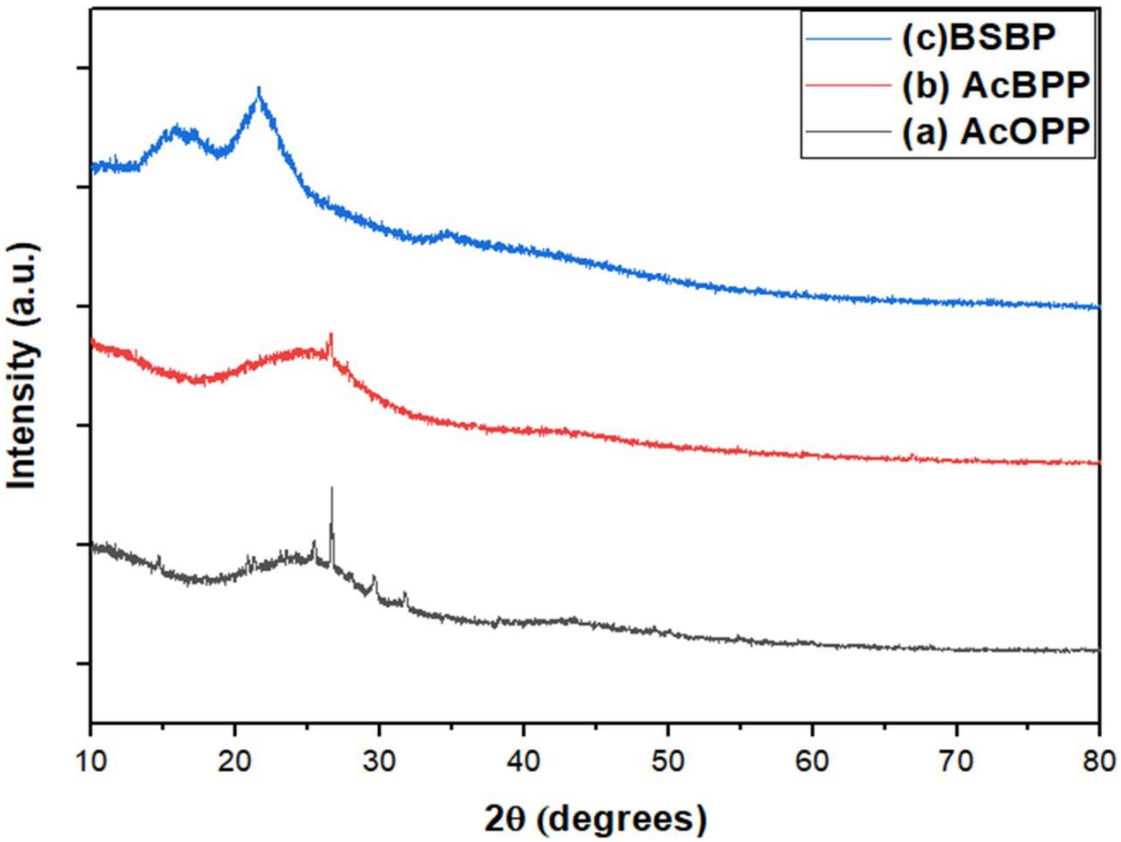

Fig. 4.6 XRD spectra of different bio-adsorbents

4.1.5 Zero point charge (pH_{ZPC}) analysis of bioadsorbents

The surface charge of any bio-adsorbent material is an essential parameter for analysing their surface chemistry in terms of acidity or basicity. The pH_{zpc} of activated orange peel powder (AcOPP), activated banana peel powder (AcBPP) and biosurfactant modified activated banana peel powder (BSBP) were found to be ~4 as represented in **Fig. 4.7(a,b,c)** respectively. FTIR and Elemental analysis as already explained further suggested the acidic nature of the bio-adsorbents mainly due to the presence of oxygen containing functional groups such as carboxylic, phenols, etc. (Ahmad & Danish, 2018; Foo & Hameed, 2012).

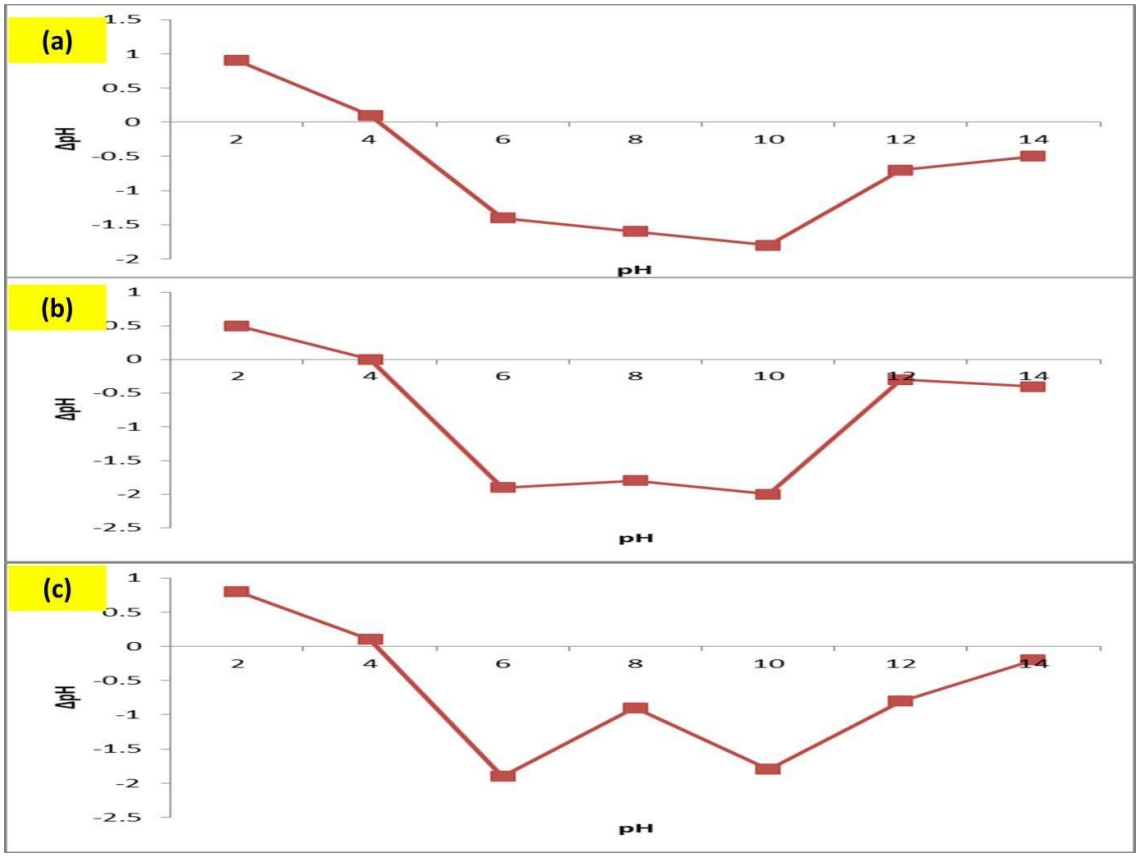

Figure 4.7 Zero point charge (a) activated orange peel powder (AcOPP); (b) activated banana peel powder (AcBPP);(c) biosurfactant modified activated banana peel powder (BSBP)

4.1.6 Bioadsorption potential of selected bio-adsorbents in a batch process

4.1.6.1 Factors affecting the performance of bio-adsorption of bio-adsorbent material

4.1.6.1.1 pH

The effect of pH on the elimination of Pb^{2+} and Cd^{2+} ions by activated orange peel powder (AcOPP) and activated banana peel powder (AcBPP) was conducted between pH ranges from 2 to 12 as explained in the chapter 3, section 3.3.2.1). pH is an important factor that strongly affects the bioadsorption capacity of any material for any pollutant being used in the adsorption study (Bian et al., 2011). Significant results were obtained using AcOPP and AcBPP for Pb^{2+} and Cd^{2+} bioadsorption from the aqueous solutions with AcBPP being better in performance than AcOPP as represented in **Fig. 4.8** and **Fig. 4.9**. The bioadsorption capacities of Pb^{2+} and Cd^{2+}

were found to enhance from 1.45 to 2.45 mg/g for Pb^{2+} and 1.54 to 2.73 mg/g for Cd^{2+} when pH was increased from 2 to 4.5 with AcOPP while the AcBPP showed enhancement from 1.59 to 2.83 mg/g for Pb^{2+} and 1.96 to 4.05 mg/g for Cd^{2+} between pH 2 to 4.5 respectively. The heavy metal ions bioadsorption was significantly high between pH 3.5 and 4.5 while highest removal of heavy metal ions was observed within pH 4 and 5 for both the metals with both the bioadsorbents. Therefore, to make it aligned, pH 4.5 was adopted for the whole set of experiments. Low bioadsorption capacities were observed at both low and high pH with fruit peel bioadsorbents for Pb^{2+} and Cd^{2+} bioadsorption as supported by previous researches (Khan & Khan, 1995). It is suggested that at low pH, the solution has more hydronium ions (H_3O^+) that competes with the heavy metal cations (Pb^{2+} and Cd^{2+}) for binding on the bioadsorbent sites. Also, the presence of H_3O^+ envelopes the cations and doesn‘t let their interactions on the bioadsorbent surface (Forján et al., 2016). However, at higher pH values, there is an inactivation of surface binding sites and Pb^{2+} and Cd^{2+} start precipitating above pH 5 and it gets deposited as their hydroxides [$Pb(OH)_2$/$Cd(OH)_2$] respectively in alkaline solutions. The bioadsorption process is blocked/not completed at higher pH (Bode-Aluko et al., 2017).

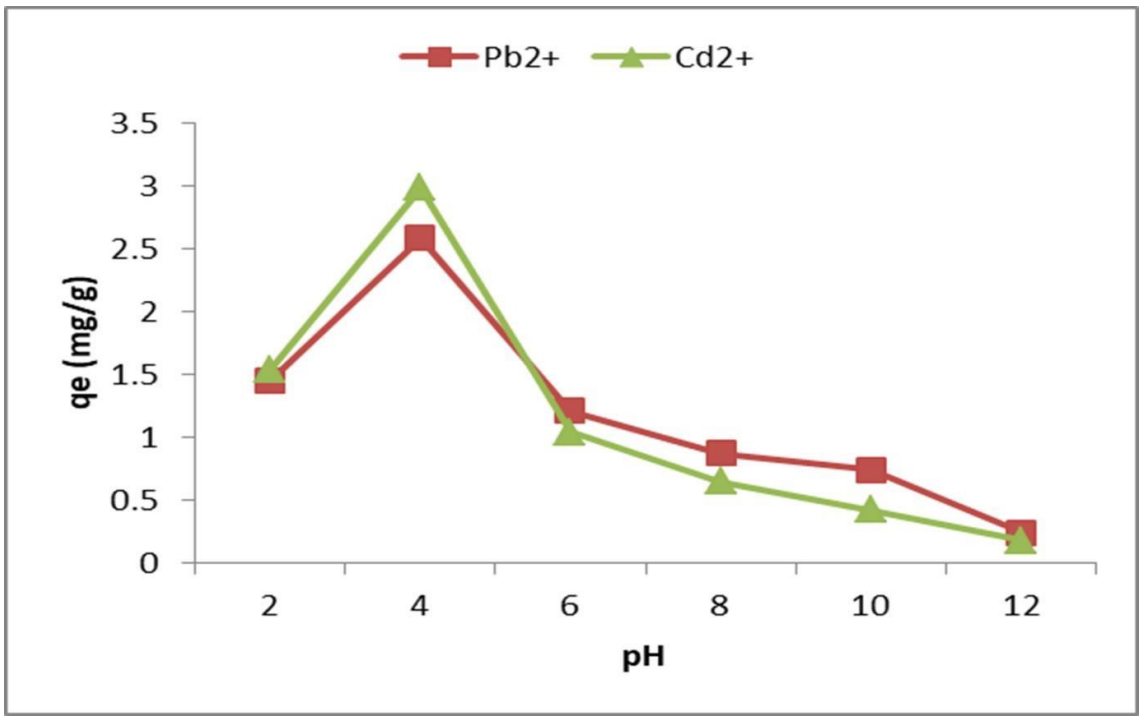

Figure 4.8 Effect of pH on the removal of Pb^{2+} and Cd^{2+} by activated orange peel powder (AcOPP)

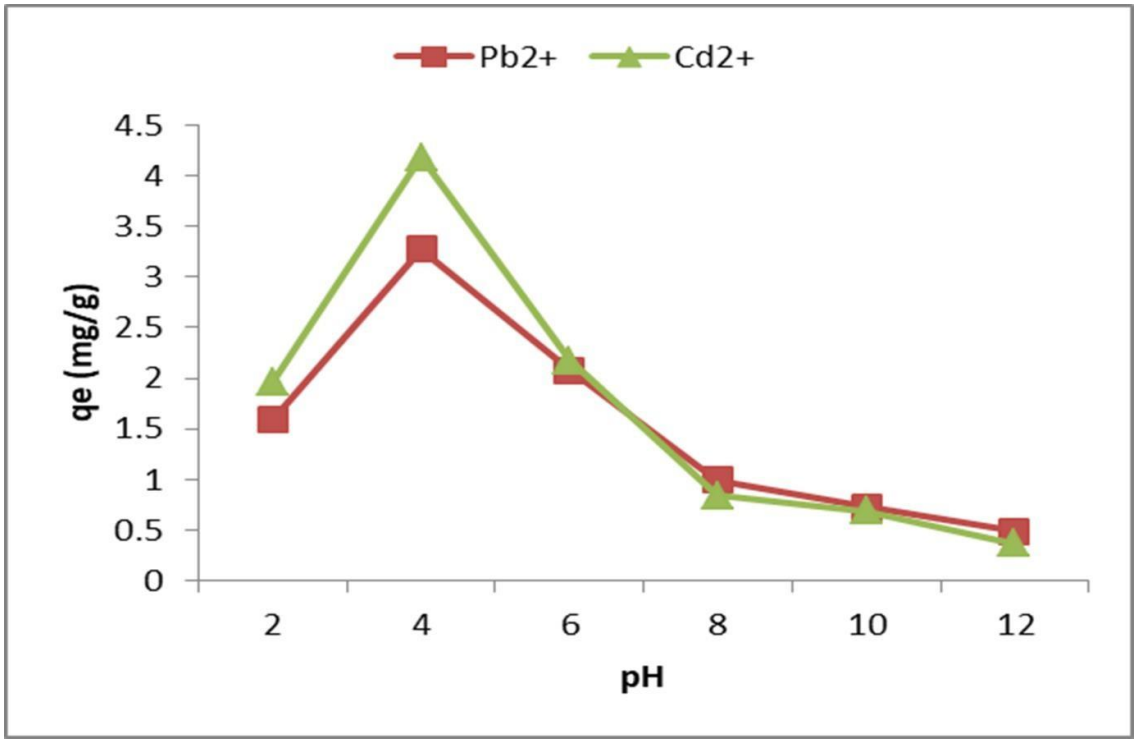

Figure 4.9 Effect of pH on the removal of Pb^{2+} and Cd^{2+} by activated banana peel powder (AcBPP)

4.1.6.1.2 Bioadsorbent doses

The effect of different dose ranges on the elimination of Pb^{2+} and Cd^{2+} was examined with 10 ppm metal concentration (chapter 3, section 3.3.2.2) and results are depicted in **Fig. 4.10** and **Fig. 4.11**. The experimental results obtained showed low metal removal at low doses of AcOPP and AcBPP while enhanced removal was observed with the enhancement in dose range gradually for both the metal ions up to a limit after which it declined. The highest Pb^{2+} and Cd^{2+} removal were with a dose of 0.5-1 g. The decreased bioadsorption at higher doses illustrated the partial clumping and aggregation of active/binding sites that retarded the heavy metals (HMs) bioadsorption on to AcOPP and AcBPP (Mohamed et al., 2019) while at low doses, there were not enough active sites for the binding of Pb^{2+} and Cd^{2+} ions (Baby et al., 2019). Therefore, 0.5 g/ 50 mL of AcOPP and AcBPP dose was selected for the whole range of experiments.

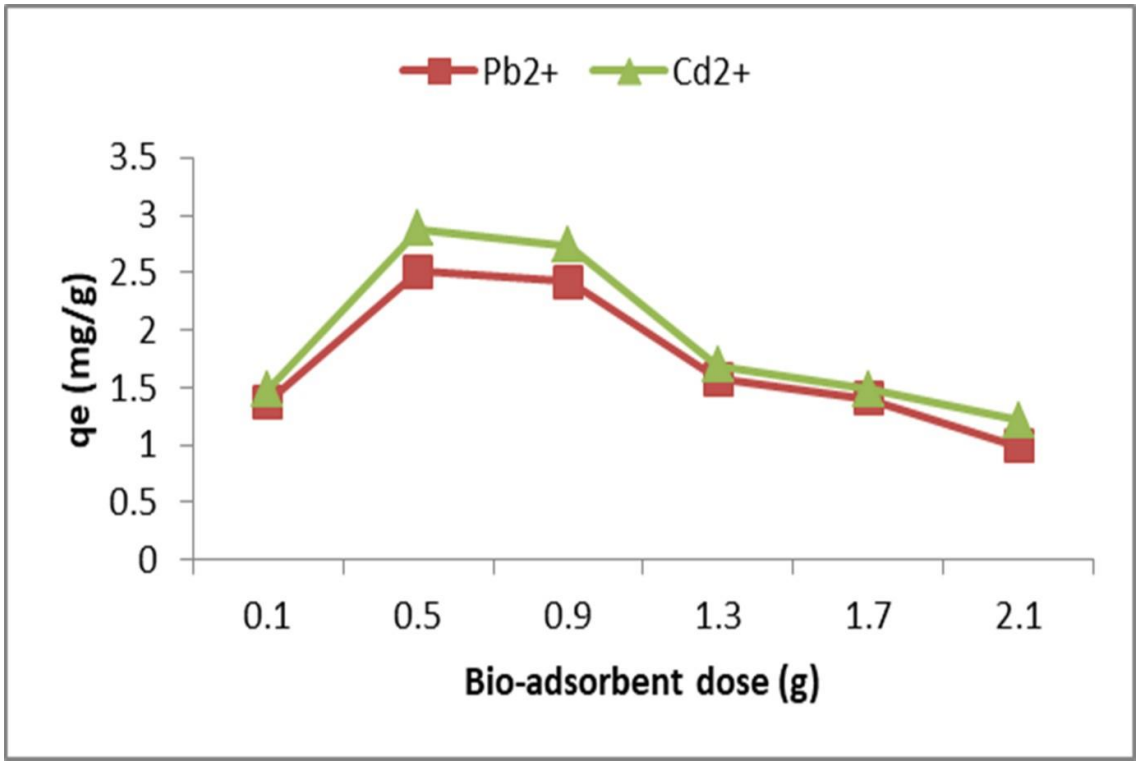

Figure 4.10 Effect of bio-adsorbent dose on the removal of Pb^{2+} and Cd^{2+} by activated orange peel powder (AcOPP)

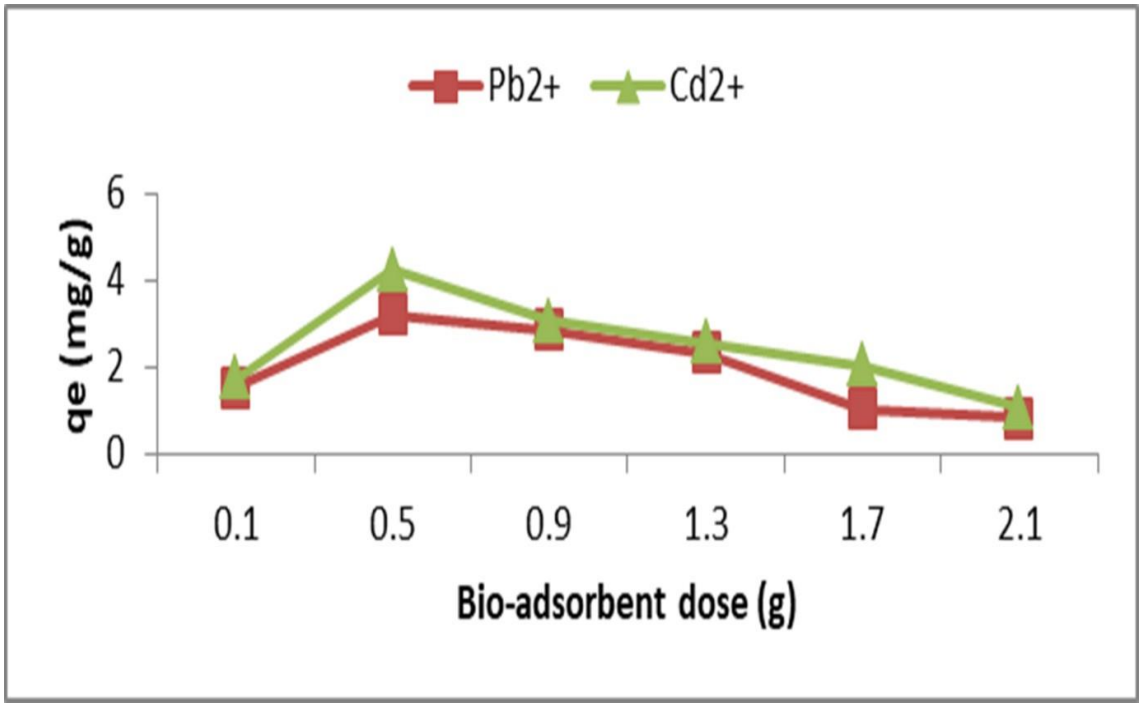

Figure 4.11 Effect of bio-adsorbent dose on the removal of Pb^{2+} and Cd^{2+} by activated banana peel powder (AcBPP)

4.1.6.1.3 Contact time

The effect of contact time on the removal of Pb^{2+} and Cd^{2+} were examined with initial metal concentration of 10 ppm using 0.5 g dose of AcOPP/AcBPP at 120 rpm in an incubating shaker for different time intervals from 30-120 min. with experimental results shown in **Fig. 4.12** and **Fig. 4.13**. The bioadsorption rate enhanced faster in the beginning of the experiment in first 30 min, and significantly increased up to 60 min, thereafter, it was found to reach equilibrium with both the bioadsorbents. It was suggested that initially the bioadsorbent surface is equipped with many vacant binding sites and metal ions can bind to it rapidly in the first stage of bioadsorption (Abdić et al., 2018), however, with the gradual passage of time, the binding sites becomes saturated and limited that leads to diminished bioadsorption rate due to the repulsion caused by already bound metal ions with the ions present in the solution phase (Çelebi, 2020). As the rate decreases, the mass driving force responsible for the dynamic transfer of metal ions also decreases with the elapsing time. Also, after the saturation of mesoporous surface, the Pb^{2+} and Cd^{2+} ions tends to move towards deeper pores where it feels more resistance which slows down the bioadsorption process in the later phase of the bioadsorption (Soliman & Moustafa, 2020).

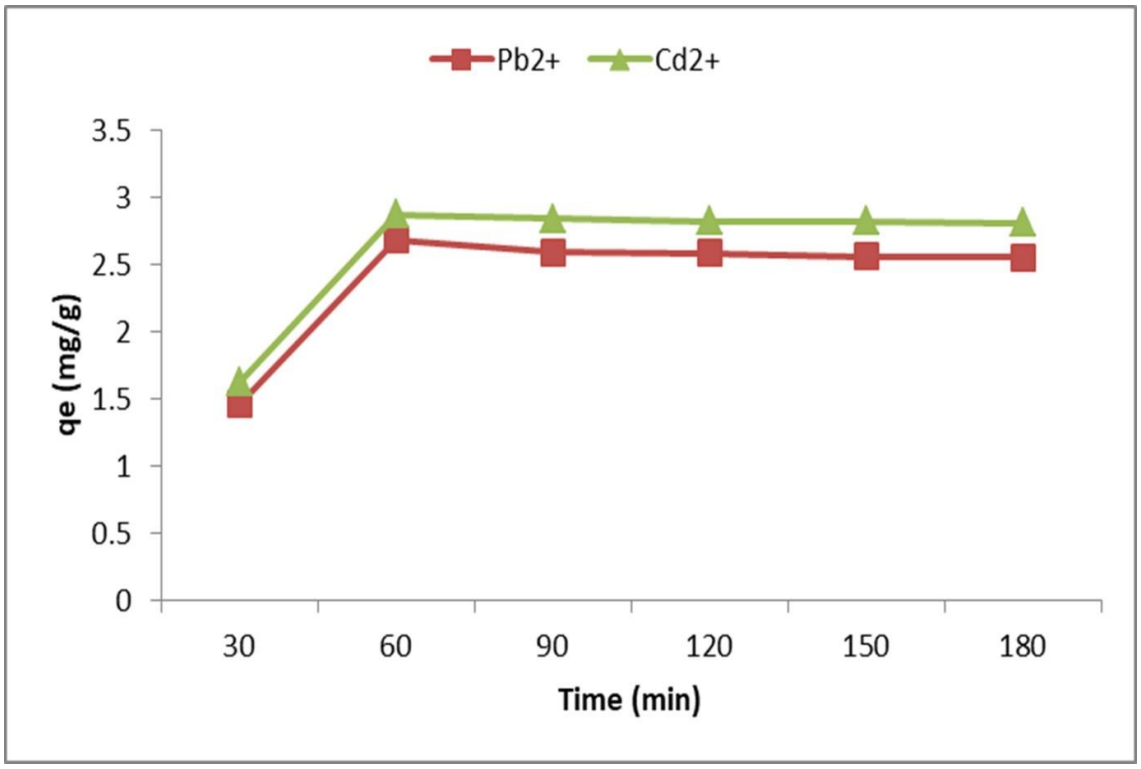

Figure 4.12 Effect of contact time on the removal of Pb^{2+} and Cd^{2+} by activated orange peel powder (AcOPP)

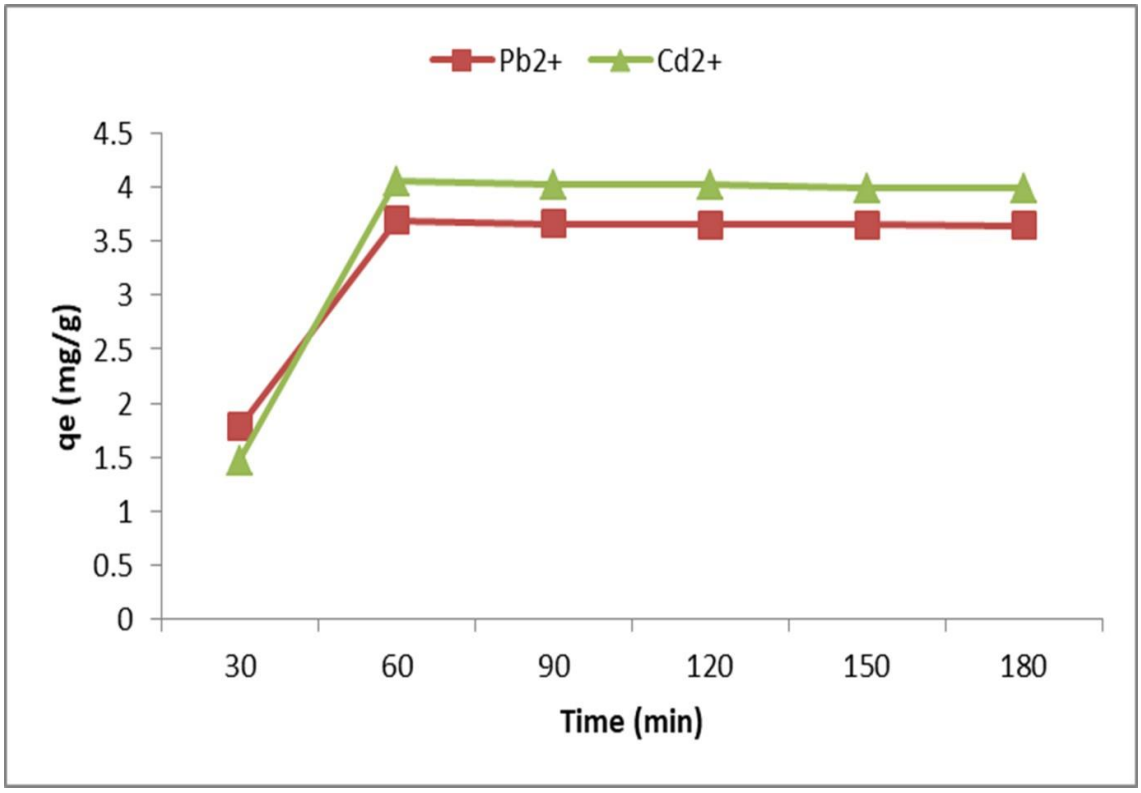

Figure 4.13 Effect of contact time on the removal of Pb^{2+} and Cd^{2+} by activated banana peel powder (AcBPP)

4.1.6.1.4 Initial metal ion concentration

The effect of initial Pb^{2+} and Cd^{2+} ions concentration were tested 0 to 200 ppm with an increment of 50 ppm in 5 Erlenmeyer flasks having 50 mL of these solutions separately. The optimized conditions obtained from the previous batch experiments were utilised i.e., 4.5 pH with bioadsorbent dose of 0.5 g and agitated for 60 min, filtered and analysed for residual metal ions concentration in the same manner.

The experimental findings are represented in **Fig. 4.14** and **Fig. 4.15**. From the data obtained, it was found that the metal removal rate was lower at low metal ion concentration (10 and 50 ppm) as less number of ions are available to get transferred from liquid to solid phase (mass transfer process will decrease) but the vacant sites on the bioadsorbents would be occupied rapidly with no further rise in uptake due to the unavailability of metal ions (Nahar et al., 2018). However, high concentrations but low bioadsorbent doses would also slow the removal rate as at low doses less number of binding sites would be present (Boostani et al., 2019). In our study, 100 ppm of Pb^{2+} and Cd^{2+} showed maximum removal rate than lower concentrations of Pb^{2+} and

Cd^{2+} (10 and 50 ppm) suggesting the suitability of the bioadsorbent to bind efficiently metal ions up to 100 ppm. In control, conditions, where no metal was taken, no binding of heavy metal was observed.

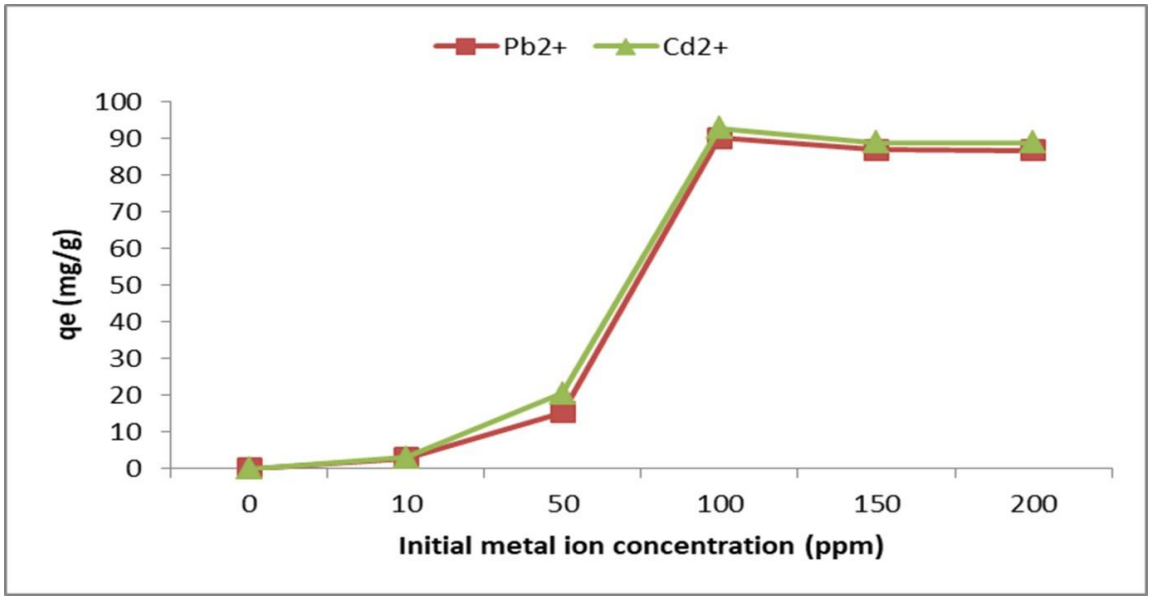

Figure 4.14 Effect of Initial metal ion concentrations on the removal of Pb^{2+} and Cd^{2+} by activated orange peel powder (AcOPP)

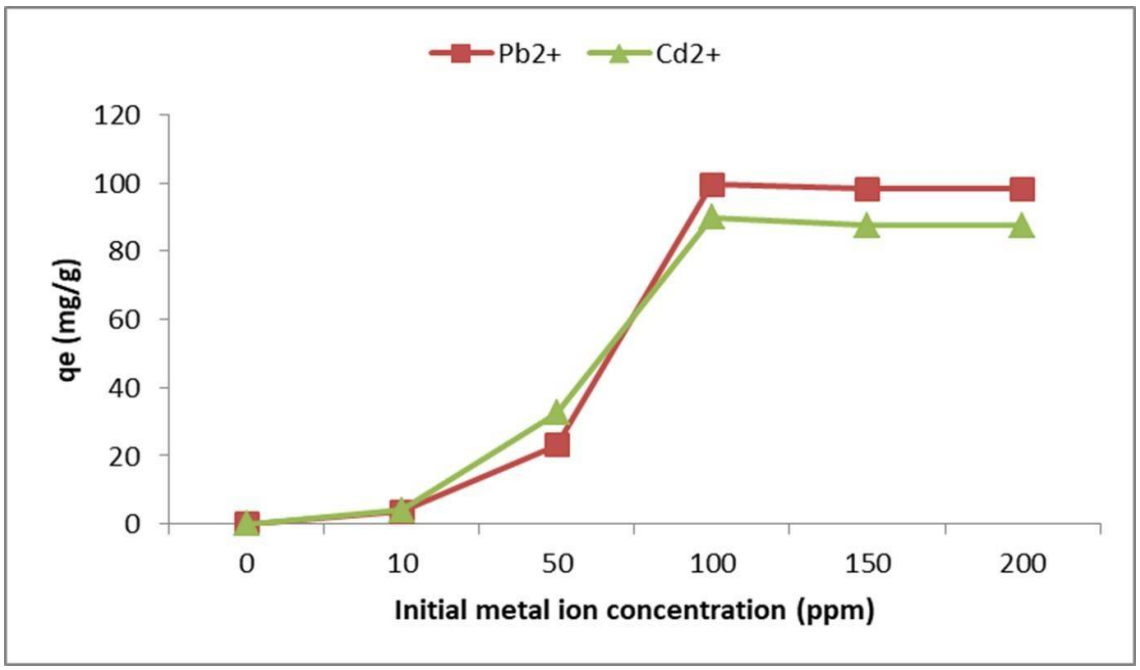

Figure 4.15 Effect of Initial metal ion concentrations on the removal of Pb^{2+} and Cd^{2+} by activated banana peel powder (AcBPP)

4.1.7 Results of Desorption studies and regeneration of the bioadsorbents

Regeneration aspect of the bio-adsorbents is essential in order to reduce the operational costs occurring in water and wastewater treatment systems. However, it is well established from the previous literature that a given bio-adsorbent is not entirely capable of releasing all the heavy metal (HM) ions adsorbed on it i.e., irreversible (Vakili et al., 2019). In the present study, 3 eluting agents such as 0.1N HNO_3, 0.1N HCl, and 0.1N NaOH were utilized for desorption of Pb^{2+} and Cd^{2+} ions from the surface of the activated orange peel powder (AcOPP) and activated banana peel powder (AcBPP) as illustrated in the **Fig. 4.16** and **Fig. 4.17**. It was found that the adsorbed heavy metal ions were easily released by using less amount of 0.1 N HNO_3. The maximum desorption were found to be 92% of Pb^{2+} and 90% of Cd^{2+} with 0.1 N HNO_3 in the case of AcOPP while 98% of Pb^{2+} and 96% of Cd^{2+} with AcBPP using 0.1 N HNO_3. The other acid (0.1N HCl) showed good desorption efficiency as well but less than 0.1 N HNO_3 while 0.1N NaOH was found to have a very low recovery rate in comparison to the acids. The usage of acids allows the deposition of hydronium ions (H_3O^+) or protons (H^+) on the surface of the bioadsorbents that allows easy desorption of cationic Pb^{2+} and Cd^{2+} ions but a high acid concentration also leads to the structural damage (Chatterjee & Abraham, 2019). The metal loaded AcOPP and AcBPP were regenerated in 3 adsorption-desorption cycle with a little decrease in their efficiency as shown in **Fig. 4.18** and **Fig. 4.19**. It is assumed that acidic solution might act as a precursor for the bioadsorbents and would have caused dissolution of the peels so that to activate the active sites on them (Bayuo et al., 2020).

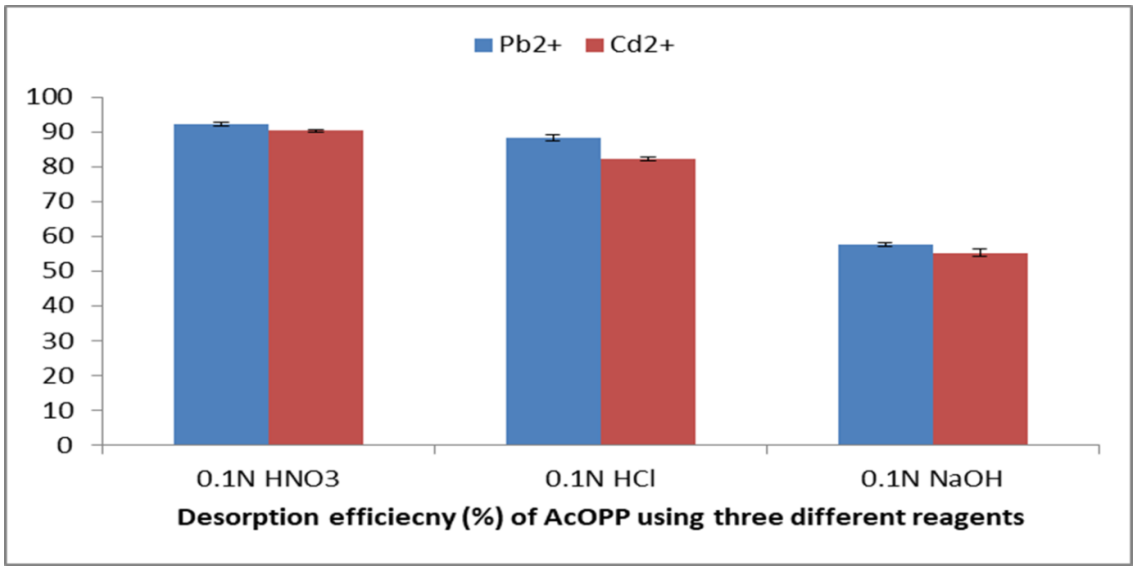

Figure 4.16 Desorption percentage of AcOPP against Pb^{2+} and Cd^{2+}

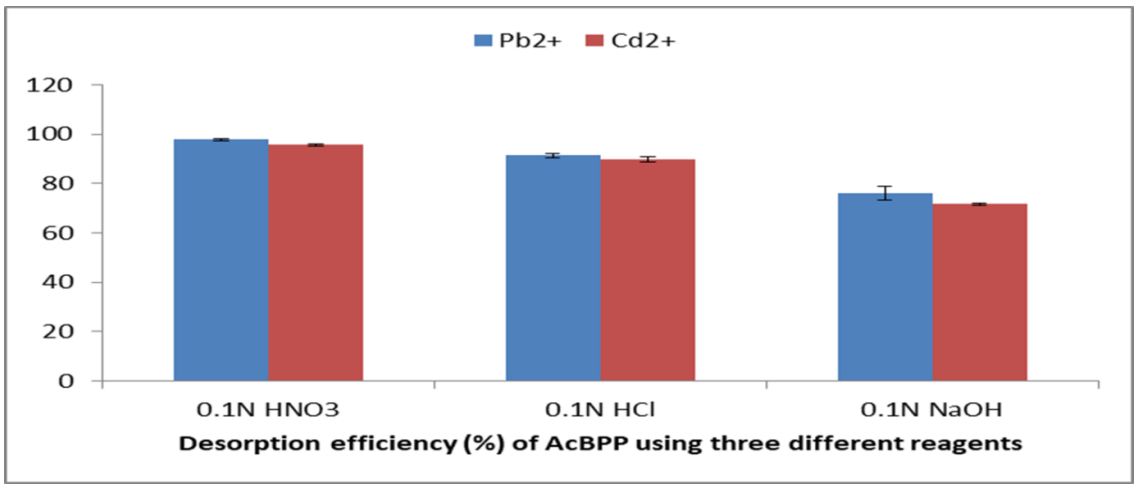

Figure 4.17 Desorption percentage of AcBPP against Pb^{2+} and Cd^{2+}

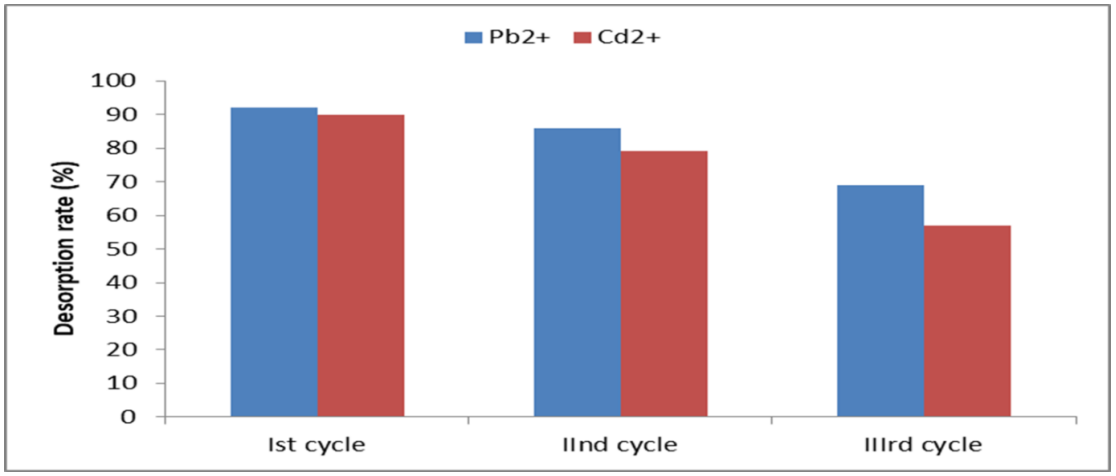

Figure 4.18 Regeneration aspect of AcOPP against Pb^{2+} and Cd^{2+} using 0.1N HNO_3

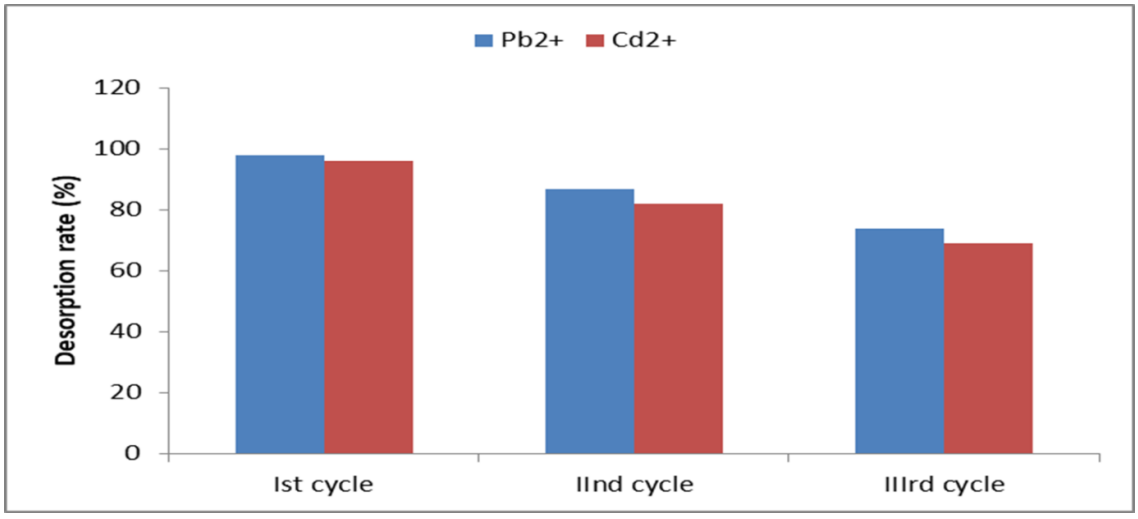

Figure 4.19 Regeneration aspect of AcBPP against Pb^{2+} and Cd^{2+} using 0.1N HNO_3

4.1.8 Adsorption equilibrium isotherms and kinetic modelling

An equilibrium isotherm model typically provides the fundamental relevance to the bioadsorbents utilised in the treatment processes and are explained through mathematical isotherm equations that illustrates the affinity and surface binding properties of the bioadsorbents (Rastogi et al., 2021b). The fitness of an isotherm model is assessed in terms of the R^2 value (regression coefficient) which is obtained from the linear regression plots. The R^2 value closer to unity is said to be best fitted for any particular model in study (Czikkely et al., 2018). In this study, three isotherm models were utilised, namely Langmuir, Freundlich, and Temkin to explain the parameters of bioadsorption of Pb^{2+} and Cd^{2+} on to AcOPP and AcBPP (**Fig. 4.20, Fig. 4.21** and **Fig. 4.22**). The model values are plotted and tabulated for Pb^{2+} and Cd^{2+} bioadsorption (**Table 4.2**).

4.1.8.1 Langmuir isotherm

Langmuir model describes monolayer biosorption based on chemical interactive forces (Can et al., 2016). The linear form of the Langmuir model as **Eq. 4.1** is given below

$$\frac{C_e}{q_e} = \frac{1}{b\,q_m} + C_e\left(\frac{1}{q_m}\right) \ldots\ldots\ldots \textbf{(4.1)}$$

A plot of 1/qe vs 1/ce gives a straight line and is used to calculate the values of R^2, qm, b and R_L from the slope and intercept. R_L is a dimensionless constant known as the equilibrium factor, is given by the **Eq. 4.2**:

$$R_L = \frac{1}{1+bC_o} \ldots\ldots\ldots \textbf{(4.2)}$$

Where ‗q_m' is the maximum adsorption capacity (mg/g), ‗b' is Langmuir constant. ‗C_o' and ‗C_e' are initial and final metal ion concentration. While calculating R_L, C_o is taken as that value that has given the highest adsorption value. The value of R_L illustrates the process of adsorption as irreversible if R_L=0, linear if R_L= 1, favourable if R_L= 0<R_L<1 and unfavourable if R_L >1 (Abd Elhafez et al., 2017).

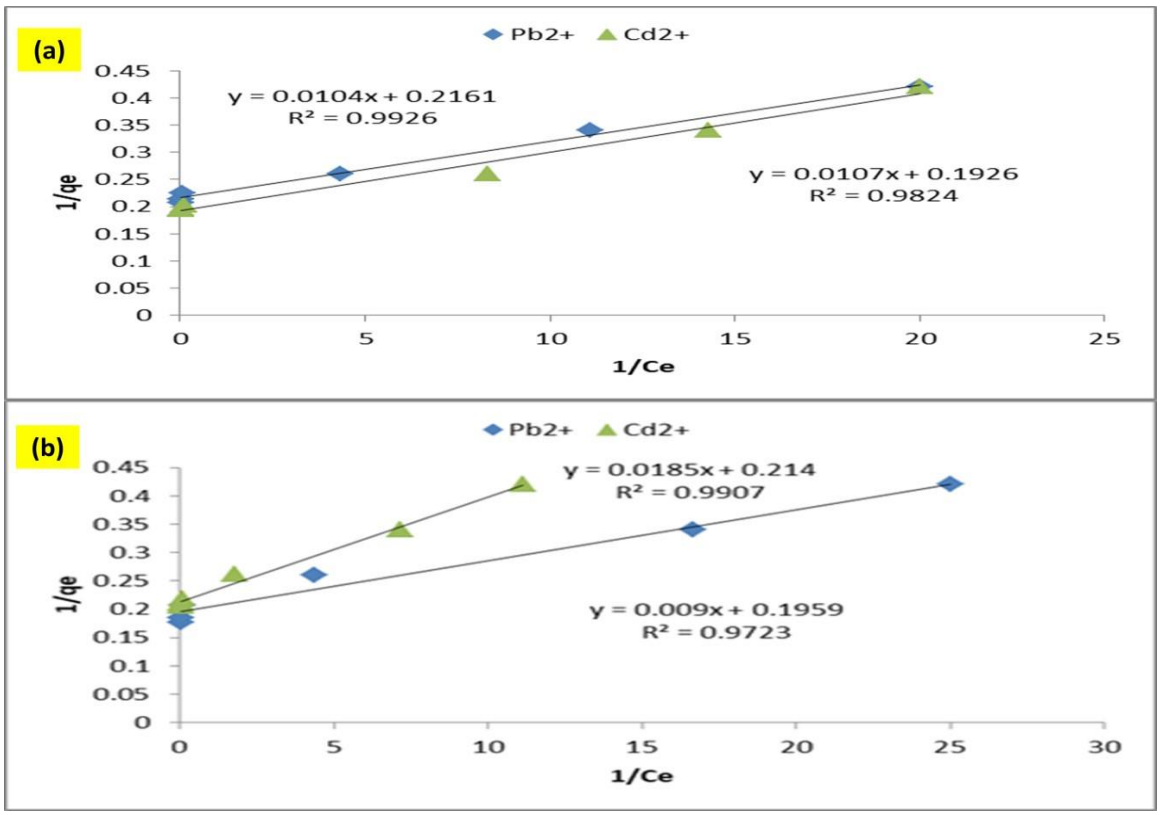

Figure 4.20 Langmuir isotherms against Pb^{2+} and Cd^{2+} bioadsorption (a) AcOPP (b) AcBPP

4.2.8.2 Freundlich isotherm

Freundlich isotherm model explains the biosorption on heterogeneous surfaces having different active sites (Can et al., 2016). Its linear form is shown as **Eq. 4.3** below:

$$logq_e = logK_f + \frac{1}{n} logC_e \ldots\ldots\ldots \textbf{(4.3)}$$

Where q_e is adsorption capacity at equilibrium (mg/g), K_f is the distribution coefficient, and ‗n' indicates favourability of biosorption. The plot of log q_e vs log C_e gives a straight line from which the values of R^2, K_f, and n are calculated.

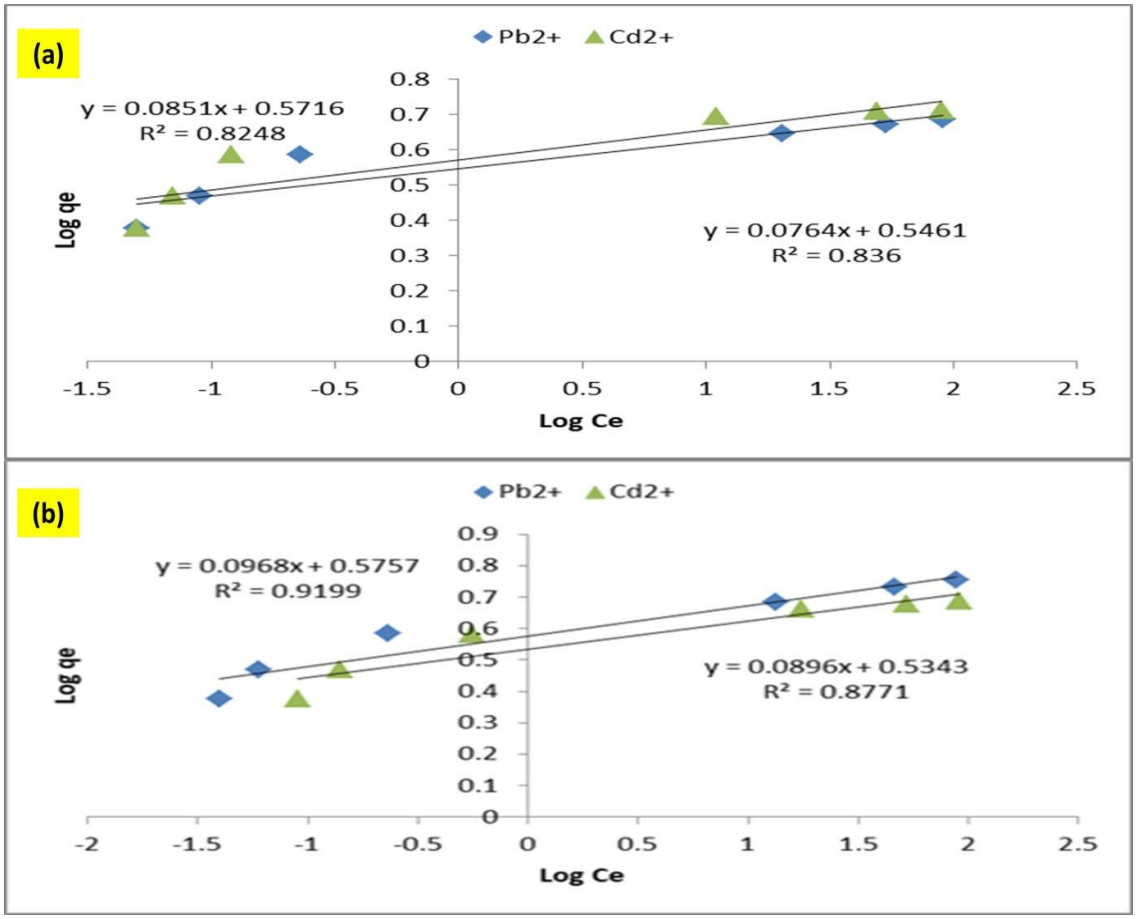

Figure 4.21 Freundlich isotherms against Pb^{2+} and Cd^{2+} bioadsorption (a) AcOPP (b) AcBPP

4.2.8.3 Temkin isotherm

Temkin isotherm is based on assumption that adsorption process heat which is a function of temperature would decrease linearly with the coverage of sites (Dada et al., 2012). This means it assumes a uniform distribution of binding energies when plotted with q_e vs ln C_e. The constants are determined from the straight line's slope and intercept. The linear form of the model equation is given as **Eq. 4.4** below:

$$q_e = \frac{RT}{b_T} lnK_T + \frac{RT}{b_T} ln\, C_e \ldots\ldots\ldots\ldots \textbf{(4.4)}$$

Where _K_T' is Temkin isotherm equilibrium binding constant (L/g), _b_T' is Temkin isotherm constant (J/mol), _R' is universal gas constant=8.314J/mol/K, and _T' is temperature at 298 K.

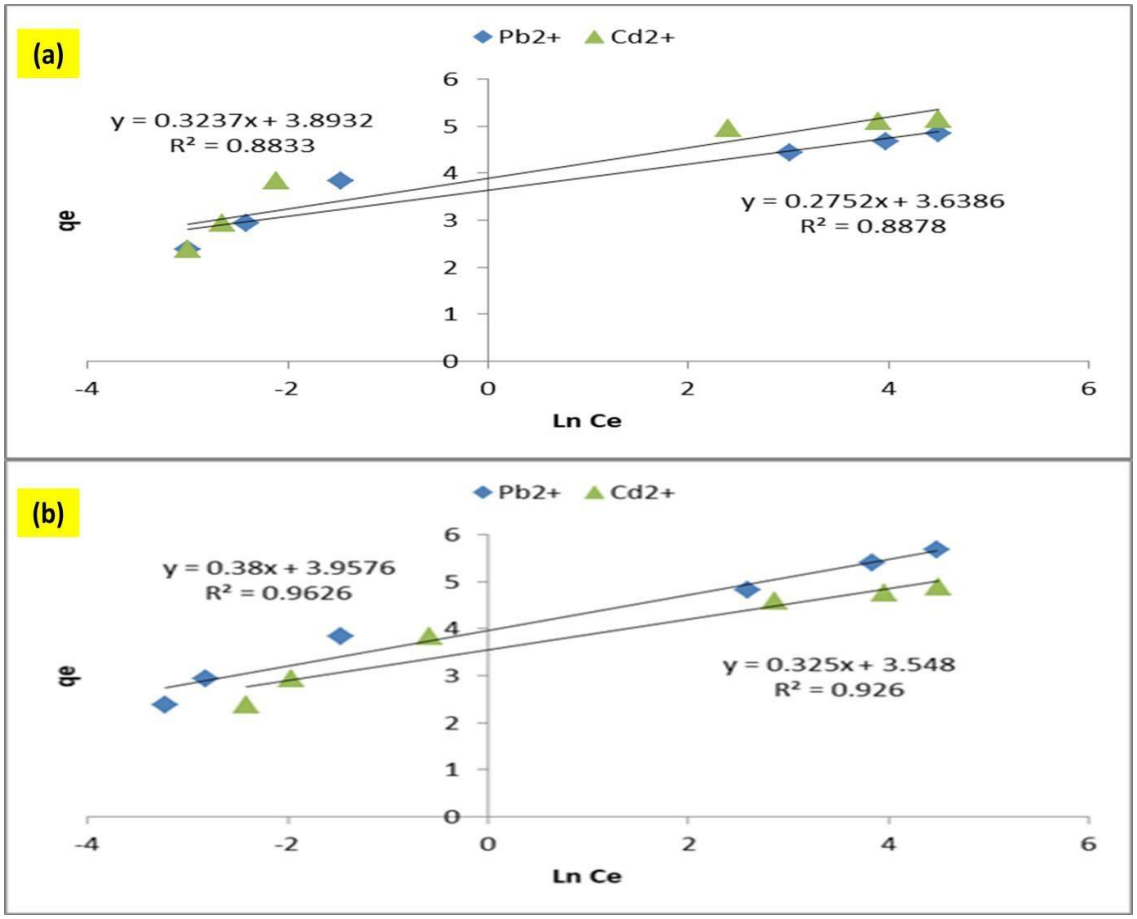

Figure 4.22 Temkin isotherms against Pb^{2+} and Cd^{2+} bioadsorption (a) AcOPP (b) AcBPP

Adsorption isotherms are applied to investigate the maximum bioadsorption rate which is not achieved in the experiments. According to the results obtained, the bioadsorption process was followed closely with the Langmuir model as estimated from the R^2 values as 0.9926 and 0.9824 for Pb^{2+} and Cd^{2+} respectively using AcOPP while it was observed 0.9723 and 0.9907 for Pb^{2+} and Cd^{2+} respectively using AcBPP [**Fig. 4.20(a,b)**]. It was observed that AcBPP performed better bioadsorption than AcOPP as indicated from the maximum bioadsorption capacities (q_m) i.e., 111.11 and 54.05 mg/g for Pb^{2+} and Cd^{2+} respectively (**Table 4.2**) and also from the previous batch optimization study. Though the bioadsorption capacity of Cd^{2+} using AcBPP is measured to be less than AcOPP in isotherm study but overall the performance of AcBPP was found to be better than AcOPP. This is also observable that the models used predicted q_m values much higher than the experimental runs for both the metals.

Table 4.2 Adsorption isotherms parameters and their values

Isotherm Model	Parameters	Values obtained using AcOPP		Values obtained using AcBPP	
		Pb^{2+}	Cd^{2+}	Pb^{2+}	Cd^{2+}
	q_m (mg/g)	96.15	93.46	111.11	54.05
Langmuir	**b (mg/g)**	0.05	0.06	0.05	0.09
	R_L	0.17	0.14	0.17	0.1
	R^2	0.9926	0.9824	0.9723	0.9907
	n	13.09	11.75	10.33	11.16
Freundlich	**K_F**	1.73	1.77	1.78	1.71
	R^2	0.836	0.8248	0.9199	0.8771
	b_T (J/mol)	9002.9	7653.9	6520	7623.4
Temkin	**K_T (L/g)**	1.0004	1.001	1.001	1.0004

The value of R_L in Langmuir isotherm is found to be between 0 to 1 indicating a favourable bioadsorption process using both the bio-adsorbents for Pb^{2+} and Cd^{2+} bioadsorption while the value of constant _b' being less than 1 illustrated weaker affinity of metal ions towards the bio-adsorbent but favourable monolayer bioadsorption (Agouborde & Navia, 2009). The overall performance of Langmuir model was found to be fitted well with the selected bioadsorption system than any other isotherm model used. However, in contrast to the experimental results, AcOPP showed better fit than AcBPP as observed from the regression coefficient values (**Fig. 4.20**) and maximum adsorption capacity (q_m) for Cd^{2+} ions than AcBPP (**Table 4.2**). But since the overall performance of AcBPP was better than AcOPP in whole batch process, AcBPP was selected for the column study.

4.1.8.4 Kinetics of bioadsorption

The biosorption process involving mass transfer and its rate kinetics were explained by applying kinetic models as represented in **Fig 4.23** to **Fig. 4.28** and their parameters are explained in **Table 4.3** and **Table 4.4** using AcOPP and AcBPP. The models chosen for studying the rate of biosorption are described in the subsequent sections.

4.1.8.4.1 Pseudo-first-order and second-order kinetics model

The Pseudo-first and second-order equations are also known as Lagrange equations. The logarithmic form of Pseudo first-order kinetic model is shown below:

$$\log(q_e - q_t) = log q_e - \left(\frac{k_1}{2.303}\right) \times t \ldots\ldots\ldots\ldots \textbf{(4.5)}$$

The Pseudo-second-order kinetic model equation is shown below

$$\frac{t}{q_t} = \frac{1}{k_2 q_e^2} + \frac{t}{q_e} \ldots\ldots\ldots\ldots \textbf{(4.6)}$$

Here, q_e (mg/g) and q_t (mg/g) are the Pb^{2+} and Cd^{2+} adsorption capacities at equilibrium and at time_t‘ (min) respectively. k_1 (min-1) and k_2 (g/mg/min) are first-order and second-order rate constants.

A plot of log (q_e-q_t) vs t and t/qt vs t gives straight lines as shown in **Fig. 4.23** to **Fig. 4.26**. the values of q_e, k_1, k_2 and regression coefficient are calculated from the slope and intercept of the straight line produced in the graph.

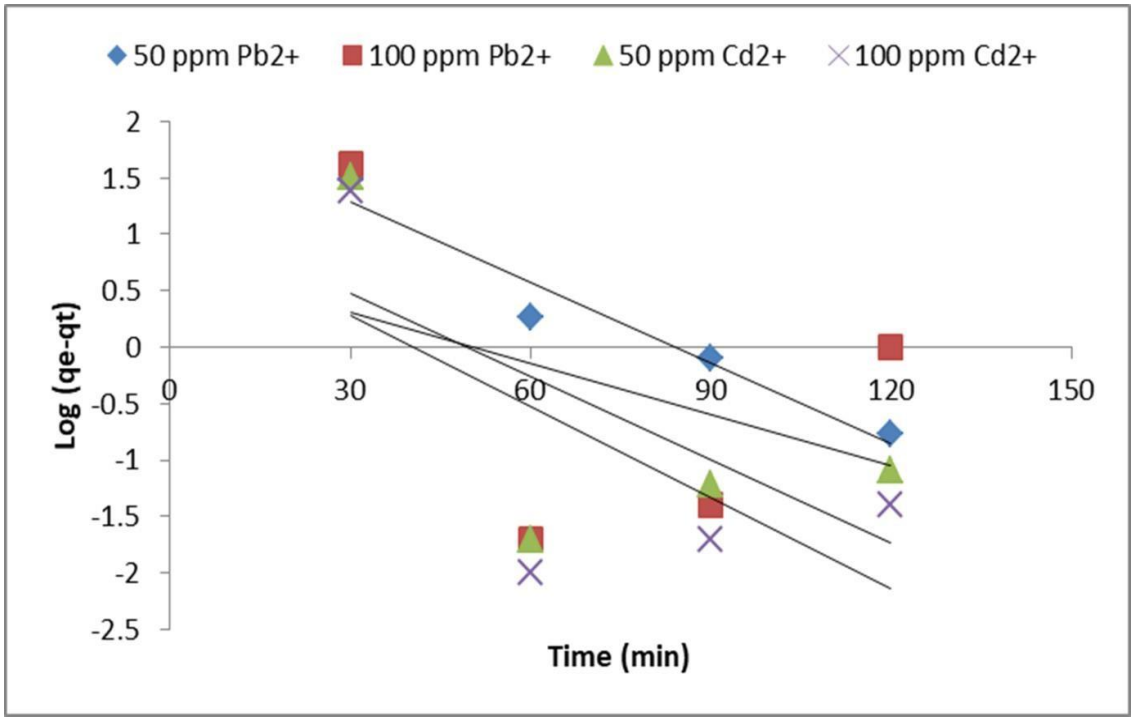

Figure 4.23 Psuedo-first-order kinetic models for Pb^{2+} and Cd^{2+} bioadsorption using AcOPP

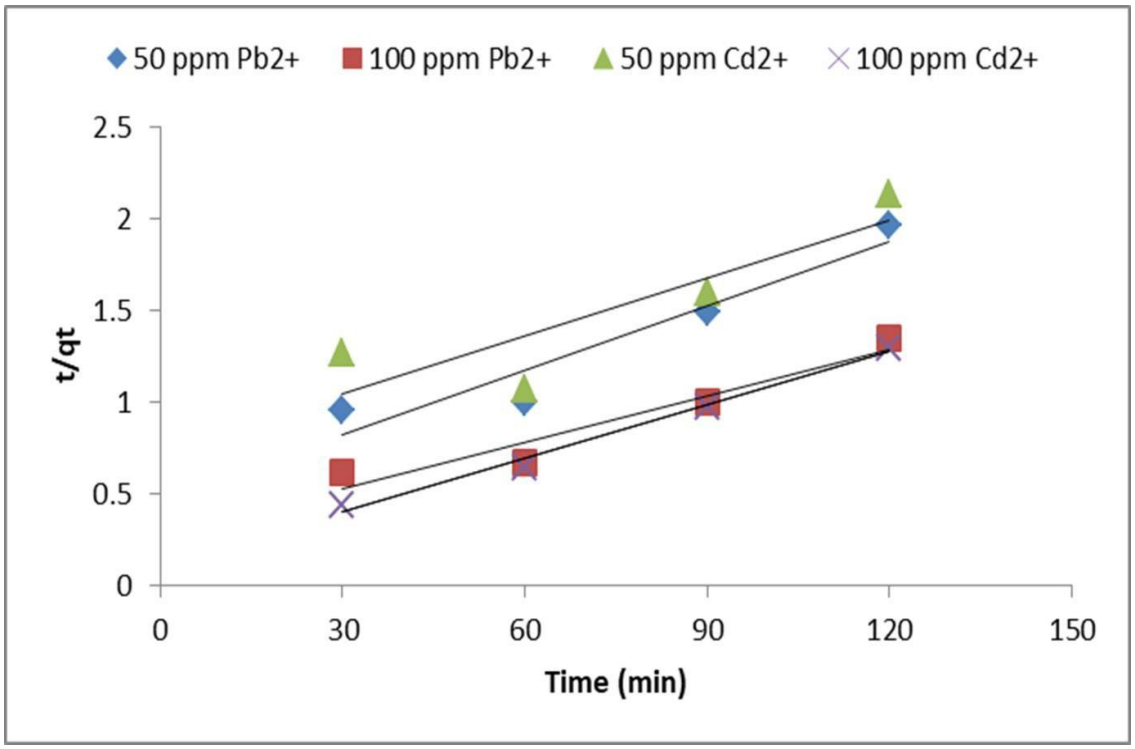

Figure 4.24 Psuedo-second-order kinetic models for Pb^{2+} and Cd^{2+} bioadsorption using AcOPP

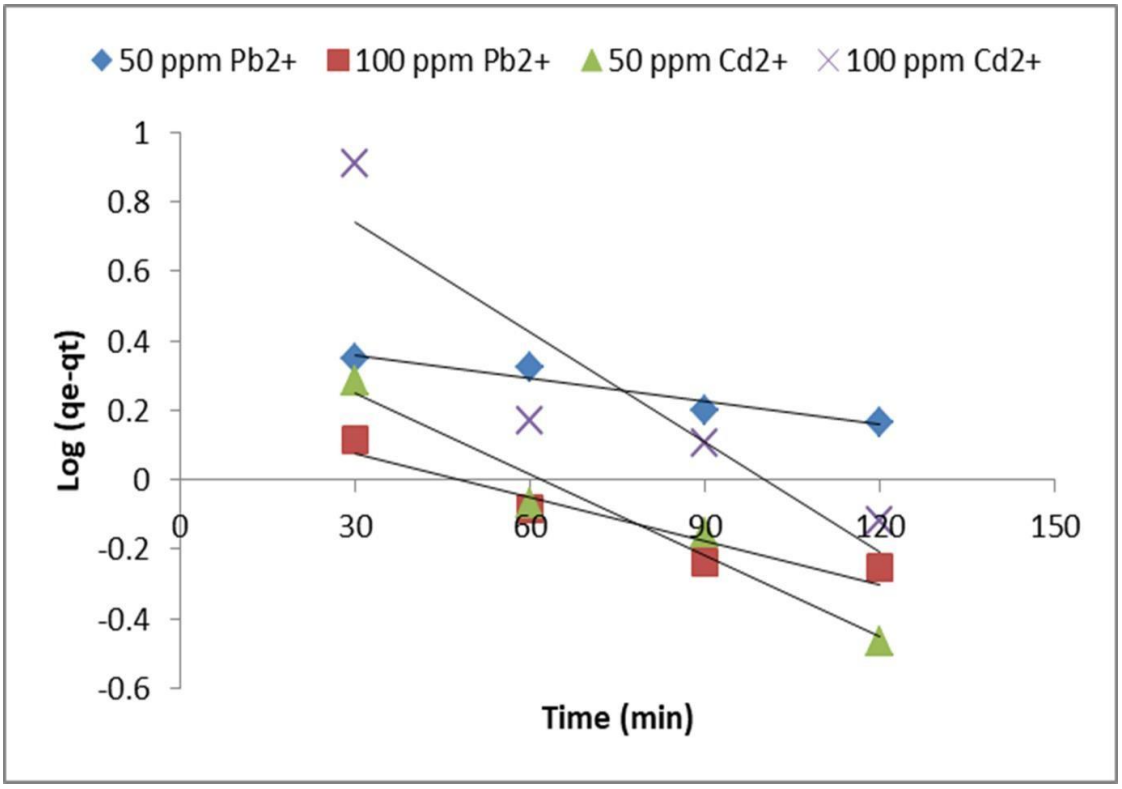

Figure 4.25 Psuedo-first-order kinetic models for Pb^{2+} and Cd^{2+} bioadsorption using AcBPP

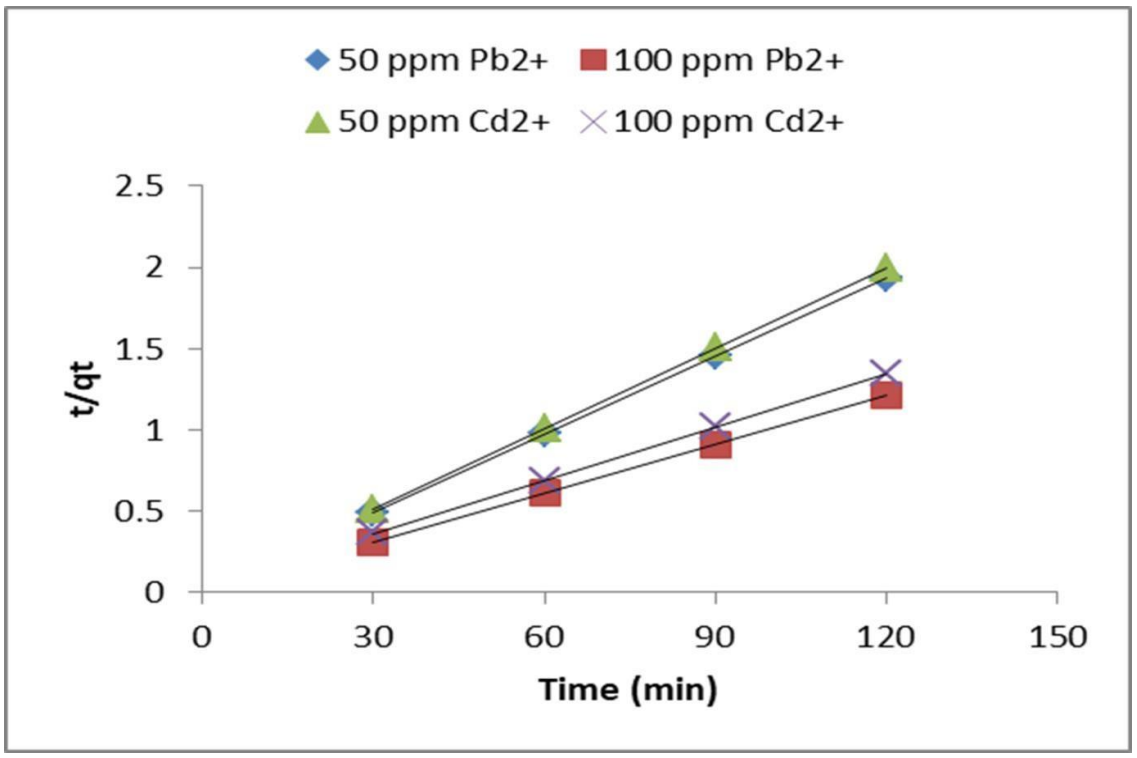

Figure 4.26 Psuedo-second-order kinetic models for Pb^{2+} and Cd^{2+} bioadsorption using AcBPP

The above two models describes about the metal bioadsorption on the outer surface of the selected bio-adsorbents (Simonin, 2016). The obtained results indicated that the experimental interpretations are well fitted with pseudo-second-order on observing their R^2 values i.e., 0.9144, 0.9265, 0.7513, 0.9907 for 50 and 100 ppm of Pb^{2+} and Cd^{2+} using activated orange peel powder (AcOPP) respectively while R^2 values as 1, 1, 1, 0.9997 for 50 and 100 ppm of Pb^{2+} and Cd^{2+} using activated banana peel powder (AcBPP) (**Table 4.3** and **Table 4.4**) and also equilibrium capacities were calculated and were quite close to the experimental values i.e., 85.47 (50 ppm Pb^{2+}), 119.05 (100 ppm Pb^{2+}), 96.15 (50 ppm Cd^{2+}) and 103.09 (100 ppm Cd^{2+}) using AcOPP. The AcBPP showed more linear correlation with the experimental values as seen from the R^2 values. Therefore, the performance of AcBPP was superior over AcOPP. The equilibrium capacities using AcBPP were estimated to be 62.5 (50 ppm Pb^{2+}), 100 (100 ppm Pb^{2+}), 60.61 (50 ppm Cd^{2+}) and 91.74 (100 ppm Cd^{2+}) as depicted in **Table 4.4**. The pseudo second-order rate constant (k_2) represented rate limiting step to be chemisorption along with the physico-sorption (Rangabhashiyam et al., 2019).

The internal diffusion of metal inside the bio-adsorbent material is explained through another kinetic model as described below.

4.1.8.4.2 Intra-particle diffusion

Weber-Morris model of particle diffusion depicts about the movement of metal ions inside adsorbent is given by the equation below:

$$q_t = x_i + k_p\, t^{1/2} \ldots\ldots\ldots \textbf{(4.7)}$$

Where q_t is the Pb^{2+} and Cd^{2+} adsorbed at given time_t‘ (min), k_p (mg/g.$min^{1/2}$) is intraparticle diffusion rate constant and X_i is the intercept. A plot of q_t vs t gives a straight line and from its slope k_p is calculated (Pholosi et al., 2020). Findings are depicted graphically in **Fig. 4.27** and **Fig. 4.28.**

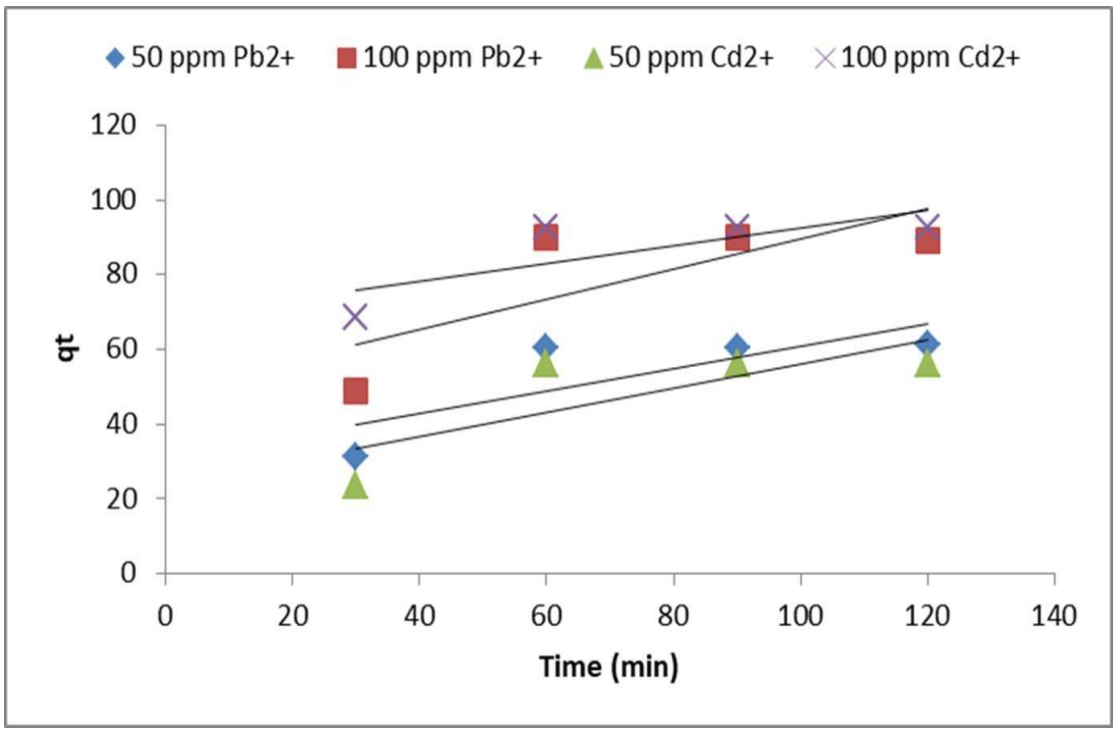

Figure 4.27 Intra-particle diffusion kinetic models for Pb^{2+} and Cd^{2+} bioadsorption using AcOPP

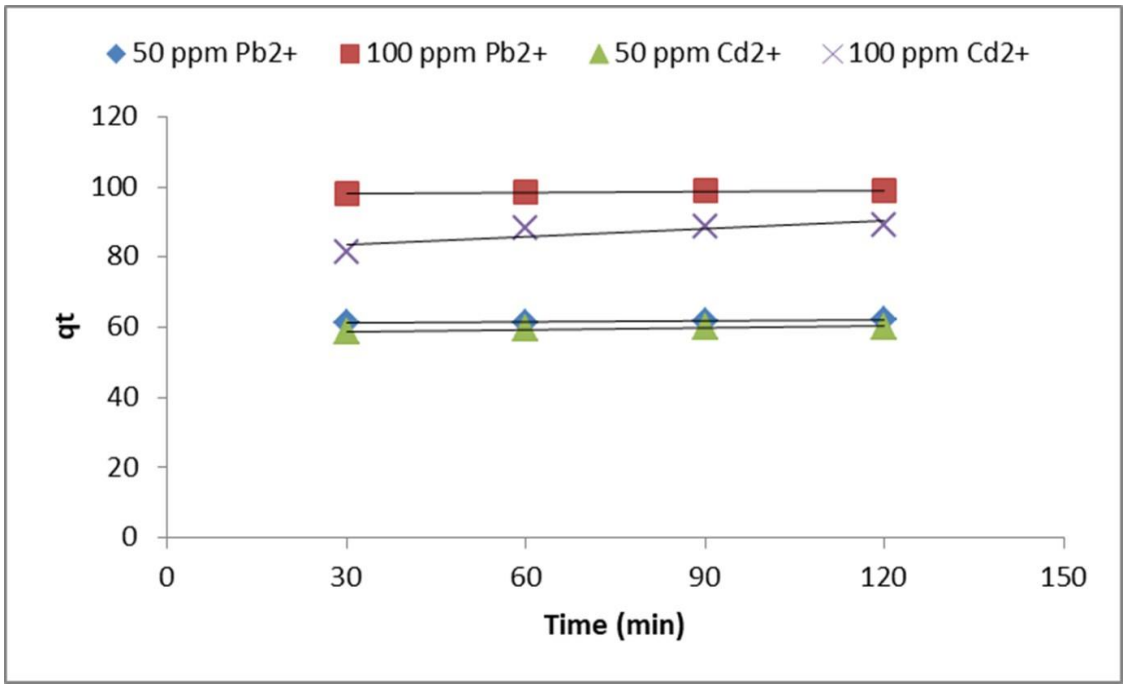

Figure 4.28 Intra-particle diffusion kinetic models for Pb^{2+} and Cd^{2+} bioadsorption using AcBPP

The experimental data moderately suited with the pseudo-first-order and intra particle model as observed from the R^2 values and more with the pseudo-second-order model (**Table 4.3** and **Table 4.4**).

Table 4.3 Kinetic models with their parameters and values using activated orange peel powder (AcOPP) bio-adsorbent

Parameters	**Initial Pb^{2+} concentrations (ppm)**		**Initial Cd^{2+} concentrations (ppm)**	
	50	**100**	**50**	**100**
Experimental q_{exp} (mg/g)	62.05	89.98	56.23	92.64
Kinetic Model				
Pseudo-first order				
k_1	5.48×10^{-2}	3.48×10^{-2}	5.6×10^{-2}	6.1×10^{-2}
q_e (mg/g)	100.05	5.79	16.29	12.09
R^2	0.9456	0.1487	0.4288	0.4427
Pseudo-second order				
k_2	2.9×10^{-4}	2.5×10^{-4}	1.4×10^{-4}	8.2×10^{-4}
q_e (mg/g)	85.47	119.05	96.15	103.09
R^2	0.9144	0.9265	0.7513	0.9907
Intra particle diffusion				
K_p	0.2982	0.402	0.3257	0.2415
X_i	30.98	49.27	23.64	68.47
R^2	0.625	0.5807	0.6	0.599

Table 4.4 Kinetic models with their parameters and values using activated banana peel powder (AcBPP) bio-adsorbent

Parameters	**Initial Pb^{2+} concentrations (ppm)**		**Initial Cd^{2+} concentrations (ppm)**	
	50	**100**	**50**	**100**
Experimental q_{exp} (mg/g)	63.47	99.45	60.48	89.74
Kinetic Model				
Pseudo-first order				
k_1	5.3×10^{-3}	9.7×10^{-3}	1.8×10^{-2}	2.4×10^{-2}
q_e (mg/g)	2.68	1.59	3.04	11.39
R^2	0.924	0.8959	0.9552	0.8306
Pseudo-second order				
k_2	2.3×10^{-2}	3.2×10^{-2}	1.54×10^{-2}	3.6×10^{-3}
q_e (mg/g)	62.5	100	60.61	91.74
R^2	1	1	1	0.9997
Intra particle diffusion				
K_p	0.0095	0.0083	0.0163	0.0747
X_i	60.92	98.01	58.31	81.22
R^2	0.923	0.8487	0.863	0.6801

4.2 Conclusion

Low cost agro/fruit peel biowastes are easily available bioadsorbents as abundant in nature. These can be explored for their bioadsorption potential in raw or modified form for environmental pollutants. The study has assessed the viability of activated orange peel powder (AcOPP) and activated banana peel powder (AcBPP) towards Pb^{2+} and Cd^{2+} removal from aqueous solutions. The prepared peels could be regenerated and reused three times without major reduction in its efficiency. The experimental data obtained were fitted with three isotherm models that showed significant degree of fitness with regression coefficient value (R^2) greater than 0.9. The Langmuir model was found to be the best fitted for removal of Pb^{2+} and Cd^{2+} ions

using AcOPP and AcBPP as evident from the maximum bioadsorption capacities using 0.5 g of bioadsorbent dose. The Langmuir model showed more linear correlation with activated orange peel powder (AcOPP) than activated banana peel powder (AcBPP) in terms of regression coefficient values obtained and high adsorption capacity (q_m) for Cd^{2+} ion. The capacities obtained are quite higher than the values obtained with many other bioadsorbents. The bioadsorption kinetics followed pseudo-second-order model equation depicting physical and chemical adsorption process that is rate controlled. Therefore, activated orange and bananapeels could be considered favourable options for heavy metal removal from water and wastewater. The overall bioadsorption efficiency of AcBPP was found to be better than AcOPP.

Chapter 5

Isolation, Screening of Bacterial Isolates from Hydrocarbon Contaminated Soil and Characterization for Biosurfactant Production and Its Extraction

5.0 Background

Microorganisms are known to play an unquestionable role in the removal of heavy metals (HMs) from the contaminated systems. Several reports are available regarding the isolation of metal resistant bacterial strains from contaminated soil (Javanbakht et al., 2014; Jiang et al., 2008; Tirry et al., 2018). These metal resistant bacteria develop intrinsic mechanisms to avoid harmful effect of heavy metal ions by maintaining their cell growth under such antagonistic environment. The popular mechanisms involved in bacteria for imparting resistance to heavy metals include efflux mechanisms, enzyme production restricting permeability of toxic metals, enzymes for transformation of metals from one form to another (toxic to non-toxic), production of secondary metabolites such as biosurfactants (BSs), and binding of HM ions on their surface or to the metabolite (Etesami, 2018; Franzetti et al., 2014; Nanda et al., 2019). The unfavourable environment triggers a stress response in microorganisms such as bacteria and fungi to produce various secondary metabolites to cope up with those antagonistic conditions. Bacterial biosurfactants (BSs) are one such compound that has proved their existence fruitful for bioremediation of inorganic contaminants particularly heavy metals (Usman et al., 2016). Such amphiphilic entities have both hydrophilic and hydrophobic moieties and functions as microemulsions and micelles between two phases by reducing the interfacial and surface tension (ST) of liquids. There are several classes of biosurfactants identified *viz.* cationic, anionic, zwitterionic, and non-ionic based on the charge present on its surface (Pacwa-Płociniczak et al., 2011). Another classification based on the type of chemical composition is also known where these are categorised as glycolipids, lipopeptides, fatty acids, phospholipids, neutral lipids, polymeric biosurfactants and particulate biosurfactants (Sobrinho et al., 2013). Some of the common properties that make a biosurfactant molecule to be preferred over chemical surfactants are surface and interfacial tension reduction ability, high tolerance to wide pH range, salinity, temperature moderations, biodegradability and biocompatibility, less toxic nature, specificity and emulsification capacity (Malik & Kerkar, 2021). Much work has been reported in recent years that has proved the role of biosurfactant producing bacteria in the bioremediation of heavy metal from contaminated soils and lesser work is reported for the remediation of heavy metals from wastewater or aqueous solutions using biosurfactants (Usman et al., 2016).

The present chapter embodies the results and discussion part for biosurfactant producing bacterial strain isolation, screening, and different methodologies employed for characterization of biosurfactants from hydrocarbon (petrol) contaminated sites. Also, it describes about mass production of biosurfactant by selected strains, its extraction, chemical composition, and characterization analysis. In the end, it discusses about the optimization process employed for maximum production of biosurfactant by the potential bacterial strains using low cost substrates (biowastes/agro-industrial wastes) as a substitute over conventional chemical and expensive carbon substrates in order to highlight the management of such biowastes for the production of economically important product and also it emphasises on reducing the operational cost that arises during its large scale production. The optimization of production process parameters would also suggest a well-defined structure for obtaining the maximum yield of biosurfactant so as to provide an alternative over chemical surfactants. The last part deals with the potential of biosurfactant producing bacterial strains in the biosorption of lead (Pb^{2+}).

5.1 Results and Discussion

A total of 23 morphologically different bacterial colonies were isolated, out of which 2 bacterial strains were shown to be potent biosurfactant producers based on various screening methods as shown in **Table 5.1** and **Fig. 5.1** that were used for further analysis.

Table 5.1 Selection of potential strains based on screening tests for biosurfactant production

S.No.	Isolate Name	Oil Displacement Assay (cm)	Drop Collapse Method	Penetration Assay	Foaming Assay (%)	Hemolytic Assay (cm)	CTAB (rhamnolipid detection)	SurfaceTension (dyne/cm)	BATH Assay (%)	Pb^{2+} MIC (ppm)	Cd^{2+} MIC (ppm)
1	A1	1.5±0.5	+	+	20.23±2.29	1.1±0.24	-	66.24±0.68	-	-	-
2	B1	2.1±0.32	+	+	15.2±1.42	0.8±0.04	-	76.41±2.16	-	-	-
3	B2	1.2±0.03	+	+	18.3±1.28	1.5±0.18	-	54.87±1.45	-	-	-
4	C1	1.2±0.06	+	+	17.54±0.59	1.2±0.05	-	58.23±0.78	-	-	-
5	D1	-	-	-	-	-	-	-	-	-	-
6	D2	2.2±0.37	+	+	21.32±1.64	1.4±0.62	-	74.12±1.24	-	-	-
7	D3	-	-	-	-	-	-	-	-	-	-
8	D4	1.7±0.04	+	+	25.14±1.28	1.6±0.04	-	56.12±0.64	-	-	-
9	E1	3.9±0.1	+	+	52.6±3.21	4.6±0.35	-	28.68±0.46	80.98±1.71	2200	500
10	E2	2.9±0.06	+	+	47.6±2.51	2.7±0.65	-	32.37±0.95	73.71±3.07	1800	300
11	F1	2.4±0.48	+	+	40.23±2.24	1.9±0.02	-	52.36±2.14	-	-	-
12	F2	2.1±0.08	+	+	36.14±0.38	1.5±0.64	-	65.14±1.47	-	-	-
13	F3	-	-	-	-	-	-	-	-	-	-
14	F4	-	-	-	-	-	-	-	-	-	-
15	F5	4.6±0.46	+	+	53.0±4.58	3.4±0.55	+	32.08 ± 0.38	91.65±2.75	2200	1000
16	G1	-	-	-	-	-	-	-	-	-	-
17	H1	2.3±0.35	+	+	52.87±2.58	1.8±0.49	-	58.48±1.27	-	-	-
18	H2	-	-	-	-	-	-	-	-	-	-
19	I1	1.8±0.09	+	+	32.56±0.43	1.4±0.75	-	65.12±0.47	-	-	-
20	J1	-	-	-	-	-	-	-	-	-	-
21	J2	-	-	-	-	-	-	-	-	-	-
22	K1	-	-	-	-	-	-	-	-	-	-
23	L1	-	-	-	-	-	-	-	-	-	-

These potential biosurfactants contain diverse functional groups such as carboxyl, hydroxyl, amine, carbonyl etc. and are grouped into different classes based on chemical composition *viz*- glycolipids (rhamnolipids), lipopeptides (surfactin, iturin) etc (Henkel & Hausmann, 2019; Mnif et al., 2018). Therefore; it becomes imperative to investigate several screening methodologies. The isolation of biosurfactant producers has gained considerable attention due to their applications in different sectors such as bioremediation, food, cosmetics, etc (Liu et al., 2020; Sarubbo et al., 2015). The levels of screening methods have been presented as primary, secondary, and indirect to provide a complete overview of experimentation as one method is not enough to identify the potential biosurfactant producers and further it will assist researchers in future to use any of the method as per their convenience. Thirteen isolates were positive for oil displacement assay (ODA), drop collapse method (DCM), and penetration assay (PA), respectively in primary screening. It was suggested that the oil displacement assay (ODA) is a reliable parameter for detecting production of surface active molecules where a large displaced diameter of oil correlates to higher activity of the testing solution (Morikawa et al., 1993; Ram et al., 2019; Yalçın et al., 2018). Also, it was reported that the efficiency of drop collapse method (DCM) method relies on the fact that a surfactant containing culture supernatant (crude biosurfactant) will reduce the interfacial tension between the liquid drop and the hydrophobic surface (oil); hence the drop will spread or collapse (Garg & Chatterjee, 2018; Tugrul & Cansunar, 2005). Another high throughput assay, penetration assay (PA) is based on contacting two insoluble phases (precipitation occurs) which causes colour change as an indicator of positive test due to the presence of moisture (culture supernatant containing biosurfactant), sensitive silica gel indicator that allows visual indication of biosurfactant containing supernatant penetration into the hydrophobic paste (Kavuthodi et al., 2015; Walter et al., 2010).

Two bacterial strains (E1, and F5) were finally found to be potential strains based on secondary screening results. The results of sheep blood agar method or hemolytic assay (HA) were found to be similar with Mulligan and Gibbs confirming the production of biosurfactant (Mulligan et al., 1989). Similar patterns of results were obtained by other researchers as well via haemolytic assay where clear zone of diameter was considered as qualitative indicator while screening for biosurfactant production (Panchariya et al., 2021; Rajesh et al., 2017; Thavasi et al., 2008). The measurement of surface tension (ST) is another reliable characteristic feature,

quantitative, and directly related to the surface activity by the biosurfactant producers (**Table 5.1**) where a good surface active metabolite can lower the surface tension of water from 72 to 35 dynes/cm (Youssef et al., 2004). In one scientific contribution, screening for biosurfactant production from *Actinimycetes nocardiopsis* A17 was assessed where they had reported reduction in surface tension to be 66.67 dyne/cm using drop count method via stalagmometer as it is an essential aspect to find CMC (critical micelle concentration) as above significant crude biosurfactant concentration, no further interfacial or surface activity is observed (Chakraborty et al., 2015).

Being amphiphilic, the hydrophobic moiety of biosurfactant (BS) helps in emulsification of any hydrocarbon compound and our study was carried out using six different hydrocarbons namely kerosene, petrol, mobil oil, lubricating oil, hexane, and toluene. It was observed that bacterial strains respond and emulsify different hydrocarbons and the emulsification is stable over a week **(Fig. 5.2)** and therefore this bioemulsification activity could be utilised in the biodegradation of hydrocarbon contaminated environment (Astuti et al., 2019; Long et al., 2017; Satpute et al., 2010).

The BATH assay is a characteristic feature of biosurfactant producing microorganisms that is based on the degree of adherence of bacterial cells to liquid hydrocarbons on account of production of surface active compounds known as biosurfactants(Nayarisseri et al., 2018; Thavasi et al., 2011). Nayarisseri and team reported >90% of affinity of bacterial cells towards hydrophobic substrate using *Bacillus* sps.(Nayarisseri et al., 2018). Hydrophobicity index of the bacterial cell surface as estimated through BATH assay using n-hexane is shown in **Table 5.1** where strain F5 illustrated maximum percentage in comparison to strain E1.

Based on screening results obtained, two bacterial strains (E1 and F5) were found to be best among all and hence, further studies were conducted with these two bacterial strains.

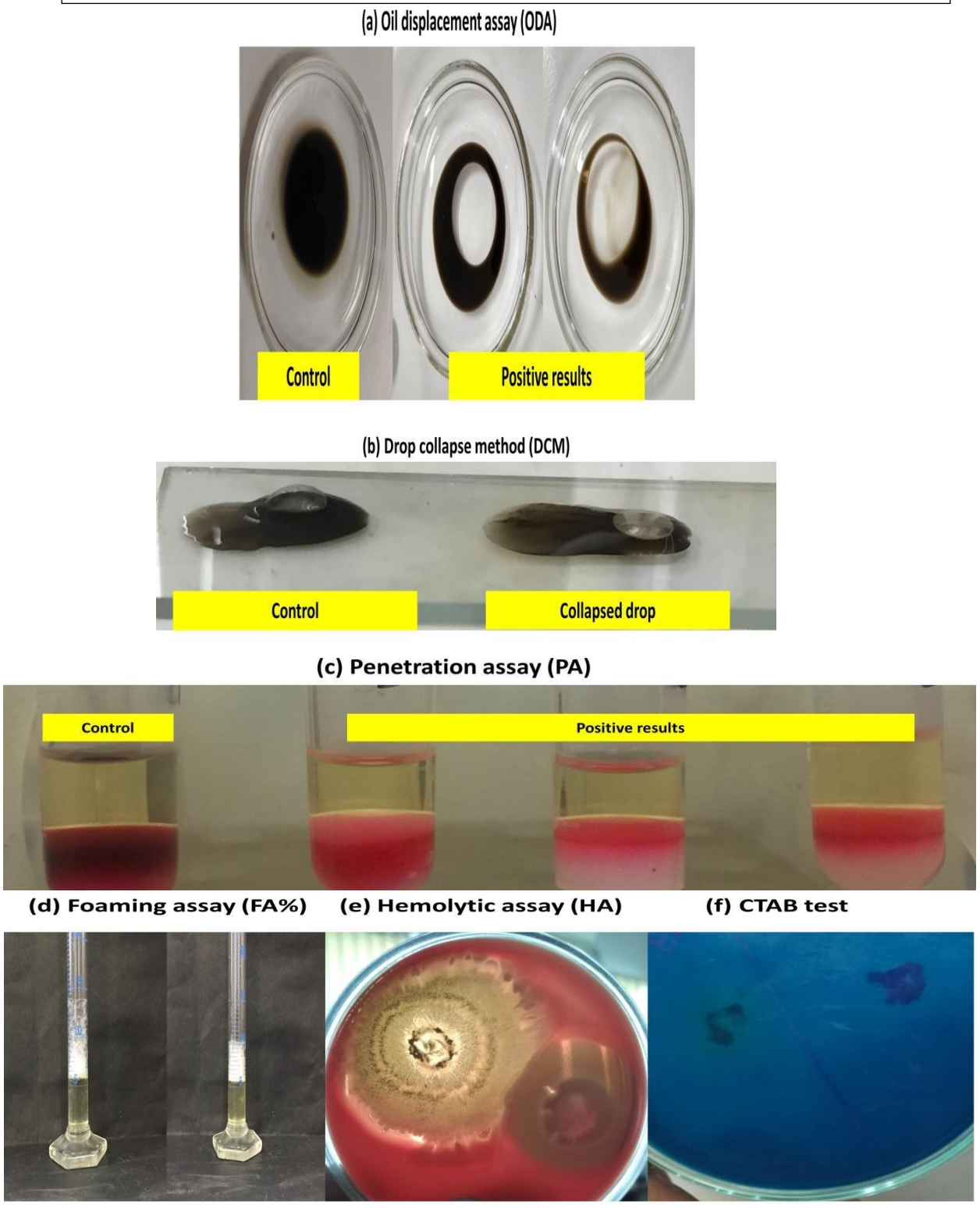

Figure 5.1 Screening results for potential bacterial strains

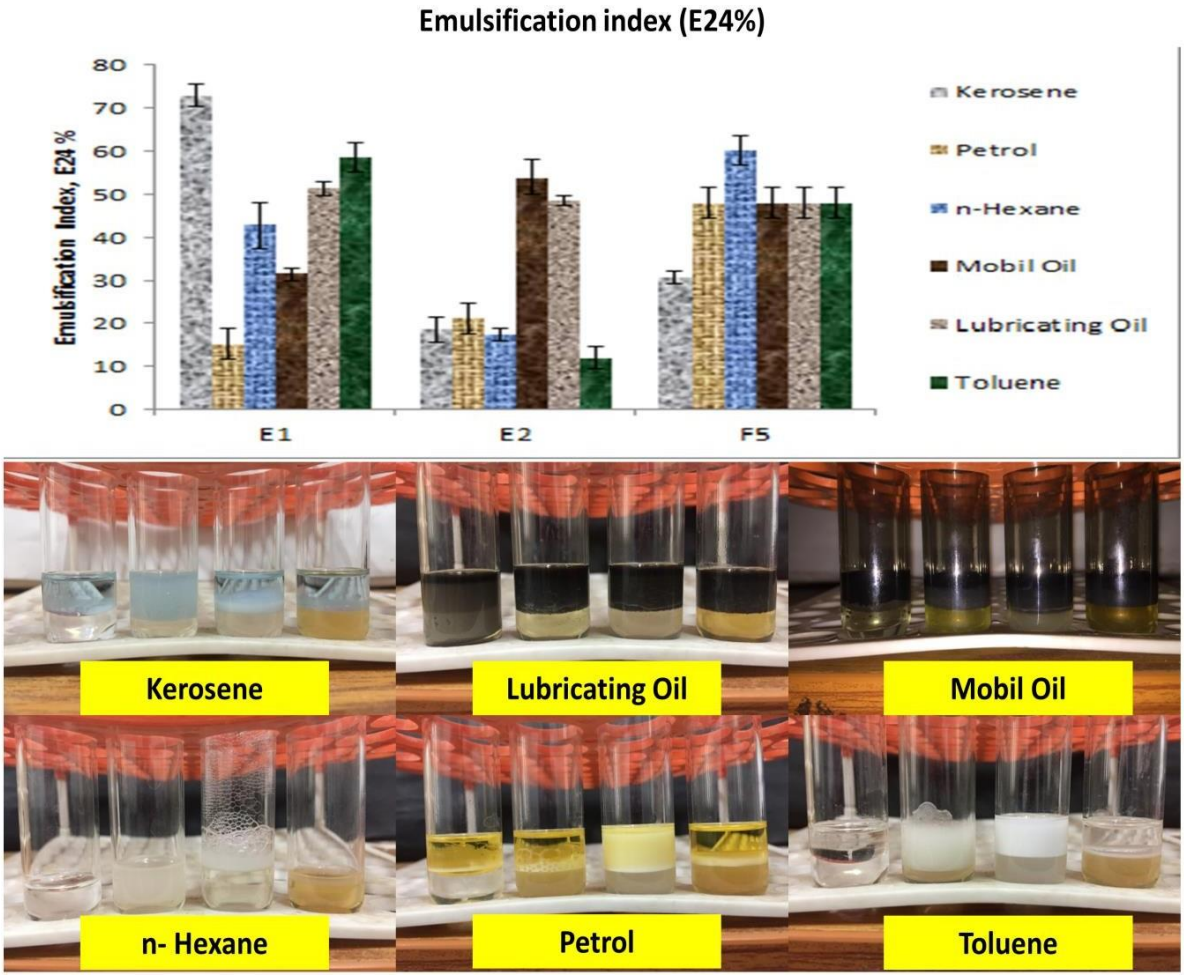

Fig. 5.2 Emulsification index (E_{24}%) of potential isolated bacterial strains

5.1.1 Morphological characterization of selected bacteria

The cultural characteristics of potent strains are shown in **Table 5.2** along with their morphology and Gram reaction.

Table 5.2 Morphological characterization of potential bacteria

Strain	Shape of the colony	Colony margin	Surface characteristics	Colony colour	Gram staining	Photograph
E1	**Circular**	**Raised**	**Mucoid**	**Creamy white translucent**	**Gram-positive**	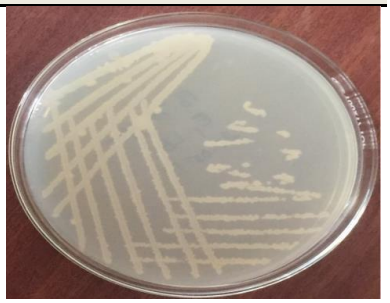
F5	**Circular**	**Flat irregular**	**Sticky**	**Yellowish-white transparent**	**Gram-negative**	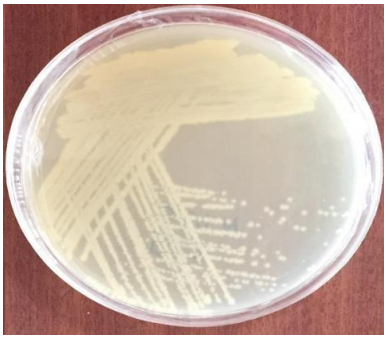

5.1.2 Biochemical Characterization of selected bacterial strains

Selected bacterial strains were also analysed biochemically and results obtained are depicted in **Fig. 5.3** and **Table 5.3**.

Figure 5.3 Biochemical characterizations of selected bacterial strains

Table 5.3 Biochemical characterization of selected bacterial strains

Biochemical tests	**E1**	**F5**
Indole test	**-**	**-**
Methyl red test	**-**	**+**
Voges Proskauer‟s test	**-**	**-**
Citrate utilization test	**-**	**-**
Glucose	**+**	**+**
Adonitol	**+**	**+**
Arabinose	**+**	**-**
Lactose	**-**	**-**
Sorbitol	**+**	**_**
Mannitol	**+**	**_**
Rhamnose	**-**	**+**
Sucrose	**+**	**+**

(Note: + = positive; - = negative)

5.1.3 Microscopic images of the selected bacterial strain under light and scanning electron microscope

The cell morphology and ultra-structure of the selected 2 bacterial strains is shown below:

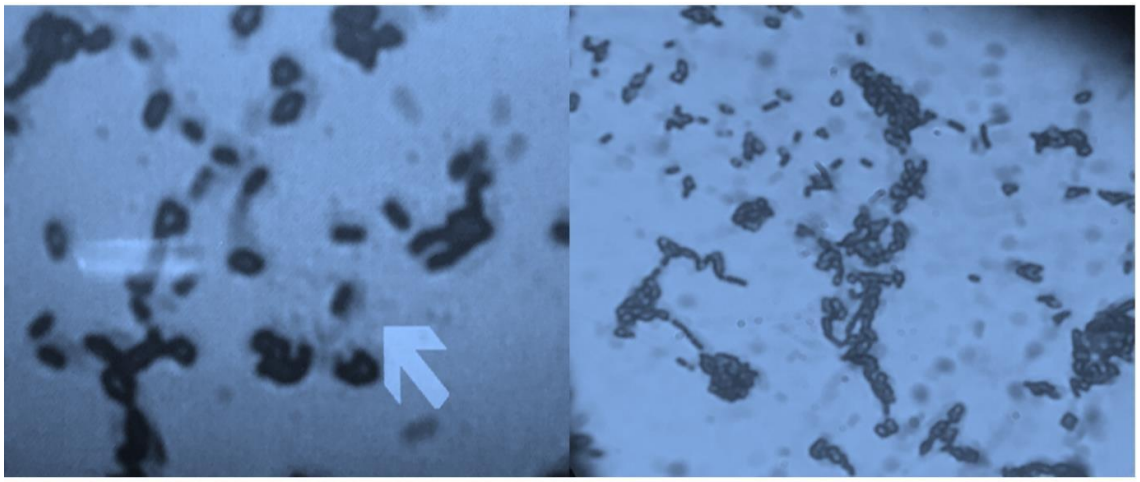

Figure 5.4 Microscopic images of the bacterial strain under light microscope

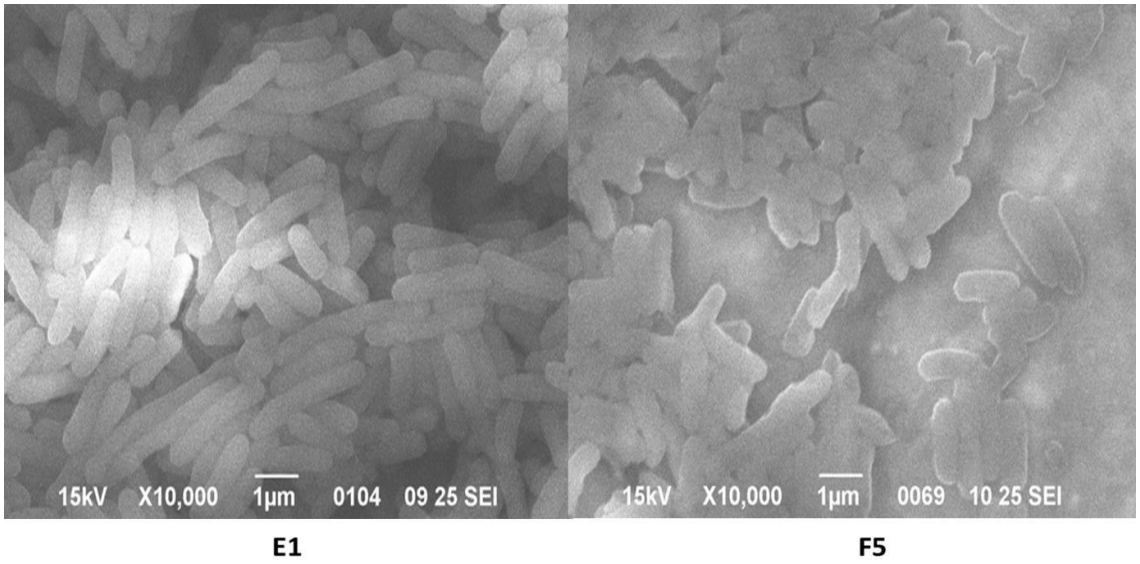

Figure 5.5 Microscopic images of the bacterial strain under scanning electron microscope

5.1.4 Molecular characterization of the isolated strains

For further confirmation of the strain, 16S rDNA sequencing was done and it revealed isolated strain E1 to be similar to *Bacillus haynesii* (accession no. MN047081), and strain F5 to be similar to *Pseudomonas aeruginosa* (accession no. MN104806) with similarity level up to 97.34%, and 99.74% respectively as shown in **Fig. 5.6**

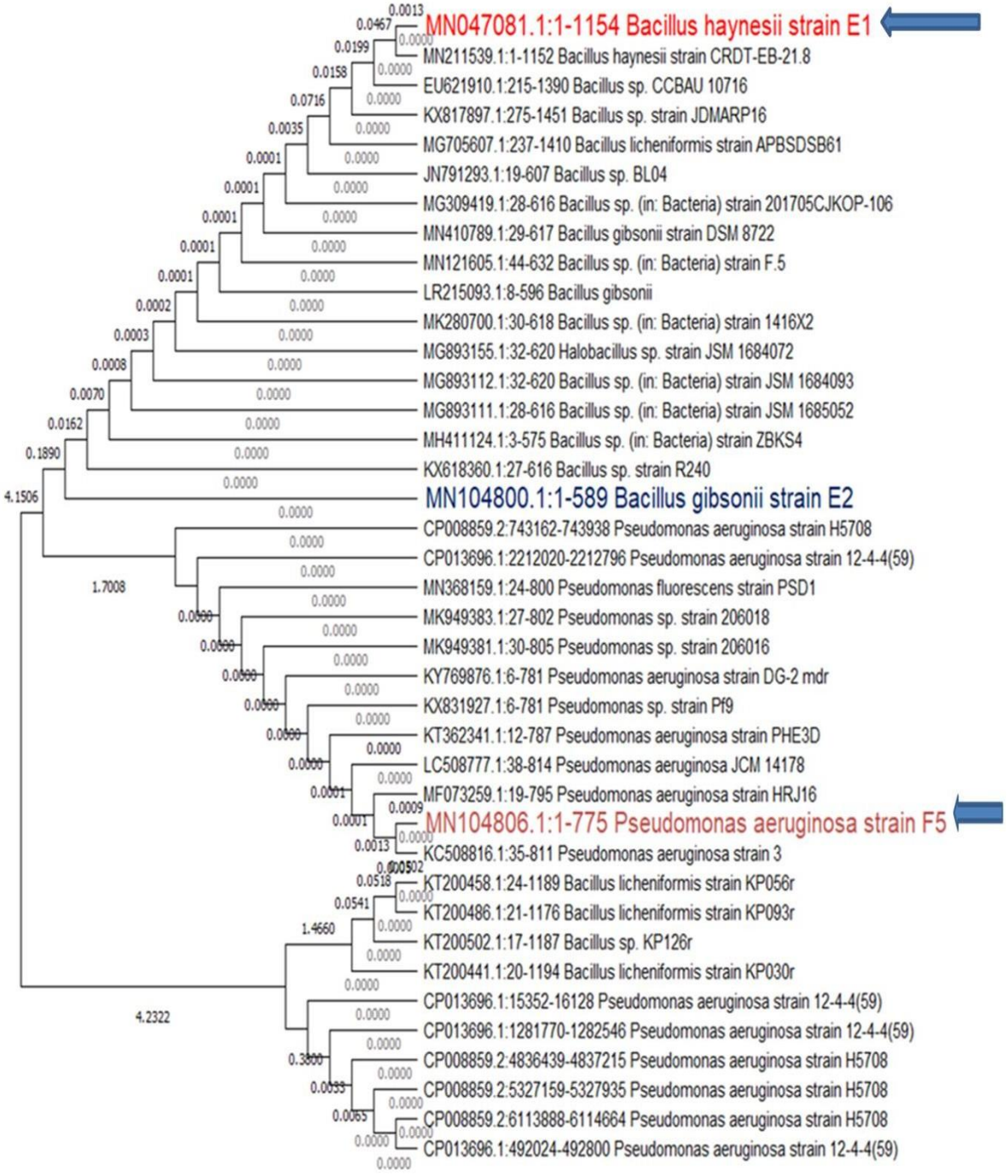

Figure 5.6 Phylogenetic tree for bacterial strain E1 and F5

5.1.5 Biosurfactant production and its related studies

The mass biosurfactant production by the potential strains and its extraction was done for further studies as shown in **Fig. 5.7**.

Figure 5.7 Schematic representations of biosurfactant production and extraction

5.1.5.1 Chemical analysis of the extracted biosurfactant

The following results were obtained for the chemical analysis by selected bacterial strains as shown in **Table 5.4 and Fig. 5.8**:

Table 5.4: Chemical analysis of biosurfactant produced by selected bacterial strains

	Chemical characterization					
Strain	**Anthrone test**	**Iodine test**	**Saponification test**	**Glycolipid test**	**Rhamnolipid test**	**Ninhydrin test**
E1	Negative	Negative	Positive	Negative	Negative	Positive
F5	Positive	Positive	Positive	Positive	Positive	Negative

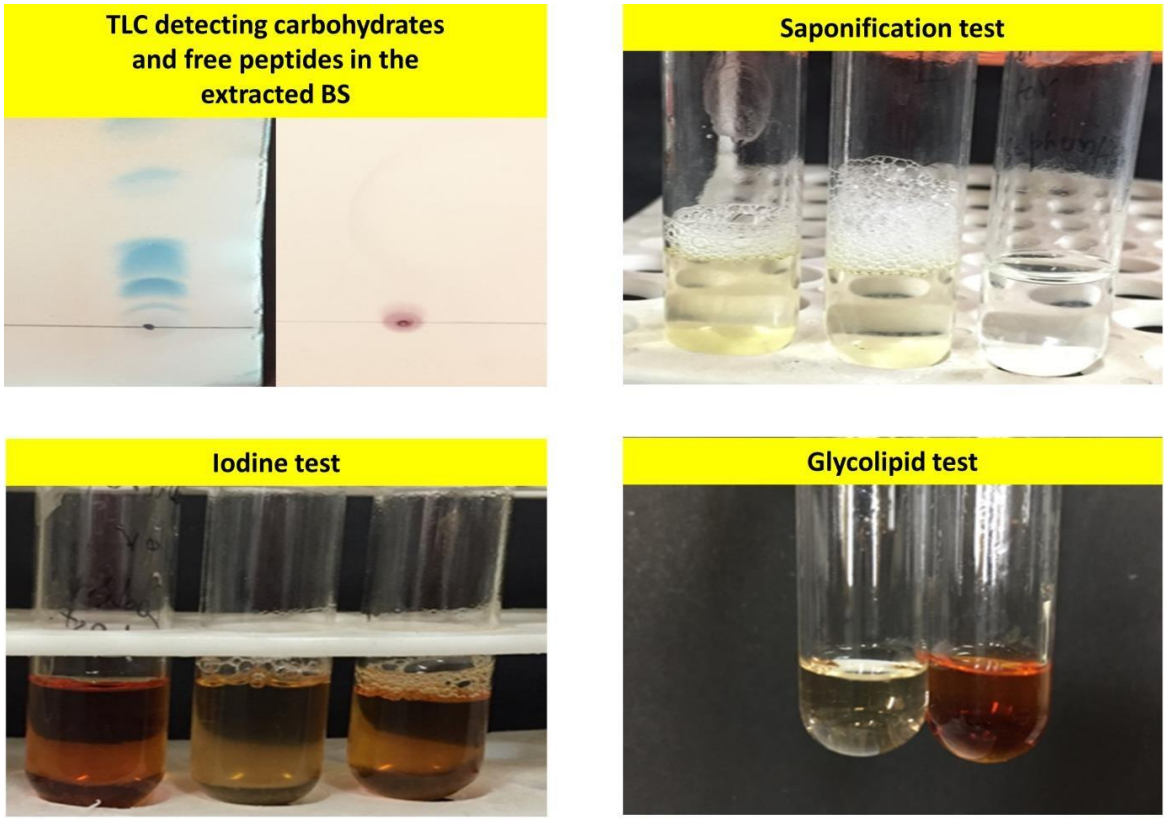

Figure 5.8: Chemical analysis of biosurfactant produced by selected bacterial strains

TLC revealed a positive reaction with ninhydrin reagent (violet spots on TLC; formation of Ruheman‘s purple complex) depicting the peptide nature of the extracted biosurfactant molecule obtained from strain E1 (*Bacillus haynesii*). Results obtained were comparable with lipopeptide (LP) surfactant and are synonymous as reported by (Dlamini et al., 2020; Goswami & Deka, 2019; Kiran et al., 2010). The appearance of pale yellow to orange colour on addition of iodine solution confirmed the presence of sugar moiety in the extracted biosurfactant for strain F5. The positive iodine test indicated the presence of monosaccharide‘s instead of polysaccharides in the F5 biosurfactant (George & Jayachandran, 2013; Ishaq et al., 2015). The strain F5 (*Pseudomonas aeruginosa*) showed positive reactions for anthrone test, glycolipid test and iodine test i.e. presence of carbohydrates were detected. The appearance ofbluish-green spots on TLC plate indicated the presence of carbohydrate in the extracted biosurfactant from strain F5 while the appearance of light orange colour in phenol: H_2SO_4 (glycolipid test) indicated the presence of glycolipid group in the extracted biosurfactant. Similar results were also reported in the previous literatures (García-Reyes & Yañez-Ocampo, 2021; Ishaq et al., 2015; Patowary et al., 2015a;

Shalini et al., 2017). Both the strains (E1 and F5) showed positive results for saponification test. In this test, NaOH causes the saponification of the extracted biosurfactant i.e. foam appearance confirming the presence of lipids in the extracted biosurfactant (Marchut-Mikolajczyk et al., 2018; Patowary et al., 2015a; Patowary et al., 2015b). Similar results indicating formation of white foaming precipitates were also observed in other studies confirming positive saponification test by selected bacterial strains (Femina Carolin et al., 2020). Therefore, the results of chemical analysis of the extracted biosurfactant from E1 and F5 illustrates that the extracted biosurfactant belong to lipopeptide group of class surfactin and glycolipid group of class rhamnolipid respectively.

5.1.5.2 Critical micelle concentration (CMC) and biosurfactant stability against environmental stress

The extracted biosurfactant from strain E1 and F5 showed a CMC of 50 and 40 mg/L, respectively. This is the minimum concentration at which the ability of the biosurfactant to reduce surface tension is maximum as shown in **Fig. 5.9**. Above critical micelle concentration (CMC), increase in biosurfactant concentration does not affect reduction in surface tension value (Rodrigues et al., 2006).

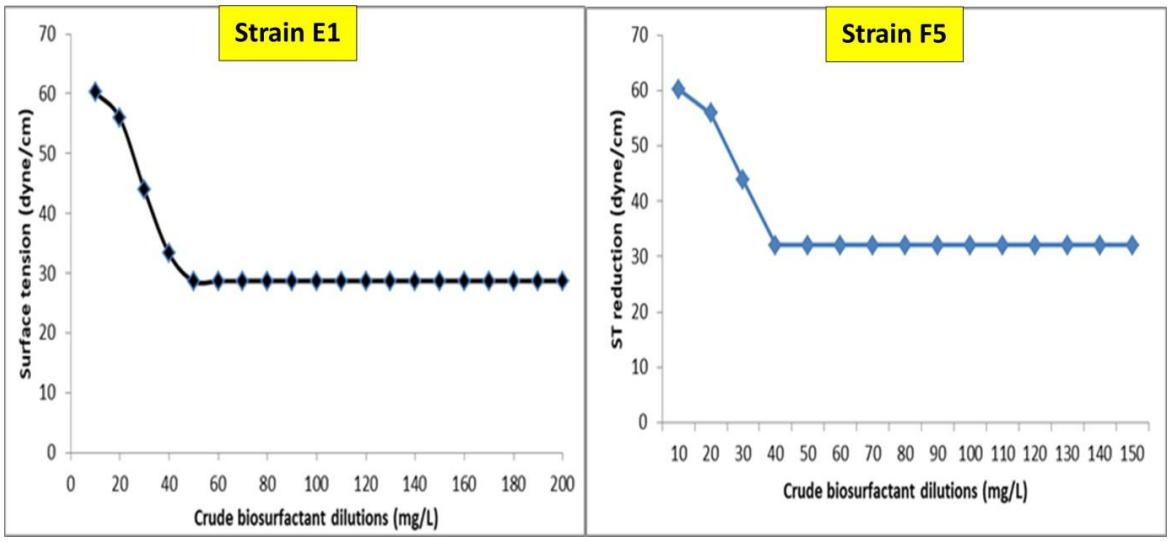

Figure 5.9 CMC of extracted biosurfactant from *Bacillus haynesii* strain E1 and *Pseudomonas aeruginosa* strain F5

The effect of pH, temperature, and salinity on the stability of the biosurfactant has been demonstrated in **Fig. 5.10**. The biosurfactant produced by strain E1 exhibited good stability in the pH range from 2 to 12 with a maximum 1.833 ± 0.24 cm oil displacement activity. The E_{24}% measured under varied pH values showed elevation from 15.83 ± 0.24 to 59.93 ± 0.09 % when shifted from acidic to alkaline conditions. These findings are in accordance with the previous reports suggested for biosurfactants extracted from *Bacillus* sps. (Goswami & Deka, 2019; Yuliani et al., 2018). Similar pattern of results were obtained with BS-VSG4 giving a maximum emulsification index of 64.1% at pH 7 (Giri et al., 2019) while crude lipopeptide biosurfactant from *Bacillus subtilis* showed a good stability over a wide pH range from 2 to 9 (Bouassida et al., 2018). From these findings, it can be conferred that for optimum utilization of biosurfactant for bioremediation, slightly alkaline environment (pH 6 to 8) will be the better.

Similarly, under the influence of different temperature ranges, extracted biosurfactant showed increased oil displacement activity with an increase in temperature from 30 to 70 ˚C. At 90 ˚C, there is a slight decrease in the diameter of the displaced oil by the extracted biosurfactant that could be attributed to the beginning of activity loss of the biosurfactant (Purwasena et al., 2019), and approximately 0.3 ± 0.14 cm zone of diameter was recorded at 121 ˚C. The E_{24}% activity of the biosurfactant was found to be most at 30 ˚C (74.83 ± 0.24 %) and thereafter, it showed moderate decline up to 90 ◦C (70.58 ± 0.66 %). The lowest E_{24}% value measured was 24.83 ± 0.24 % at 121 ˚C. From the data values, it can be concluded that the optimum temperature range for the activity of the thermo-stable biosurfactant lies from 30 to 90 ˚C that may facilitate its application in diverse environmental conditions. The temperature stability studies with *Bacillus subtilis* indicated the stable activity of the crude biosurfactant in the range from 80% to 50% over 60 min of incubation at 70 and 80 ºC respectively (Bouassida et al., 2018; Ram et al., 2019).

Further, the oil displacement activity of the extracted biosurfactant at different salt concentrations remained almost the same (~3.4 ± 0.08 mm) with slight precipitation noted at higher salt concentrations (> 6%). The elevated E_{24}% was measured at higher salt concentrations between 10 to 20% (~ 64.9 ± 0.29%). The results obtained were supported by the previous literature depicting the overall good stability of the

extracted biosurfactant under a diverse range of factors studied here (Liu et al., 2021; Mhamdi et al., 2017; Somoza-Coutiño et al., 2020).

The stability of the extracted biosurfactant from *Pseudomonas aeruginosa* F5 was also found to be quite good (**Fig. 5.10**). It exhibited good stability at pH range from 2 to 12 with a maximum 3.93 ± 0.05 cm oil displacement activity obtained at pH 10. There was an increment in oil displacement activity with the enhancement in the value of pH range up to 10. The emulsification index (E_{24}%) measured under varied pH values showed elevation from 10 ± 4.08 to 79.96 ± 0.05 % when shifted from acidic to alkaline conditions up to pH 10. These findings were in accordance with the previous reports suggested for biosurfactants extracted from *Pseudomonas* sps (Abouseoud et al., 2008; Chen et al., 2018; Somoza-Coutiño et al., 2020; Sun et al., 2019). In one study involving *Pseudomonas* sps., the instability of the biosurfactant in acidic conditions on account of precipitation and insolubility was observed and found to be stable (alkali resistant) between pH 6 to 12, similar findings were presented in the present study as well (Chen et al., 2018). Under the effect of different temperature ranges, the extracted biosurfactant showed decreased oil displacement activity and E24 % with an increase in temperature from 30 to 121 °C. At 30 °C, the maximum oil displacement activity in terms of the diameter of the displaced oil by the extracted biosurfactant was found to be 4.3 ± 0.17 cm and E24% value as 64 ± 1.4 % that could be attributed to the maximum stability of the biosurfactant. There was a decrease in the oil displacement activity and E24% value with the increase in the salt concentrations from 2 to 20 % depicting the lower structural and compositional stability of the extracted biosurfactant at higher saline conditions. The results obtained were similar to the previously published reports (Khademolhosseini et al., 2019; Silva et al., 2010; Sood et al., 2020).

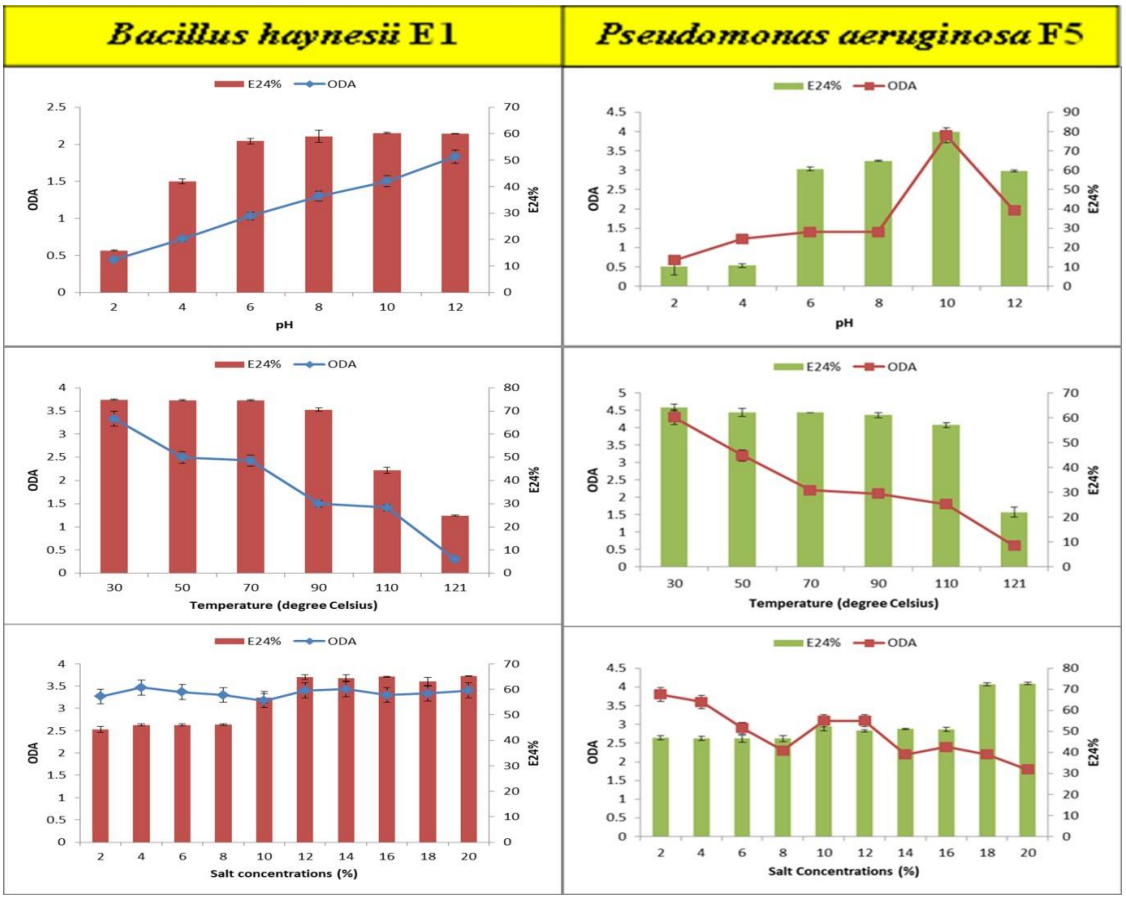

Figure 5.10 Effect of pH, temperature, and salt concentration on biosurfactant performance

5.1.5.3 Characterization of the extracted biosurfactant

Fourier transform infrared spectroscopy (FTIR)

FTIR characterization of the biosurfactant extracted from the strain E1

With FTIR analysis, the partially purified biosurfactant showed peaks at wave number 3308.4, 2946.9, and 2834.1 cm^{-1} indicating carbon atom stretching defining lipopeptide nature of the molecule, aliphatic chain, and carbon-containing alkyl groups (-C-CH_3) along with long carbon-hydrogen (C-H) stretching respectively (Bezza & Chirwa, 2015; Cruz et al., 2018). The peak at 1656.8 cm^{-1} depicts the bonding of a lactone ring having amino group (N-H) bending of primary and secondary amide and at 1450.2 cm^{-1} indicates the presence of a carbonyl group (C═O) stretching attached to the carbon chain in the biosurfactant molecule. The same patterns of results were obtained in previous literatures depicting peptide functional groups (Lin et al., 1994; Pradhan et al., 2013). The peak at 1114.4 cm^{-1} showed

carbon-oxygen (C-O) deformation and all this leading to the surfactin nature of the partially purified biosurfactant molecule as represented in **Fig. 5.11.**

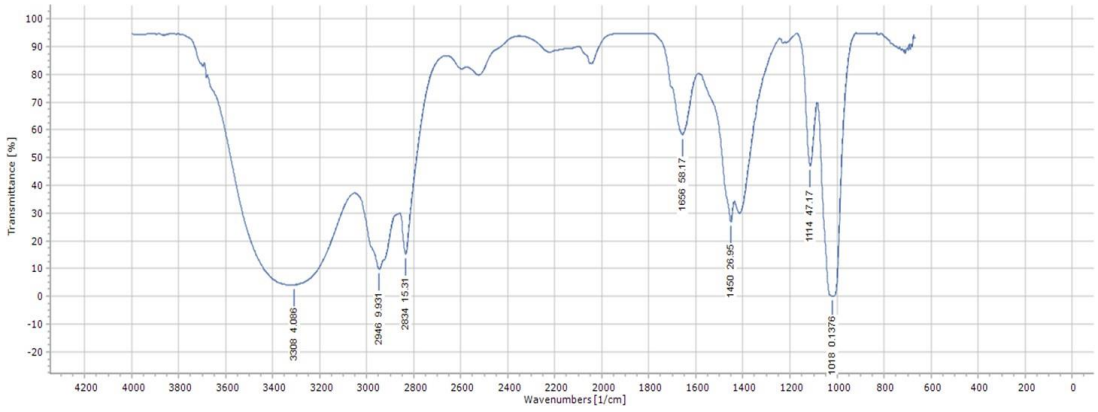

Figure 5.11 FTIR spectroscopy of extracted biosurfactant from *Bacillus haynesii* strain E1

FTIR characterization of the biosurfactant extracted from the strain F5

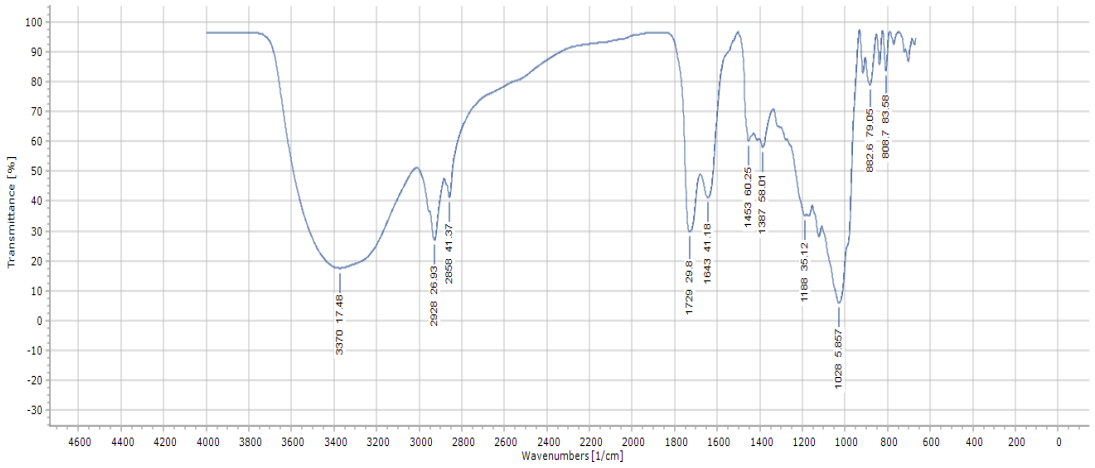

Figure 5.12 FTIR spectroscopy of extracted biosurfactant from *Pseudomonas aeruginosa* strain F5

Spectral analysis revealed that crude biosurfactant showed strong absorption bands at 3370 cm^{-1} indicating stretching of the hydroxyl (─OH) group while peaks obtained at 2928 cm^{-1} and 2858 cm^{-1} ascertained the presence of long aliphatic hydrocarbon (carbon-hydrogen stretching) ─C─H stretching as methylene (─CH_2) and methyl (─CH_3) moiety (Priji et al., 2017; Sabarinathan et al., 2021). An absorption band seen at 1729 cm^{-1} corresponded to the carbonyl (─C═O) stretching of ester compounds and a peak at 1643 cm^{-1} showed ─COO─ group **(Fig. 5.12**). The band at 1028 cm^{-1}

indicated ─C─O─C stretching in rhamnose depicting the structure similar to the rhamnolipids (Pornsunthorntawee et al., 2008; Saikia et al., 2012).

Proton nuclear magnetic resonance spectroscopy (^{1}H-NMR)

A comparative assessment of ^{1}H-NMR spectrum of strain E1 with the previously published reports (Sousa et al., 2014), established the nature of the extracted biosurfactant to be of lipopeptide and more precisely to be a surfactin isomer. The ^{1}H-NMR spectrum in **Fig. 5.13** illustrated signals at δ= 6.5 – 7.3 ppm corresponding to the benzene ring protons and imide (─NH) binding protons while signals received at δ = 1.2 – 4.5 ppm were of ά/β/γ- protons of amino acid sequences (Joshi et al., 2015; Liu et al., 2016). The concentration at δ = 0.5 – 1.5 ppm corresponded to the methylene (─CH_2) group attached to the fatty acid chain and terminal methyl (─CH_3) group in the surfactin type of biosurfactant . The presence of lactone ring was observed at δ = 4.6-5.2 ppm and lipopeptide monoester (GluOMe) peaks at δ = 3.5-3.8ppm (Biria et al., 2010).

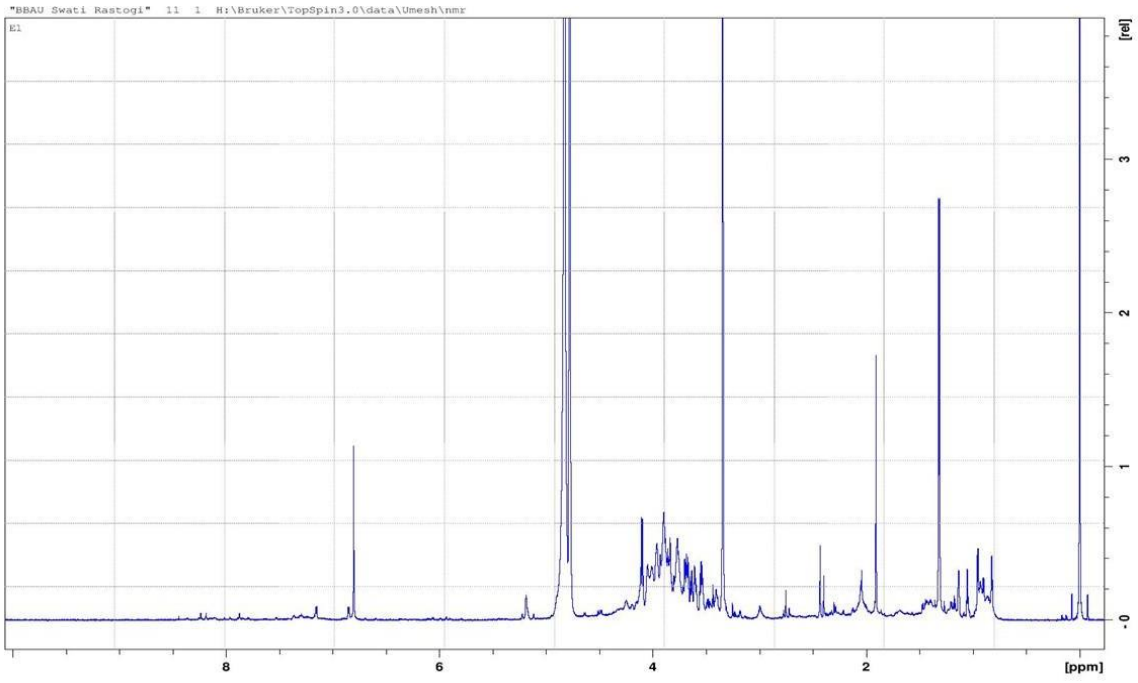

Figure 5.13 ^{1}H-NMR spectrum of extracted biosurfactant from *Bacillus haynesii* strain E1

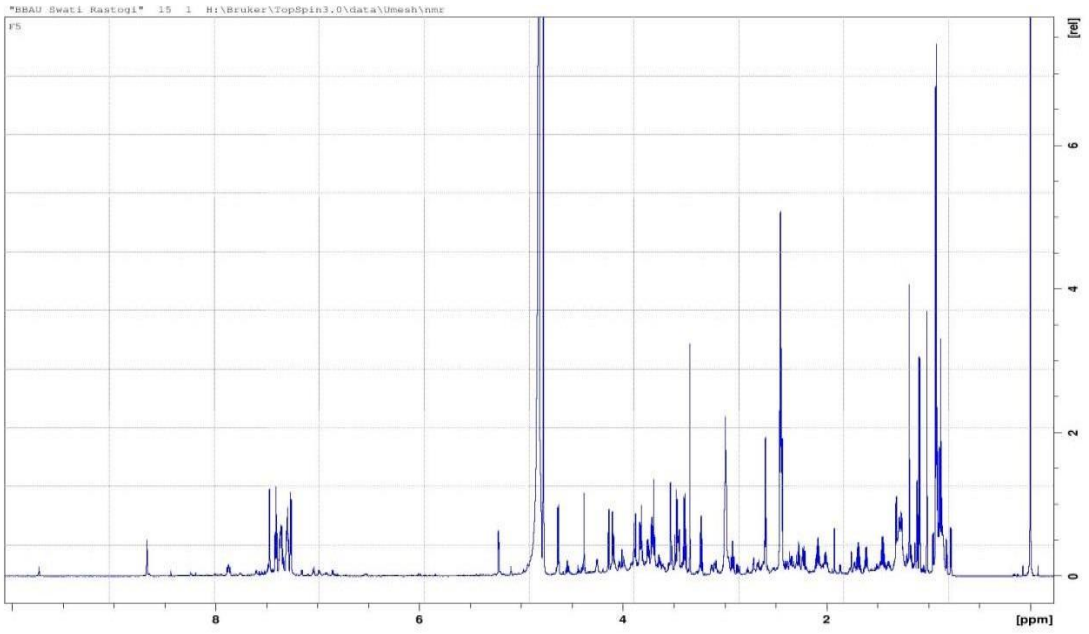

Figure 5.14 ^{1}H-NMR spectrum of extracted biosurfactant from *Pseudomonas aeruginosa* strain F5

An understanding of ^{1}H-NMR spectrum of strain F5 estimated that the crude biosurfactant belongs to a glycolipid class (a rhamnolipid) as shown in **Fig 5.14**. The corresponding signals observed from δ= 0.88 to 1.1/1.2 ppm corresponded to the presence of methyl (─CH_3) group on lipid [beta (β)-hydroxy fatty acids] and rhamnose moiety having singlet and doublet multiplicity respectively (Lotfabad et al., 2010; Sharma et al., 2019). The peaks obtained at concentration, δ = 1.26 ppm is of methylene (─CH_2)$_5$ while at δ = 2.5 ppm indicated a multiplet of aldehyde (─CHO) or carboxylic (─CH_2COO) present on the chain of (β)-hydroxy fatty acids (Pornsunthorntawee et al., 2008; Shekhar et al., 2019). The peak of rhamnose as (─CH─OH) was seen at δ = 3.33 to 3.37 ppm and δ = 4.9 ppm respectively (Oluwaseun et al., 2017; Victor et al., 2019). Also, a doublet peak at δ = 5.27 ppm corresponded to the rhamnose (─CH─O─C).

Liquid chromatography- mass spectrometry (LC-MS)

Our findings for the characterization of biosurfactant from strain E1 were further affirmed by mass spectra obtained through LC-MS analysis [**Fig. 5.15(a-d)**]. The m/z peaks at 1008.9, 1022.8, 1026.8, 1007.9, 685.4, and 683.5 suggested that the extracted biosurfactant is a surfactin C-13 isomer (Mohd Isa et al., 2020; Pecci et al., 2010).

The peak at 1026.8 represented a linear nature of surfactin which are characterized as uncyclized intermediates in the biosynthetic pathway of surfactin (Pathak et al., 2014). Our findings are supported by the previously published reports of (Deng et al., 2017; Jasim et al., 2016).

(a)

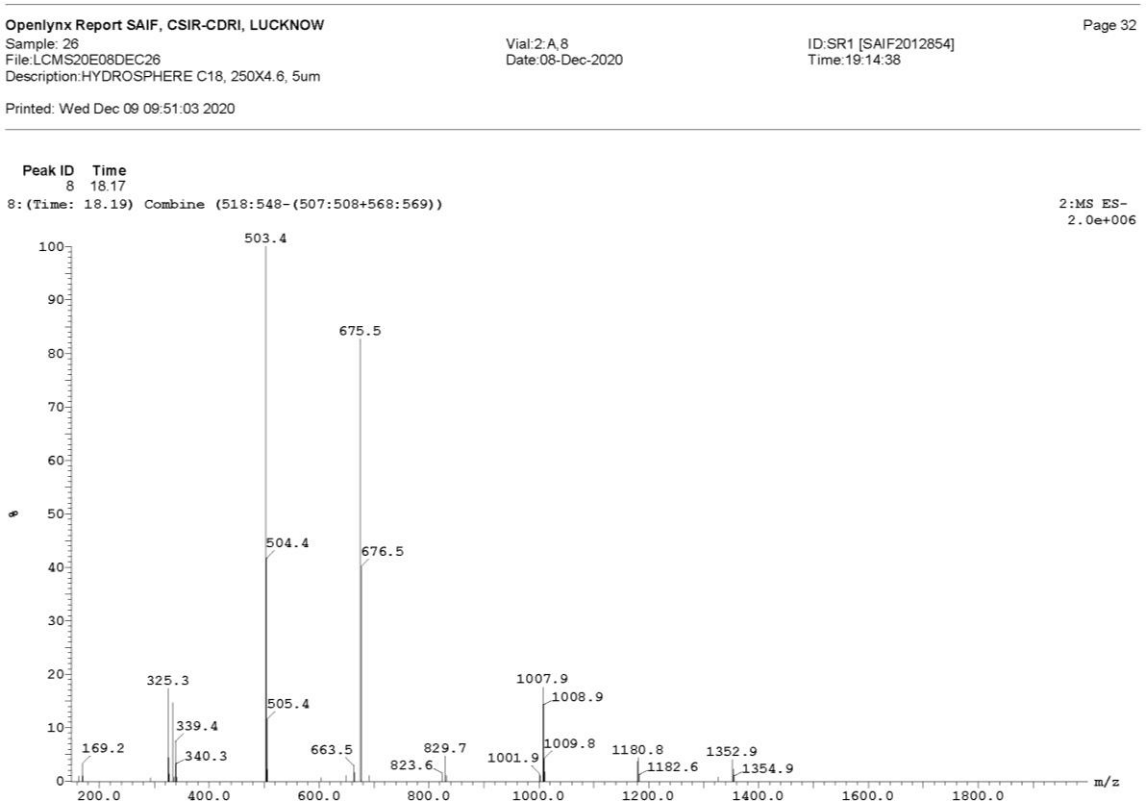

(b)

Openlynx Report SAIF, CSIR-CDRI, LUCKNOW Page 8
Sample: 26 Vial:2:A,8 ID:SR1 [SAIF2012854]
File:LCMS20E08DEC26 Date:08-Dec-2020 Time:19:14:38
Description:HYDROSPHERE C18, 250X4.6, 5um

Printed: Wed Dec 09 09:51:03 2020

Peak ID Time
8 18.17
8:(Time: 18.17) Combine (518:548-(507:508+569:570))

1:MS ES+
4.2e+005

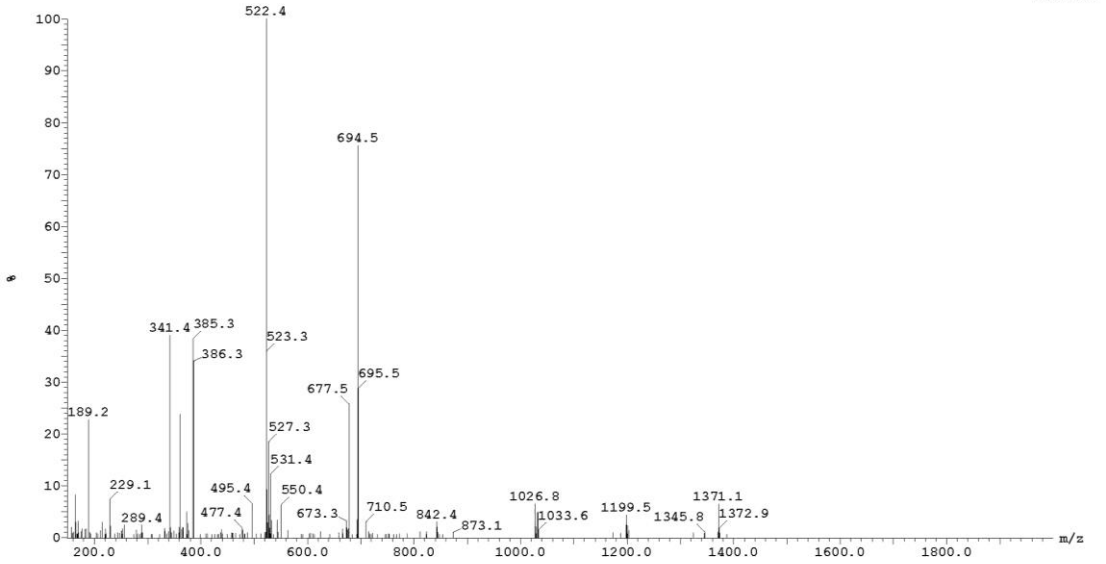

(c)

Openlynx Report SAIF, CSIR-CDRI, LUCKNOW Page 15
Sample: 26 Vial:2:A,8 ID:SR1 [SAIF2012854]
File:LCMS20E08DEC26 Date:08-Dec-2020 Time:19:14:38
Description:HYDROSPHERE C18, 250X4.6, 5um

Printed: Wed Dec 09 09:51:03 2020

Peak ID Time
16 23.80
16:(Time: 23.80) Combine (683:713-(668:669+722:723))

1:MS ES+
8.9e+006

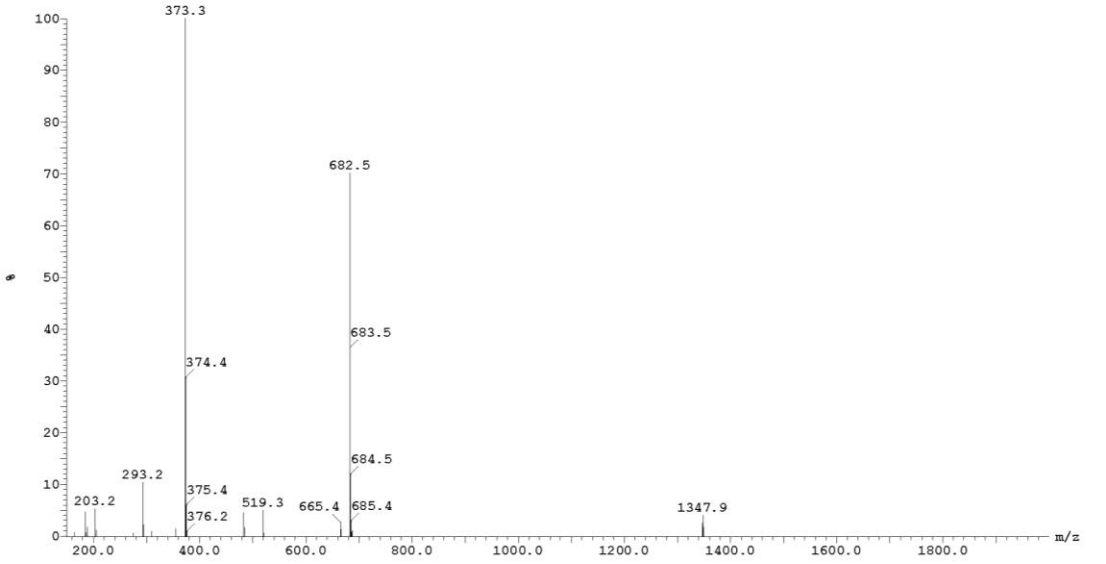

(d)

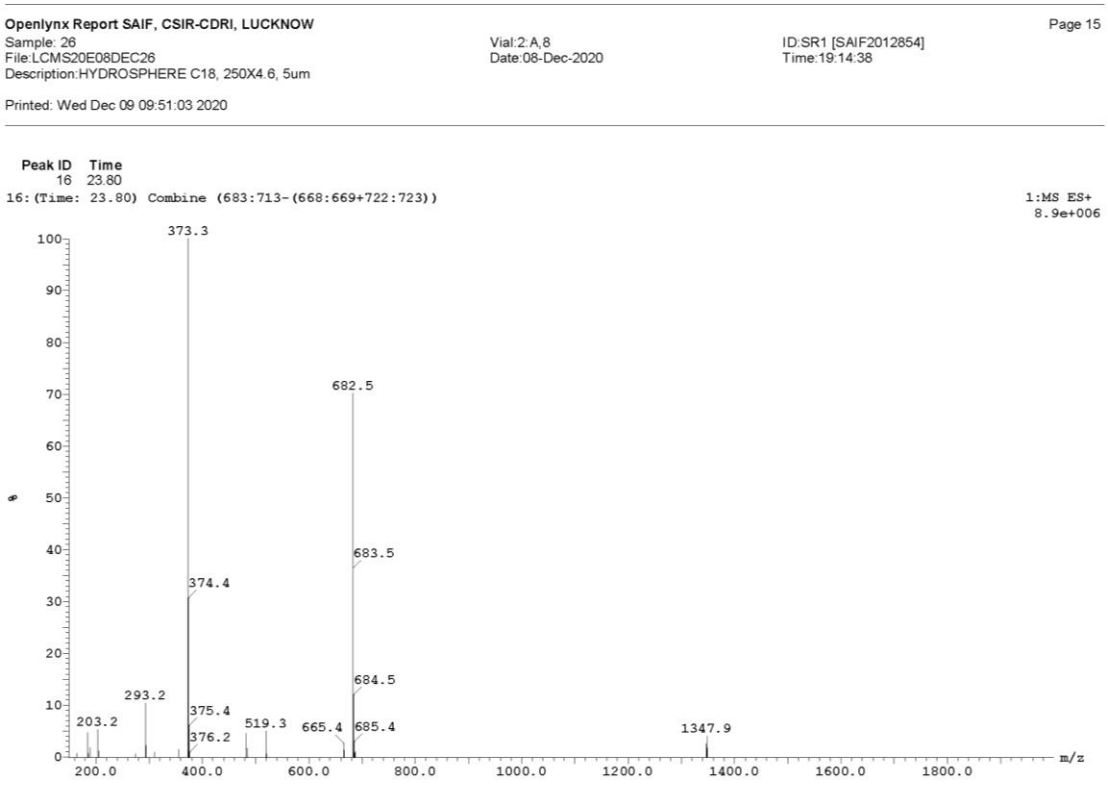

Figure 5.15 LC-MS profile (a-d) of extracted biosurfactant from *Bacillus haynesii* strain E1

Comparative analysis and earlier spectral findings in case of strain F5 reported the extracted biosurfactant to be of rhamnolipid nature where mono-rhamnolipids were found to be in greater extent than the di-rhamnolipids [**Fig. 5.16 S(a)-S(d)**]. The respective m/z peaks were observed at 678.5, 576.3, 516.6, 515.3, 503.3 and our results obtained were also found to be congruent with previous studies (Bajpai et al., 2020; Gogoi et al., 2016; Thaniyavarn et al., 2006).

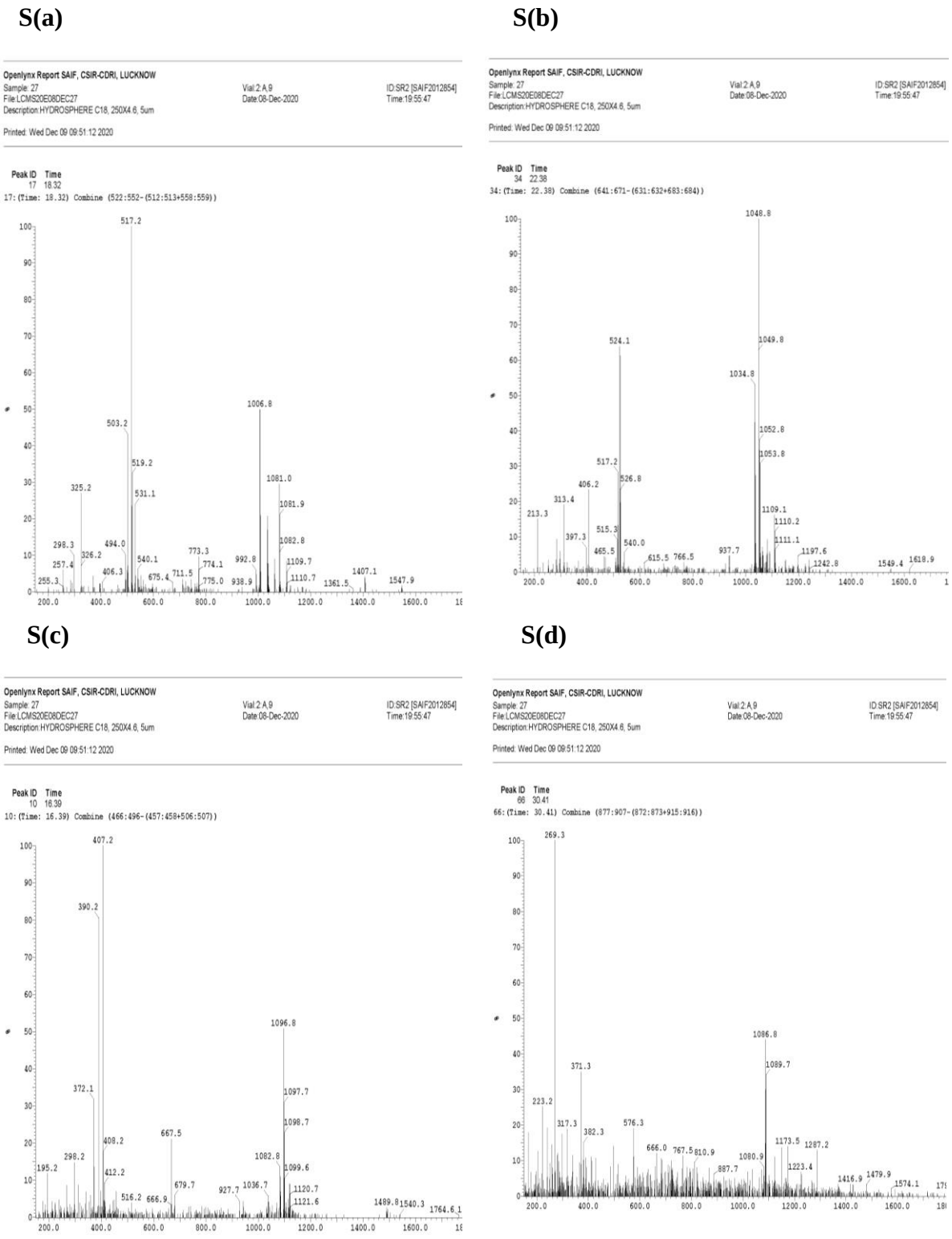

Figure 5.16 LC-MS profile (Sa –Sd) of extracted biosurfactant from *Pseudomonas aeruginosa* strain F5

5.1.5.4 Optimization of biosurfactant production by *Bacillus haynesii* and *Pseudomonas aeruginosa* using biowaste

For the production of maximum biosurfactant using orange peel extract (biowaste), the four process parameters were evaluated using central composite design (from Design-Expert version 8 software) for both the isolated bacterial strains and results are shown in **Table 5.5** and **Table 5.7** respectively**.** The individual and interactive effects of the variables i.e., biowaste concentration (A), temperature (B), pH (C), and agitation rate (D) were studied. The ST reduction was taken as the response. The least-square method was applied to the experimental data and the second-order polynomial **Eq. 3.8** (provided in chapter 3, section 3.3.6.3.4), gave the apt explanation of surface tension reduction in terms of only significant terms. In case of optimization done for *Bacillus haynesii*, on submitting the model equation to analysis, the coefficient of regression, R^2 was measured to be 0.9820 indicating that 98.20 % of the experimental data were congruent with the data predicted by the model. The predicted R^2 (0.9088) was found to be in reasonable agreement with the adjusted R^2 of 0.9653 explaining the validity of the model. The closer the value of the regression coefficient (R^2) to unity; the better is the correlation between the obtained and predicted value (Almansoory et al., 2017; Mutalik et al., 2008).

The validity of the model and interaction of factors with their effect for *B. haynesii* is explained through the ANOVA table **(Table 5.6).** A Quadratic model was suggested by the Design Expert software. The model terms with ‗Prob>F' < 0.05 are considered significant terms. In our study, the model terms A, B, C, D, AD, BC, BD, A^2, B^2, C^2, and D^2 are significant terms. The appropriateness of the model applied was suggested by analysing normal plots of residuals, an approximately straight line indicates the normal distribution and a good fit model which can be applied to predict the value of surface tension reduction by produced biosurfactant within a given set of the independent variables.

The optimized values of four factors are biowaste concentration (10%; v/v), temperature (35°C), pH (6), and agitation rate (130 rpm). The maximum surface tension reduction value was estimated to be 33.04 dyne/cm (**Run 13** from **Table 5.5**) which yielded an approximately 3.7 g/L of biosurfactant using orange peel extract as carbon substrate. This optimized value obtained using biowaste was found to be approximately equal to the yield value using dextrose as carbon substrate (~3.9g/L), suggesting utilization of such biowastes over chemical and expensive carbon

substrates leading to reduce the operational cost of the production process at a large scale.

Table 5.5: A four variable central composite design (CCD) design with experimental and predicted surface tension (ST) reduction (dyne/cm) values for *Bacillus haynesii* (E1).

Run	A: Biowaste Concentration (%)	B: Temperature (˚C)	C: pH	D: Agitation rate (rpm)	Experimental surface tension reduction (dyne/cm)	Predicted surface tension reduction (dyne/cm)
1	10	35	6	130	35.56	34.93
2	6	35	8	130	60.34	59.44
3	4	30	5	150	67.23	67.12
4	4	40	5	150	62.32	61.12
5	8	30	7	110	52.12	52.92
6	6	25	6	130	68.25	65.36
7	6	35	6	130	35.93	34.93
8	6	35	6	170	61.45	59.29
9	2	35	6	130	46.23	45.48
10	4	40	5	110	62.42	63.35
11	4	40	7	150	58.32	59.60
12	8	40	5	150	52.65	53.20
13	6	35	6	130	33.04	34.93
14	8	30	5	110	58.23	57.71
15	6	35	6	130	35.63	34.93
16	6	35	6	130	33.22	34.93
17	8	30	7	150	48.46	48.29
18	4	30	7	110	54.36	54.57
19	6	35	4	130	65.23	65.75
20	8	30	5	150	52.30	54.69
21	6	35	6	130	36.98	34.93
22	4	30	7	150	54.23	57.16
23	8	40	7	110	65.42	66.30
24	8	40	5	110	65.98	62.65
25	6	35	6	90	64.39	66.16
26	4	30	5	110	62.32	62.92
27	6	45	6	130	70.23	72.74
28	8	40	7	150	56.23	55.23
29	6	35	6	130	34.76	34.93
30	4	40	7	110	66.23	63.44

Table 5.6: Anova analysis for the quadratic model for *Bacillus haynesii* E1

	Sum of Squares	df	Mean Square	F-value	p-value	
Model	4202.47	14	300.18	58.54	<0.0001	**Significant**
A- Agro waste concentration	137.19	1	137.19	26.76	0.0001	
B- Temperature	81.70	1	81.70	15.93	0.0012	
C-pH	59.72	1	59.72	11.65	0.0039	
D-Agitation speed	70.80	1	70.80	13.81	0.0021	
AB	20.30	1	20.30	3.96	0.0652	
AC	12.64	1	12.64	2.46	0.1373	
AD	52.13	1	52.13	10.17	0.0061	
BC	71.15	1	71.15	13.88	0.0020	
BD	41.34	1	41.34	8.06	0.0124	
CD	2.59	1	2.59	0.5056	0.4880	
A2	57.19	1	57.19	11.15	0.0045	
B2	1995.83	1	1995.83	389.26	<0.0001	
C2	1312.11	1	1312.11	255.91	<0.0001	
D2	1324.95	1	1324.95	258.41	<0.0001	
Residual	76.91	15	5.13			
Lack of Fit	64.70	10	6.47	2.65	0.1469	**Not significant**
Pure Error	12.21	5	2.44			
Cor Total	4279.38	29				

5.1.5.4.1 Response surface plots

The 3D response surface plots obtained, explain the interactions of the two independent variables at a time by keeping the other variables constant. The interactions of the variables were studied for minimum surface tension that corresponded to the maximum biosurfactant production. From the Anova **Table 5.6**, the model terms AD (Agro-waste concentration X agitation speed), BC (Temperature X pH), and BD (Temperature X agitation speed) were found to be significant for the

selected design ($p<0.05$). **Fig 5.17(a)** represents the decrease in agitation rate and biowaste concentration near the middle value in the graph signifies reduction in the surface tension value. This is because a very high biowaste concentration does not necessarily reduce the surface tension of the medium and ultimately high biosurfactant production. A high dose of low-cost carbon substrate will lead to enhancement in cellular biomass which in turn will cause competition for growth maintenance, low pH rather than an increase in biosurfactant yield (Almeida et al., 2017). Likewise, a very high agitation rate will result in a decrease in surface oxygen leaving behind anoxic conditions for cellular respiration, and also wear and tear of cells might be seen (Moshtagh et al., 2019). Similarly, in **Fig 5.17(b)**, the lowest surface tension value was obtained when the pH was reduced up to the middle value along with the temperature value when kept in the middle range. An optimum temperature and pH value are required for maximum surface tension reduction and biosurfactant yield as it will facilitate various enzymatic activities for cell growth and reproduction and enzyme permeability across the cellular membrane (Phulpoto et al., 2020). In present study, an optimum temperature of 35 ºC and pH 6 was observed. Further, minimum surface tension reduction value was observed when agitation rate and temperature value were kept low up till middle level. The ellipsoidal curves are seen in **Fig 5.17(c)** indicating a high level of interaction between the variables.

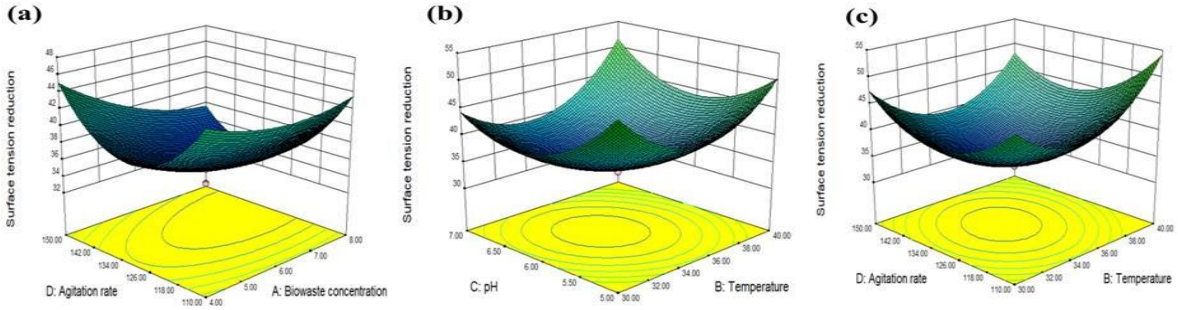

Figure 5.17 3D plots of interactive variables for *Bacillus haynesii* E1 biosurfactant production

Similarly for biosurfactant production, optimization by *Pseudomonas aeruginosa*, the polynomial equation **Eq. 3.9** (provided in chapter 3, section 3.3.6.3.4) explained the correct explanation for surface tension reduction through selected parameters. The value of regression coefficient (R^2) was calculated to be 0.9863 (~close to unity) estimating 98.63% of similarity with predicted data from the model. The predicted R^2

(0.9088) was observed to be compatible with the adjusted R^2 of 0.9653 indicating a valid model design. Further, the interaction and justification of the Quadratic model is analysed through ANOVA table **(Table 5.8).** The model terms A, C, AC, AD, BC, A^2, B^2, C^2, and D^2 having _Prob>F' < 0.05 are considered significant terms. The study of straight normal plots of residuals and actual and predicted response explains befitting of the model in a set of the selected independent variables (Nalini & Parthasarathi, 2018).

The optimum value of variables for maximum surface tension reduction (32.41 dyne/cm) was estimated to be 5%; v/v (agro waste concentration), 35 °C (temperature), 7 (pH), and 140 rpm (agitation rate). At this reduced surface tension, the strain F5 produced an approximately 2.4 g/L biosurfactant which was quite akin to the yield obtained when dextrose as carbon substrate was used (~2.6 g/L), indicating suitable competitiveness over uneconomical chemical substrates for their large scale usage.

Table 5.7: A four variable CCD design with experimental and predicted surface tension (ST) reduction (dyne/cm) values for *Pseudomonas aeruginosa* F5

Run	A: Agrowaste Concentration (%)	B: Temperature (°C)	C: pH	D: Agitation rate (rpm)	Experimental ST reduction (dyne/cm)	Predicted ST reduction (dyne/cm)
1	4.00	40.00	8.00	130.00	63.99	62.13
2	3.00	35.00	7.00	140.00	49.17	47.18
3	5.00	35.00	9.00	140.00	63.14	63.62
4	6.00	40.00	8.00	130.00	64.89	62.97
5	4.00	40.00	6.00	150.00	65.23	65.82
6	4.00	30.00	6.00	130.00	64.33	64.57
7	5.00	35.00	7.00	140.00	32.15	33.34
8	6.00	40.00	6.00	150.00	54.89	54.12
9	5.00	35.00	7.00	140.00	34.99	33.34
10	5.00	35.00	5.00	140.00	67.54	67.86
11	5.00	35.00	7.00	140.00	32.56	33.32
12	5.00	35.00	7.00	120.00	55.24	59.01
13	6.00	30.00	8.00	130.00	55.63	54.78
14	6.00	40.00	6.00	130.00	56.98	55.05
15	6.00	30.00	6.00	130.00	56.85	55.19
16	5.00	35.00	7.00	140.00	33.99	33.34
17	6.00	30.00	6.00	150.00	54.4	55.83
18	6.00	30.00	8.00	150.00	50.99	51.29
19	5.00	45.00	7.00	140.00	71.89	74.72
20	7.00	35.00	7.00	140.00	34.02	36.05
21	5.00	35.00	7.00	140.00	33.84	33.34
22	4.00	30.00	8.00	150.00	56.34	57.97
23	5.00	35.00	7.00	140.00	32.41	33.34
24	4.00	40.00	8.00	150.00	60.49	61.85
25	4.00	30.00	8.00	130.00	56.23	56.65
26	5.00	35.00	7.00	160.00	62.47	59.34
27	4.00	30.00	6.00	150.00	69.06	70.66
28	6.00	40.00	8.00	150.00	58.16	57.61
29	4.00	40.00	6.00	130.00	62.31	61.59
30	5.00	25.00	7.00	140.00	72.64	70.61

Table 5.8: Anova analysis for the quadratic model for *Pseudomonas aeruginosa* F5

	Sum of Squares	df	Mean Square	F-value	p-value	
Model	24.63	14	1.76	77.04	< 0.0001	**Significant**
A- Agro waste concentration	1.16	1	1.16	51.01	< 0.0001	
B- Temperature	0.087	1	0.087	3.82	0.0695	
C-pH	0.11	1	0.11	5.00	0.0410	
D-Agitation speed	9.357E-004	1	9.357E-004	0.041	0.8423	
AB	0.032	1	0.032	1.39	0.2569	
AC	0.23	1	0.23	10.17	0.0061	
AD	0.11	1	0.11	4.69	0.0469	
BC	0.30	1	0.30	12.93	0.0027	
BD	0.011	1	0.011	0.49	0.4950	
CD	0.080	1	0.080	3.49	0.0812	
A^2	0.78	1	0.78	34.00	< 0.0001	
B^2	12.98	1	12.98	568.22	< 0.0001	
C^2	9.33	1	9.33	408.45	< 0.0001	
D^2	6.31	1	6.31	276.31	< 0.0001	
Residual	0.34	15	0.023			
Lack of Fit	0.30	10	0.030	3.15	0.1085	**Not significant**
Pure Error	0.047	5	9.380E-003			
Cor Total	24.98	29				

The combined action of two independent factors while keeping the others constant was illustrated through response surface plots against surface tension reduction as response to check for its efficacy in maximising the biosurfactant production (Rodrigues et al., 2017). **Fig. 5.18(a)** illustrates required agitation rate to be optimum up to the middle value as enhanced rpm would produce anoxic environment by decreasing surface oxygen and damage to the cell‘s structure (Moshtagh et al., 2019).

Likewise, an optimum temperature range is required for maximum enzymatic activities (Phulpoto et al., 2020) and our study showed maximum surface tension reduction up to the middle range i.e., 35 °C as shown in **Fig 5.18(b)** indicating highly interactive ellipsoidal curves. The positive correlation of pH and agrowaste concentration indicated reduced surface tension value up to the middle as seen from the plot in **Fig. 5.18(c)** indicating an optimum range for maximum biosurfactant yield as high agrowaste concentration will produce an acidic environment leading to the hindered metabolism and also nutrient competition due to the enhancement in cell biomass (Almeida et al., 2017).

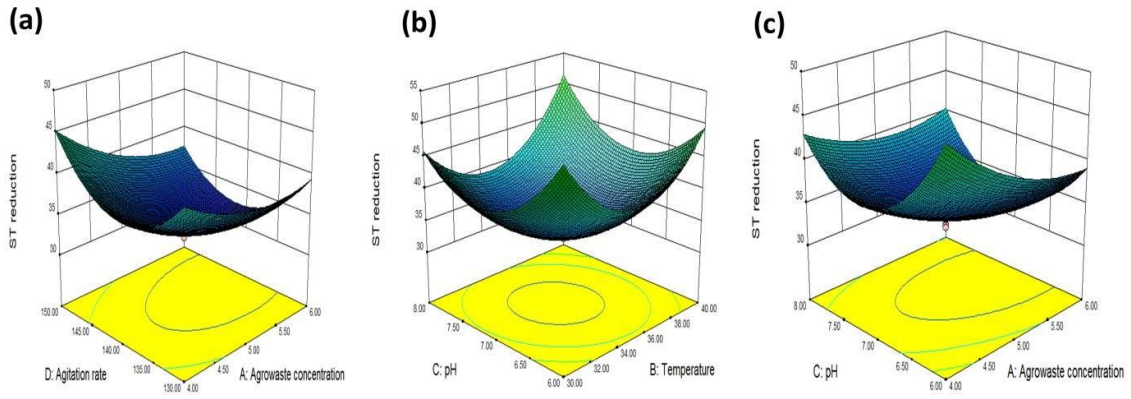

Fig. 5.18 Interactive effect of variables for maximum biosurfactant production by *Pseudomonas aeruginosa* F5

5.1.5.5 Simultaneous Biosurfactant production and metal biosorption by *Bacillus haynesii* and *Pseudomonas aeruginosa* study findings

A batch study involving synchronic biosurfactant production and metal biosorption capacity of bacterial strains ***Bacillus haynesii* and *Pseudomonas aeruginosa*** and its interaction with the Pb^{2+} was executed and studied through adsorption isotherm models (Langmuir, Freundlich, and Temkin models).

The potential of isolated bacterial strains to produce biosurfactant in good yield under lead (Pb^{2+}) stress was also evaluated to assess the stability of the bacterial strains to withstand metal stress and perform their metabolic activities. Findings are summarized below:

The *B. haynesii* E1 and *P. aeruginosa* F5 upon screening showed good Pb^{2+} resistance on nutrient agar plates at varied metal concentrations and were resistant up to 2000

ppm with MIC (minimum inhibitory concentration) at 2200 ppm **(Fig. 5.19)**. This high resistance of both the strains could aid beneficially in the bioremediation of Pb^{2+} from the polluted systems. Similarly, it could lay a foundation for the resistance of bacteria against other heavy metals that could be checked for its efficacy in concomitant metal systems.

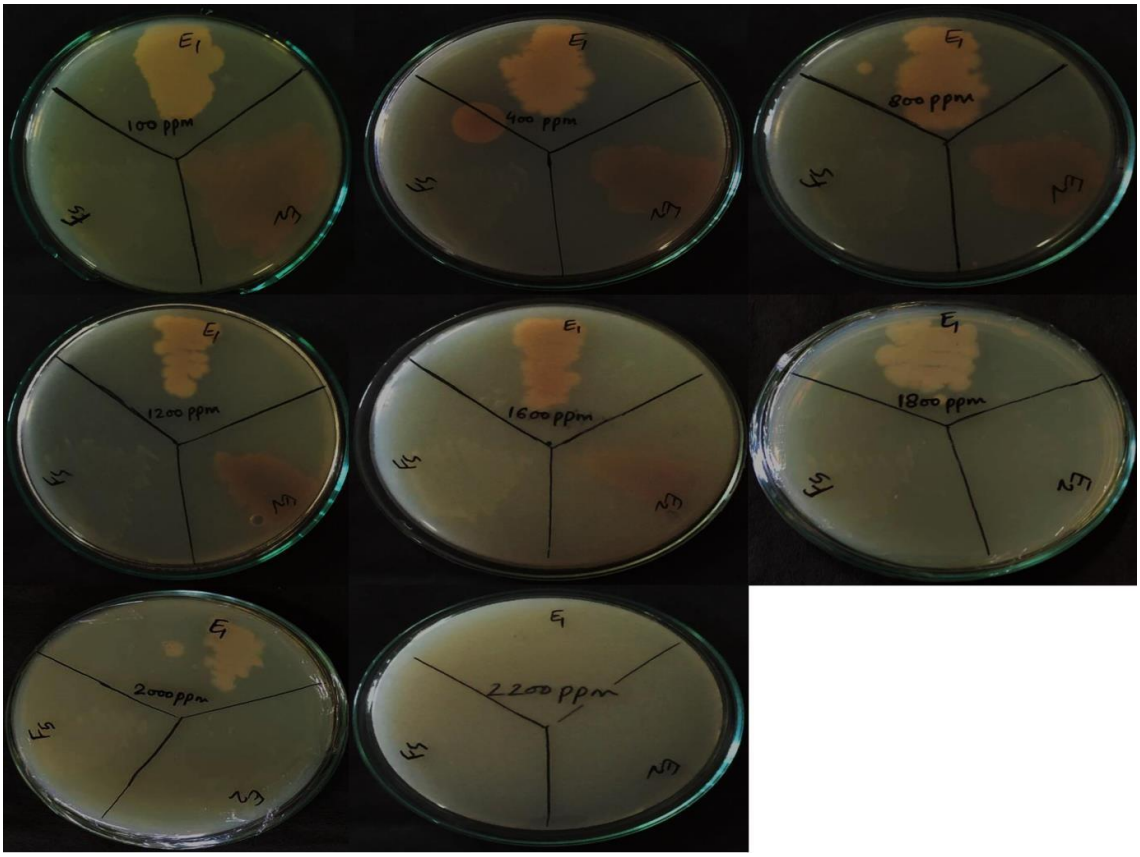

Figure 5.19 Bacterial growths at different Pb^{2+} concentrations

5.1.5.5.1 Biosurfactant production and growth kinetics of *Bacillus haynesii* E1 at different Pb^{2+} concentration

The growth pattern of *B. haynesii* E1 in MSM broth and simultaneous biosurfactant production against different Pb^{2+} concentrations (100,200, 300, 400 and 500 ppm) along with control (MSM broth without $Pb^{2+)}$ was evaluated as shown in **Fig. 5.20**. From the study performed, it was estimated to be a concentration-dependent growth model where increased Pb^{2+} concentration led to decreased growth rate and ultimately decreased biosurfactant production. The control and metal amended flasks were incubated at 35 $^{\circ}$C for 5 days and bacterial growth was measured at 620 nm using UV-Vis spectrophotometer (Thermo scientific, Evolution 201) while the biosurfactant

production ability was assessed in terms of emulsification index (E_{24}%) taken consecutively for 5 days for selected Pb^{2+} concentrations.

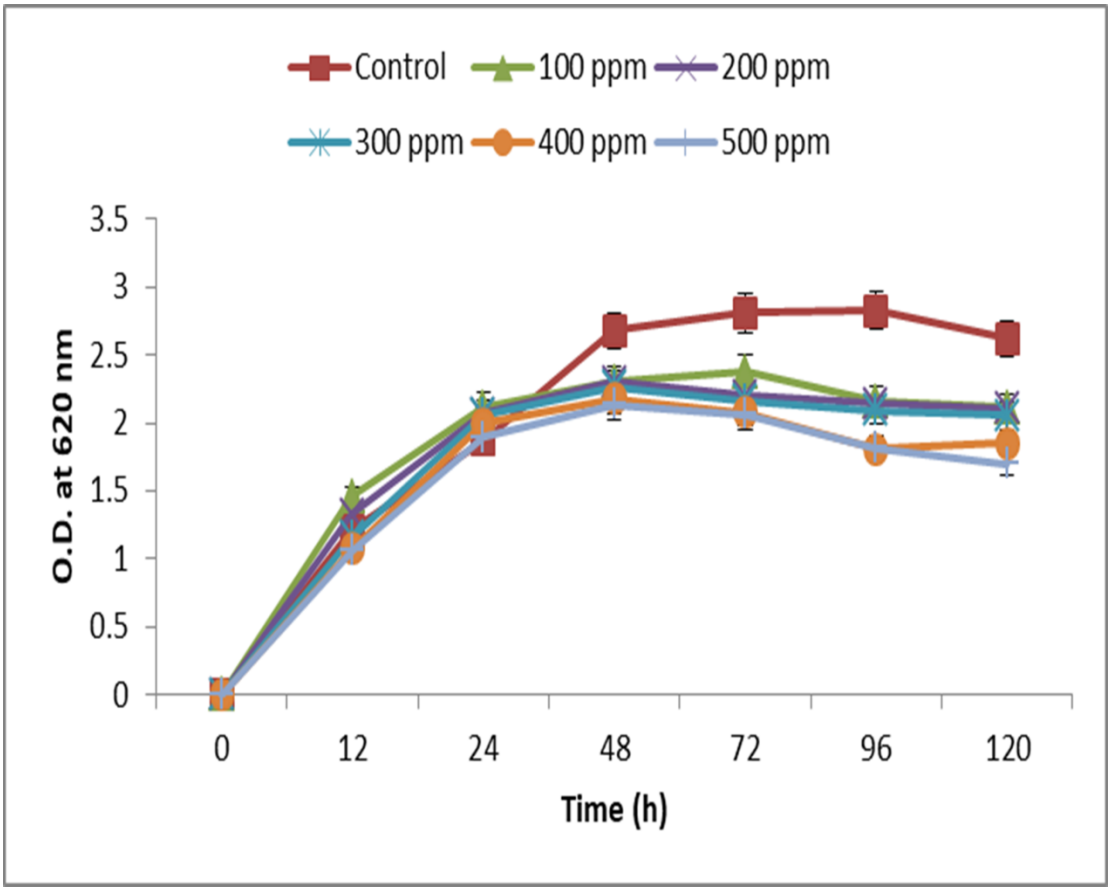

Figure 5.20 Growth kinetics of *Bacillus haynesii* E1 in the absence (control) and presence of different Pb^{2+} concentrations

The lag phase of the bacterium ***Bacillus haynesii* E1** was extended in absence and presence of lead upto 8 hours and then it entered the logarithmic phase in control as well as in presence of metal. Till 24 h, logarithmic phase lasted in presence of the metal and then it stabilized till 72 hours. After 72 hours, growth of the bacterial strain started declining in presence of lead and again stabilized from 96 hours to 120 hours (**Fig. 5.20**). There was no noticeable change in the growth with 100 and 200 ppm of Pb^{2+} as visible with foaming but growth was hindered slightly at higher Pb^{2+} concentrations.

Samples (2ml each) withdrawn from the experimental flasks above at 24h, 48h, 72h, 96h, 120h was centrifuged at 10000 rpm for 10 min. Emulsification index ability of each sample drawn at different time interval was assessed for 24 hours by mixing supernatant (crude biosurfactant) and hydrocarbon (lubricating oil) in a tube, vortexed

and allowed to stand for 24 h. Emulsification index was taken as a criterion for biosurfactant production. More the Emulsification of hydrocarbon more is the biosurfactant production. Results are depicted in **Fig. 5.21**.

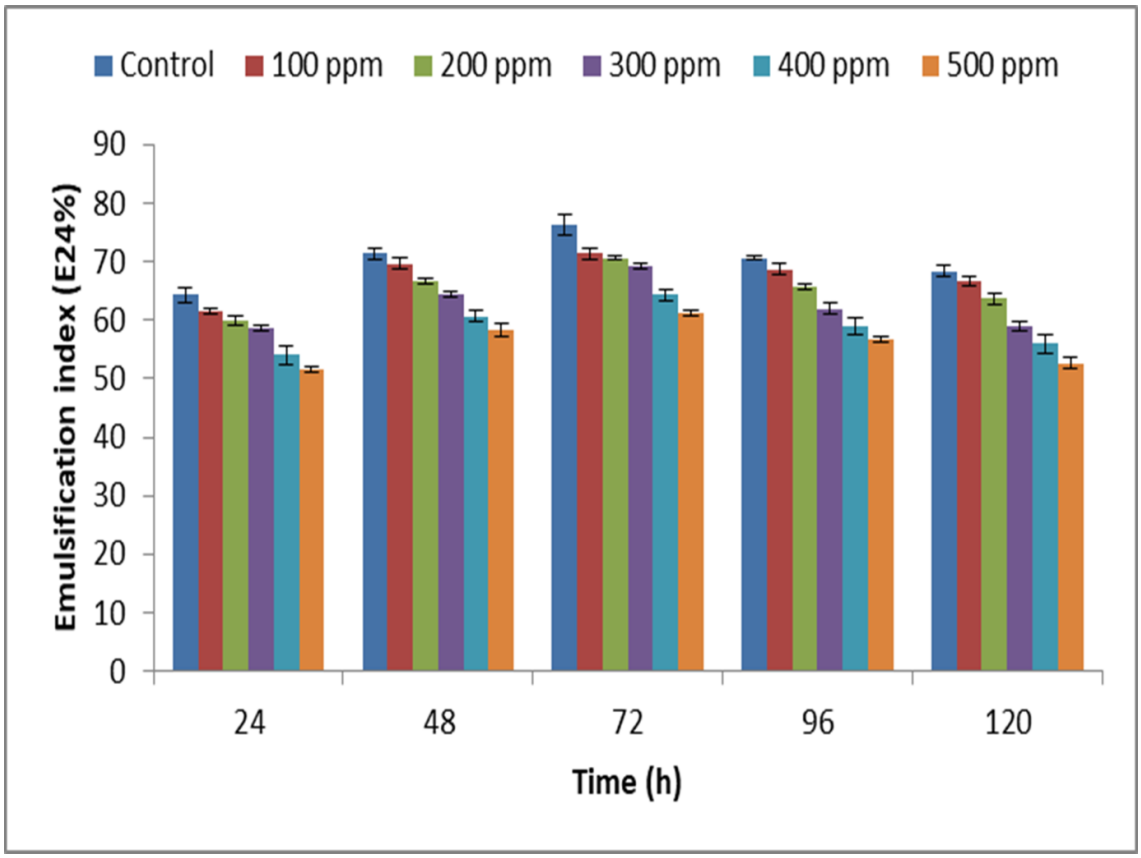

Figure 5.21 Emulsification index (E_{24}%) of *Bacillus haynesii* E1 in the absence (control) and presence of different Pb^{2+} concentrations using lubricating oil

Emulsification ability of the crude biosurfactant drawn at 72 hours was found to be maximum indicating that till 72 h, biosurfactant production increased and thereafter it started declining. Good emulsification was detected up to 72 h with an E_{24}% value at 100, 200, 300, 400 and 500 ppm of Pb^{2+} ions respectively and after which it started to decline. The high E_{24}% value at low initial Pb^{2+} concentration suggests adaptability of the bacterium to optimize its growth under metal stress. The bacterium showed maximum emulsification potential at 100 ppm Pb^{2+}. The optimized growth is due to the bioaccumulation ability developed in the bacterium on account of continuous exposure in the Pb^{2+} medium. The biosorption of Pb^{2+} ions also increased gradually and became constant after an optimum time interval with a higher dose of metal concentration which might be due to the nutrient exhaustion and the toxicity caused

by Pb^{2+} ions (Hossain & Anantharaman, 2006). However, it could be concluded that the overall growth of bacterium E1 in the presence of different Pb^{2+} concentrations was showing the adaptive nature of the bacterium and present findings are supported by previous reports on *Bacillus* sp. growth at different Pb^{2+} concentrations (Ayangbenro & Babalola, 2020; Hossain & Anantharaman, 2006; Murthy et al., 2014; Shin et al., 2012).

5.1.5.5.2 Biosorption study

5.1.5.5.2.1 Effect of initial metal ion concentration

The dynamic force required to facilitate mass transfer in a metal biosorption system is highly influenced by the initial metal ion concentrations (Yang et al., 2017). Metal biosorption experiments depicted nearly identical Pb^{2+} removal percentages at 100 and 200 ppm of initial Pb^{2+} concentration with about 50 to 99 % of biosorption in 330 min of incubation time. Thereafter, it reached its saturation point. It is to be noted here that though almost 99% Pb^{2+} biosorption completed in nearly 6-7 hours of incubation, flasks were kept to check for biosurfactant production which continued to reach its higher value up to 72 h of incubation. This period of incubation is optimum for biosurfactant production as CMC reached at the end of this time period and studies by researchers had reported similar findings for *Bacillus* sps. (Ayangbenro & Babalola, 2020; Datta et al., 2018). In one scientific study, researchers studied the biosorption of Pb^{2+} by *Bacillus subtilis* where bacterium immediately entered into log phase in the presence of Pb^{2+} ions and showed maximum optical density after 72 h. They had also reported maximum 82 % Pb^{2+} removal in 2.5 h owing to its maximum removal in first 30 min of the incubation only (Salamat et al., 2018). One significant relation could be derived from this finding that bacterium adapted its internal physiology under metal stress precisely up to 72 h but began to decline in growth which might be due to the nutrient deprivation and metal toxicity. The biosorption of Pb^{2+} ions was found to be enhanced with the increase in initial metal ion concentration as evident from the maximum adsorption capacities recorded at 100 ppm (99.05 mg/g) and 213.96 mg/g at 500 ppm. This elevated biosorption of Pb^{2+} ions might be influenced by the binding interaction of metal ions with the surface of the bacterium that resulted in overcoming the opposing force of mass transfer exhibiting between solution and solid phase (Mohapatra et al., 2019). On the other hand, the biosorption rate declined with the

increase in the initial metal ion concentration on account of less or no availability of binding sites with saturation level attained at 72 h of incubation with no significant change thereafter. At low initial Pb^{2+} concentration, more of the surface sites on the bacterium was available for binding but a gradual increase in Pb^{2+} concentration will lead to unavailable vacant sites to hold extra Pb^{2+} ions (Vishan et al., 2019). The maximum Pb^{2+} biosorption percentage observed was 99.05, 97.94, 69.19, 51.92, and 42.79 % in case of 100, 200, 300, 400, and 500 ppm Pb^{2+} ions respectively. The maximum Pb^{2+} loading capacity i.e. 213.96 mg/g at 500 ppm was found to be higher as compared with the metal adsorption study done with different bacteria (Cai et al., 2018). Also, the live bacterial cells showed a higher rate of biosorption than dead biomass (Mohapatra et al., 2019). It is hypothesized that low initial metal concentration prefers surface binding but a slow increase in concentration transports the metal ions into the cell via energy-based metabolic action of living cells through a metal transport system. It is also observed that at high metal concentration, live cells might become toxic and metal ions mimic the transporter substrates as well resulting in less adsorption rate and might lead to the death of the bacterial cell (Ayangbenro & Babalola, 2020).

5.1.5.5.2.2 Biosorption equilibrium isotherm

Out of the three different isotherm models plotted as shown in **Fig 5.22(a,b,c),** the Langmuir isotherm model was found to be fitted well. The value of R^2, q_m, b, R_L, K_F, n, b_T, and K_T are depicted in **Table 5.9**. In our study, the R_L for bacterium E1 was found to be 0.009 at 35 $^{\circ}$C indicating affirmative adsorption of Pb^{2+} ions on the bacterial cells. The regression coefficients (R^2) for Langmuir, Freundlich, and Temkin isotherm are 0.9724, 0.6587, and 0.6924 respectively. The high value of R^2 obtained in Langmuir isotherm approving monolayer biosorption resulting from the interaction between homogenous cell surface (Can et al., 2016) and this type of adsorption is found to be shown by other studies regarding Pb^{2+} removal using bacteria (Mohapatra et al., 2019). The Freundlich constant (n) value (9.469) ascertains favorable biosorption even at high initial Pb^{2+} concentration.

Table 5.9 Adsorption isotherm and kinetic parameters obtained during biosorption of Pb^{2+} ions by *Bacillus haynesii* E1

Parameters	**Initial Pb^{2+} concentrations (ppm)**	
	100	**200**
Experimental q_e (mg/g)	99.05	195.88
Kinetic Model		
Pseudo-first order		
k_1	1.49×10^{-2}	1.358×10^{-2}
q_e (mg/g)	46.49	38.81
R^2	0.7115	0.968
Pseudo-second order		
k_2	7.9×10^{-4}	7.3×10^{-5}
q_e (mg/g)	101.01	196.07
R^2	0.9974	0.9996
Intra particle diffusion		
K_p	2.6887	5.7046
X_i	15.906	31.556
R^2	0.8648	0.9018
Isotherm Model	**Parameters**	**Values obtained**
	q_m (mg/g)	196.08
Langmuir		
	b (mg/g)	1.087
	R_L	0.009
	R^2	0.9724
Freundlich	n	9.469
	K_F	8.137
	R^2	0.6587
Temkin	b_T (J/mol)	155.812
	K_T (L/g)	2.324

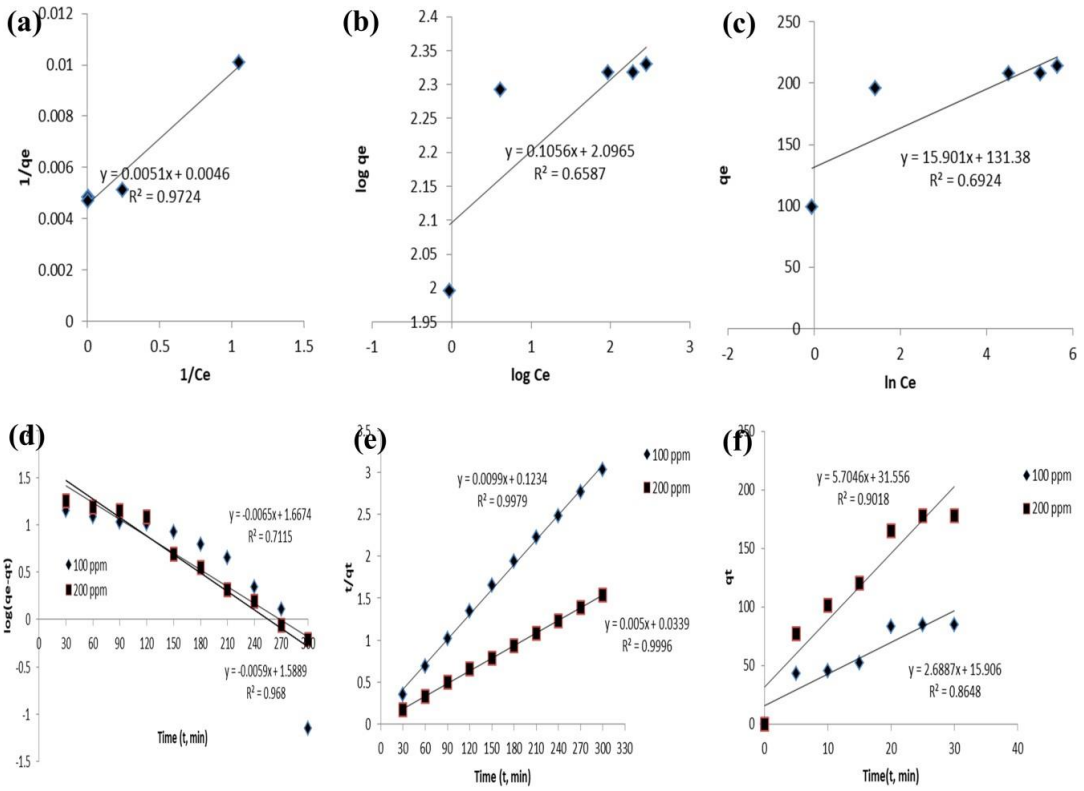

Figure 5.22 Adsorption isotherms and kinetics data for Pb2+ biosorption by *Bacillus haynesii* E1: (a) Langmuir isotherm; (b) Freundlich isotherm; (c) Temkin isotherm; (d) Pseudo first-order reaction; (e) Pseudo second-order reaction; (f) Intra-particle diffusion

5.1.5.5.2.3 Effect of contact time and biosorption rate kinetics

The effect of varying time ranges from 30 to 330 min for the biosorption of different Pb^{2+} ion concentrations was studied. The biosorption rate of Pb^{2+} ions was found to be fast (> 50 %) at the beginning of the experiment only (within 15-30 min) and later become slow and steady as the experiment preceded further up to 330 min coinciding with other published reports (Salamat et al., 2018). There was no increase in biosorption capacity after 330 min indicating the attainment of the equilibrium stage. The reason for an initial rapid rate of biosorption could be attributed to the fact that initially, the surface of bacterial biomass has free active available sites so that more of the Pb^{2+} ions could have adhered to it leading to gradual saturation of the surface with the further increase in initial Pb^{2+} concentration. A similar patterns of studies were reported by other researchers (Cai et al., 2018). It is interesting to note that the rapid initial biosorption is based on metabolism independent pathway i.e., surface

adsorption pathway which is usually fast while the latter slow rate is observed as it is based on metabolism dependent i.e., intracellular bioaccumulation of Pb^{2+} ions by the bacterium E1 (Mohapatra et al., 2019). The mechanism and biosorption rate under different contact time is best understood through biosorption kinetics model. These models explain the mass transfer chemical reaction (by Pseudo first and second-order kinetics) and intracellular diffusion of metal ions via the intraparticle diffusion kinetic model.

In our study, pseudo second-order kinetics was found to be best fitted with R^2 value of 0.9979 and 0.9996 at 100 and 200 ppm respectively in comparison to the pseudo first-order model having R^2 value of 0.7115 and 0.968 at 100 and 200 ppm of Pb^{2+} ions respectively [**Fig 5.22 (d,e)**]. The plot against t/q_t versus time (t) gave a straight line and the value of k_2 and q_e were calculated as shown in **Table 5.9**. Our findings are also supported by previous researches where bacterial biosorption was found to be fitted well by using pseudo second-order kinetics only suggesting chemisorption behavior of Pb^{2+} ions and bacterial biomass (Wen et al., 2018). While some of the metal ions get passed into the intracellular positions of the bacterial cell using enzymatic pathway via metal transporters leading to their deposition which is confirmed by ‗X_i‘ value from **Table 5.9**, **Fig 5.22(f)**; found to be higher for 200 ppm of Pb^{2+} ions. The higher the initial Pb^{2+} concentration, the higher is the possibility of diffusion of Pb^{2+} ions inside the cell due to the saturation of the surface ligand sites by binding of Pb^{2+} ions on it (Chintalpudi et al., 2021).

5.1.5.5.3 Biosurfactant production, growth rate, and biosorption kinetics during Pb^{2+} stress by *Pseudomonas aeruginosa*

The biosurfactant production ability of the *P. aeruginosa* F5 was evaluated and assessed to be a concentration-dependent framework that involved depreciative growth rate (also declined biosurfacatnt production) with the enhanced Pb^{2+} concentration. The growth of the bacterium in the presence of varied Pb^{2+} concentration extended lag phase (0-8 h) along with control flasks without Pb^{2+} with a logarithmic stage lasting up to 72 h. The growth became static after 3 days and begins to decline at the end of 5^{th} day (**Fig. 5.23**). At low initial Pb^{2+} concentration (100 and 200 ppm), good foaming was observed in the flasks corresponding to the biosurfactant production but it was slightly affected at 500 ppm. It was estimated that

maximum biosurfactant production (better adaptation under metal stress) is enhanced up to 72 h as noted from the emulsification index (E_{24}%) value obtained at different Pb^{2+} concentration (**Fig. 5.24**), suggesting CMC is reached at the end of 72 h by many previously published literatures (Rastogi et al., 2021b). The affected growth at high Pb^{2+} (500 ppm) concentration could be due to the noxiousness of Pb^{2+} ions and nutrient enfeeblement but the good metal bioaccumulation capability and optimum growth illustrated accommodative feature of the bacterium at various Pb^{2+} concentrations (Ayangbenro & Babalola, 2020).

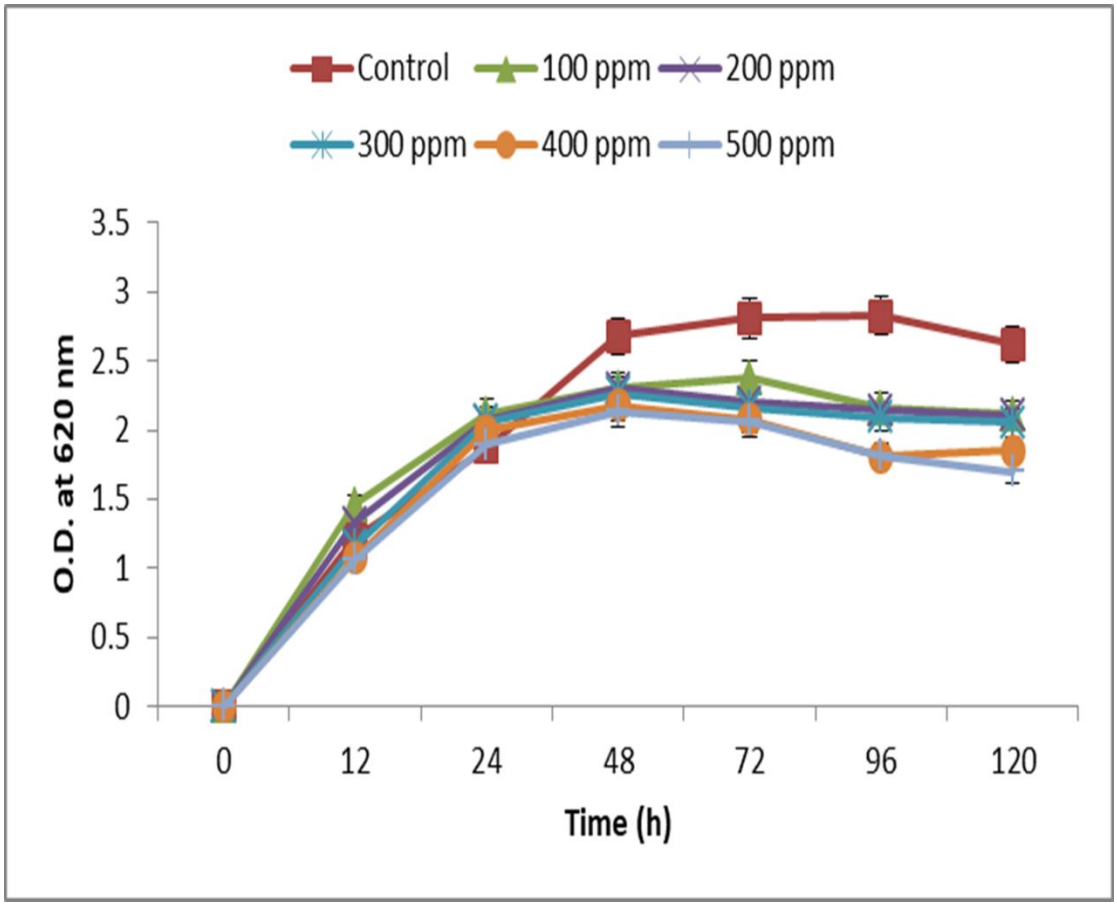

Figure 5.23 Growth kinetics of *Psuedomonas aeruginosa* F5 in the absence (control) and presence of different Pb^{2+} concentrations

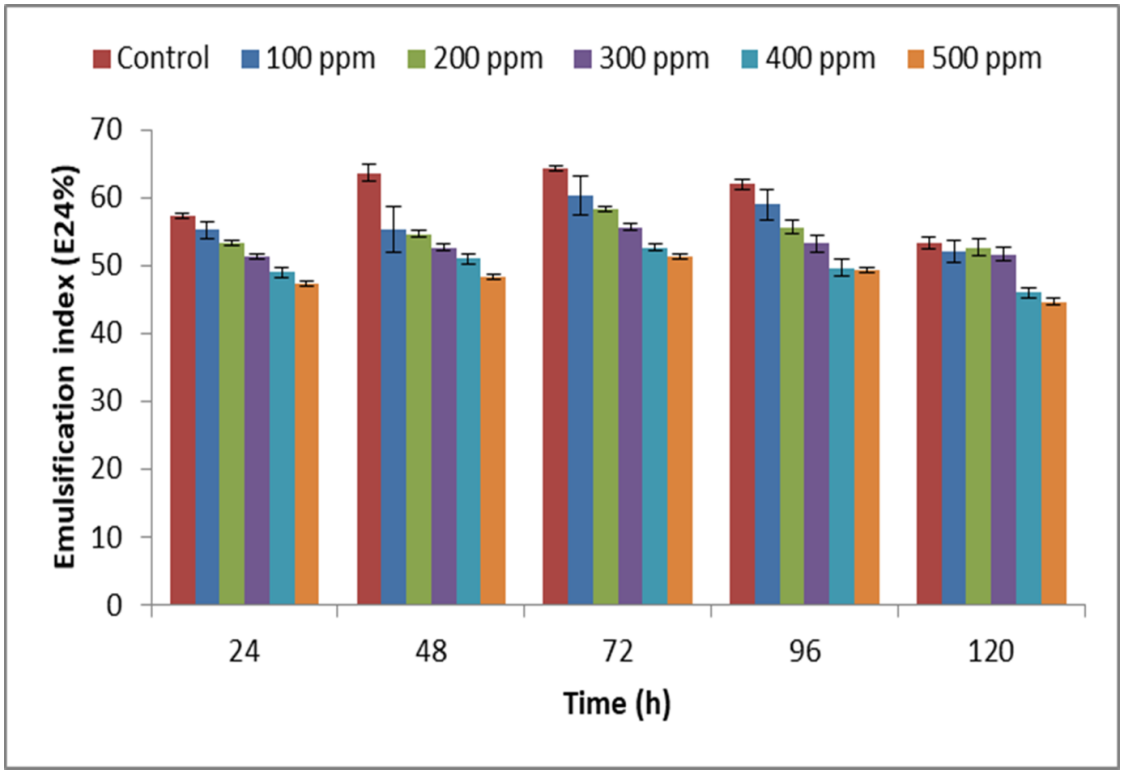

Figure 5.24 Emulsification index of *Psuedomonas aeruginosa* F5 in the absence (control) and presence of different Pb^{2+} concentrations using n-hexane

5.1.5.5.3.1 Effect of initial Pb^{2+} ion concentration

The biosorption efficacy of the strain F5 was ascertained to be enhanced with the increase of initial Pb^{2+} concentrations as reported from the adsorption capacities observed from 100 to 500 ppm to be 99.44 to 267.86 mg/g respectively. This high value of adsorption capacity trait shown by the bacterium could be attributed to adjustment of its intrinsic physiology during metal stress and also due to the strong metal binding interactions available at its cell surface leading to the suppression of resisting mass transfer forces occurring between solid and solution phase (Tiwari et al., 2017). While the biosorption percentage was noted to be enhanced with the increment of initial metal concentration but the metal removal percent kept on declining on account of less or no vacant binding site available on the bacterium‘s cell surface (Mohapatra et al., 2019). The highest metal removal rate observed was 99.44% at 100 ppm of Pb^{2+} while lowest recorded was 53.57% at 500 ppm of Pb^{2+}. It was also noted that nearly identical removal percentage was seen at 100 and 200 ppm of Pb^{2+} from ~16-21 to 97-99% in 5-6 h of incubation time but the metal amended flasks were kept to look for maximum biosurfactant production that existed up to 72 h of incubation thereafter no further increment in emulsification index (E_{24}%) value was

noted. Our study illustrated a high value of adsorption capacity as compared to the previous studies (Karimpour et al., 2018) using live bacterium (shows better adsorption than dead biomass) on account of its energy dependent metabolic machinery that causes internalization of Pb^{2+} ions through metal transporters but at high concentrations its rate is declined due to the mimicry shown by Pb^{2+} ions as substrates of transportation leading to lesser adsorption kinetics, and ultimately death of the cell (Ayangbenro & Babalola, 2020).

The biosorption study fitted well with Langmuir isotherm model [R^2= 0.9859; **Fig. 5.25(a)**] suggesting monolayer adsorption and it is supported by other studies as well (Vimalnath & Subramanian, 2018). The values of respective constants obtained in different isotherm models are depicted in **Table 5.10**.

5.1.5.5.3.2 Effect of contact time

There are two types of pathway a bacterium adopts in the metal biosorption study at different time interval. A rapid initial Pb^{2+} biosorption rate (> 33% within 5-30 min) was observed at the beginning of the experiment owing its ability to the availability of numerous free binding sites on the cell surface i.e., a metabolism independent (surface adsorption) mechanism. With the gradual passing of contact time, the surface began to become saturated with the increment in initial Pb^{2+} ion concentration and equilibrium was achieved at 330 min as noted from no further enhancement in adsorption capacity. The slow biosorption rate was observed after the mid-time on account of activation of metabolism dependent (internal bioaccumulation) pathway due to the saturation of surface sites (Ayangbenro & Babalola, 2017). The effect of varied contact time is illustrated through biosorption kinetics model (Rastogi et al., 2021b).

In our study, pseudo second-order kinetic model (chemisorption process) was reported to be well fitted that was also supported by other studies (Manirethan et al., 2018). The regression coefficient (R^2) value of 0.9913 and 0.9975 at 100 and 200 ppm of Pb^{2+} ions respectively were obtained from the plot against t/q_t versus time (t) and the value of rate constant (k_2) and equilibrium capacity (q_e) were calculated [**Fig. 5.25(b)**]. The high value of _X_i‘ at 200 ppm in intra-particle diffusion model (**Table 5.10)**, established the intracellular movement of Pb^{2+} ions through metal transporters due to the saturation of Pb^{2+} experienced at the cell surface on enhancement of initial Pb^{2+} concentration.

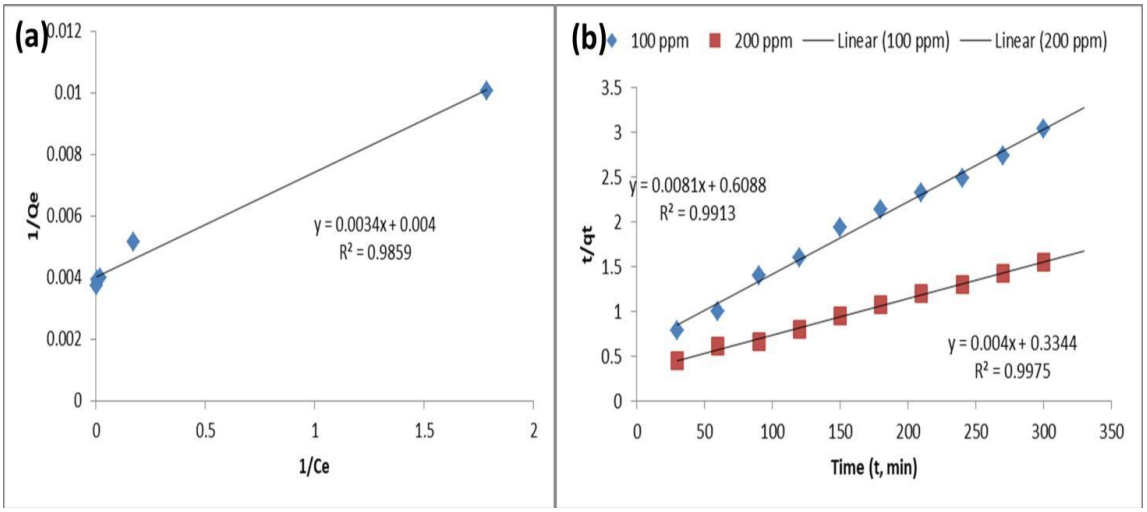

Figure 5.25 (a) Langmuir adsorption isotherm; (b) Pseudo second-order kinetics during biosorption of lead by *Pseudomonas aeruginosa* F5

Table 5.10 Adsorption kinetics and isotherm parameters obtained during biosorption of Pb^{2+} ions by *Pseudomonas aeruginosa* F5

Parameters	**Initial Pb^{2+} concentrations (ppm)**	
	100	**200**
Experimental q_e (mg/g)	99.44	194.22
Kinetic Model		
Pseudo-first order		
k_1	1.82×10^{-2}	1.71×10^{-2}
q_e (mg/g)	158.49	316.23
R^2	0.8787	0.8514
Pseudo-second order		
k_2	1.07×10^{-4}	4.78×10^{-5}
q_e (mg/g)	123.46	250
R^2	0.9913	0.9975
Intra particle diffusion		
K_p	0.9345	1.9106
X_i	9.8653	12.97
R^2	0.9595	0.985
Isotherm Model	**Parameters**	**Values obtained**
Langmuir	q_m (mg/g)	294.12

	b (mg/g)	0.8
	R_L	0.01235
	R^2	0.9859
Freundlich	n	6.378
	K_F	8.101
	R^2	0.9041
Temkin	b_T (J/mol)	91.36
	K_T (L/g)	4.104

5.1.5.5.3.3 Mechanism of biosorption of Pb2+ by *Bacillus haynesii* E1 and *Psuedomonas aeruginosa* F5

The possible mechanism of biosorption of Pb^{2+} ions by cells of both bacteria could be estimated to be ion-exchange and complex formation. Our estimations were further confirmed by SEM and EDX analysis. The SEM micrographs clearly indicated an alteration in the morphology of bacterial cells when treated with Pb^{2+} as compared to the control cell (without Pb^{2+}) as shown in **Fig. 5.26(a,c) and Fig. 5.27(a,b)** The analysis revealed the presence of sticky white bright Pb^{2+} particles on bacterial biomass giving an appearance of irregular, patchy, rough, and spongy surface whereas in the case of a control cell, we can see the distinct rod-shaped smooth surface. The altered bacterial cell morphology occurred due to the interaction of Pb^{2+} ions with the surface causing abrupt changes. The Pb^{2+} ions are mostly present as $Pb(OH)_2$ particles on the surface coming from the interaction of water molecules with the ions and making them soluble in the solution phase. Also, complexation and ion–exchange interactions occurred with the negatively charged ligands and positively charged molecules present on the bacterial surface confirming the settlement of Pb^{2+} ions as $Pb(OH)_2$ particles on the cell surface (Qiao et al., 2019).

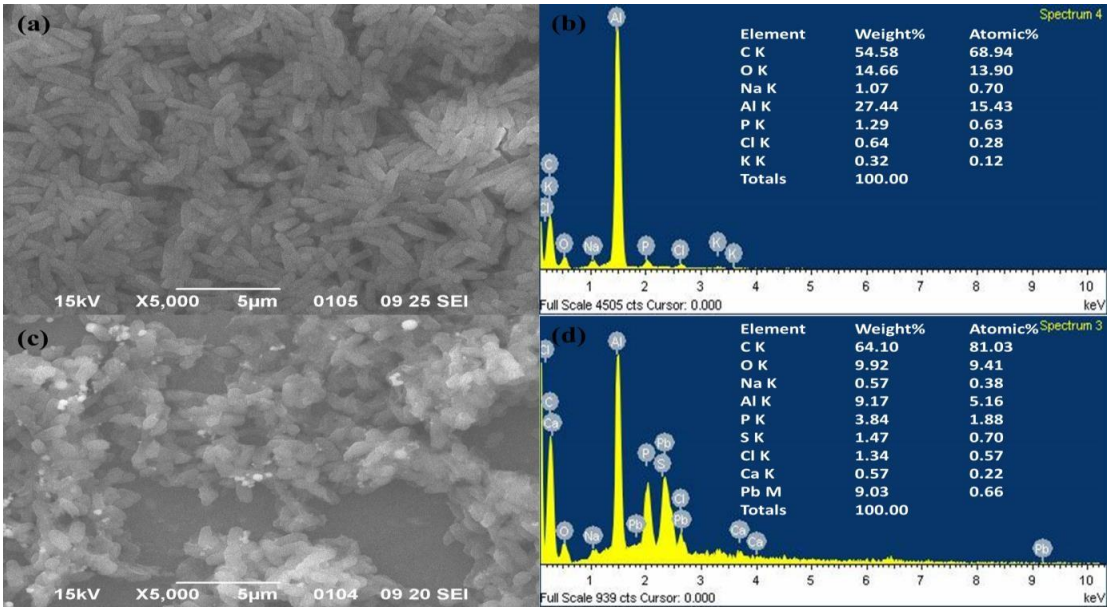

Figure 5.26 Mechanism of biosorption of Pb2+ by *Bacillus haynesii* E1

Further EDX analysis [**Fig 5.26(b, d)]** explained the significant changes in the elemental composition of both bacteria before and after Pb^{2+} treatment. The atomic percentage of Pb^{2+} was 0.66 and 9.03 % was weight percentage at 100 ppm of Pb^{2+} treatment in the case of biosorption by *B. haynesii* E1. The reduction in the atomic and weight percentage value of sodium (Na^{+}) from 0.72 and 1.21 % to 0.38 and 0.57 % indicates the removal of Na^{+} ions from the surface ligands and binding of Pb^{2+} ions with it confirming the possible ion-exchange mechanism of biosorption. One peak at about 6.359 keV corresponding to potassium (K^{+}) was omitted in the treated sample that ensured affinity between Pb^{2+} with carbon, oxygen, nitrogen atoms of surface molecules, and possibly the ion-exchange with K^{+} ions (Chintalpudi et al., 2021) while **Fig. 5.27(c, d)** depicts the noticeable changes in the elemental composition of strain F5 with and without Pb^{2+} treatment. The atomic and weight percent of Pb^{2+} was found to be 0.10 and 1.49% at 100 ppm of Pb^{2+} ions with enhanced atomic carbon (C) percent from 63.81 to 74.84%. EDX analysis also revealed the reduction in the aluminium atomic percent as compared to control i.e., 29.85 to 2.36% establishing ion-exchange reactions as a part of the biosorption mechanism as supported by previous studies as well (Xu et al., 2017). Similar patterns of SEM and EDX studies has been reported in the past related to support our findings and ascertaining the capability of both bacteria to take up Pb^{2+} via surface adsorption. The intracellular Pb^{2+} deposition via bioaccumulation mechanism as reported by previous researchers

(Mohapatra et al., 2019) is also possible and could be ascertained by using analytical techniques such as transmission electron microscopy (TEM).

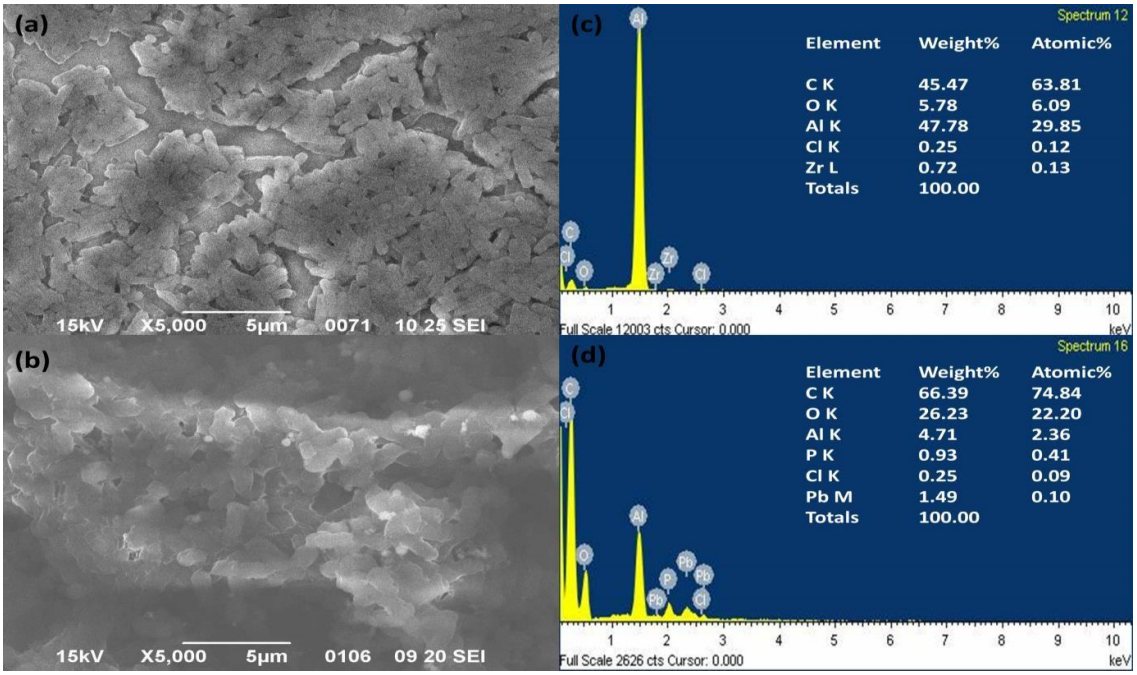

Figure 5.27 Mechanism of biosorption of Pb2+ by *Psuedomonas aeruginosa* F5

5.2 Conclusion

The present chapter discussed the isolation of bacterial strains from hydrocarbon (petrol) contaminated sites and their screening showed them as efficient biosurfactant producers. Also, their high MIC towards Pb^{2+} and Cd^{2+} shows their adaptability towards heavy metal stress and could be employed for management and bioremediation (biosorption) of heavy metal contaminated systems. Also, it revealed the potential of selected strains to utilize biowaste to produce good yield of biosurfactant. The biosurfactant produced by bacteria had good stability over a varied range of factors and retained their emulsification and oil displacement property along with their good Pb^{2+} biosorption capability. The findings suggest the implementation of such biosurfactant producing strains or their product (metabolite) alone for covering the demand of surfactants and their role in bioremediation industry.

Chapter 6

Biosurfactant Modified Activated Bio-Adsorbent for Heavy Metal Removal From Wastewater - Fixed Bed Column Study

6.0 Background

The efficacy of a particular bio-adsorbent is validated by its application in a dynamic operating column based on the conditions employed and data obtained in the batch bioadsorption process. The performance of any bio-adsorbent is also altered/ assessed in terms of its uptake capacity when applied in a mixed metal system along with other parameters. Also, the amount of time required to reach equilibrium varies differently under continuous and batch adsorption system (Arora, 2019). A fixed-bed column study is a simple continuous process where a fresh solution of an adsorbate (here, heavy metal ions from an aqueous solution or wastewater) having a particular concentration is allowed to come in contact with the fixed-bed of adsorbent (here, biosurfactant modified activated banana peel powder, BSBP) establishing a dynamic equilibrium (Khan et al., 2004). The process of adsorption is initially rapid due to the presence of numerous vacant/binding sites on the surface of the bio-adsorbent that reaches the stage of saturation over a course of time and it deals with relatively large volumes of wastewater or aqueous solutions that provides or generates results in such a way which suggests economic feasibility to treat or design any treatment methodology for an industrial effluent treatment plant with more accuracy / precision (Afroze & Sen, 2018).

In a fixed-bed column, the performance of biosurfactant modified activated banana peel powder (BSBP) for the continuous elimination of Pb^{2+} and Cd^{2+} from an aqueous solution separately and also when present concomitantly in an electroplating wastewater is investigated. The breakthrough curves (BTCs) resulting from different operating conditions was fitted with an adsorption model to assess appropriate scaling and design of the bioadsorption column. The activated carbon obtained from acidified banana peel waste (AcBPP) as shown in chapter 4 was found to be effective than the activated carbon obtained from acidified orange peel waste (AcOPP). Due to the effectiveness, AcBPP was used here with further surface fabrication using surfactin (biosurfactant) extracted from *Bacillus haynesii* strain E1. The conditions obtained in the batch process using AcBPP were kept same such as pH to evaluate the influence of column parameters *viz.* flow rate, bed height, and initial metal concentrations (feed concentrations) on column adsorption process by biosurfactant modified activated banana peel powder (BSBP).

6.1 Results and discussions

A glass column of dimensions 18 X 300 mm was taken to perform the column experiments using different column conditions to examine the metal bioadsorption potential of BSBP and the results are discussed below:

6.1.1 Effect of flow rate

Two flow rates of 15 mL/min and 20 mL/min were selected with bed height of 4 cm, approximately having 3.5 g of biosurfactant modified activated banana peel powder (BSBP) and an initial metal concentration of 50 ppm was kept constant. The breakthrough curves obtained are represented in **Fig, 6.1** and **Fig. 6.2** for Pb^{2+} and Cd^{2+}, respectively. Although, batch study showed optimum removal of metal ions at 100 ppm but an initial feed concentration of 50 ppm was selected in order to remain closer to the real wastewater concentrations.

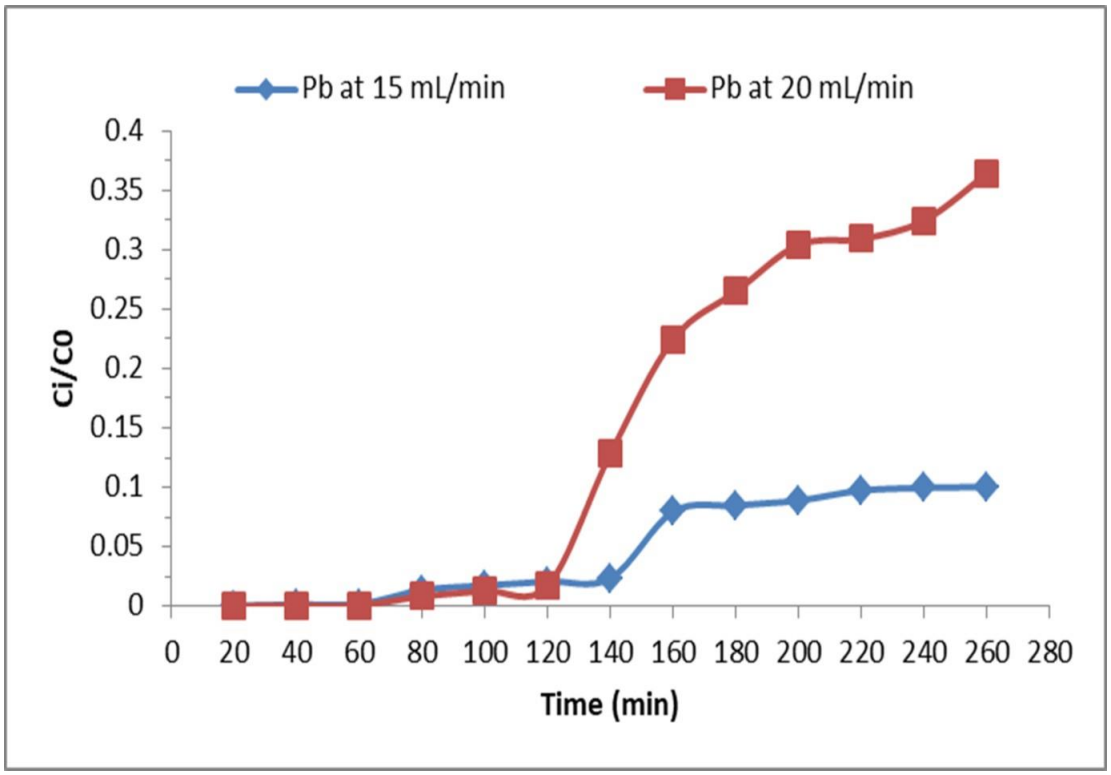

Figure 6.1 Breakthrough curves for Pb^{2+} bioadsorption onto BSBP at different flow rates (bed height= 4cm, inlet Pb^{2+} concentrations= 50 ppm, temperature= room temperature and influent pH= 4.0-4.5)

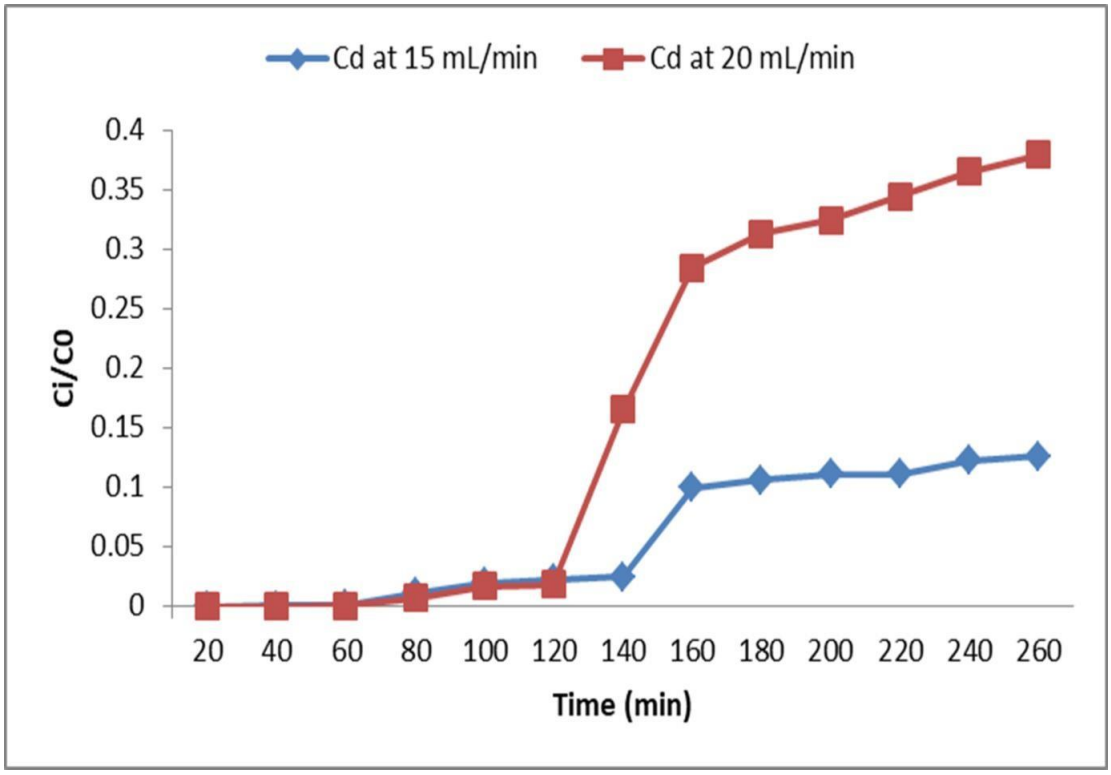

Figure 6.2 Breakthrough curves for Cd^{2+} bioadsorption onto BSBP at different flow rates (bed height= 4cm, inlet Cd^{2+} concentrations= 50 ppm, temperature= room temperature and influent pH= 4.0-4.5)

The breakthrough and the exhaustion time were found to increase with a decrease in flow rate from 20 mL/min (1.2 L/h) to 15 mL/min (0.9 L/h) for both Pb^{2+} and Cd^{2+} bioadsorption i.e., 140 min is the breakthrough time for both Pb^{2+} and Cd^{2+} while the slope of the plots increased with an increase in the flow rates. This means breakthrough curves obtained have steeper slopes with the increase in the flow rates for both the metal ions. In case of low flow rate i.e., Pb^{2+} and Cd^{2+} bioadsorption showed earlier exhaustion (saturation) time (160 min) than the higher flow rate indicating enhanced bioadsorption and more cleaner effluent. This finding is quite similar to results obtained by other researchers and also a higher flow rate leads to lower residence time in the column and vice versa (de Freitas et al., 2018; Dong et al., 2019; Jin et al., 2018). A high flow rate will reduce the contact time between the adsorbate (Pb^{2+} and Cd^{2+} ions here) and the bio-adsorbent (BSBP) and also less volume of the effluent is treated before the bed saturation point is achieved leading to reduction in the service time of the bed (Yahya et al., 2020a; Zhang et al., 2020). Adsorption capacity [q_e(exp); **Table 6.1**] was found to be high at 20 mL/min flow rate

which could be attributed to higher metal loading, hence enhanced uptake. In present study, since there was only slight difference in the percentage adsorption (Y %) at different flow rates (**Table 6.1**), therefore, treatment of the feed solution at higher flow rate (more adsorption capacity also) was selected for further studies as it is a requisite aspect when dealing in commercial applications which deals with large volumes of effluent.

6.1.2 Effect of bed height

In order to have an efficient continuous wastewater treatment system in a dynamic column mode, bed height or bed depth has an essential role. Here, two bed heights of 2 and 4 cm for the elimination of Pb^{2+} and Cd^{2+} from an artificial metal solution were utilised and the results are presented in **Fig. 6.3** and **Fig. 6.4**.

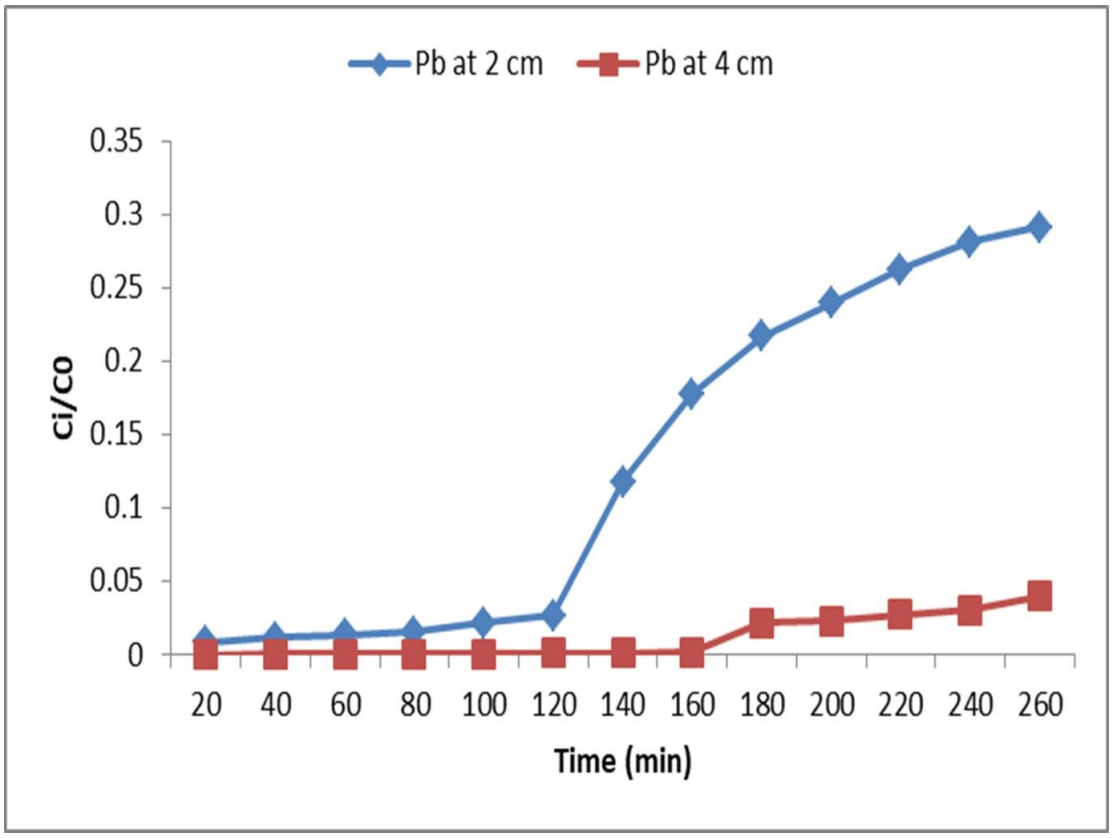

Figure 6.3 Breakthrough curves for Pb^{2+} bioadsorption onto BSBP at different bed heights (flow rate= 20 mL/min, inlet Pb^{2+} concentrations= 50 ppm, temperature= room temperature and influent pH= 4.0-4.5)

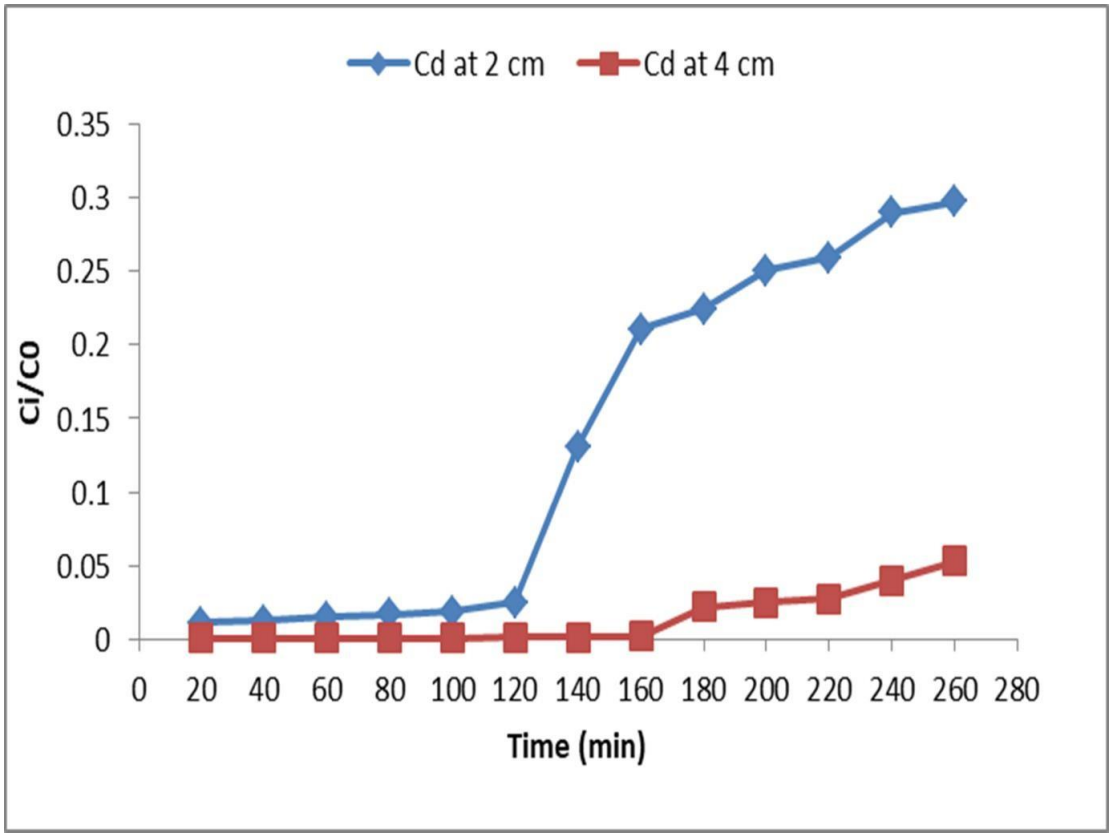

Figure 6.4 Breakthrough curves for Cd^{2+} bioadsorption onto BSBP at different bed heights (flow rate= 20 mL/min, inlet Cd^{2+} concentrations= 50 ppm, temperature= room temperature and influent pH= 4.0-4.5)

At an uniform flow rate of 20 mL/min and initial metal concentration of 50 ppm, it is evident that the breakthrough volume is different at different bed heights along with the appearance of characteristic ‗S' shaped plots representing the dominance of axial dispersion during mass transfer over diffusion process at low bed height (Luo et al., 2017; Yahya et al., 2020b). The metal ions do not get enough residence time to diffuse into the whole bio-adsorbent mass while the treated volume obtained was significantly less for a used flow rate from 5200 to 3600 mL for both Pb^{2+} and Cd^{2+} , respectively as evidently seen in **Fig. 6.3** and **Fig. 6.4** as ions do not gets dispersed efficiently in the column as the bed height was increased (Biswas et al., 2020; Renu et al., 2020). Present study revealed, steady enhancement in the percentage adsorption (Y %) from 80.48 to 91.32 % and 79.97 to 91.18 % for Pb^{2+} and Cd^{2+} ions, respectively when bed height was increased from 2 to 4 cm (**Table 6.1**). It indicates production of cleaner effluent with the rise in the bed height of the column as more binding sites would be available for the attachment of the metal ions (Amin et al.,

2017). Therefore bed height of 4 cm was selected as it gave maximum adsorption percentage i.e., removal of metal ions. The high adsorption capacity [q_e(exp); **Table 6.1**] at low bed height corresponded to the maximum exploitation of the binding sites available as reported in other studies as well (Hayati et al., 2018; Kausar et al., 2017).

6.1.3 Effect of initial metal concentrations

The change in the shape of the breakthrough curves at two different inlet metal concentrations of 50 and 100 ppm was examined at uniform bed height of 4 cm and a flow rate of 20 mL/min. The results are shown in the **Fig. 6.5** and **Fig. 6.6**.

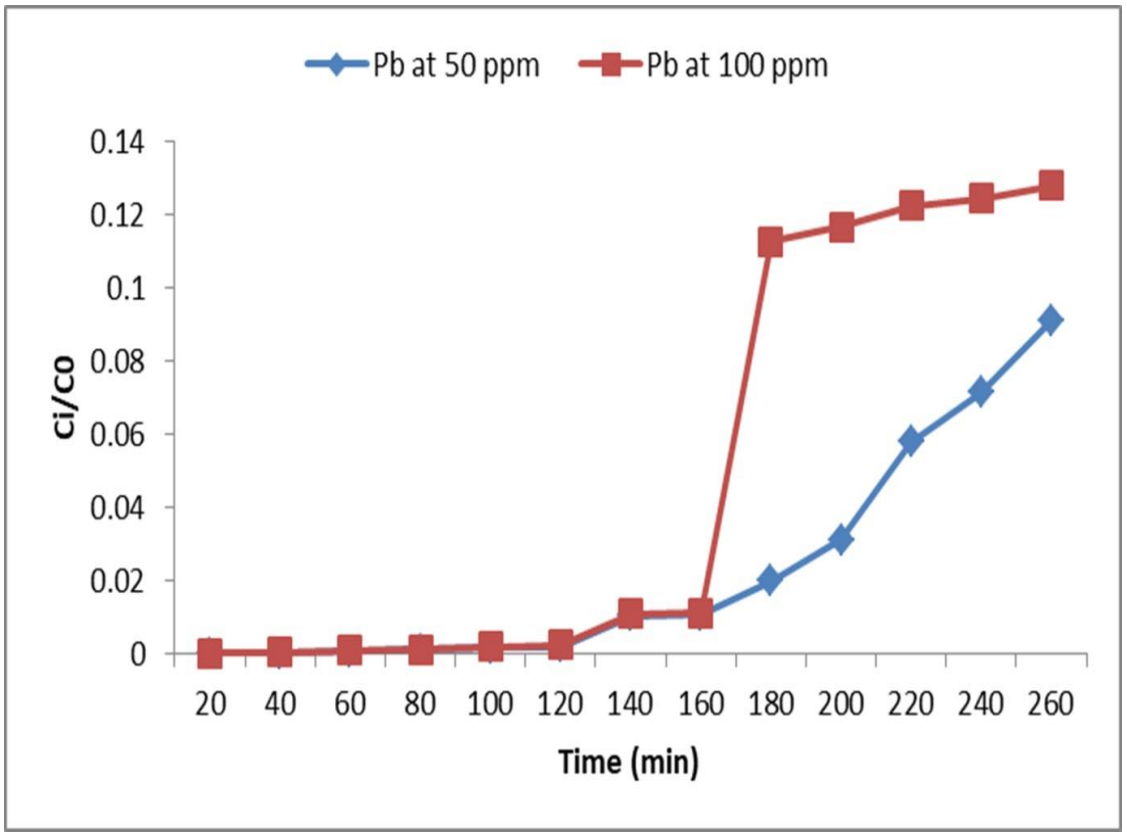

Figure 6.5 Breakthrough curves for Pb^{2+} bioadsorption onto BSBP at different inlet Pb^{2+} concentrations (bed height= 4 cm, flow rate= 20 mL/min, temperature= room temperature and influent pH= 4.0-4.5)

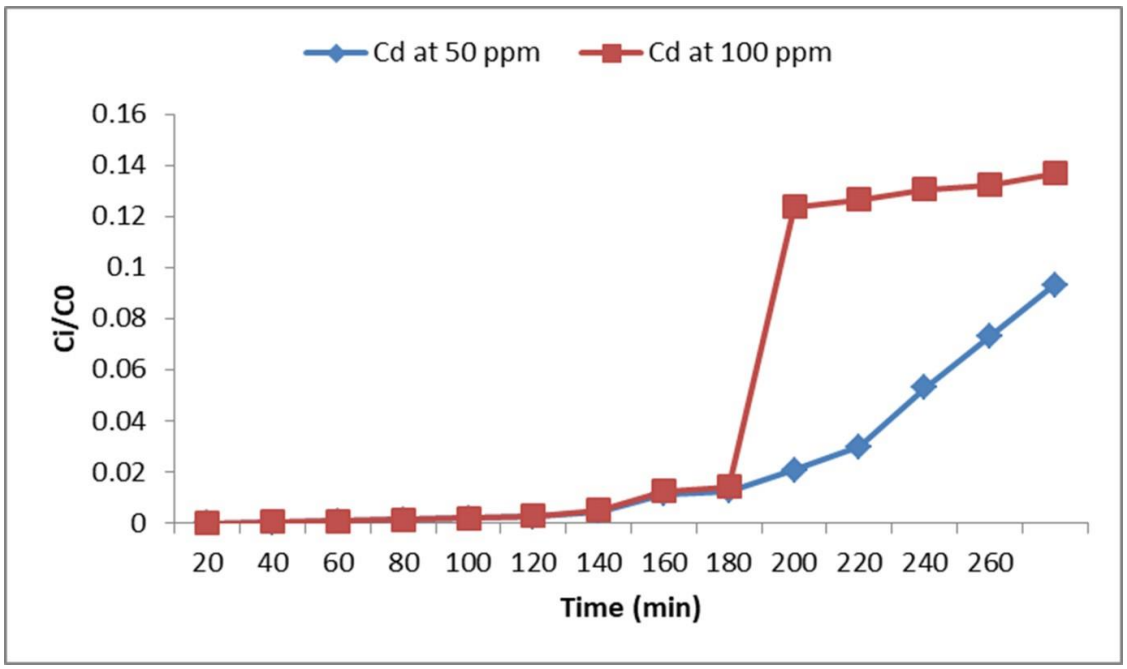

Figure 6.6 Breakthrough curves for Cd^{2+} bioadsorption onto BSBP at different inlet Cd^{2+} concentrations (bed height= 4 cm, flow rate= 20 mL/min, temperature= room temperature and influent pH= 4.0-4.5)

As can be observed from the breakthrough curves in **Fig. 6.5** and **Fig. 6.6,** breakthrough time is reduced with the increase in the inlet metal concentration with steeper lines at higher inlet concentrations for both Pb^{2+} and Cd^{2+}. The volume of the treated solution before reaching the bed saturation time is also reduced at higher inlet concentrations from 5200 mL to 3600 mL for Pb^{2+} and 6000 mL to 4000 mL for Cd^{2+} respectively. This is the case observed because high inlet metal concentration would saturate the bed rapidly thereby reducing the whole operation/contact time and vice versa (Hayati et al., 2018). At low inlet metal concentration, the breakthrough curves would shift more towards right and more volume will be required to treat the feed solution (Luo et al., 2017). The value of C_i/C_0 reached nearly 0.1 at 180 and 200 min for high inlet concentration of 100 ppm in case of both Pb^{2+} and Cd^{2+} respectively. The adsorption capacity [q_e(exp); **Table 6.1**] was assessed to be enhanced from 67.13 to 130.65 mg/g and 67.09 to 130.05 mg/g for Pb^{2+} and Cd^{2+} respectively when feed concentration was doubled to 100 ppm. However, percentage adsorption (Y %) was not altered much as bio-adsorbent dose (same bed height) was constant that leads to same number of binding sites available for both the feed concentrations (Vilvanathan & Shanthakumar, 2017). It could be estimated that the number of binding sites were not adequate at higher feed concentration as seen from the percentage adsorption (Y %) values **(Table 6.1)**.

6.1.4 Metal ion uptake at different column design parameters and their influence on breakthrough curves

The maximum column capacity, q_{total} (mg) for a set condition in the column was calculated from area under the curve plotted against adsorbed metal ions (C_{ad} in ppm) and time as shown below:

$$q_{total} = \frac{QA}{1000}\int_{t_0}^{t_{total}} C_{ad}\,dt \quad \text{..... (6.1)}$$

Here, Q is the flow rate (mL/min), A is the area under the BTC in cm^2, C_{ad} is C_0-C_i in ppm, t_{total} is the total time flow in min.

The equilibrium (adsorption) capacity, $q_{e\,(exp)}$ was calculated using:

$$q_{e(exp)} = \frac{q_{total}}{m} \quad \text{..... (6.2)}$$

Here, m is the amount of bio-adsorbent in the column (g).

The total treated volume, V_{eff} in mL was measured using:

$$V_{eff} = Qt_{total} \quad \text{..... (6.3)}$$

The column data obtained for a given set of conditions are represented in **Table 6.1**. The evaluation of results obtained using lab scale experiments is quite efficient for the design of a full scale bio-adsorbent column (Qu et al., 2019). From the data in **Table 6.1**, it is quite evident that the increase in the flow rate led to decreased percentage adsorption (Y %) and increased inlet treated volume. The optimum conditions produced for the Pb^{2+} and Cd^{2+} bioadsorption from aqueous solutions using biosurfactant modified activated banana peel powder (BSBP) were 100 ppm inlet metal ion concentration at 4 cm bed height using a flow rate of 20 mL/min that generated a breakthrough time of 3 h (**Table 6.1**). At this optimized conditions, the uptake (adsorption) capacity, q_e(exp) was found to be 130.65 mg/g for Pb^{2+} and 130.05 mg/g for Cd^{2+} ions, respectively using biosurfactant modified activated banana peel powder (BSBP). The adsorption capacities for removal of Pb^{2+} and Cd^{2+} from aqueous solutions reported in this study using BSBP are quite better from the previous literatures available. An adsorption capacity of 100 and 19.5 mg/g was reported for Pb^{2+} and Cd^{2+} using pectin-xanthan gum based bioadsorbent (Jakóbik-Kolon & Bok-Badura, 2020); 18.8 mg/g for Pb^{2+} using *Bauhinia purpurea* bioadsorbent (Sharma et

al., 2017); 53.90 mg/g for Pb^{2+} using *Liagora viscida* (Srikanth et al., 2021); 55.20 mg/g for Cd^{2+} with xanthate treated *Ficus religiosa* (Tariq et al., 2021).

Table 6.1 Pb^{2+} and Cd^{2+} uptake at different column parameters

Metal ion	Flow rate (Q) (mL/min)	Bed height (Z) (cm)	Feed concentration (C_0)	Total metals removed (q_{total}); mg	Total treated volume (V_{eff} in mL)	Adsorption capacity (q_e(exp)) (mg/g)	Percentage adsorption, Y (%)
	15	4	50	171.31	2400	48.95	87.85
	20	4	50	204.42	5200	58.41	78.62
	20	2	50	209.25	5200	139.5	80.48
Pb	20	4	50	237.44	3600	67.84	91.32
	20	4	50	234.95	5200	67.13	90.37
	20	4	100	457.26	4400	130.65	87.93
	15	4	50	169.59	2400	48.45	86.97
	20	4	50	199.42	5200	56.98	76.7
Cd	20	2	50	207.93	5200	138.62	79.97
	20	4	50	237.06	3600	67.73	91.18
	20	4	50	234.84	5200	67.09	90.32
	20	4	100	455.16	4600	130.05	87.53

The adsorption capacities obtained in column study for Pb^{2+} and Cd^{2+} were better than the batch process at optimized conditions. The possible bioadsorption capacity might be attributed to the presence of hydroxyl (─OH), and carboxylate (─COO^-) groups on the surface of the bio-adsorbent that are involved in the removal of Pb^{2+} and Cd^{2+} metal ions from aqueous solutions. The other minor factors that are also involved would be micro precipitation and electrostatic forces of attraction (Amin et al., 2017; Calero et al., 2018).

The design parameters selected for column study showed varied influence on the uptake capacity of Pb^{2+} and Cd^{2+} bioadsorption onto biosurfactant modified activated banana peel powder (BSBP). For instance, low flow rate had more percentage of adsorption as it favoured higher residence time for the influent or allowed more contact with the fixed bed leading to proper diffusion into the pores of the biosurfactant modified activated banana peel powder (BSBP) via intra-particle

diffusion kinetics. On the contrary, high flow rate resulted in rapid leaving of influent from the column before it gets to be adsorbed or equilibrium is achieved (Abdolali et al., 2017; Fallah & Taghizadeh, 2020). In our study, another parameter i.e., bed height also had a significant effect on the bioadsorption of Pb^{2+} and Cd^{2+} ions onto biosurfactant modified activated banana peel powder (BSBP). With the increase in the bed height, percentage adsorption (Y %) was found to be enhanced as metal ions had more contact time with BSBP particles (**Table 6.1**). Hence, it could be said that the maximum generation of cleaner effluent was collected at the outlet of the column (Alalwan et al., 2018). But, all high bed heights does not always produces the same trend at high bed height, the bed is more compact and restricts the contact of metal ions with its particles that results in enhanced slope of the breakthrough curves i.e., large or broad mass transfer zone would be observed. In the last, a high concentration gradient would provide a large driving force for the bioadsorption process and delayed saturation of the bed but breakthrough time is reached before all the active sites of the biosurfactant modified activated banana peel powder (BSBP) gets occupied by Pb^{2+} or Cd^{2+} ions (Hymavathi & Prabhakar, 2019).

6.1.5 Evaluation of column data by dynamic models

A number of efficient mathematical models are available for their usage in the design of continuous fixed bed column bioadsorption study. Most commonly used Thomas model has been used in this study for predicting the behaviour of breakthrough curves. At the same time, it has to be kept in mind that each adsorption process would be different with different materials and fitting of present experimental data having R^2 values closer to unity does not guarantees its applicability to produce same results for any other adsorption system, it only validates a particular experimental finding. So, for other metal ions (other than lead and cadmium), different set of conditions may have to be optimised for removal of those heavy metals from industrial wastewaters.

6.1.5.1 Thomas model

This model is widely used to describe the behaviour of breakthrough curves and is based on Langmuir model of adsorption-desorption system (Nwabanne & Igbokwe, 2012). It is also based on the assumption that axial dispersion is negligible during column adsorption and it follows pseudo second-order kinetics (Dalhat et al., 2021). The model was applied to the experimental data obtained and model parameters were

calculated from the linear plot made between Ln (C_0/C_i-1) against time _t'. The model **Eq. 6.4** is presented below:

$$\mathrm{Ln}\left[\frac{C_o}{C_i} - 1\right] = \frac{k_{th} q_o m}{Q} - k_{th} C_0 t \ldots\ldots\ldots\ldots\ldots \textbf{(6.4)}$$

From the intercept and the slope of the straight line plot obtained, the values of k_{TH} (Thomas model constant) and q_0 in mg/g (adsorption capacity) are measured respectively as shown in **Fig. 6.7** and **Table 6.2** for Pb^{2+} and Cd^{2+} , respectively.

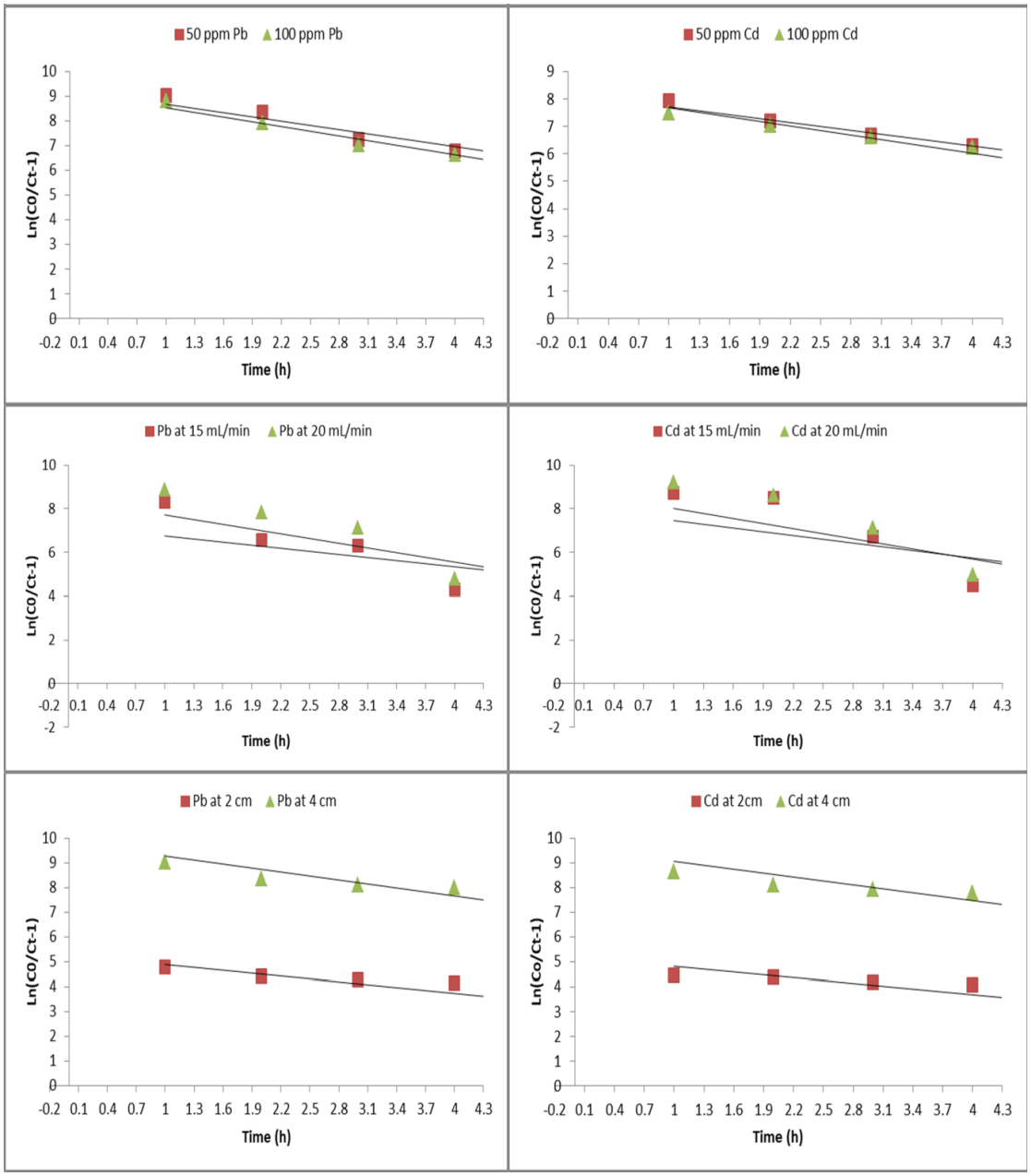

Figure 6.7 Thomas model graphs for Pb^{2+} and Cd^{2+} bioadsorption onto BSBP at different feed concentrations, flow rates and bed heights

Table 6.2 Evaluation of Thomas model parameters

Metal ion	Bed height „Z‟ (cm)	Flow rate „Q‟ (mL/min)	Feed concentration „C_0‟ (ppm)	Adsorption capacity „q_0‟ (mg/g)	Thomas model constant „k_{TH}‟ (mL/mg.min)	Regression coefficient „R^2‟
	4	15	50	3.43	9	0.8338
	4	20	50	3.45	14	0.8878
Pb	2	20	50	8.8	8	0.9192
	4	20	50	5.11	11	0.9323
	4	20	50	4.79	11	0.9784
	4	20	100	8.74	6.0	0.9399
	4	15	50	3.13	11	0.8189
	4	20	50	3.34	15	0.8687
	2	20	50	8.63	8	0.8878
Cd	4	20	50	4.98	11	0.9344
	4	20	50	4.93	9.5	0.992
	4	20	100	7.83	6.0	0.938

The results of the Thomas model indicated an increase in q_0 with the increase in flow rate and initial metal concentration over the entire bioadsorption period. However, the adsorption capacity, q_o from **Table 6.2** obtained were not in agreement with the experimental results q_e(exp) from **Table 6.1** . Although a good fit was observed for both the metal ions with regression coefficient (R^2) value lying between 0.83-0.99. The value of k_{TH} (**Table 6.2**) was found to be enhanced with the increasing flow rate. Similar trend was observed with the already published reports for chromium adsorption onto coconut coir pith (Suksabye et al., 2008) while decreased k_{TH} value was observed at increasing feed concentrations akin to the reports available indicating favourable driving force for bioadsorption on account of concentration difference (Basu et al., 2019). Higher flow rates lead to the rise in the mass transfer of ions from aqueous solutions onto the biosurfactant modified activated banana peel powder (BSBP) surface leading to enhanced q_0 value due to proper distribution and diffusion into the BSBP bed. However, it is suggested that this model might not be adequate to depict bioadsorption process in this study on account of deviation from q_0 values with the experimental values and hence, it is not considered as a suitable model for the design of the BSBP column bioadsorption.

6.1.6 Real effluent study

The optimised column conditions of flow rate (20 mL/min), bed height (4 cm) obtained for the Pb^{2+} and Cd^{2+} bioadsorption from aqueous solutions using biosurfactant modified activated banana peel powder (BSBP) were utilised for the removal of Pb^{2+} and Cd^{2+} from an electroplating wastewater at inlet concentrations of 20.86±0.197 ppm for Pb^{2+} and 6.39±0.029 ppm for Cd^{2+} that was originally present in the wastewater at pH 3.3±0.05. The selectivity of the biosurfactant modified activated banana peel powder (BSBP) towards Pb^{2+} and Cd^{2+} was examined when present in a concomitant metal system containing chromium, magnesium, manganese, iron, and zinc along with other physicochemical parameters whose concentrations were found above their permissible limits. The pH and temperature of the effluent was not altered and the study was performed to maintain the real world conditions.

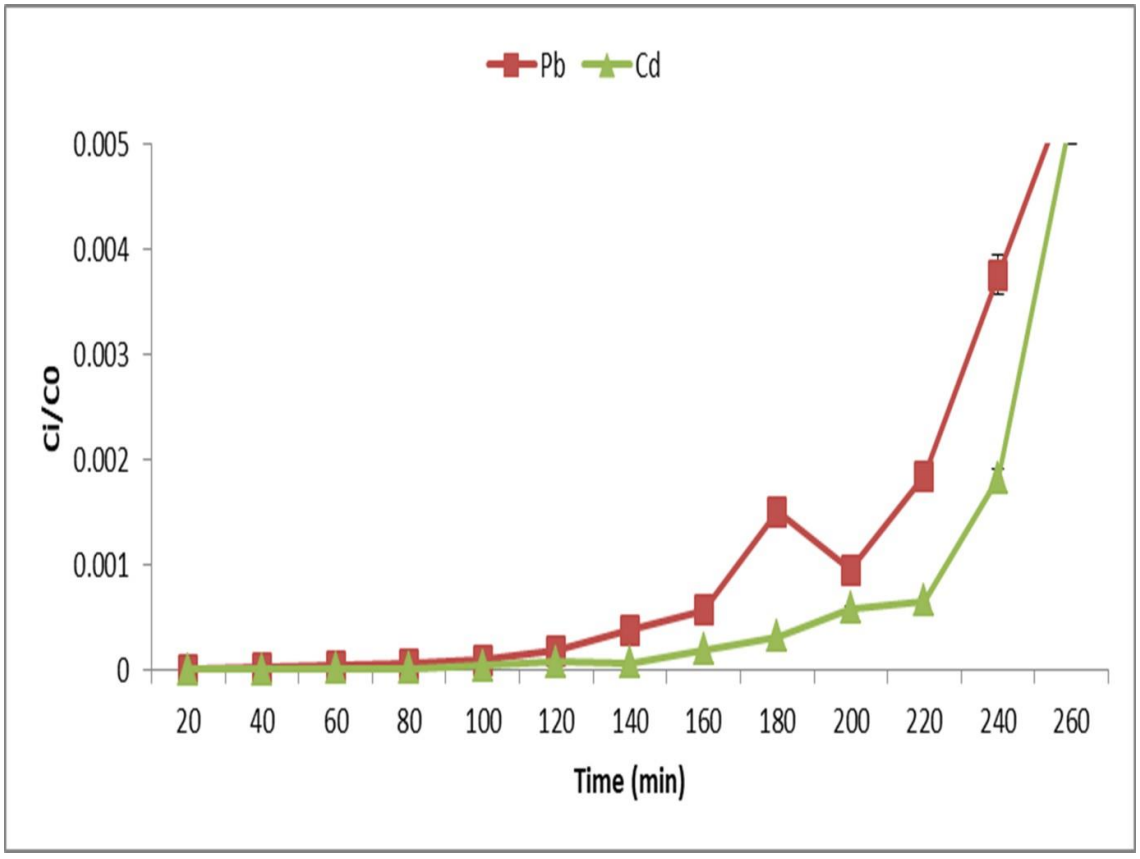

Figure 6.8 Breakthrough curves for Pb^{2+} and Cd^{2+} bioadsorption onto BSBP at different inlet Pb^{2+} and Cd^{2+} concentrations present in an electroplating wastewater (bed height= 4 cm, flow rate= 20 mL/min, temperature= 24.9±0.08 and influent pH=3.3±0.05)

Table 6.3 Pb^{2+} and Cd^{2+} uptake from an electroplating wastewater

Metal ion	Flow rate (Q) (mL/min)	Bed height (Z) (cm)	Feed concentration (C_0)	Total metals removed (q_{total}); mg	Total treated volume (V_{eff} in mL)	Adsorption capacity (q_e) (mg/g)	Percentage adsorption, Y (%)
Pb^{2+}	20	4	20.86±0.197	100	4600	28.57	92.19
Cd^{2+}	20	4	6.39±0.029	30.65	4600	8.76	92.24

The electroplating effluent from a local industry was utilised in an undiluted form and breakthrough curves for the removal of Pb^{2+} and Cd^{2+} are represented in **Fig. 6.8**. From the **Table 6.3**, it was found to have an adsorption capacity (q_e) of 28.57 and 8.76 mg/g for Pb^{2+} and Cd^{2+} respectively at a flow rate of 20 mL/min and a bed height of 4 cm yielding cleaner effluent containing 1.63±0.02 and 1.01±0.036 ppm of Pb^{2+} and Cd^{2+} , respectively (**Fig. 6.9)**. The biosurfactant modified activated banana peel powder (BSBP) particles indicated sufficient binding sites that efficiently adsorbed the metal ions on its surface without any significant loss in the rate of bioadsorption. Due to the presence of other heavy and light metal ions, considerable competition for the binding sites was observed. The light metal ions such as magnesium (Mg^{2+}) showed less strong binding behaviour, hence, it didn‘t interfere in the heavy metal ions binding due to their complexation with anionic chlorides, sulphates present in the solution (Jusoh et al., 2007; Kumar et al., 2011). The percentage adsorption (Y %) was also noted to be high (>90%) till the end of ~4 h. The performance of the BSBP column in the treatment of an industrial effluent was well established indicating its good prospects in practical applications (Ghorbani et al., 2018).

Figure 6.9 Schematic representation of bioadsorption study using electroplating effluent

As per Bureau of Indian Standards (BIS 10500: 2012) for land irrigation, most of the parameters for wastewater/effluent from electroplating industry were beyond the permissible limits. Overall pH, temperature and electrical conductivity (E_c) directly puts its effect on the ionic balance of the wastewater thereby affecting the chemical processes in the aqueous environment (Bharti & Kumar, 2018). The different concentrations of the total dissolved solids (TDS), total suspended solids (TSS), biological oxygen demand (BOD), dissolved oxygen (DO), chemical oxygen demand (COD) indicated the level of pollution present in the effluent on account of various organic and inorganic contaminants, hence affecting the water quality (Poonkothai & Vijayavathi, 2015). The colour of the effluent was observed to be muddy yellow with unpleasant odour that might be the reason for high value of BOD and COD leading to decline in dissolved oxygen (DO). The overall turbidity of the effluent was much reduced into a clean colourless effluent after treatment with permitted pH values in the range of BIS standards (5.5-9.0). Therefore, the overall comparison of various physicochemical parameters of an electroplating effluent before and after the dynamic

bioadsorption process were also observed to be reduced significantly with BSBP bio-adsorbent as shown in **Table 6.4**. This indicated that BSBP biomass is environmental-friendly, feasible that could be effectively utilised for the treatment of wastewaters discharged from different industries.

Table 6.4 Characterization of electroplating effluent before and after the bioadsorption treatment (all values are in ppm except pH (range), temperature (°C), electrical conductivity (mS/m; results are expressed as mean of three replicates±SD (n=3))

Parameters	Before treatment	After treatment
pH	3.3±0.05	6.8±0.048
Temperature	24.9±0.08	25.5±0.01
E_c	1236.2±4.35	624.25±0.007
TSS	1379.7±7.13	195±0.08
TDS	574±21.4	223.64±0.03
COD	475±10.98	124.54±0.008
BOD	80±1.63	11.09±0.01
Sulphate	311.67±11.95	95.45±0.07
Phosphate	0.323±0.088	0.145±0.09
Chromium	0.226±0.01	0.001±0.01
Magnesium	22.39±0.11	15.24±0.08
Manganese	3.99±0.08	1.58±0.04
Iron	30.88±0.39	14.68±0.14
Zinc	0.22±0.001	0.001±0.01
Cadmium	6.39±0.029	1.01±0.036
Lead	20.86±0.197	1.63±0.02

6.2 Conclusions

The present column design using biosurfactant modified activated banana peel powder (BSBP) suggested better Pb^{2+} and Cd^{2+} uptake capacities at higher flow rate, and feed concentrations but low bed height in aqueous solutions having almost similar adsorption capacities for both the metal ions with a service breakthrough time of ~4-5 h. High bed height is preferred on account of better adsorption percentage of metal

ions. Thomas model selected for the prediction of metal ions breakthrough was found to be poor but the adsorption capacities found by the Thomas model were higher than the batch process. The removal of Pb^{2+} and Cd^{2+} ions from real effluent showed efficient 92.19 and 92.24% adsorption with much reduced physicochemical parameters in the presence of multi-metal system. The efficiency of the BSBP for Pb^{2+} and Cd^{2+} was not hindered in the presence of other heavy metal ions. Biosurfactant (surfactin from *Bacillus haynesii*) modified activated banana peel powder (BSBP) illustrated a good practical implication for the treatment of industrial effluents.

Chapter 7
Conclusions and Recommendations

Some of the common industries that generate heavy metal containing effluent include tanneries, mining, electroplating, fertilizer, smelting plants, etc. On account of various industrial operations, copious measures of wastewater are produced and are being dismissed nonchalantly into the water bodies affecting its environment (Agarwal et al., 2020; Ahmed et al., 2021). Such wastewaters contain toxic, carcinogenic, indelible heavy metal ions therefore, it requires their efficient treatment before dumping into the ecosystem (Gupta et al., 2020). Lead, Cadmium, Mercury, Arsenic, Chromium, Copper, etc. are most common heavy metal ions found in such industrial effluents that has high binding affinity for biological macromolecules composed of oxygen, nitrogen, etc. thereby, exerts interference towards the normal functioning of different organ systems by exhibiting their harmful effects such as diseases like Itai-Itai in Japan due to cadmium toxicity, etc. (Calabrò et al., 2021; Saini et al., 2020).

Numerous conventional treatment techniques such as chemical precipitation, flotation, coagulation, etc., are available for heavy metal remediation but all are associated with certain advantages and disadvantages. Major drawback includes high operational costs and generation of secondary toxic by-products (Vo et al., 2020). However, adsorption seems to be a promising, an economically feasible, environmental friendly process that involves flexible process factors (Sheth et al., 2021). Some of the conventional materials such as zeolites, commercial activated carbon are widely explored adsorbents but has limitations like difficult regeneration, and are expensive (Bagchi & Behera, 2020; Qasem et al., 2021; Wadhawan et al., 2020).Therefore, their limitations has shifted the direction in search of an economical alternative that poses less or no threat to the environment as well. The extensive usage of agro-industrial based bio-adsorbents have given rise to greener non-conventional remediation technology that are low cost, have numerous binding sites containing rich functional groups, and give good bioadsorption capacities comparable to the conventional adsorbents (Chai et al., 2021; Sabir et al., 2021; Vo et al., 2020). Further, their (bio-adsorbents) modification with suitable agents enhances their performance ability for a particular pollutant in study (Gupta et al., 2020; Surgutskaia et al., 2020).

Keeping in view of background of this problem, the present study was designed to assess the potential of low cost and efficient bioadsorption system for the removal of Pb^{2+} and Cd^{2+} from aqueous solutions and real effluents through batch and column based experiments. To fulfil the objectives of the present study, economical

agro/biowastes i.e., rice husk powder (RHP), *Eucalyptus* saw dust powder (SDP), orange peel powder (OPP), banana peel powder (BPP), activated carbon from orange and banana fruit peel wastes (AcOPP and AcBPP) were prepared. The activated banana peel powder performed (AcBPP) well in the batch adsorption process and hence, it was fabricated with bacterial metabolite i.e., surfactin to be used in the column adsorption process for heavy metal removal. To prepare biosurfactant modified activated banana peel powder (BSBP); bacterial isolates from hydrocarbon contaminated sites were screened for their biosurfactant production. The potential bacterial strains were further subjected to the mass production of biosurfactant and extraction. The evaluation of the prepared bio-adsorbents were done in terms of their characterization, effect of process conditions, regeneration and desorption percentages by utilizing Pb^{2+} and Cd^{2+} as primary pollutants in aqueous solutions and in a multi metal wastewater system.

Salient findings of the present study entitled ‒Assessment of agro-industrial and bacterial surfactant based bioadsorbent column for heavy metal removal from industrial wastewater‖ are summarised below:

1. All the bio-adsorbents that were used in the study i.e., activated orange peel powder (AcOPP), activated banana peel powder (AcBPP) and biosurfactant modified activated banana peel powder (BSBP) illustrated the presence of microporous particles in their asymmetric structures and pores which contributed towards the affinity for high binding of the pollutants (heavy metals such as Pb^{2+} and Cd^{2+}).

2. Prepared bio-adsorbent surfaces represented diverse functional moieties such as anionic oxygen containing functional groups as carboxylic, phenolics, hydroxyls and amines that served as high binding sites for positively charged heavy metal ions.

3. BET (Brunauer-Emmett-Teller) analysis revealed that orange peel powder (OPP) possessed highest while rice husk powder (RHP) had lowest surface area, respectively.

4. The bioadsorption process was affected by change in the experimental conditions such as pH, contact time, bio-adsorbent dose, and initial metal ion

concentration. Bio-adsorbents were best regenerated using 0.1N HNO_3 and were reusable up to 3 times with little loss in the efficiency.

5. The Langmuir adsorption isotherm model showed best fit as regression coefficient i.e., R^2 value ranging between 0.97 to 0.99 than the other two Freundlich and Temkin model for the removal of Pb^{2+} and Cd^{2+} ions from aqueous solutions having maximum bioadsorption capacities (q_m) of 96.15 and 93.46 mg/g respectively with activated orange peel powder (AcOPP) while 111.11 and 54.05 mg/g, respectively using activated banana peel powder (AcBPP).

6. The Langmuir isotherm model behaviour depicted performance of activated orange peel powder (AcOPP) to be better than activated banana peel powder (AcBPP) in terms of regression coefficient value in comparison to the experimental results where AcBPP performed better than AcOPP for Pb^{2+} and Cd^{2+} removal. However, according to the overall batch adsorption results obtained, AcBPP presented better bioadsorption potential than AcOPP in the order $Pb^{2+} > Cd^{2+}$.

7. The pseudo-second-order kinetic model was found to be in agreement with the bioadsorption process for both the bio-adsorbents with bioadsorption capacity values of 85.47 mg/g at 50 ppm Pb^{2+} , 119.05 mg/g at 100 ppm Pb^{2+}, 96.15 mg/g at 50 ppm Cd^{2+} and 103.09 mg/g at 100 ppm Cd^{2+} using AcOPP.

8. The AcBPP depicted adsorption 62.5 mg/g at 50 ppm Pb^{2+}, 100 mg/g at 100 ppm Pb^{2+}, 60.61 mg/g at 50 ppm Cd^{2+} and 91.74 mg/g at 100 ppm Cd^{2+} which was quite similar to the experimental results indicating the role of physico- and chemisorption processes.

9. The biosurfactant producing bacterial strains were reported to yield ~3.7 g/L surfactin biosurfactant and ~2.4 g/L rhamnolipid biosurfactant using raw orange peel extract wastes as carbon substrates with *Bacillus haynesii* E1 and *Pseudomonas aeruginosa* F5 respectively.

10. On account of high yield of surfactin from *Bacillus haynesii* E1, it was utilised to modify the activated banana peel powder (AcBPP) to make biosurfactant modified activated banana peel powder (BSBP) for column mode study.

11. Fixed-bed column experiments explained better removal of Pb^{2+} and Cd^{2+} ions at parameters such as higher feed concentrations, higher feed flow rate, and higher bio-adsorbent bed height giving uptake (bioadsorption) capacity of 130.65 and 130.05 mg/g for Pb^{2+} and Cd^{2+} removal from aqueous solutions.

12. The removal of metal ions from an electroplating effluent depicted bioadsorption percentage of 92.19 and 92.24 % for Pb^{2+} and Cd^{2+}, respectively.

7.1 Conclusion:

The continuous column mode study showed better results than the batch process. The modification of activated banana peel powder with surfactin biosurfactant presented an economical aspect of bio-adsorbent preparation having good heavy metal removal efficiency giving it an equal weightage among its other representatives. This recommends its application at industrial scale as biofilter material for the treatment of effluents and their discharge into natural bodies of water.

7.2 Recommendations

The prepared bio-adsorbents showed good metal removal efficiencies and could be regenerated multiple times without significant loss in their efficiency. These could also be applied in continuous mode for industrial effluents/wastewater. Based on the experimental investigation, following recommendations are provided for the future study:

1. A pilot-scale bio-adsorbent column containing prepared bio-adsorbent could be utilised for other industrial effluents.

2. Fabrication of the bio-adsorbent with surfactin biosurfactant showed promising results in metal removal, the tailoring of the bio-adsorbent with other biosurfactant molecules of other class or in combination could be explored in the removal of metals from concomitant (organic/inorganic) systems.

3. A desirable modification (and/or statistical optimisation) of the methodology employed in the preparation of the bio-adsorbent can be explored to achieve higher metal removal efficiencies.

4. A bioreactor based study could be conducted to remove organic pollutants and nutrients such as organic carbon that are being added on account of dissolving bio-adsorbent in aqueous solutions.

These recommendations will be helpful for future research for exploring more alternates with different types of wastewater and their subsequent application in Industrial wastewater treatment having metals other than lead and cadmium.

Bibliography

Abd-Elwahed, M.S. 2018. Influence of long-term wastewater irrigation on soil quality and its spatial distribution. *Annals of Agricultural Sciences*, **63**(2), 191-199.

Abd Elhafez, S., Hamad, H., Zaatout, A., Malash, G. 2017. Management of agricultural waste for removal of heavy metals from aqueous solution: adsorption behaviors, adsorption mechanisms, environmental protection, and techno-economic analysis. *Environmental Science and Pollution Research*, **24**(2), 1397-1415.

Abdić, Š., Memić, M., Šabanović, E., Sulejmanović, J., Begić, S. 2018. Adsorptive removal of eight heavy metals from aqueous solution by unmodified and modified agricultural waste: tangerine peel. *International Journal of Environmental Science and Technology*, **15**(12), 2511-2518.

Abdolali, A., Ngo, H.H., Guo, W., Zhou, J.L., Zhang, J., Liang, S., Chang, S.W., Nguyen, D.D., Liu, Y. 2017. Application of a breakthrough biosorbent for removing heavy metals from synthetic and real wastewaters in a lab-scale continuous fixed-bed column. *Bioresource technology*, **229**, 78-87.

Abdullah, N., Yusof, N., Lau, W., Jaafar, J., Ismail, A. 2019. Recent trends of heavy metal removal from water/wastewater by membrane technologies. *Journal of Industrial and Engineering Chemistry*, **76**, 17-38.

Abouseoud, M., Maachi, R., Amrane, A., Boudergua, S., Nabi, A. 2008. Evaluation of different carbon and nitrogen sources in production of biosurfactant by Pseudomonas fluorescens. *Desalination*, **223**(1-3), 143-151.

Afroze, S., Sen, T.K. 2018. A review on heavy metal ions and dye adsorption from water by agricultural solid waste adsorbents. *Water, Air, & Soil Pollution*, **229**(7), 1-50.

Agarwal, A., Upadhyay, U., Sreedhar, I., Singh, S.A., Patel, C.M. 2020. A review on valorization of biomass in heavy metal removal from wastewater. *Journal of Water Process Engineering*, **38**, 101602.

Agouborde, L., Navia, R. 2009. Heavy metals retention capacity of a non-conventional sorbent developed from a mixture of industrial and agricultural wastes. *Journal of hazardous materials*, **167**(1-3), 536-544.

Ahmad, R., Mirza, A. 2015. Sequestration of heavy metal ions by Methionine modified bentonite/Alginate (Meth-bent/Alg): A bionanocomposite. *Groundwater for Sustainable Development*, **1**(1-2), 50-58.

Ahmad, T., Danish, M. 2018. Prospects of banana waste utilization in wastewater treatment: A review. *Journal of environmental management*, **206**, 330-348.

Ahmed, S.F., Mofijur, M., Parisa, T.A., Islam, N., Kusumo, F., Inayat, A., Badruddin, I.A., Khan, T.Y., Ong, H.C. 2021. Progress and challenges of contaminate removal from wastewater using microalgae biomass. *Chemosphere*, 131656.

Ajsuvakova, O.P., Tinkov, A.A., Aschner, M., Rocha, J.B., Michalke, B., Skalnaya, M.G., Skalny, A.V., Butnariu, M., Dadar, M., Sarac, I. 2020. Sulfhydryl groups as targets of mercury toxicity. *Coordination chemistry reviews*, **417**, 213343.

Akbari, S., Abdurahman, N.H., Yunus, R.M., Fayaz, F., Alara, O.R. 2018. Biosurfactants—a new frontier for social and environmental safety: a mini review. *Biotechnology Research and Innovation*, **2**(1), 81-90.

Al-Alawi, A., Van de Voort, F.R., Sedman, J. 2004. New FTIR method for the determination of FFA in oils. *Journal of the American Oil Chemists' Society*, **81**(5), 441-446.

Al-Ghouti, M.A., Da'ana, D.A. 2020. Guidelines for the use and interpretation of adsorption isotherm models: A review. *Journal of hazardous materials*, **393**, 122383.

Al Naggar, Y., Khalil, M.S., Ghorab, M.A. 2018. Environmental pollution by heavy metals in the aquatic ecosystems of Egypt. *Open Acc. J. Toxicol*, **3**, 555603.

Alak, G., Parlak, V., Aslan, M.E., Ucar, A., Atamanalp, M., Turkez, H. 2019. Borax supplementation alleviates hematotoxicity and DNA damage in rainbow trout (Oncorhynchus mykiss) exposed to copper. *Biological trace element research*, **187**(2), 536-542.

Alalwan, H.A., Abbas, M.N., Abudi, Z.N., Alminshid, A.H. 2018. Adsorption of thallium ion (Tl+ 3) from aqueous solutions by rice husk in a fixed-bed column: Experiment and prediction of breakthrough curves. *Environmental Technology & Innovation*, **12**, 1-13.

Algül, F., Beyhan, M. 2020. Concentrations and sources of heavy metals in shallow sediments in Lake Bafa, Turkey. *Scientific reports*, **10**(1), 1-12.

Almansoory, A.F., Hasan, H.A., Idris, M., Abdullah, S.R.S., Anuar, N. 2017. Biosurfactant production by the hydrocarbon-degrading bacteria (HDB) Serratia marcescens: Optimization using central composite design (CCD). *Journal of industrial and engineering chemistry*, **47**, 272-280.

Almeida, D.G., Soares da Silva, R.d.C.F., Luna, J.M., Rufino, R.D., Santos, V.A., Sarubbo, L.A. 2017. Response surface methodology for optimizing the production of biosurfactant by Candida tropicalis on industrial waste substrates. *Frontiers in microbiology*, **8**, 157.

Amin, M., Alazba, A., Shafiq, M. 2017. Batch and fixed-bed column studies for the biosorption of Cu (II) and Pb (II) by raw and treated date palm leaves and orange peel. *Global Nest Journal*, **19**(3), 464-478.

Arora, R. 2019. Adsorption of heavy metals–A review. *Materials Today: Proceedings*, **18**, 4745-4750.

Astuti, D.I., Purwasena, I.A., Putri, R.E., Amaniyah, M., Sugai, Y. 2019. Screening and characterization of biosurfactant produced by Pseudoxanthomonas sp. G3 and its applicability for enhanced oil recovery. *Journal of Petroleum Exploration and Production Technology*, **9**(3), 2279-2289.

Attari, M., Bukhari, S.S., Kazemian, H., Rohani, S. 2017. A low-cost adsorbent from coal fly ash for mercury removal from industrial wastewater. *Journal of Environmental Chemical Engineering*, **5**(1), 391-399.

Ayangbenro, A.S., Babalola, O.O. 2020. Genomic analysis of Bacillus cereus NWUAB01 and its heavy metal removal from polluted soil. *Scientific reports*, **10**(1), 1-12.

Ayangbenro, A.S., Babalola, O.O. 2018. Metal (loid) bioremediation: strategies employed by microbial polymers. *Sustainability*, **10**(9), 3028.

Ayangbenro, A.S., Babalola, O.O. 2017. A new strategy for heavy metal polluted environments: a review of microbial biosorbents. *International journal of environmental research and public health*, **14**(1), 94.

Azimi, A., Azari, A., Rezakazemi, M., Ansarpour, M. 2017. Removal of heavy metals from industrial wastewaters: a review. *ChemBioEng Reviews*, **4**(1), 37-59.

Baby, R., Saifullah, B., Hussein, M.Z. 2019. Palm Kernel Shell as an effective adsorbent for the treatment of heavy metal contaminated water. *Scientific reports*, **9**(1), 1-11.

Bagchi, S., Behera, M. 2020. Assessment of heavy metal removal in different bioelectrochemical systems: A review. *Journal of Hazardous, Toxic, and Radioactive Waste*, **24**(3), 04020010.

Bajpai, A., Sharma, M., Gond, L. 2019. Nanocomposites for environmental pollution remediation. in: *Sustainable Polymer Composites and Nanocomposites*, Springer, pp. 1407-1440.

Bajpai, A., Singh, B., Johri, B.N. 2020. Rhamnolipids and siderophores from Pseudomonas protegens strain BNJ-SS-45 isolated from wheat rhizosphere. *Environmental Sustainability*, **3**, 219-228.

Bakos, V., Szombathy, P., Simon, J., Jobbágy, A. 2020. Implementing Cost-effective Co-treatment of Domestic and Food-industrial Wastewater by Novel Methods for Estimating Industrial Load. *Periodica Polytechnica Chemical Engineering*, **64**(4), 505-513.

Bankar, A., Joshi, B., Kumar, A.R., Zinjarde, S. 2010. Banana peel extract mediated novel route for the synthesis of silver nanoparticles. *Colloids and Surfaces A: Physicochemical and Engineering Aspects*, **368**(1-3), 58-63.

Bashir, A., Malik, L.A., Ahad, S., Manzoor, T., Bhat, M.A., Dar, G., Pandith, A.H. 2019. Removal of heavy metal ions from aqueous system by ion-exchange and biosorption methods. *Environmental Chemistry Letters*, **17**(2), 729-754.

Basu, M., Guha, A.K., Ray, L. 2019. Adsorption of lead on lentil husk in fixed bed column bioreactor. *Bioresource technology*, **283**, 86-95.

Bayuo, J., Abukari, M.A., Pelig-Ba, K.B. 2020. Desorption of chromium (VI) and lead (II) ions and regeneration of the exhausted adsorbent. *Applied Water Science*, **10**(7), 1-6.

Bediako, J.K., Sarkar, A.K., Lin, S., Zhao, Y., Song, M.-H., Choi, J.-W., Cho, C.-W., Yun, Y.-S. 2019. Characterization of the residual biochemical components of sequentially extracted banana peel biomasses and their environmental remediation applications. *Waste management*, **89**, 141-153.

Bernhoft, R.A. 2013. Cadmium toxicity and treatment. *The Scientific World Journal*, **2013**.

Bezza, F.A., Chirwa, E.M.N. 2016. Biosurfactant-enhanced bioremediation of aged polycyclic aromatic hydrocarbons (PAHs) in creosote contaminated soil. *Chemosphere*, **144**, 635-644.

Bezza, F.A., Chirwa, E.M.N. 2015. Production and applications of lipopeptide biosurfactant for bioremediation and oil recovery by Bacillus subtilis CN2. *Biochemical engineering journal*, **101**, 168-178.

Bharti, S.K., Kumar, N. 2018. Kinetic study of lead (Pb 2+) removal from battery manufacturing wastewater using bagasse biochar as biosorbent. *Applied Water Science*, **8**(4), 1-13.

Bhatnagar, A., Minocha, A. 2006. Conventional and non-conventional adsorbents for removal of pollutants from water–A review.

Bhosale, S.S., Rohiwal, S.S., Chaudhary, L.S., Pawar, K.D., Patil, P.S., Tiwari, A.P. 2019. Photocatalytic decolorization of methyl violet dye using Rhamnolipid biosurfactant modified iron oxide nanoparticles for wastewater treatment. *Journal of Materials Science: Materials in Electronics*, **30**(5), 4590-4598.

Bian, S.-W., Mudunkotuwa, I.A., Rupasinghe, T., Grassian, V.H. 2011. Aggregation and dissolution of 4 nm ZnO nanoparticles in aqueous environments: influence of pH, ionic strength, size, and adsorption of humic acid. *Langmuir*, **27**(10), 6059-6068.

Biria, D., Maghsoudi, E., Roostaazad, R., Dadafarin, H., Lotfi, A.S., Amoozegar, M. 2010. Purification and characterization of a novel biosurfactant produced by Bacillus licheniformis MS3. *World Journal of Microbiology and Biotechnology*, **26**(5), 871-878.

Biswas, S., Sharma, S., Mukherjee, S., Meikap, B.C., Sen, T.K. 2020. Process modelling and optimization of a novel Semifluidized bed adsorption column operation for aqueous phase divalent heavy metal ions removal. *Journal of Water Process Engineering*, **37**, 101406.

Bode-Aluko, C.A., Pereao, O., Ndayambaje, G., Petrik, L. 2017. Adsorption of toxic metals on modified polyacrylonitrile nanofibres: a review. *Water, Air, & Soil Pollution*, **228**(1), 1-11.

Boostani, H.R., Najafi-Ghiri, M., Hardie, A.G. 2019. Single and competitive adsorption isotherms of some heavy metals onto a light textured calcareous soil amended with agricultural wastes-biochars. *Archives of Agronomy and Soil Science*, **65**(3), 360-373.

Bouassida, M., Fourati, N., Ghazala, I., Ellouze-Chaabouni, S., Ghribi, D. 2018. Potential application of Bacillus subtilis SPB1 biosurfactants in laundry detergent formulations: Compatibility study with detergent ingredients and washing performance. *Engineering in Life Sciences*, **18**(1), 70-77.

Brame, J., Griggs, C. 2016a. Surface Area Analysis Using the Brunauer-Emmett-Teller (BET) Method: Standard Operating Procedure Series: SOP-C. US Army Engineer Research and Development Center-Environmental Laboratory ….

Brame, J.A., Griggs, C.S. 2016b. Surface area analysis using the Brunauer-Emmett-Teller (BET) method: scientific operation procedure series: SOP-C.

Briffa, J., Sinagra, E., Blundell, R. 2020. Heavy metal pollution in the environment and their toxicological effects on humans. *Heliyon*, **6**(9), e04691.

Cai, Y., Li, X., Liu, D., Xu, C., Ai, Y., Sun, X., Zhang, M., Gao, Y., Zhang, Y., Yang, T. 2018. A novel Pb-resistant Bacillus subtilis bacterium isolate for co-biosorption of hazardous Sb (III) and Pb (II): thermodynamics and application strategy. *International journal of environmental research and public health*, **15**(4), 702.

Calabrò, P.S., Bilardi, S., Moraci, N. 2021. Advancements in the use of filtration materials for the removal of heavy metals from multicontaminated solutions. *Current Opinion in Environmental Science & Health*, 100241.

Calero, M., Iáñez-Rodríguez, I., Pérez, A., Martín-Lara, M., Blázquez, G. 2018. Neural fuzzy modelization of copper removal from water by biosorption in fixed-bed columns using olive stone and pinion shell. *Bioresource technology*, **252**, 100-109.

Calvert, J.G. 1990. Glossary of atmospheric chemistry terms (Recommendations 1990). *Pure and applied chemistry*, **62**(11), 2167-2219.

Can, N., Ömür, B.C., Altındal, A. 2016. Modeling of heavy metal ion adsorption isotherms onto metallophthalocyanine film. *Sensors and Actuators B: Chemical*, **237**, 953-961.

Cariccio, V.L., Samà, A., Bramanti, P., Mazzon, E. 2019. Mercury involvement in neuronal damage and in neurodegenerative diseases. *Biological trace element research*, **187**(2), 341-356.

Castro, L., Blázquez, M.L., González, F., Muñoz, J.A., Ballester, A. 2018. Heavy metal adsorption using biogenic iron compounds. *Hydrometallurgy*, **179**, 44-51.

Çelebi, H. 2020. Recovery of detox tea wastes: usage as a lignocellulosic adsorbent in Cr6+ adsorption. *Journal of Environmental Chemical Engineering*, **8**(5), 104310.

Chai, W.S., Cheun, J.Y., Kumar, P.S., Mubashir, M., Majeed, Z., Banat, F., Ho, S.-H., Show, P.L. 2021. A review on conventional and novel materials towards heavy metal adsorption in wastewater treatment application. *Journal of Cleaner Production*, 126589.

Chakraborty, S., Ghosh, M., Chakraborti, S., Jana, S., Sen, K.K., Kokare, C., Zhang, L. 2015. Biosurfactant produced from Actinomycetes nocardiopsis A17: characterization and its biological evaluation. *International journal of biological macromolecules*, **79**, 405-412.

Charkiewicz, A.E., Backstrand, J.R. 2020. Lead toxicity and pollution in Poland. *International Journal of Environmental Research and Public Health*, **17**(12), 4385.

Chatterjee, A., Abraham, J. 2019. Desorption of heavy metals from metal loaded sorbents and e-wastes: A review. *Biotechnology letters*, **41**(3), 319-333.

Chen, C., Sun, N., Li, D., Long, S., Tang, X., Xiao, G., Wang, L. 2018. Optimization and characterization of biosurfactant production from kitchen waste oil using Pseudomonas aeruginosa. *Environmental Science and Pollution Research*, **25**(15), 14934-14943.

Chen, W., Qu, Y., Xu, Z., He, F., Chen, Z., Huang, S., Li, Y. 2017. Heavy metal (Cu, Cd, Pb, Cr) washing from river sediment using biosurfactant rhamnolipid. *Environmental Science and Pollution Research*, **24**(19), 16344-16350.

Chetty, S., Pillay, L. 2019. Assessing the influence of human activities on river health: a case for two South African rivers with differing pollutant sources. *Environmental monitoring and assessment*, **191**(3), 1-11.

Chintalpudi, V., Kanamarlapudi, R., Mallu, U., Muddada, S. 2021. Isolation, identification, biosorption optimization, characterization, isotherm, kinetic and application of novel bacterium Chelatococcus sp. biomass for removal of Pb (II) ions from aqueous solutions. *International Journal of Environmental Science and Technology*, 1-14.

Chung, K.W., Dhillon, P., Huang, S., Sheng, X., Shrestha, R., Qiu, C., Kaufman, B.A., Park, J., Pei, L., Baur, J. 2019. Mitochondrial damage and activation of the STING pathway lead to renal inflammation and fibrosis. *Cell metabolism*, **30**(4), 784-799. e5.

Claus, D. 1992. A standardized Gram staining procedure.

Crini, G., Lichtfouse, E., Wilson, L.D., Morin-Crini, N. 2019. Conventional and non-conventional adsorbents for wastewater treatment. *Environmental Chemistry Letters*, **17**(1), 195-213.

Crockett, S.A. 2012. A five-step guide to conducting SEM analysis in counseling research. *Counseling Outcome Research and Evaluation*, **3**(1), 30-47.

Cruz, J.M., Hughes, C., Quilty, B., Montagnolli, R.N., Bidoia, E.D. 2018. Agricultural feedstock supplemented with manganese for biosurfactant production by Bacillus subtilis. *Waste and biomass valorization*, **9**(4), 613-618.

Czikkely, M., Neubauer, E., Fekete, I., Ymeri, P., Fogarassy, C. 2018. Review of heavy metal adsorption processes by several organic matters from wastewaters. *Water*, **10**(10), 1377.

Dąbrowski, A. 2001. Adsorption—from theory to practice. *Advances in colloid and interface science*, **93**(1-3), 135-224.

Dada, A., Olalekan, A., Olatunya, A., Dada, O. 2012. Langmuir, Freundlich, Temkin and Dubinin–Radushkevich isotherms studies of equilibrium sorption of Zn2+ unto phosphoric acid modified rice husk. *IOSR Journal of Applied Chemistry*, **3**(1), 38-45.

Dalhat, M., Mu'azu, N.D., Essa, M.H. 2021. Generalized decay and artificial neural network models for fixed-Bed phenolic compounds adsorption onto activated date palm biochar. *Journal of Environmental Chemical Engineering*, **9**(1), 104711.

Das, S.C., Al-Naemi, H.A. 2019. Cadmium toxicity: oxidative stress, inflammation and tissue injury.

Datar, A., Chung, Y.G., Lin, L.-C. 2020. Beyond the BET analysis: the surface area prediction of nanoporous materials using a machine learning method. *The Journal of Physical Chemistry Letters*, **11**(14), 5412-5417.

Datta, P., Tiwari, P., Pandey, L.M. 2018. Isolation and characterization of biosurfactant producing and oil degrading Bacillus subtilis MG495086 from formation water of Assam oil reservoir and its suitability for enhanced oil recovery. *Bioresource technology*, **270**, 439-448.

de Freitas, E.D., de Almeida, H.J., de Almeida Neto, A.F., Vieira, M.G.A. 2018. Continuous adsorption of silver and copper by Verde-lodo bentonite in a fixed bed flow-through column. *Journal of cleaner production*, **171**, 613-621.

Deng, Q., Wang, W., Sun, L., Wang, Y., Liao, J., Xu, D., Liu, Y., Ye, R., Gooneratne, R. 2017. A sensitive method for simultaneous quantitative determination of surfactin and iturin by LC-MS/MS. *Analytical and bioanalytical chemistry*, **409**(1), 179-191.

Devda, V., Chaudhary, K., Varjani, S., Pathak, B., Patel, A.K., Singhania, R.R., Taherzadeh, M.J., Ngo, H.H., Wong, J.W., Guo, W. 2021. Recovery of resources from industrial wastewater employing electrochemical technologies: status, advancements and perspectives. *Bioengineered*, **12**(1), 4697-4718.

Diarra, I., Prasad, S. 2021. The current state of heavy metal pollution in Pacific Island Countries: a review. *Applied Spectroscopy Reviews*, **56**(1), 27-51.

Dilmohamud, B., Seeneevassen, J., Rughooputh, S., Ramasami, P. 2005. Surface tension and related thermodynamic parameters of alcohols using the Traube stalagmometer. *European journal of physics*, **26**(6), 1079.

Dlamini, B., Rangarajan, V., Clarke, K.G. 2020. A simple thin layer chromatography based method for the quantitative analysis of biosurfactant surfactin vis-a-vis the presence of lipid and protein impurities in the processing liquid. *Biocatalysis and Agricultural Biotechnology*, **25**, 101587.

Dong, J., Du, Y., Duyu, R., Shang, Y., Zhang, S., Han, R. 2019. Adsorption of copper ion from solution by polyethylenimine modified wheat straw. *Bioresource Technology Reports*, **6**, 96-102.

Dotto, G.L., McKay, G. 2020. Current scenario and challenges in adsorption for water treatment. *Journal of Environmental Chemical Engineering*, **8**(4), 103988.

El-Naggar, N.E.-A., Hamouda, R.A., Mousa, I.E., Abdel-Hamid, M.S., Rabei, N.H. 2018. Biosorption optimization, characterization, immobilization and application of Gelidium amansii biomass for complete Pb 2+ removal from aqueous solutions. *Scientific reports*, **8**(1), 1-19.

Elazzazy, A.M., Abdelmoneim, T., Almaghrabi, O. 2015. Isolation and characterization of biosurfactant production under extreme environmental conditions by alkali-halo-thermophilic bacteria from Saudi Arabia. *Saudi Journal of Biological Sciences*, **22**(4), 466-475.

Etesami, H. 2018. Bacterial mediated alleviation of heavy metal stress and decreased accumulation of metals in plant tissues: mechanisms and future prospects. *Ecotoxicology and environmental safety*, **147**, 175-191.

Fallah, N., Taghizadeh, M. 2020. Continuous fixed-bed adsorption of Mo (VI) from aqueous solutions by Mo (VI)-IIP: Breakthrough curves analysis and mathematical modeling. *Journal of Environmental Chemical Engineering*, **8**(5), 104079.

Farraji, H., Zaman, N.Q., Tajuddin, R., Faraji, H. 2016. Advantages and disadvantages of phytoremediation: A concise review. *Int J Env Tech Sci*, **2**, 69-75.

Femina Carolin, C., Senthil Kumar, P., Janet Joshiba, G., Ramamurthy, R., Varjani, S.J. 2020. Bioremediation of 2, 4-diaminotoluene in aqueous solution enhanced by lipopeptide biosurfactant production from bacterial strains. *Journal of Environmental Engineering*, **146**(7), 04020069.

Foo, K., Hameed, B. 2012. Preparation, characterization and evaluation of adsorptive properties of orange peel based activated carbon via microwave induced K2CO3 activation. *Bioresource technology*, **104**, 679-686.

Forján, R., Asensio, V., Rodríguez-Vila, A., Covelo, E. 2016. Contribution of waste and biochar amendment to the sorption of metals in a copper mine tailing. *Catena*, **137**, 120-125.

Franzetti, A., Gandolfi, I., Fracchia, L., Van Hamme, J., Gkorezis, P., Marchant, R., Banat, I.M. 2014. Biosurfactant use in heavy metal removal from industrial effluents and contaminated sites. *Biosurfactants: Production and utilization—Processes, technologies, and economics*, **159**, 361.

Fratesi, S.E., Lynch, F.L., Kirkland, B.L., Brown, L.R. 2004. Effects of SEM preparation techniques on the appearance of bacteria and biofilms in the Carter Sandstone. *Journal of Sedimentary Research*, **74**(6), 858-867.

García-Reyes, S., Yañez-Ocampo, G. 2021. Microbial biosurfactants: Methods for their isolation and characterization. *Journal of Microbiology, Biotechnology and Food Sciences*, **2021**, 641-648.

Garg, M., Chatterjee, M. 2018. Isolation, characterization and antibacterial effect of biosurfactant from Candida parapsilosis. *Biotechnology Reports*, **18**, e00251.

Gautam, P., Kumar, S., Lokhandwala, S. 2019. Advanced oxidation processes for treatment of leachate from hazardous waste landfill: A critical review. *Journal of Cleaner Production*, **237**, 117639.

George, S., Jayachandran, K. 2013. Production and characterization of rhamnolipid biosurfactant from waste frying coconut oil using a novel P seudomonas aeruginosa D. *Journal of Applied Microbiology*, **114**(2), 373-383.

Ghaith, E.-S.I., Rizvi, S., Namasivayam, C., Rahman, P. 2019. Removal of Cd++ from contaminated water using bio-surfactant modified ground grass as a bio-sorbent. *2019 Advances in Science and Engineering Technology International Conferences (ASET)*. IEEE. pp. 1-7.

Ghaneian, M., Bhatnagar, A., Ehrampoush, M., Amrollahi, M., Jamshidi, B., Dehvari, M., Taghavi, M. 2017. Biosorption of hexavalent chromium from aqueous solution onto pomegranate seeds: kinetic modeling studies. *International journal of environmental science and technology*, **14**(2), 331-340.

Ghorbani, M., Shams, A., Seyedin, O., Lahoori, N.A. 2018. Magnetic ethylene diamine-functionalized graphene oxide as novel sorbent for removal of lead and cadmium ions from wastewater samples. *Environmental Science and Pollution Research*, **25**(6), 5655-5667.

Giri, S.S., Ryu, E., Sukumaran, V., Park, S.C. 2019. Antioxidant, antibacterial, and anti-adhesive activities of biosurfactants isolated from Bacillus strains. *Microbial pathogenesis*, **132**, 66-72.

Gogoi, D., Bhagowati, P., Gogoi, P., Bordoloi, N.K., Rafay, A., Dolui, S.K., Mukherjee, A.K. 2016. Structural and physico-chemical characterization of a dirhamnolipid biosurfactant purified from Pseudomonas aeruginosa: application of crude biosurfactant in enhanced oil recovery. *RSC advances*, **6**(74), 70669-70681.

Goswami, M., Deka, S. 2019. Biosurfactant production by a rhizosphere bacteria Bacillus altitudinis MS16 and its promising emulsification and antifungal activity. *Colloids and Surfaces B: Biointerfaces*, **178**, 285-296.

Guez, J.-S., Vassaux, A., Larroche, C., Jacques, P., Coutte, F. 2021. New Continuous Process for the Production of Lipopeptide Biosurfactants in Foam Overflowing Bioreactor. *Frontiers in Bioengineering and Biotechnology*, **9**.

Guo, X., Cui, X., Li, H. 2020. Effects of fillers combined with biosorbents on nutrient and heavy metal removal from biogas slurry in constructed wetlands. *Science of the Total Environment*, **703**, 134788.

Gupta, P., Diwan, B. 2017. Bacterial exopolysaccharide mediated heavy metal removal: a review on biosynthesis, mechanism and remediation strategies. *Biotechnology Reports*, **13**, 58-71.

Gupta, S., Sireesha, S., Sreedhar, I., Patel, C.M., Anitha, K. 2020. Latest trends in heavy metal removal from wastewater by biochar based sorbents. *Journal of Water Process Engineering*, **38**, 101561.

Guyo, U., Phiri, L.Y., Chigondo, F. 2017. Application of central composite design in the adsorption of Ca (II) on metakaolin zeolite. *Journal of Chemistry*, **2017**.

Haroon, B., Ping, A., Pervez, A., Faridullah, F., Irshad, M. 2019. Characterization of heavy metal in soils as affected by long-term irrigation with industrial wastewater. *Journal of Water Reuse and Desalination*, **9**(1), 47-56.

Haryanto, B., Chang, C.-H. 2015. Removing adsorbed heavy metal ions from sand surfaces via applying interfacial properties of rhamnolipid. *Journal of oleo science*, **64**(2), 161-168.

Hasanin, T.H., Ahmed, S.A., Barakat, T. 2019. Nano-chamomile Waste as a Low-cost Biosorbent for Rapid Removal of Heavy Metal Ions from Natural Water Samples. *Egyptian Journal of Chemistry*, **62**(5), 937-953.

Hashem, A.H., Saied, E., Hasanin, M.S. 2020. Green and ecofriendly bio-removal of methylene blue dye from aqueous solution using biologically activated banana peel waste. *Sustainable Chemistry and Pharmacy*, **18**, 100333.

Hashemian, S., Salari, K., Yazdi, Z.A. 2014. Preparation of activated carbon from agricultural wastes (almond shell and orange peel) for adsorption of 2-pic from aqueous solution. *Journal of Industrial and Engineering Chemistry*, **20**(4), 1892-1900.

Hayati, B., Maleki, A., Najafi, F., Gharibi, F., McKay, G., Gupta, V.K., Puttaiah, S.H., Marzban, N. 2018. Heavy metal adsorption using PAMAM/CNT nanocomposite from aqueous solution in batch and continuous fixed bed systems. *Chemical Engineering Journal*, **346**, 258-270.

He, J., Bardelli, F., Gehin, A., Silvester, E., Charlet, L. 2016. Novel chitosan goethite bionanocomposite beads for arsenic remediation. *Water research*, **101**, 1-9.

Henkel, M., Hausmann, R. 2019. Diversity and classification of microbial surfactants. in: *Biobased surfactants*, Elsevier, pp. 41-63.

Heyd, M., Kohnert, A., Tan, T.-H., Nusser, M., Kirschhöfer, F., Brenner-Weiss, G., Franzreb, M., Berensmeier, S. 2008. Development and trends of biosurfactant

analysis and purification using rhamnolipids as an example. *Analytical and bioanalytical chemistry*, **391**(5), 1579-1590.

Hino, K., Nishina, S., Sasaki, K., Hara, Y. 2019. Mitochondrial damage and iron metabolic dysregulation in hepatitis C virus infection. *Free Radical Biology and Medicine*, **133**, 193-199.

Hossain, S.M., Anantharaman, N. 2006. Studies on bacterial growth and lead (IV) biosorption using Bacillus subtilis.

Hu, X., Zhang, X., Ngo, H.H., Guo, W., Wen, H., Li, C., Zhang, Y., Ma, C. 2020. Comparison study on the ammonium adsorption of the biochars derived from different kinds of fruit peel. *Science of The Total Environment*, **707**, 135544.

Hubadillah, S.K., Othman, M.H.D., Harun, Z., Ismail, A., Rahman, M.A., Jaafar, J. 2017. A novel green ceramic hollow fiber membrane (CHFM) derived from rice husk ash as combined adsorbent-separator for efficient heavy metals removal. *Ceramics International*, **43**(5), 4716-4720.

Hymavathi, D., Prabhakar, G. 2019. Modeling of cobalt and lead adsorption by Ficus benghalenesis L. in a fixed bed column. *Chemical Engineering Communications*, **206**(10), 1264-1272.

Ibrahim, B.M. 2021. Heavy metal ions removal from wastewater using various low-cost agricultural wastes as adsorbents: a survey. *Zanco Journal of Pure and Applied Sciences*, **33**(2), 76-91.

Igiri, B.E., Okoduwa, S.I., Idoko, G.O., Akabuogu, E.P., Adeyi, A.O., Ejiogu, I.K. 2018. Toxicity and bioremediation of heavy metals contaminated ecosystem from tannery wastewater: a review. *Journal of toxicology*, **2018**.

Immerzeel, W.W., Lutz, A., Andrade, M., Bahl, A., Biemans, H., Bolch, T., Hyde, S., Brumby, S., Davies, B., Elmore, A. 2020. Importance and vulnerability of the world‘s water towers. *Nature*, **577**(7790), 364-369.

Indhumathi, P., Sathiyaraj, S., Koelmel, J.P., Shoba, S.U., Jayabalakrishnan, C., Saravanabhavan, M. 2018. The efficient removal of heavy metal ions from industry effluents using waste biomass as low-cost adsorbent: thermodynamic and kinetic models. *Zeitschrift für Physikalische Chemie*, **232**(4), 527-543.

Ishaq, U., Akram, M., Iqbal, Z., Rafiq, M., Akrem, A., Nadeem, M., Shafi, F., Shafiq, Z., Mahmood, S., Baig, M. 2015. Production and characterization of novel self-assembling biosurfactants from Aspergillus flavus. *Journal of applied microbiology*, **119**(4), 1035-1045.

Jaiswal, A., Verma, A., Jaiswal, P. 2018a. Detrimental effects of heavy metals in soil, plants, and aquatic ecosystems and in humans. *Journal of Environmental Pathology, Toxicology and Oncology*, **37**(3).

Jaiswal, V., Saxena, S., Kaur, I., Dubey, P., Nand, S., Naseem, M., Singh, S.B., Srivastava, P.K., Barik, S.K. 2018b. Application of four novel fungal strains to remove arsenic from contaminated water in batch and column modes. *Journal of hazardous materials*, **356**, 98-107.

Jakóbik-Kolon, A., Bok-Badura, J. 2020. Sorption and desorption of cadmium and lead on pectin-based biosorbents–batch and column studies. *Separation Science and Technology*, **55**(12), 2108-2121.

James, A., Percy, M., Ameh, O.S. 2020. Heavy metals pollution status of the Katima Mulilo Urban open land wastewater disposal centre and the immediate vicinity. *Cogent Environmental Science*, **6**(1), 1726093.

Jasim, B., Sreelakshmi, K., Mathew, J., Radhakrishnan, E. 2016. Surfactin, iturin, and fengycin biosynthesis by endophytic Bacillus sp. from Bacopa monnieri. *Microbial ecology*, **72**(1), 106-119.

Javanbakht, V., Alavi, S.A., Zilouei, H. 2014. Mechanisms of heavy metal removal using microorganisms as biosorbent. *Water Science and Technology*, **69**(9), 1775-1787.

Javed, M., Ahmad, M.I., Usmani, N., Ahmad, M. 2017. Multiple biomarker responses (serum biochemistry, oxidative stress, genotoxicity and histopathology) in Channa punctatus exposed to heavy metal loaded waste water. *Scientific reports*, **7**(1), 1-11.

Jawad, A.H., Abdulhameed, A.S., Wilson, L.D., Syed-Hassan, S.S.A., ALOthman, Z.A., Khan, M.R. 2021. High surface area and mesoporous activated carbon from KOH-activated Dragon fruit peels for methylene blue dye adsorption: Optimization and mechanism study. *Chinese Journal of Chemical Engineering*, **32**, 281-290.

Jiang, C.-y., Sheng, X.-f., Qian, M., Wang, Q.-y. 2008. Isolation and characterization of a heavy metal-resistant Burkholderia sp. from heavy metal-contaminated paddy field soil and its potential in promoting plant growth and heavy metal accumulation in metal-polluted soil. *Chemosphere*, **72**(2), 157-164.

Jiang, C., Wang, X., Hou, B., Hao, C., Li, X., Wu, J. 2020. Construction of a lignosulfonate–lysine hydrogel for the adsorption of heavy metal ions. *Journal of agricultural and food chemistry*, **68**(10), 3050-3060.

Jin, X., Xiang, Z., Liu, Q., Chen, Y., Lu, F. 2017. Polyethyleneimine-bacterial cellulose bioadsorbent for effective removal of copper and lead ions from aqueous solution. *Bioresource technology*, **244**, 844-849.

Jin, Y., Teng, C., Yu, S., Song, T., Dong, L., Liang, J., Bai, X., Liu, X., Hu, X., Qu, J. 2018. Batch and fixed-bed biosorption of Cd (II) from aqueous solution using immobilized Pleurotus ostreatus spent substrate. *Chemosphere*, **191**, 799-808.

Joshi, S.J., Geetha, S., Desai, A.J. 2015. Characterization and application of biosurfactant produced by Bacillus licheniformis R2. *Applied biochemistry and biotechnology*, **177**(2), 346-361.

Jusoh, A., Shiung, L.S., Noor, M. 2007. A simulation study of the removal efficiency of granular activated carbon on cadmium and lead. *Desalination*, **206**(1-3), 9-16.

Kamsonlian, S., Suresh, S., Majumder, C., Chand, S. 2011. Characterization of banana and orange peels: biosorption mechanism. *International Journal of Science Technology & Management*, **2**(4), 1-7.

Karimpour, M., Ashrafi, S.D., Taghavi, K., Mojtahedi, A., Roohbakhsh, E., Naghipour, D. 2018. Adsorption of cadmium and lead onto live and dead cell mass of Pseudomonas aeruginosa: A dataset. *Data in brief*, **18**, 1185-1192.

Kausar, A., Bhatti, H.N., Iqbal, M., Ashraf, A. 2017. Batch versus column modes for the adsorption of radioactive metal onto rice husk waste: conditions optimization through response surface methodology. *Water Science and Technology*, **76**(5), 1035-1043.

Kavuthodi, B., Thomas, S.K., Sebastian, D. 2015. Co-production of pectinase and biosurfactant by the newly isolated strain Bacillus subtilis BKDS1. *Microbiology Research Journal International*, 1-12.

Keshavarzi, B., Hassanaghaei, M., Moore, F., Mehr, M.R., Soltanian, S., Lahijanzadeh, A.R., Sorooshian, A. 2018. Heavy metal contamination and health risk assessment in three commercial fish species in the Persian Gulf. *Marine pollution bulletin*, **129**(1), 245-252.

Khademolhosseini, R., Jafari, A., Mousavi, S.M., Hajfarajollah, H., Noghabi, K.A., Manteghian, M. 2019. Physicochemical characterization and optimization of

glycolipid biosurfactant production by a native strain of Pseudomonas aeruginosa HAK01 and its performance evaluation for the MEOR process. *RSC advances*, **9**(14), 7932-7947.

Khan, M.A., Ozturk, I. 2020. Examining foreign direct investment and environmental pollution linkage in Asia. *Environmental Science and Pollution Research*, **27**(7), 7244-7255.

Khan, N.A., Ibrahim, S., Subramaniam, P. 2004. Elimination of heavy metals from wastewater using agricultural wastes as adsorbents. *Malaysian journal of science*, **23**(1), 43-51.

Khan, S.A., Khan, M.A. 1995. Adsorption of chromium (III), chromium (VI) and silver (I) on bentonite. *Waste Management*, **15**(4), 271-282.

Khopade, A., Biao, R., Liu, X., Mahadik, K., Zhang, L., Kokare, C. 2012. Production and stability studies of the biosurfactant isolated from marine Nocardiopsis sp. B4. *Desalination*, **285**, 198-204.

Kiran, G.S., Thomas, T.A., Selvin, J., Sabarathnam, B., Lipton, A. 2010. Optimization and characterization of a new lipopeptide biosurfactant produced by marine Brevibacterium aureum MSA13 in solid state culture. *Bioresource technology*, **101**(7), 2389-2396.

Kumar, A., MMS, C.-P., Chaturvedi, A.K., Shabnam, A.A., Subrahmanyam, G., Mondal, R., Gupta, D.K., Malyan, S.K., Kumar, S.S., A Khan, S. 2020. Lead toxicity: health hazards, influence on food chain, and sustainable remediation approaches. *International journal of environmental research and public health*, **17**(7), 2179.

Kumar, R., Bhatia, D., Singh, R., Rani, S., Bishnoi, N.R. 2011. Sorption of heavy metals from electroplating effluent using immobilized biomass Trichoderma viride in a continuous packed-bed column. *International Biodeterioration & Biodegradation*, **65**(8), 1133-1139.

Kutuzova, A., Dontsova, T. 2017. Synthesis, characterization and properties of titanium dioxide obtained by hydrolytic method. *2017 IEEE 7th International Conference Nanomaterials: Application & Properties (NAP)*. IEEE. pp. 01NNPT02-1-01NNPT02-5.

Lahlou, F.-z., Namany, S., Mackey, H.R., Al-Ansari, T. 2020. Treated industrial wastewater as a water and nutrients source for tomatoes cultivation: an

optimisation approach. in: *Computer Aided Chemical Engineering*, Vol. 48, Elsevier, pp. 1819-1824.

Lakherwal, D. 2014. Adsorption of heavy metals: a review. *International journal of environmental research and development*, **4**(1), 41-48.

Lathiya, D.R., Bhatt, D.V., Maheria, K.C. 2018. Synthesis of sulfonated carbon catalyst from waste orange peel for cost effective biodiesel production. *Bioresource Technology Reports*, **2**, 69-76.

Li, D., Zhou, L. 2018. Adsorption of heavy metal tolerance strains to Pb 2+ and Cd 2+ in wastewater. *Environmental Science and Pollution Research*, **25**(32), 32156-32162.

Lin, S.-C., Minton, M.A., Sharma, M.M., Georgiou, G. 1994. Structural and immunological characterization of a biosurfactant produced by Bacillus licheniformis JF-2. *Applied and environmental microbiology*, **60**(1), 31-38.

Liu, B., Liu, J., Ju, M., Li, X., Yu, Q. 2016. Purification and characterization of biosurfactant produced by Bacillus licheniformis Y-1 and its application in remediation of petroleum contaminated soil. *Marine pollution bulletin*, **107**(1), 46-51.

Liu, J., Mwamulima, T., Wang, Y., Fang, Y., Song, S., Peng, C. 2017. Removal of Pb (II) and Cr (VI) from aqueous solutions using the fly ash-based adsorbent material-supported zero-valent iron. *Journal of Molecular Liquids*, **243**, 205-211.

Liu, K., Sun, Y., Cao, M., Wang, J., Lu, J.R., Xu, H. 2020. Rational design, properties, and applications of biosurfactants: a short review of recent advances. *Current Opinion in Colloid & Interface Science*, **45**, 57-67.

Liu, L., Li, W., Song, W., Guo, M. 2018. Remediation techniques for heavy metal-contaminated soils: Principles and applicability. *Science of the Total Environment*, **633**, 206-219.

Liu, Q., Niu, J., Yu, Y., Wang, C., Lu, S., Zhang, S., Lv, J., Peng, B. 2021. Production, characterization and application of biosurfactant produced by Bacillus licheniformis L20 for microbial enhanced oil recovery. *Journal of Cleaner Production*, **307**, 127193.

Lodhi, R.S., Das, S., Zhang, A., Das, P. 2021. Nanotechnology for the Remediation of Heavy Metals and Metalloids in Contaminated Water. in: *Water Pollution and Remediation: Heavy Metals*, Springer, pp. 177-209.

Long, X., He, N., He, Y., Jiang, J., Wu, T. 2017. Biosurfactant surfactin with pH-regulated emulsification activity for efficient oil separation when used as emulsifier. *Bioresource technology*, **241**, 200-206.

Lotfabad, T.B., Abassi, H., Ahmadkhaniha, R., Roostaazad, R., Masoomi, F., Zahiri, H.S., Ahmadian, G., Vali, H., Noghabi, K.A. 2010. Structural characterization of a rhamnolipid-type biosurfactant produced by Pseudomonas aeruginosa MR01: enhancement of di-rhamnolipid proportion using gamma irradiation. *Colloids and Surfaces B: Biointerfaces*, **81**(2), 397-405.

Luo, X., Yuan, J., Liu, Y., Liu, C., Zhu, X., Dai, X., Ma, Z., Wang, F. 2017. Improved solid-phase synthesis of phosphorylated cellulose microsphere adsorbents for highly effective Pb2+ removal from water: batch and fixed-bed column performance and adsorption mechanism. *ACS Sustainable Chemistry & Engineering*, **5**(6), 5108-5117.

Maharana, M., Manna, M., Sardar, M., Sen, S. 2021. Heavy Metal Removal by Low-Cost Adsorbents. in: *Green Adsorbents to Remove Metals, Dyes and Boron from Polluted Water*, Springer, pp. 245-272.

Malik, R., Kerkar, S. 2021. Biosurfactant Mediated Remediation of Heavy Metals: A Review. *Rhizobiont in Bioremediation of Hazardous Waste*, 73-85.

Manasa, R.L., Mehta, A. 2020. Wastewater: Sources of Pollutants and Its Remediation. *Environmental Biotechnology*, **2**, 197-219.

Manirethan, V., Raval, K., Rajan, R., Thaira, H., Balakrishnan, R.M. 2018. Kinetic and thermodynamic studies on the adsorption of heavy metals from aqueous solution by melanin nanopigment obtained from marine source: Pseudomonas stutzeri. *Journal of environmental management*, **214**, 315-324.

Mao, G., Hu, H., Liu, X., Crittenden, J., Huang, N. 2021. A bibliometric analysis of industrial wastewater treatments from 1998 to 2019. *Environmental Pollution*, **275**, 115785.

Marchut-Mikolajczyk, O., Drożdżyński, P., Pietrzyk, D., Antczak, T. 2018. Biosurfactant production and hydrocarbon degradation activity of endophytic bacteria isolated from Chelidonium majus L. *Microbial cell factories*, **17**(1), 1-9.

Mhamdi, S., Bkhairia, I., Nasri, R., Mechichi, T., Nasri, M., Kamoun, A.S. 2017. Evaluation of the biotechnological potential of a novel purified protease BS1

from Bacillus safensis S406 on the chitin extraction and detergent formulation. *International journal of biological macromolecules*, **104**, 739-747.

Mnif, I., Chaabouni-Ellouze, S., Ghribi, D. 2012. Optimization of the nutritional parameters for enhanced production of B. subtilis SPB1 biosurfactant in submerged culture using response surface methodology. *Biotechnology research international*, **2012**.

Mnif, I., Ellouz-Chaabouni, S., Ghribi, D. 2018. Glycolipid biosurfactants, main classes, functional properties and related potential applications in environmental biotechnology. *Journal of Polymers and the Environment*, **26**(5), 2192-2206.

Mohamed, H.S., Soliman, N., Abdelrheem, D.A., Ramadan, A.A., Elghandour, A.H., Ahmed, S.A. 2019. Adsorption of Cd2+ and Cr3+ ions from aqueous solutions by using residue of Padina gymnospora waste as promising low-cost adsorbent. *Heliyon*, **5**(3), e01287.

Mohapatra, R.K., Parhi, P.K., Pandey, S., Bindhani, B.K., Thatoi, H., Panda, C.R. 2019. Active and passive biosorption of Pb (II) using live and dead biomass of marine bacterium Bacillus xiamenensis PbRPSD202: Kinetics and isotherm studies. *Journal of environmental management*, **247**, 121-134.

Mohd Isa, M.H., Shamsudin, N.H., Al-Shorgani, N.K.N., Alsharjabi, F.A., Kalil, M.S. 2020. Evaluation of antibacterial potential of biosurfactant produced by surfactin-producing Bacillus isolated from selected Malaysian fermented foods. *Food Biotechnology*, **34**(1), 1-24.

Mondal, N.K., Samanta, A., Chakraborty, S., Shaikh, W.A. 2018. Enhanced chromium (VI) removal using banana peel dust: isotherms, kinetics and thermodynamics study. *Sustainable Water Resources Management*, **4**(3), 489-497.

Morikawa, M., Daido, H., Takao, T., Murata, S., Shimonishi, Y., Imanaka, T. 1993. A new lipopeptide biosurfactant produced by Arthrobacter sp. strain MIS38. *Journal of bacteriology*, **175**(20), 6459-6466.

Moshtagh, B., Hawboldt, K., Zhang, B. 2019. Optimization of biosurfactant production by Bacillus subtilis N3-1P using the brewery waste as the carbon source. *Environmental technology*, **40**(25), 3371-3380.

Moussout, H., Ahlafi, H., Aazza, M., Maghat, H. 2018. Critical of linear and nonlinear equations of pseudo-first order and pseudo-second order kinetic models. *Karbala International Journal of Modern Science*, **4**(2), 244-254.

Muhammad, N., Nafees, M., Ge, L., Khan, M.H., Bilal, M., Chan, W.P., Lisak, G. 2021. Assessment of industrial wastewater for potentially toxic elements, human health (dermal) risks, and pollution sources: A case study of Gadoon Amazai industrial estate, Swabi, Pakistan. *Journal of Hazardous Materials*, **419**, 126450.

Mulligan, C.N., Chow, T.Y.-K., Gibbs, B.F. 1989. Enhanced biosurfactant production by a mutant Bacillus subtilis strain. *Applied microbiology and biotechnology*, **31**(5), 486-489.

Mulligan, C.N., Yong, R., Gibbs, B. 2001. Surfactant-enhanced remediation of contaminated soil: a review. *Engineering geology*, **60**(1-4), 371-380.

Murthy, S., Bali, G., Sarangi, S. 2014. Effect of lead on growth, protein and biosorption capacity of Bacillus cereus isolated from industrial effluent. *Journal of Environmental Biology*, **35**(2), 407.

Mutalik, S.R., Vaidya, B.K., Joshi, R.M., Desai, K.M., Nene, S.N. 2008. Use of response surface optimization for the production of biosurfactant from Rhodococcus spp. MTCC 2574. *Bioresource Technology*, **99**(16), 7875-7880.

Naga Babu, A., Krishna Mohan, G., Kalpana, K., Ravindhranath, K. 2017. Removal of lead from water using calcium alginate beads doped with hydrazine sulphate-activated red mud as adsorbent. *Journal of Analytical Methods in Chemistry*, **2017**.

Nahar, K., Chowdhury, M.A.K., Chowdhury, M.A.H., Rahman, A., Mohiuddin, K. 2018. Heavy metals in handloom-dyeing effluents and their biosorption by agricultural byproducts. *Environmental Science and Pollution Research*, **25**(8), 7954-7967.

Nalini, S., Parthasarathi, R. 2018. Optimization of rhamnolipid biosurfactant production from Serratia rubidaea SNAU02 under solid-state fermentation and its biocontrol efficacy against Fusarium wilt of eggplant. *Annals of Agrarian Science*, **16**(2), 108-115.

Nanda, M., Kumar, V., Sharma, D. 2019. Multimetal tolerance mechanisms in bacteria: The resistance strategies acquired by bacteria that can be exploited to

_clean-up‘heavy metal contaminants from water. *Aquatic toxicology*, **212**, 1-10.

Naranjo, V.I., Hendricks, M., Jones, K.S. 2020. Lead toxicity in children: an unremitting public health problem. *Pediatric Neurology*.

Nasim, A.K., Shaliza, I., Piarapakaran, S. 2004. Elimination of heavy metals from wastewater using agricultural wastes as adsorbents. *Malaysian Journal of Science*, **23**(1), 43-51.

Nasir, A.M., Goh, P.S., Abdullah, M.S., Ng, B.C., Ismail, A.F. 2019. Adsorptive nanocomposite membranes for heavy metal remediation: Recent progresses and challenges. *Chemosphere*, **232**, 96-112.

Navasumrit, P., Chaisatra, K., Promvijit, J., Parnlob, V., Waraprasit, S., Chompoobut, C., Binh, T.T., Hai, D.N., Bao, N.D., Hai, N.K. 2019. Exposure to arsenic in utero is associated with various types of DNA damage and micronuclei in newborns: a birth cohort study. *Environmental Health*, **18**(1), 1-16.

Nayarisseri, A., Singh, P., Singh, S.K. 2018. Screening, isolation and characterization of biosurfactant producing Bacillus subtilis strain ANSKLAB03. *Bioinformation*, **14**(6), 304.

Nguyen, T.C., Loganathan, P., Nguyen, T.V., Kandasamy, J., Naidu, R., Vigneswaran, S. 2018. Adsorptive removal of five heavy metals from water using blast furnace slag and fly ash. *Environmental science and pollution research*, **25**(21), 20430-20438.

Nishanthi, R., Kumaran, S., Palani, P., Chellaram, C., Anand, T.P., Kannan, V. 2010. Screening of biosurfactants from hydrocarbon degrading bacteria. *Journal of Ecobiotechnology*, **2**(5).

Niu, Y., Jiang, X., Wang, K., Xia, J., Jiao, W., Niu, Y., Yu, H. 2020. Meta analysis of heavy metal pollution and sources in surface sediments of Lake Taihu, China. *Science of the Total Environment*, **700**, 134509.

Nwabanne, J., Igbokwe, P. 2012. Kinetic modeling of heavy metals adsorption on fixed bed column.

Oluwaseun, A.C., Kola, O.J., Mishra, P., Singh, J.R., Singh, A.K., Cameotra, S.S., Micheal, B.O. 2017. Characterization and optimization of a rhamnolipid from Pseudomonas aeruginosa C1501 with novel biosurfactant activities. *Sustainable Chemistry and Pharmacy*, **6**, 26-36.

Onwosi, C.O., Odibo, F.J.C. 2012. Effects of carbon and nitrogen sources on rhamnolipid biosurfactant production by Pseudomonas nitroreducens isolated from soil. *World Journal of Microbiology and Biotechnology*, **28**(3), 937-942.

Özdemir, G., Yapar, S. 2009. Adsorption and desorption behavior of copper ions on Na-montmorillonite: Effect of rhamnolipids and pH. *journal of Hazardous Materials*, **166**(2-3), 1307-1313.

Pacwa-Płociniczak, M., Płaza, G.A., Piotrowska-Seget, Z., Cameotra, S.S. 2011. Environmental applications of biosurfactants: recent advances. *International journal of molecular sciences*, **12**(1), 633-654.

Pan, W., Ye, X., Zhu, Z., Li, C., Zhou, J., Liu, J. 2021. Urinary cadmium concentrations and risk of primary ovarian insufficiency in women: a case–control study. *Environmental Geochemistry and Health*, **43**(5), 2025-2035.

Panchariya, V., Bhati, V., Madhyastha, H., Madhyastha, R., Prasad, J., Sharma, P., Sharma, P., Saini, M.K., Rajput, V.D., Nakajima, Y. 2021. Chromatic intervention and biocompatibility assay for biosurfactant derived from Balanites aegyptiaca (L.) Del. *Scientific reports*, **11**(1), 1-12.

Pankow, J.F., Cherry, J.A. 1996. Dense chlorinated solvents and other DNAPLs in groundwater: History, behavior, and remediation.

Parastar, M., Sheshmani, S., Shokrollahzadeh, S. 2021. Cross-linked chitosan into graphene oxide-iron (III) oxide hydroxide as nano-biosorbent for Pd (II) and Cd (II) removal. *International Journal of Biological Macromolecules*, **166**, 229-237.

Park, D., Yun, Y.-S., Park, J.M. 2010. The past, present, and future trends of biosorption. *Biotechnology and Bioprocess Engineering*, **15**(1), 86-102.

Pathak, K.V., Bose, A., Keharia, H. 2014. Characterization of novel lipopeptides produced by Bacillus tequilensis P15 using liquid chromatography coupled electron spray ionization tandem mass spectrometry (LC–ESI–MS/MS). *International Journal of Peptide Research and Therapeutics*, **20**(2), 133-143.

Pathak, P.D., Mandavgane, S.A., Kulkarni, B.D. 2015. Fruit peel waste as a novel low-cost bio adsorbent. *Reviews in Chemical Engineering*, **31**(4), 361-381.

Patidar, K., Chouhan, A., Thakur, L.S. 2017. Removal of heavy metals from water and waste water by electrocoagulation process—a review. *Int Res J Eng Technol*, **4**(11), 16-25.

Patowary, K., Kalita, M.C., Deka, S. 2015a. Degradation of polycyclic aromatic hydrocarbons (PAHs) employing biosurfactant producing Pseudomonas aeruginosa KS3.

Patowary, K., Saikia, R.R., Kalita, M.C., Deka, S. 2015b. Degradation of polyaromatic hydrocarbons employing biosurfactant-producing Bacillus pumilus KS2. *Annals of microbiology*, **65**(1), 225-234.

Pauli, B.J. 2020. The Flint water crisis. *Wiley Interdisciplinary Reviews: Water*, **7**(3), e1420.

Pavón, N., Buelna-Chontal, M., Macías-López, A., Correa, F., Uribe-Álvarez, C., Hernández-Esquivel, L., Chávez, E. 2019. On the oxidative damage by cadmium to kidney mitochondrial functions. *Biochemistry and Cell Biology*, **97**(2), 187-192.

Pecci, Y., Rivardo, F., Martinotti, M.G., Allegrone, G. 2010. LC/ESI-MS/MS characterisation of lipopeptide biosurfactants produced by the Bacillus licheniformis V9T14 strain. *Journal of mass spectrometry*, **45**(7), 772-778.

Pereira, J.F., Gudiña, E.J., Costa, R., Vitorino, R., Teixeira, J.A., Coutinho, J.A., Rodrigues, L.R. 2013. Optimization and characterization of biosurfactant production by Bacillus subtilis isolates towards microbial enhanced oil recovery applications. *Fuel*, **111**, 259-268.

Perez-Ameneiro, M., Vecino, X., Cruz, J.M., Moldes, A.B. 2015. Wastewater treatment enhancement by applying a lipopeptide biosurfactant to a lignocellulosic biocomposite. *Carbohydrate polymers*, **131**, 186-196.

Pholosi, A., Naidoo, E.B., Ofomaja, A.E. 2020. Intraparticle diffusion of Cr (VI) through biomass and magnetite coated biomass: A comparative kinetic and diffusion study. *South African Journal of Chemical Engineering*, **32**, 39-55.

Phulpoto, I.A., Yu, Z., Hu, B., Wang, Y., Ndayisenga, F., Li, J., Liang, H., Qazi, M.A. 2020. Production and characterization of surfactin-like biosurfactant produced by novel strain Bacillus nealsonii S2MT and it's potential for oil contaminated soil remediation. *Microbial cell factories*, **19**(1), 1-12.

Płaza, G.A., Zjawiony, I., Banat, I.M. 2006. Use of different methods for detection of thermophilic biosurfactant-producing bacteria from hydrocarbon-contaminated and bioremediated soils. *Journal of Petroleum Science and Engineering*, **50**(1), 71-77.

Poole, K., Hay, T., Gilmour, C., Fruci, M. 2019. The aminoglycoside resistance-promoting AmgRS envelope stress-responsive two-component system in Pseudomonas aeruginosa is zinc-activated and protects cells from zinc-promoted membrane damage. *Microbiology*, **165**(5), 563-571.

Poonkothai, M., Vijayavathi, B.S. 2015. Physicochemical characterisation of nickel electroplating effluent before and after treatment with dead Aspergillus niger. *International Research Journal of Pharmaceutical and Biosciences*, **2**(6), 1-13.

Pornsunthorntawee, O., Wongpanit, P., Chavadej, S., Abe, M., Rujiravanit, R. 2008. Structural and physicochemical characterization of crude biosurfactant produced by Pseudomonas aeruginosa SP4 isolated from petroleum-contaminated soil. *Bioresource technology*, **99**(6), 1589-1595.

Posati, T., Nocchetti, M., Kovtun, A., Donnadio, A., Zambianchi, M., Aluigi, A., Capobianco, M.L., Corticelli, F., Palermo, V., Ruani, G. 2019. Polydopamine nanoparticle-coated polysulfone porous granules as adsorbents for water remediation. *ACS omega*, **4**(3), 4839-4847.

Pradhan, A.K., Pradhan, N., Mall, G., Panda, H.T., Sukla, L.B., Panda, P.K., Mishra, B.K. 2013. Application of lipopeptide biosurfactant isolated from a halophile: Bacillus tequilensis CH for inhibition of biofilm. *Applied biochemistry and biotechnology*, **171**(6), 1362-1375.

Priji, P., Sajith, S., Unni, K.N., Anderson, R.C., Benjamin, S. 2017. Pseudomonas sp. BUP6, a novel isolate from Malabari goat produces an efficient rhamnolipid type biosurfactant. *Journal of basic microbiology*, **57**(1), 21-33.

Priyantha, N., Kotabewatta, P. 2019. Biosorption of heavy metal ions on peel of Artocarpus nobilis fruit: 1—Ni (II) sorption under static and dynamic conditions. *Applied Water Science*, **9**(2), 1-10.

Purwasena, I.A., Astuti, D.I., Syukron, M., Amaniyah, M., Sugai, Y. 2019. Stability test of biosurfactant produced by Bacillus licheniformis DS1 using experimental design and its application for MEOR. *Journal of Petroleum Science and Engineering*, **183**, 106383.

Qasem, N.A., Mohammed, R.H., Lawal, D.U. 2021. Removal of heavy metal ions from wastewater: A comprehensive and critical review. *Npj Clean Water*, **4**(1), 1-15.

Qiao, W., Zhang, Y., Xia, H., Luo, Y., Liu, S., Wang, S., Wang, W. 2019. Bioimmobilization of lead by Bacillus subtilis X3 biomass isolated from lead mine soil under promotion of multiple adsorption mechanisms. *Royal Society open science*, **6**(2), 181701.

Qu, J., Song, T., Liang, J., Bai, X., Li, Y., Wei, Y., Huang, S., Dong, L., Jin, Y. 2019. Adsorption of lead (II) from aqueous solution by modified Auricularia matrix waste: A fixed-bed column study. *Ecotoxicology and Environmental Safety*, **169**, 722-729.

Rajesh, M., Samundeeswari, M., Archana, B. 2017. Isolation of biosurfactant producing bacteria from garbage soil. *Journal of Applied & Environmental Microbiology*, **5**(2), 74-78.

Rajkumar, D., Palanivelu, K. 2004. Electrochemical treatment of industrial wastewater. *Journal of hazardous materials*, **113**(1-3), 123-129.

Ram, H., Sahu, A.K., Said, M.S., Banpurkar, A.G., Gajbhiye, J.M., Dastager, S.G. 2019. A novel fatty alkene from marine bacteria: A thermo stable biosurfactant and its applications. *Journal of hazardous materials*, **380**, 120868.

Ram, R., Morrisroe, L., Etschmann, B., Vaughan, J., Brugger, J. 2021. Lead (Pb) sorption and co-precipitation on natural sulfide, sulfate and oxide minerals under environmental conditions. *Minerals Engineering*, **163**, 106801.

Rana, M.N., Tangpong, J., Rahman, M.M. 2018. Toxicodynamics of lead, cadmium, mercury and arsenic-induced kidney toxicity and treatment strategy: a mini review. *Toxicology reports*, **5**, 704-713.

Rangabhashiyam, S., Sayantani, S., Balasubramanian, P. 2019. Assessment of hexavalent chromium biosorption using biodiesel extracted seeds of Jatropha sp., Ricinus sp. and Pongamia sp. *International Journal of Environmental Science and Technology*, **16**(10), 5707-5724.

Rao, C., Yan, B. 2020. Study on the interactive influence between economic growth and environmental pollution. *Environmental Science and Pollution Research*, **27**(31), 39442-39465.

Rastogi, S., Kumar, J., Kumar, R. 2019. An investigation into the efficacy of fungal biomass as a low cost bio-adsorbent for the removal of lead from aqueous solutions. *Int Res J Eng Technol*, **6**(3), 7144-7149.

Rastogi, S., Kumar, R. 2020. Remediation of heavy metals using non-conventional adsorbents and biosurfactant-producing bacteria. *Environmental degradation: causes and remediation strategies*, 133-153.

Rastogi, S., Kumar, R. 2021. Statistical optimization of biosurfactant production using waste biomaterial and biosorption of Pb2+ under concomitant submerged fermentation. *Journal of Environmental Management*, **295**, 113158.

Rastogi, S., Ratna, S., Said, O.B., Kumar, R. 2021a. Physiological and Molecular Aspects of Retrieving Environmental Stress in Plants by Microbial Interactions. in: *Microbes and Signaling Biomolecules Against Plant Stress*, Springer, pp. 107-125.

Rastogi, S., Tiwari, S., Ratna, S., Kumar, R. 2021b. Utilization of Agro-industrial waste for Biosurfactant Production under Submerged Fermentation and its Synergistic Application in Biosorption of Pb2+. *Bioresource Technology Reports*, 100706.

Ratna, S., Rastogi, S., Kumar, R. 2021a. Current trends for distillery wastewater management and its emerging applications for sustainable environment. *Journal of Environmental Management*, **290**, 112544.

Ratna, S., Rastogi, S., Kumar, R. 2021b. Phytoremediation: A Synergistic Interaction Between Plants and Microbes for Removal of Unwanted Chemicals/Contaminants. in: *Microbes and Signaling Biomolecules Against Plant Stress*, Springer, pp. 199-222.

Renu, Agarwal, M., Singh, K., Gupta, R., Dohare, R. 2020. Continuous fixed-bed adsorption of heavy metals using biodegradable adsorbent: modeling and experimental study. *Journal of Environmental Engineering*, **146**(2), 04019110.

Rezapour, S., Atashpaz, B., Moghaddam, S.S., Kalavrouziotis, I.K., Damalas, C.A. 2019. Cadmium accumulation, translocation factor, and health risk potential in a wastewater-irrigated soil-wheat (Triticum aestivum L.) system. *Chemosphere*, **231**, 579-587.

Rodrigues, L.R., Teixeira, J.A., van der Mei, H.C., Oliveira, R. 2006. Physicochemical and functional characterization of a biosurfactant produced by Lactococcus lactis 53. *Colloids and Surfaces B: Biointerfaces*, **49**(1), 79-86.

Rodrigues, M.S., Moreira, F.S., Cardoso, V.L., de Resende, M.M. 2017. Soy molasses as a fermentation substrate for the production of biosurfactant using

Pseudomonas aeruginosa ATCC 10145. *Environmental Science and Pollution Research*, **24**(22), 18699-18709.

Rosales, E., Escudero, S., Pazos, M., Sanromán, M. 2019. Sustainable removal of Cr (vi) by lime peel and pineapple core wastes. *Applied Sciences*, **9**(10), 1967.

Rosenberg, M. 1984. Bacterial adherence to hydrocarbons: a useful technique for studying cell surface hydrophobicity. *FEMS Microbiology Letters*, **22**(3), 289-295.

Sabarinathan, D., Vanaraj, S., Sathiskumar, S., Poorna Chandrika, S., Sivarasan, G., Arumugam, S., Preethi, K., Li, H., Chen, Q. 2021. Characterization and application of rhamnolipid from Pseudomonas plecoglossicida BP03. *Letters in Applied Microbiology*, **72**(3), 251-262.

Sabir, A., Altaf, F., Batool, R., Shafiq, M., Khan, R.U., Jacob, K.I. 2021. Agricultural Waste Absorbents for Heavy Metal Removal. in: *Green Adsorbents to Remove Metals, Dyes and Boron from Polluted Water*, Springer, pp. 195-228.

Saikia, R.R., Deka, S., Deka, M., Sarma, H. 2012. Optimization of environmental factors for improved production of rhamnolipid biosurfactant by Pseudomonas aeruginosa RS29 on glycerol. *Journal of Basic Microbiology*, **52**(4), 446-457.

Saini, S., Gill, J.K., Kaur, J., Saikia, H.R., Singh, N., Kaur, I., Katnoria, J.K. 2020. Biosorption as environmentally friendly technique for heavy metal removal from wastewater. *Fresh water pollution dynamics and remediation*, 167-181.

Sakamoto, M., Rôças, I., Siqueira Jr, J., Benno, Y. 2006. Molecular analysis of bacteria in asymptomatic and symptomatic endodontic infections. *Oral microbiology and immunology*, **21**(2), 112-122.

Salamat, N., Lamoochi, R., Shahaliyan, F. 2018. Metabolism and removal of anthracene and lead by a B. subtilis-produced biosurfactant. *Toxicology reports*, **5**, 1120-1123.

Saleem, H., Pal, P., Haija, M.A., Banat, F. 2019. Regeneration and reuse of bio-surfactant to produce colloidal gas aphrons for heavy metal ions removal using single and multistage cascade flotation. *Journal of Cleaner Production*, **217**, 493-502.

Samuel PN, K.J., Soosai, M.R., Ganesh Moorthy, I., Sankar, K. 2020. Material and Process Selection for Biosorption. *Bioprocess Engineering for Bioremediation: Valorization and Management Techniques*, 241-259.

Sanaei, F., Amin, M.M., Alavijeh, Z.P., Esfahani, R.A., Sadeghi, M., Bandarrig, N.S., Fatehizadeh, A., Taheri, E., Rezakazemi, M. 2021. Health risk assessment of potentially toxic elements intake via food crops consumption: Monte Carlo simulation-based probabilistic and heavy metal pollution index. *Environmental Science and Pollution Research*, **28**(2), 1479-1490.

Sangeetha, J., Thangadurai, D., Hospet, R., Purushotham, P., Manowade, K.R., Mujeeb, M.A., Mundaragi, A.C., Jogaiah, S., David, M., Thimmappa, S.C. 2017. Production of bionanomaterials from agricultural wastes. in: *Nanotechnology*, Springer, pp. 33-58.

Sankpal, S.T., Naikwade, P.V. 2012. Physicochemical analysis of effluent discharge of fish processing industries in Ratnagiri India. *Bioscience Discovery*, **3**(1), 107-111.

Santucci, R.J., Scully, J.R. 2020. The pervasive threat of lead (Pb) in drinking water: Unmasking and pursuing scientific factors that govern lead release. *Proceedings of the National Academy of Sciences*, **117**(38), 23211-23218.

Sarkar, S., Sarkar, S., Biswas, P. 2017. Effective utilization of iron ore slime, a mining waste as adsorbent for removal of Pb (II) and Hg (II). *Journal of environmental chemical engineering*, **5**(1), 38-44.

Sarubbo, L., Rocha Jr, R., Luna, J., Rufino, R.D., Santos, V., Banat, I.M. 2015. Some aspects of heavy metals contamination remediation and role of biosurfactants. *Chemistry and Ecology*, **31**(8), 707-723.

Satpute, S.K., Banpurkar, A.G., Dhakephalkar, P.K., Banat, I.M., Chopade, B.A. 2010. Methods for investigating biosurfactants and bioemulsifiers: a review. *Critical reviews in biotechnology*, **30**(2), 127-144.

Selvaraju, G., Bakar, N.K.A. 2017. Production of a new industrially viable green-activated carbon from Artocarpus integer fruit processing waste and evaluation of its chemical, morphological and adsorption properties. *Journal of cleaner production*, **141**, 989-999.

Shahat, A., Awual, M.R., Naushad, M. 2015. Functional ligand anchored nanomaterial based facial adsorbent for cobalt (II) detection and removal from water samples. *Chemical Engineering Journal*, **271**, 155-163.

Shalini, D., Benson, A., Gomathi, R., Henry, A.J., Jerritta, S., Joe, M.M. 2017. Isolation, characterization of glycolipid type biosurfactant from endophytic Acinetobacter sp. ACMS25 and evaluation of its biocontrol efficiency against

Xanthomonas oryzae. *Biocatalysis and Agricultural Biotechnology*, **11**, 252-258.

Sharma, R., Sarswat, A., Pittman, C.U., Mohan, D. 2017. Cadmium and lead remediation using magnetic and non-magnetic sustainable biosorbents derived from Bauhinia purpurea pods. *RSC advances*, **7**(14), 8606-8624.

Sharma, S., Datta, P., Kumar, B., Tiwari, P., Pandey, L.M. 2019. Production of novel rhamnolipids via biodegradation of waste cooking oil using Pseudomonas aeruginosa MTCC7815. *Biodegradation*, **30**(4), 301-312.

Shekhar, S., Sundaramanickam, A., Saranya, K., Meena, M., Kumaresan, S., Balasubramanian, T. 2019. Production and characterization of biosurfactant by marine bacterium Pseudomonas stutzeri (SSASM1). *International Journal of Environmental Science and Technology*, **16**(8), 4697-4706.

Sheth, Y., Dharaskar, S., Khalid, M., Sonawane, S. 2021. An environment friendly approach for heavy metal removal from industrial wastewater using chitosan based biosorbent: A review. *Sustainable Energy Technologies and Assessments*, **43**, 100951.

Shin, M.-N., Shim, J., You, Y., Myung, H., Bang, K.-S., Cho, M., Kamala-Kannan, S., Oh, B.-T. 2012. Characterization of lead resistant endophytic Bacillus sp. MN3-4 and its potential for promoting lead accumulation in metal hyperaccumulator Alnus firma. *Journal of hazardous materials*, **199**, 314-320.

Shoushtarian, F., Negahban-Azar, M. 2020. Worldwide regulations and guidelines for agricultural water reuse: a critical review. *Water*, **12**(4), 971.

Sidkey, N., Mohamed, H., Elkhouly, H. 2016. Evaluation of different screening methods for biosurfactant producers isolated from contaminated Egyptian samples grown on industrial olive oil processing waste. *Microbiology Research Journal International*, 1-19.

Silva, S., Farias, C., Rufino, R., Luna, J., Sarubbo, L. 2010. Glycerol as substrate for the production of biosurfactant by Pseudomonas aeruginosa UCP0992. *Colloids and Surfaces B: Biointerfaces*, **79**(1), 174-183.

Sim, L., Ward, O., Li, Z. 1997. Production and characterisation of a biosurfactant isolated from Pseudomonas aeruginosa UW-1. *Journal of Industrial Microbiology and Biotechnology*, **19**(4), 232-238.

Simonin, J.-P. 2016. On the comparison of pseudo-first order and pseudo-second order rate laws in the modeling of adsorption kinetics. *Chemical Engineering Journal*, **300**, 254-263.

Sjöström, J.K., Bindler, R., Granberg, T., Kylander, M.E. 2019. Procedure for organic matter removal from peat samples for XRD mineral analysis. *Wetlands*, **39**(3), 473-481.

Sneath, P.H., Mair, N.S., Sharpe, M.E., Holt, J.G. 1986. *Bergey's manual of systematic bacteriology. Volume 2*. Williams & Wilkins.

Sobrinho, H.B., Luna, J.M., Rufino, R.D., Porto, A., Sarubbo, L.A. 2013. Biosurfactants: classification, properties and environmental applications. *Recent developments in biotechnology*, **11**(14), 1-29.

Soliman, N., Moustafa, A. 2020. Industrial solid waste for heavy metals adsorption features and challenges; a review. *Journal of Materials Research and Technology*, **9**(5), 10235-10253.

Soltanighias, T., Singh, A.E., Satpute, S.K., Banpurkar, A.G., Koolivand, A., Rahi, P. 2019. Assessment of biosurfactant-producing bacteria from oil contaminated soils and their hydrocarbon degradation potential. *Environmental Sustainability*, **2**(3), 285-296.

Somoza-Coutiño, G., Wong-Villarreal, A., Blanco-González, C., Pérez-Sariñana, B., Mora-Herrera, M., Mora-Herrera, S.I., Rivas-Caceres, R.R., de la Portilla-López, N., Lugo, J., Vaca-Paulín, R. 2020. A bacterial strain of Pseudomonas aeruginosa B0406 pathogen opportunistic, produce a biosurfactant with tolerance to changes of pH, salinity and temperature. *Microbial pathogenesis*, **139**, 103869.

Song, Y., Yang, T., Li, Z., Zhang, X., Zhang, M. 2020. Research on the direct and indirect effects of environmental regulation on environmental pollution: Empirical evidence from 253 prefecture-level cities in China. *Journal of Cleaner Production*, **269**, 122425.

Sonone, S.S., Jadhav, S., Sankhla, M.S., Kumar, R. 2020. Water contamination by heavy metals and their toxic effect on aquaculture and human health through food Chain. *Letters in applied NanoBioScience*, **10**(2), 2148-2166.

Sood, U., Singh, D.N., Hira, P., Lee, J.-K., Kalia, V.C., Lal, R., Shakarad, M. 2020. Rapid and solitary production of mono-rhamnolipid biosurfactant and biofilm

inhibiting pyocyanin by a taxonomic outlier Pseudomonas aeruginosa strain CR1. *Journal of biotechnology*, **307**, 98-106.

Sotomayor, F.J., Cychosz, K.A., Thommes, M. 2018. Characterization of micro/mesoporous materials by physisorption: concepts and case studies. *Acc. Mater. Surf. Res*, **3**(2), 34-50.

Sousa, M., Dantas, I., Feitosa, F., Alencar, A., Soares, S., Melo, V., Gonçalves, L., Sant'ana, H. 2014. Performance of a biosurfactant produced by Bacillus subtilis LAMI005 on the formation of oil/biosurfactant/water emulsion: study of the phase behaviour of emulsified systems. *Brazilian Journal of Chemical Engineering*, **31**(3), 613-623.

Souza, S.C., Souza, L.A., Schiavinato, M.A., de Oliveira Silva, F.M., de Andrade, S.A. 2020. Zinc toxicity in seedlings of three trees from the Fabaceae associated with arbuscular mycorrhizal fungi. *Ecotoxicology and environmental safety*, **195**, 110450.

Souza, W.D., Rodrigues, W.S., Lima Filho, M.M., Alves, J.J., Oliveira, T.M. 2018. Heavy metals uptake on Malpighia emarginata DC seed fiber microparticles: Physicochemical characterization, modeling and application in landfill leachate. *Waste Management*, **78**, 356-365.

Srikanth, K., King, P., Pujari, M. 2021. Breakthrough studies of the adsorption of lead from synthetic solution using Liagora viscida in a fixed bed column. *Environmental Progress & Sustainable Energy*, e13628.

Srivastava, S., Mondal, M.K., Agrawal, S.B. 2021. Biosurfactants for Heavy Metal Remediation and Bioeconomics. *Biosurfactants for a Sustainable Future: Production and Applications in the Environment and Biomedicine*, 79-98.

Srivastava, V., Sarkar, A., Singh, S., Singh, P., de Araujo, A.S., Singh, R.P. 2017. Agroecological responses of heavy metal pollution with special emphasis on soil health and plant performances. *Frontiers in Environmental Science*, **5**, 64.

Stathi, P., Litina, K., Gournis, D., Giannopoulos, T.S., Deligiannakis, Y. 2007. Physicochemical study of novel organoclays as heavy metal ion adsorbents for environmental remediation. *Journal of colloid and interface science*, **316**(2), 298-309.

Suksabye, P., Thiravetyan, P., Nakbanpote, W. 2008. Column study of chromium (VI) adsorption from electroplating industry by coconut coir pith. *Journal of hazardous materials*, **160**(1), 56-62.

Sun, S., Wang, Y., Zang, T., Wei, J., Wu, H., Wei, C., Qiu, G., Li, F. 2019. A biosurfactant-producing Pseudomonas aeruginosa S5 isolated from coking wastewater and its application for bioremediation of polycyclic aromatic hydrocarbons. *Bioresource technology*, **281**, 421-428.

Surgutskaia, N.S., Di Martino, A., Zednik, J., Ozaltin, K., Lovecká, L., Bergerová, E.D., Kimmer, D., Svoboda, J., Sedlarik, V. 2020. Efficient Cu2+, Pb2+ and Ni2+ ion removal from wastewater using electrospun DTPA-modified chitosan/polyethylene oxide nanofibers. *Separation and Purification Technology*, **247**, 116914.

Taer, E., Taslim, R., Aini, Z., Hartati, S., Mustika, W. 2017. Activated carbon electrode from banana-peel waste for supercapacitor applications. *AIP Conference Proceedings*. AIP Publishing LLC. pp. 040004.

Tamele, I.J., Vázquez Loureiro, P. 2020. Lead, mercury and cadmium in fish and shellfish from the Indian Ocean and Red Sea (African Countries): Public health challenges. *Journal of Marine Science and Engineering*, **8**(5), 344.

Tang, J., He, J., Liu, T., Xin, X., Hu, H. 2017. Removal of heavy metal from sludge by the combined application of a biodegradable biosurfactant and complexing agent in enhanced electrokinetic treatment. *Chemosphere*, **189**, 599-608.

Tang, J., He, J., Tang, H., Wang, H., Sima, W., Liang, C., Qiu, Z. 2020. Heavy metal removal effectiveness, flow direction and speciation variations in the sludge during the biosurfactant-enhanced electrokinetic remediation. *Separation and Purification Technology*, **246**, 116918.

Tariq, M., Farooq, U., Athar, M., Salman, M., Tariq, M., Shahida, S., Farooqi, Z.H. 2021. Lab-scale continuous flow studies for comparative biosorption of cadmium (II) on untreated and xanthated Ficus religiosa biomass. *Water Environment Research*.

Thaniyavarn, J., Chongchin, A., Wanitsuksombut, N., Thaniyavarn, S., Pinphanichakarn, P., Leepipatpiboon, N., Morikawa, M., Kanaya, S. 2006. Biosurfactant production by Pseudomonas aeruginosa A41 using palm oil as carbon source. *The Journal of general and applied microbiology*, **52**(4), 215-222.

Thavasi, R., Jayalakshmi, S., Balasubramanian, T., Banat, I.M. 2008. Production and characterization of a glycolipid biosurfactant from Bacillus megaterium using

economically cheaper sources. *World Journal of Microbiology and Biotechnology*, **24**(7), 917-925.

Thavasi, R., Sharma, S., Jayalakshmi, S. 2011. Evaluation of screening methods for the isolation of biosurfactant producing marine bacteria. *J Pet Environ Biotechnol S*, **1**(2).

Thomas, R. 2008. *Practical guide to ICP-MS: a tutorial for beginners*. CRC press.

Tirry, N., Joutey, N.T., Sayel, H., Kouchou, A., Bahafid, W., Asri, M., El Ghachtouli, N. 2018. Screening of plant growth promoting traits in heavy metals resistant bacteria: prospects in phytoremediation. *Journal of genetic engineering and biotechnology*, **16**(2), 613-619.

Tiwari, S., Hasan, A., Pandey, L.M. 2017. A novel bio-sorbent comprising encapsulated Agrobacterium fabrum (SLAJ731) and iron oxide nanoparticles for removal of crude oil co-contaminant, lead Pb (II). *Journal of environmental chemical engineering*, **5**(1), 442-452.

Tortajada, C. 2020. Contributions of recycled wastewater to clean water and sanitation Sustainable Development Goals. *NPJ Clean Water*, **3**(1), 1-6.

Tsamo, C., Djonga, P.D., Dikdim, J.D., Kamga, R. 2018. Kinetic and equilibrium studies of Cr (VI), Cu (II) and Pb (II) removal from aqueous solution using red mud, a low-cost adsorbent. *Arabian Journal for Science and Engineering*, **43**(5), 2353-2368.

Tugrul, T., Cansunar, E. 2005. Detecting surfactant-producing microorganisms by the drop-collapse test. *World Journal of Microbiology and Biotechnology*, **21**(6), 851-853.

Ucankus, G., Ercan, M., Uzunoglu, D., Culha, M. 2018. Methods for preparation of nanocomposites in environmental remediation. in: *New Polymer Nanocomposites for Environmental Remediation*, Elsevier, pp. 1-28.

Usman, M.M., Dadrasnia, A., Lim, K.T., Mahmud, A.F., Ismail, S. 2016. Application of biosurfactants in environmental biotechnology; remediation of oil and heavy metal. *AIMS Bioengineering*, **3**(3), 289-304.

Vafaeifard, M., Ibrahim, S., Wong, K.T., Pasbakhsh, P., Pichiah, S., Choi, J., Yoon, Y., Jang, M. 2019. Novel self-assembled 3D flower-like magnesium hydroxide coated granular polyurethane: Implication of its potential application for the removal of heavy metals. *Journal of Cleaner Production*, **216**, 495-503.

Vakili, M., Deng, S., Cagnetta, G., Wang, W., Meng, P., Liu, D., Yu, G. 2019. Regeneration of chitosan-based adsorbents used in heavy metal adsorption: A review. *Separation and Purification Technology*, **224**, 373-387.

Vanhaecke, F., Degryse, P. 2012. *Isotopic analysis: fundamentals and applications using ICP-MS*. John Wiley & Sons.

Vardhan, K.H., Kumar, P.S., Panda, R.C. 2019. A review on heavy metal pollution, toxicity and remedial measures: Current trends and future perspectives. *Journal of Molecular Liquids*, **290**, 111197.

Vasistha, P., Ganguly, R. 2020. Water quality assessment of natural lakes and its importance: an overview. *Materials Today: Proceedings*, **32**, 544-552.

Victor, I.U., Kwiencien, M., Tripathi, L., Cobice, D., McClean, S., Marchant, R., Banat, I.M. 2019. Quorum sensing as a potential target for increased production of rhamnolipid biosurfactant in Burkholderia thailandensis E264. *Applied microbiology and biotechnology*, **103**(16), 6505-6517.

Vilvanathan, S., Shanthakumar, S. 2017. Column adsorption studies on nickel and cobalt removal from aqueous solution using native and biochar form of Tectona grandis. *Environmental Progress & Sustainable Energy*, **36**(4), 1030-1038.

Vimalnath, S., Subramanian, S. 2018. Studies on the biosorption of Pb (II) ions from aqueous solution using extracellular polymeric substances (EPS) of Pseudomonas aeruginosa. *Colloids and Surfaces B: Biointerfaces*, **172**, 60-67.

Vishan, I., Saha, B., Sivaprakasam, S., Kalamdhad, A. 2019. Evaluation of Cd (II) biosorption in aqueous solution by using lyophilized biomass of novel bacterial strain Bacillus badius AK: biosorption kinetics, thermodynamics and mechanism. *Environmental Technology & Innovation*, **14**, 100323.

Vo, T.S., Hossain, M.M., Jeong, H.M., Kim, K. 2020. Heavy metal removal applications using adsorptive membranes. *Nano Convergence*, **7**(1), 1-26.

Vojoudi, H., Badiei, A., Bahar, S., Ziarani, G.M., Faridbod, F., Ganjali, M.R. 2017. A new nano-sorbent for fast and efficient removal of heavy metals from aqueous solutions based on modification of magnetic mesoporous silica nanospheres. *Journal of magnetism and magnetic materials*, **441**, 193-203.

Wadhawan, S., Jain, A., Nayyar, J., Mehta, S.K. 2020. Role of nanomaterials as adsorbents in heavy metal ion removal from waste water: A review. *Journal of Water Process Engineering*, **33**, 101038.

Walter, V., Syldatk, C., Hausmann, R. 2010. Screening concepts for the isolation of biosurfactant producing microorganisms. *Biosurfactants*, 1-13.

Wang, J., Guo, X. 2020. Adsorption isotherm models: Classification, physical meaning, application and solving method. *Chemosphere*, 127279.

Wang, S., Liu, Y., Lü, Q.-F., Zhuang, H. 2020. Facile preparation of biosurfactant-functionalized Ti2CTX MXene nanosheets with an enhanced adsorption performance for Pb (II) ions. *Journal of Molecular Liquids*, **297**, 111810.

Wang, S., Mulligan, C.N. 2009. Rhamnolipid biosurfactant-enhanced soil flushing for the removal of arsenic and heavy metals from mine tailings. *Process Biochemistry*, **44**(3), 296-301.

Wen, X., Du, C., Zeng, G., Huang, D., Zhang, J., Yin, L., Tan, S., Huang, L., Chen, H., Yu, G. 2018. A novel biosorbent prepared by immobilized Bacillus licheniformis for lead removal from wastewater. *Chemosphere*, **200**, 173-179.

Xiang, W., Zhang, X., Chen, J., Zou, W., He, F., Hu, X., Tsang, D.C., Ok, Y.S., Gao, B. 2020. Biochar technology in wastewater treatment: A critical review. *Chemosphere*, **252**, 126539.

Xie, W.-M., Zhou, F.-P., Bi, X.-L., Chen, D.-D., Li, J., Sun, S.-Y., Liu, J.-Y., Chen, X.-Q. 2018. Accelerated crystallization of magnetic 4A-zeolite synthesized from red mud for application in removal of mixed heavy metal ions. *Journal of hazardous materials*, **358**, 441-449.

Xu, X., Li, H., Wang, Q., Li, D., Han, X., Yu, H. 2017. A facile approach for surface alteration of Pseudomonas putida I3 by supplying K2SO4 into growth medium: enhanced removal of Pb (II) from aqueous solution. *Bioresource technology*, **232**, 79-86.

Xu, Z., Mi, W., Mi, N., Fan, X., Zhou, Y., Tian, Y. 2020. Characteristics and sources of heavy metal pollution in desert steppe soil related to transportation and industrial activities. *Environmental Science and Pollution Research*, **27**(31), 38835-38848.

Yahya, M.D., Abubakar, H., Obayomi, K., Iyaka, Y., Suleiman, B. 2020a. Simultaneous and continuous biosorption of Cr and Cu (II) ions from industrial tannery effluent using almond shell in a fixed bed column. *Results in Engineering*, **6**, 100113.

Yahya, M.D., Aliyu, A., Obayomi, K., Olugbenga, A., Abdullahi, U. 2020b. Column adsorption study for the removal of chromium and manganese ions from

electroplating wastewater using cashew nutshell adsorbent. *Cogent Engineering*, **7**(1), 1748470.

Yalçın, H.T., Ergin-Tepebaşı, G., Uyar, E. 2018. Isolation and molecular characterization of biosurfactant producing yeasts from the soil samples contaminated with petroleum derivatives. *Journal of basic microbiology*, **58**(9), 782-792.

Yang, M., Liang, Y., Dou, Y., Lan, M., Gao, X. 2017. Characterisation of an extracellular polysaccharide produced by Bacillus mucilaginosus MY6-2 and its application in metal biosorption. *Chemistry and Ecology*, **33**(7), 625-636.

Yang, Z., Shi, W., Yang, W., Liang, L., Yao, W., Chai, L., Gao, S., Liao, Q. 2018. Combination of bioleaching by gross bacterial biosurfactants and flocculation: A potential remediation for the heavy metal contaminated soils. *Chemosphere*, **206**, 83-91.

Yazdi, M.E.T., Amiri, M.S., Nourbakhsh, F., Rahnama, M., Forouzanfar, F., Mousavi, S.H. 2021. Bio-indicators in cadmium toxicity: Role of HSP27 and HSP70. *Environmental Science and Pollution Research*, 1-21.

Youssef, N.H., Duncan, K.E., Nagle, D.P., Savage, K.N., Knapp, R.M., McInerney, M.J. 2004. Comparison of methods to detect biosurfactant production by diverse microorganisms. *Journal of microbiological methods*, **56**(3), 339-347.

Yu, Z., Liu, E., Lin, Q., Zhang, E., Yang, F., Wei, C., Shen, J. 2021. Comprehensive assessment of heavy metal pollution and ecological risk in lake sediment by combining total concentration and chemical partitioning. *Environmental Pollution*, **269**, 116212.

Yuliani, H., Perdani, M.S., Savitri, I., Manurung, M., Sahlan, M., Wijanarko, A., Hermansyah, H. 2018. Antimicrobial activity of biosurfactant derived from Bacillus subtilis C19. *Energy Procedia*, **153**, 274-278.

Zanin, E., Scapinello, J., de Oliveira, M., Rambo, C.L., Franscescon, F., Freitas, L., de Mello, J.M.M., Fiori, M.A., Oliveira, J.V., Dal Magro, J. 2017. Adsorption of heavy metals from wastewater graphic industry using clinoptilolite zeolite as adsorbent. *Process Safety and Environmental Protection*, **105**, 194-200.

Zdravkov, B., Čermák, J., Šefara, M., Janků, J. 2007. Pore classification in the characterization of porous materials: A perspective. *Open Chemistry*, **5**(2), 385-395.

Zeng, G., He, Y., Zhan, Y., Zhang, L., Pan, Y., Zhang, C., Yu, Z. 2016. Novel polyvinylidene fluoride nanofiltration membrane blended with functionalized halloysite nanotubes for dye and heavy metal ions removal. *Journal of hazardous materials*, **317**, 60-72.

Zhang, L., Niu, W., Sun, J., Zhou, Q. 2020. Efficient removal of Cr (VI) from water by the uniform fiber ball loaded with polypyrrole: Static adsorption, dynamic adsorption and mechanism studies. *Chemosphere*, **248**, 126102.

Zhang, Q., Wang, C. 2020. Natural and human factors affect the distribution of soil heavy metal pollution: a review. *Water, Air, & Soil Pollution*, **231**(7), 1-13.

Zhou, Q., Yang, N., Li, Y., Ren, B., Ding, X., Bian, H., Yao, X. 2020. Total concentrations and sources of heavy metal pollution in global river and lake water bodies from 1972 to 2017. *Global ecology and conservation*, **22**, e00925.

Zhu, F., Zheng, Y.-M., Zhang, B.-G., Dai, Y.-R. 2021. A critical review on the electrospun nanofibrous membranes for the adsorption of heavy metals in water treatment. *Journal of Hazardous Materials*, **401**, 123608.

Zhu, W., Wang, J., Wu, D., Li, X., Luo, Y., Han, C., Ma, W., He, S. 2017. Investigating the heavy metal adsorption of mesoporous silica materials prepared by microwave synthesis. *Nanoscale research letters*, **12**(1), 1-9.

Scientific Publications

&

Achievements

ACHIEVEMENTS:

- Achieved **second position** in **Poster Participation** on _Utility of Biologically treated molasses spent wash as fertigation tool in Horticulture‘ in National Seminar on _Horticulture: A Boon for Indian Economy‘ held at BBAU, Lucknow on 31st October, 2019.

SCIENTIFIC PUBLICATIONS:

RESEARCH PAPERS:

- **Rastogi, S.,** Ratna, S. & Kumar, R. (2021). Screening of Biosurfactant Producing Bacteria Isolated from Hydrocarbon Contaminated Site and Their Potential in Biosorption of Pb(II) and Oil Biodegradation. *Tenside Surfactants Detergents, 58*(6), 435-441. https://doi.org/10.1515/tsd-2020-2341
- **Rastogi, S.**, Tiwari, S., Ratna, S., & Kumar, R. (2021). Utilization of agro-industrial waste for biosurfactant production under submerged fermentation and its synergistic application in biosorption of Pb^{2+}. *Bioresource Technology Reports*, *15*, 100706. https://doi.org/10.1016/j.biteb.2021.100706
- **Rastogi, S.**, & Kumar, R. (2021). Statistical optimization of biosurfactant production using waste biomaterial and biosorption of Pb^{2+} under concomitant submerged fermentation. *Journal of Environmental Management, 295*, 113158. https://doi.org/10.1016/j.jenvman.2021.113158
- Kumar, S., Kumar, S., Kumar, A., **Rastogi, S.**, & Kumar, D. (2021). Synthesis and Characterization of Chitosan-Alginate-Based Cross-linked Copolymer for the Effective Removal of Methylene Blue from Its Aqueous Solution. *Water, Air, & Soil Pollution, 232*(11), 1-17. https://doi.org/10.1007/s11270-021-05334-6
- **Rastogi, S.**, Kumar, J., & Kumar, R. (2019). An investigation into the efficacy of fungal biomass as a low cost bio-adsorbent for the removal of lead from aqueous solutions. *Int Res J Eng Technol*, *6*(3), 7144-7149.

BOOK CHAPTERS:

- **Rastogi, S.**, Ratna, S., Said, O. B., & Kumar, R. (2021). Physiological and molecular aspects of retrieving environmental stress in plants by microbial interactions. In *Microbes and Signaling Biomolecules Against Plant Stress* (pp. 107-125). Springer, Singapore.
- Ratna, S., **Rastogi, S.**, & Kumar, R. (2021). Phytoremediation: a synergistic interaction between plants and microbes for removal of unwanted chemicals/contaminants. In *Microbes and Signaling Biomolecules Against Plant Stress* (pp. 199-222). Springer, Singapore.
- **Rastogi, S.**, & Kumar, R. (2020). Remediation of heavy metals using non-conventional adsorbents and biosurfactant-producing bacteria. *Environmental degradation: causes and remediation strategies*, 133-153.

REVIEW PAPER:

- Ratna, S., **Rastogi, S.**, & Kumar, R. (2021). Current trends for distillery wastewater management and its emerging applications for sustainable environment. *Journal of Environmental Management*, *290*, 112544. https://doi.org/10.1016/j.jenvman.2021.112544

NATIONAL TRAINING/COURSE ATTENDED:

- Attended an Online Societal skill/ Training program on –Water safety plan‖ organised by CSIR- National Environmental Engineering Research Institute on March 4-5, 2021.
- Attended a two-week GIAN course on _Principles of Environmental Catalysis‘ held at Central University of Haryana, Mahendragarh (Haryana) from 6th to 17th August, 2018.

Reprints

 Published by De Gruyter November 30, 2021

Screening of Biosurfactant Producing Bacteria Isolated from Hydrocarbon Contaminated Site and Their Potential in Biosorption of Pb(II) and Oil Biodegradation

Screening von Biosurfactant-produzierenden Bakterien, die von Kohlenwasserstoff-kontaminierten Standorten isoliert wurden, und ihr Potenzial für die Biosorption von Pb(II) und den Abbau von Öl

Swati Rastogi, Sheel Ratna and Rajesh Kumar

From the journal Tenside Surfactants Detergents
https://doi.org/10.1515/tsd-2020-2341

Abstract

In the present study, three potentially Pb(II)-resistant and biosurfactant-producing bacterial strains were isolated from a total of 23 strains using various screening methods, investigated for their biosorption of Pb(II) and used for the biodegradation of used motor oil. The results show that strain E1 (Bacillus haynesii) has significantly high efficiency in biodegradation of used motor oil, up to 82 % in the first three days. Maximum Pb(II) biosorption capacities of 238.09 mg/g and 99.01 mg/g were determined for strains E1 and F5 (Pseudomonas aeruginosa), respectively. The biosorption process was found to be in good agreement with the Langmuir isotherm for both E1 (R^2 = 0.9614) and F5 (R^2 = 0.9646), suggesting monolayer biosorption. The four common screening methods, namely the haemolytic assay, the determination of surface tension, the emulsifying activity and the foam test, were also correlated with the Pearson correlation method.

Zusammenfassung

In der vorliegenden Studie wurden drei potenziell Pb(II)-resistente und Biotensid-produzierende Bakterienstämme aus insgesamt 23 Stämmen mit Hilfe verschiedener Screening-Methoden isoliert, auf ihre Biosorption von Pb(II) untersucht und für den biologischen Abbau von gebrauchtem Motoröl eingesetzt. Die Ergebnisse zeigen, dass der Stamm E1 (Bacillus haynesii) eine signifikant hohe Effizienz beim biologischen Abbau von gebrauchtem Motoröl aufweist, nämlich bis zu 82 % in den ersten drei Tagen. Für die Stämme E1 und F5 (Pseudomonas aeruginosa) wurden maximale Pb(II)-Biosorptionskapazitäten von 238,09 mg/g bzw. 99,01 mg/g ermittelt. Es wurde festgestellt, dass der Biosorptions-prozess sowohl für E1 (R^2 = 0,9614) als auch für F5 (R^2 = 0,9646) gut mit der Langmuir-Isotherme übereinstimmt, was auf eine Monolayerbiosorption schließen lässt. Die vier gängigen Screening-Methoden, nämlich der hämolytische Assay, die Bestimmung der Oberflächenspannung, die Emulgieraktivität und der Schaumtest, wurden ebenfalls mit der Pearson-Korrelationsmethode korreliert.

Journal of Environmental Management 295 (2021) 113158

Contents lists available at ScienceDirect

Journal of Environmental Management

journal homepage: www.elsevier.com/locate/jenvman

Statistical optimization of biosurfactant production using waste biomaterial and biosorption of Pb^{2+} under concomitant submerged fermentation

Swati Rastogi *, Rajesh Kumar

Rhizosphere Biology Laboratory, Department of Environmental Microbiology, Babasaheb Bhimrao Ambedkar (A Central) University, Vidya Vihar Raebareli Road, Lucknow, 226025, India

ARTICLE INFO

Keywords:
Agrowastes
Waste management
Bioremediation
Biosorption
Mathematical modelling

ABSTRACT

The present study was conducted to statistically optimize the biosurfactant production yield of *Pseudomonas* sp. F5 using raw orange peel extract (Central composite design (CCD) design; Surface tension (ST) reduction = 32.41 dyne/cm; biosurfactant yield = ~2.4 g/L). The extracted biosurfactant was characterized as a glycolipid having predominant mono-rhamnolipids than di-rhamnolipids with a critical micelle concentration (CMC) of 40 mg/L. The potential of strain F5 for good biosurfactant yield during Pb^{2+} stress and the inherent mechanism for simultaneous biosorption of Pb^{2+} was also investigated. During concomitant submerged fermentation from 100 to 500 mg/L of Pb^{2+} showed enhancement in adsorption capacity from 99.44 to 267.86 mg/g respectively having 60.33 ± 2.87 of emulsification index (E_{24}%) measured at 100 mg/L Pb^{2+} corresponding to maximum biosurfactant production during metal stress. The bacterium showed a high Pb^{2+} MIC (minimum inhibitory concentration) of 2200 mg/L and efficiently biosorbed Pb^{2+} ions at pH 7 and a dosage of 0.05 g under varying initial metal ion concentration and contact time. The exothermic biosorption (chemisorption) mechanism was found to be fitted well with Langmuir (R^2 = 0.9859) and Pseudo second-order kinetic model (R^2 = 0.9975; 200 mg/L) having a maximum adsorption capacity of 294.12 mg/g. These findings indicated the excellent potential of biosurfactant producing strain F5 in the removal of Pb^{2+} ions from aqueous system and management of agrowastes as suitable carbon substrate.

1. Introduction

The alarming extent of industrialization and consequent environmental pollution has jeopardised the goals of sustainable development and raises the concern for its amelioration worldwide (Nasir et al., 2021). Due to the natural weathering processes and several anthropogenic acts have given rise to the heavy metal (HM) contamination and their persistent accumulation in the environment. Though, these HMs are necessary for the proper growth when taken in optimum concentrations, however, enhanced dosages and their release above permissible limits causes various anomalies in humans, animals, and plants as well (Rastogi et al., 2019). Lead (Pb^{2+}) has been known to exert deleterious effects on flora and fauna by inducing declined growth and photosynthetic rate in plants while neurological to physiological dysfunction has been reported in humans and animals. The major sources of Pb^{2+} discharge includes mining, batteries, electroplating, paints and pigment industries (Rastogi et al., 2021a; Schileo and Grancini, 2021). Therefore, proper remediation strategies are needed to prevent its toxic effects. Several physical, chemical, and biological methods of remediation have been reported in the past but the present situation demands an integrated modified approach to avail maximum benefits from the prenominal treatment technologies by eliminating/reducing their secondary non-biodegradable obnoxious by-product load (Rastogi and Kumar, 2020; Ratna et al., 2021b; Zamora-Ledezma et al., 2021).

Biosurfactants (BSs) are secondary metabolites that are usually produced by microorganism extracellulary or on their cellular surface. They belong to different class's viz. Glycolipids, lipopeptides, lipoproteins, phospholipids, sophorolipids, and polymer (Banat et al., 2020). Recently, their usage has been increased and has been recognised as potential superior HM bioremediating agents over chemical surfactants/agents due to their several properties such as amphiphilic nature, less or no toxicity, ability to reduce surface and interfacial tension, stable structure in harsh environment, biocompatibility, etc. (Guo and Gao, 2021). However, their large scale commercial production is still an economical stimulating issue and many scientists have addressed the role of agricultural residues like fruit peel wastes, etc. For their cost

* Corresponding author.
E-mail addresses: sswatirrastogi73@gmail.com (S. Rastogi), rajesh_skumar@yahoo.co.in (R. Kumar).

https://doi.org/10.1016/j.jenvman.2021.113158
Received 4 April 2021; Received in revised form 17 June 2021; Accepted 23 June 2021

Bioresource Technology Reports 15 (2021) 100706

Contents lists available at ScienceDirect

Bioresource Technology Reports

journal homepage: www.sciencedirect.com/journal/bioresource-technology-reports

Utilization of agro-industrial waste for biosurfactant production under submerged fermentation and its synergistic application in biosorption of Pb^{2+}

Swati Rastogi *, Shweta Tiwari, Sheel Ratna, Rajesh Kumar

Rhizosphere Biology Laboratory, Department of Environmental Microbiology, Babasaheb Bhimrao Ambedkar (A Central) University, Vidya Vihar Raebareli Road, Lucknow 226025, India

ARTICLEINFO

Keywords:
Biowastes
Waste management
Bioremediation
Biosorption
Mathematical modelling

ABSTRACT

The biosurfactant production process was optimized using raw orange peel extract (ST reduction = 33.04 dyne cm^{-1}; biosurfactant yield = ~3.7 g L^{-1}) and the extracted metabolite was characterized in terms of its nature, and class/family. To the best of our knowledge, a first report utilizing biowaste as a sole carbon substrate for simultaneous biosurfactant production and Pb^{2+} removal under submerged fermentation by *Bacillus haynesii* strain E1. The results depicted the extracted biosurfactant to be of lipopeptide nature belonging to surfactin family having 50 mg L^{-1} of CMC. The crude biosurfactant was found to be tensioactive at temperature 70 °C, 6% salt concentration, and varying pH range. The biosurfactant-producing bacterium effectively remediated Pb^{2+} (high MIC = 2200 mg L^{-1}) with a maximum adsorption capacity of 196.08 mg g^{-1}. The biosorption mechanism followed Langmuir (R^2 = 0.9724) and Pseudo second-order adsorption kinetics (R^2 = 0.9996; 200 mg L^{-1}).

1. Introduction

Microorganisms secrete metabolites that are known to ameliorate environmental stress. Biosurfactants (BSs) are one such secondary metabolite that are produced on the microbial cell surface or are released extracellularly. These are considered amphiphilic molecules on account of both hydrophilic and hydrophobic moieties that confer the potential to reduce surface and interfacial tension between the surfaces (Banat et al., 2021). In recent years, BSs have gained popularity as bioremediating agents due to the characteristics that offer them an edge over synthetic surfactants. Such characteristics include stability towards harsh temperature, pH, and saline conditions. Also, they are biocompatible; possess low toxicity, biodegradability, and specificity (Rastogi and Kumar, 2020). It is still a challenge regarding large scale production of BSs from an economical point but the environmental damage caused by chemical surfactants makes BSs potential representatives for bioremediation purposes. As per these benefits, BSs are promising candidates for many commercial applications. But, their production must be cost-effective and to resolve this issue, various authors have recommended the usage of renewable agro-industrial wastes (biowastes) such as fruit and vegetable peels, etc. (Kumar and Ngueagni, 2021; Ratna et al., 2021). Such lignocellulosic biowastes would render a cheaper source of carbon substrate and parameters such as pH, temperature, agitation rate, etc. that would impact its production. But limited literature is available on the usage of these biowastes for biosurfactant production. The implementation of such bio wastes could resolve issues of biowastes management and also foster biosurfactant production simultaneously.

Various anthropogenic activities and natural weathering have resulted in heavy metal accumulation in the environment. Some of them are required as growth supplements in optimum dosages. These heavy metals, for instance, lead (Pb^{2+}) is released from paint, metal pipe factories, batteries, mining, electroplating industries, etc. (Nassiri et al., 2021). They are persistent in nature, non-biodegradable, and confer toxicity to the different flora and fauna of the ecosystem (Rastogi et al., 2019). The chronic Pb^{2+} exposure could lead to neurological, metamorphosis, and developmental abnormalities in aquatic organisms while stunted growth, diminished photosynthetic rate, etc. in plants. Kidney failure, reduced fertility, cardiovascular disorders, etc. are some malicious consequences in humans (Kumar et al., 2020). Few studies have been conducted regarding accelerated BS production in the presence of metal ions (Kiran et al., 2014). BSs are reported to remove heavy metal ions from the contaminated systems (Rastogi et al., 2021). BS mediated heavy metal remediation/ removal occurs via adsorption and precipitation reactions based on Le Chatelier's principle. An adsorption

* Corresponding author.
E-mail address: sswatirrastogi73@gmail.com (S. Rastogi).

https://doi.org/10.1016/j.biteb.2021.100706
Received 29 March 2021; Received in revised form 16 April 2021; Accepted 19 April 2021
Available online 28 April 2021

Water Air Soil Pollut (2021) 232:445
https://doi.org/10.1007/s11270-021-05334-6

Synthesis and Characterization of Chitosan-Alginate-Based Cross-linked Copolymer for the Effective Removal of Methylene Blue from Its Aqueous Solution

Sumit Kumar · Shailesh Kumar · Ashok Kumar · Swati Rastogi · Deepak Kumar

Received: 17 February 2021 / Accepted: 1 September 2021

Abstract The objective of the present study was the synthesis and characterization of chitosan-alginate-based cross-linked copolymer (CACC) for the effective removal of methylene blue (MB) from its aqueous solution. The CACC before and after the removal of MB was confirmed by in-depth characterization techniques. The thermal stability of the materials before and after adsorption of MB was determined by thermal gravimetric analysis. The solid–liquid phase interactions between CACC and MB during the adsorption/removal was observed employing several affecting operating parameters like the concentration of MB, CACC dose, pH, contact time and temperature were studied. Langmuir isotherm model described better MB adsorption onto CACC than the model of Freundlich model with determination coefficient R^2-value of 0.990 in Langmuir equation. Thus, being an eco-friendly, biodegradable, biocompatible and low-cost material, the CACC could be a potential polymeric-based adsorbent for the effective removal of MB from its aqueous solution and wastewater.

Keywords Chitosan-based polymeric composite · Sodium alginate · Ceric ammonium nitrate · Glutaraldehyde · Methylene blue · Adsorption isotherms

S. Kumar · S. Kumar (✉) · A. Kumar
Department of Applied Chemistry, School of Physical Sciences, Babasaheb Bhimrao Ambedkar University (A Central University), Lucknow 226025, India
e-mail: drskum10@gmail.com

S. Rastogi
Department of Environmental Microbiology, School of Environmental Sciences, Babasaheb Bhimrao Ambedkar University (A Central University), Lucknow 226025, India

D. Kumar
Department of Chemical Engineering, Indian Institute of Technology Roorkee, Roorkee, Uttarakhand 247667, India

1 Introduction

Nowadays, unplanned urbanization, industrialization, excessive use of chemicals in agriculture and excessive growth in the world population have greatly promoted environmental pollution (Gupta, 2009). Water is being heavily contaminated by biological and inorganic waste generated by the activities done by humans, by which the health of humans and other organisms is becoming increasingly threatened (Ceyhan & BAYBAŞ, 2001). The discharge of dye inside water bodies is not only harmful to ecology and biological organisms but is also causing human beauty and health issues (Prasad & Santhi, 2012). Apart from the textile industry, the dyeing industry is mainly leather plastic and the food industry is the main source of polluting freshwater. There is usually about 40 to 60 L/kg waste material within the volume of wastewater at each stage of the textile industry (Mezohegyi et al., 2012). The presence of mixed

Published online: 20 October 2021

International Research Journal of Engineering and Technology (IRJET) e-ISSN: 2395-0056
Volume: 06 Issue: 03 | Mar 2019 www.irjet.net p-ISSN: 2395-0072

An Investigation into the efficacy of Fungal Biomass as a Low Cost Bio-adsorbent for the removal of Lead from aqueous solutions

Swati Rastogi[1], Jeetendra Kumar[2], Rajesh Kumar[3]

[1]Research Scholar, Rhizosphere Biology Laboratory, Department of Microbiology, Babasaheb Bhimrao Ambedkar University (a central university) vidya vihar raebareli road, Lucknow, India

[2]M.Sc. Student, Rhizosphere Biology Laboratory, Department of Microbiology, Babasaheb Bhimrao Ambedkar University (a central university) vidya vihar raebareli road, Lucknow, India

[3]Professor, Rhizosphere Biology Laboratory, Department of Microbiology, Babasaheb Bhimrao Ambedkar University (a central university) vidya vihar raebareli road, Lucknow, India

---

Abstract - *Some of the heavy metals such as lead (Pb^{2+}) even in low concentration pose a threat to human wellbeing and other life forms. Various anthropogenic and industrial sources discharge this toxic metal into the biosphere. The present study explores the efficiency of untreated dead biomass of Penicillium sp. (a fungus) in the bio-sorption of Pb^{2+} ions from aqueous solutions. Different factors viz., initial Pb^{2+} ion concentration, adsorbent dose and contact time were studied. The maximum adsorption percentage (78.03%) of Pb^{2+} was found under the optimum conditions of 10 mg/l of Pb^{2+}, an adsorbent dose of 1g/L and contact time of 2 hours. Langmuir adsorption isotherm was best fitted for the present study (R^2=0.9984). Bio-sorption reaction mechanism was explained through FTIR analysis of fungal biomass which revealed the presence of carbonyl, methylene, phosphate, carbonate and phenolic groups and their possible involvement in the Pb^{2+} ions bio-sorption process. SEM and EDX details provide the structural characterization and optical absorption peaks of dead fungal biomass and explain its surface morphology in the adsorption and removal of Pb^{2+} ions from aqueous solutions respectively. It can be concluded that untreated dead biomass of Penicillium sp. is a promising, efficient, low-cost bio-adsorbent for the removal of Pb^{2+} ions from the environment and wastewater effluents.*

***Key Words*: Biosorption; low-cost bio-adsorbent; SEM; FTIR; Langmuir isotherm model**

1. INTRODUCTION

Enhanced industrial and economic development has resulted in heavy metal pollution and their vast distribution in the environment which in turn poses a major challenge for their effective treatment and management due to their toxic and persistent nature and accumulation in the food chain [1].

Many conventional technologies including filtration, ion-exchange, precipitation, coagulation, membrane separation, solvent extraction are available for mitigation of these dangerous pollutants but demands high energy and operation costs even lead to the generation of secondary pollutants/sludge. Due to which focus has been shifted towards the application of cost-effective, eco-friendly non-conventional methods for remediation of these heavy metals. Bioadsorption is one of the emerging process/methods which is considered to be beneficial for the removal of metal ions from aqueous solutions. Microbial biomass either living or dead as bioadsorbents has been found to be effective in the amelioration of heavy metal ions from wastewater/soil. Literature survey supports the use of fungi, algae, and bacteria as adsorbents for several heavy metals [2] [3].

Recently, lead removal from soil and aqueous samples have been reported by many fungal species like *Aspergillus niger* [4][6][11][14], *Trichoderma reesi* [4], *Mucor arcindloides* [4], *Saccharomyces cerevisiae* [4][9] , *Penicillium austurianum* [4], *Penicillium verrucosum* [5], *Botrytis cinerea* [7], *Phanerochaete chrysosporium* [8], *Mucor rouxii* [10], *Aspergillus fumigatus* [11], *Penicillum simplicissimum* [11], *Trichoderma asperellum*[11],*Penicillium chrysogenum*[12] [13] [15], *Aspegillus nidulans* [15], *Aspergillus flavus* [15], *Rhizopus arrhizus* [15], *Trichoderma viride* [15].

The utility of fungal biomass as bioadsorbent is in the fact as are easy to separate, rarely sensitive to nutrient variation, pH etc, has less nucleic content in biomass, easily cultivated for large scale production, provides large surface area for adsorption reactions and are non-toxic [16][17].

Journal of Environmental Management 290 (2021) 112544

Contents lists available at ScienceDirect

Journal of Environmental Management

journal homepage: http://www.elsevier.com/locate/jenvman

Review

Current trends for distillery wastewater management and its emerging applications for sustainable environment

Sheel Ratna *, Swati Rastogi, Rajesh Kumar

Rhizosphere Biology Laboratory, Department of Environmental Microbiology, Babasaheb Bhimrao Ambedkar University, (A Central University), Vidya Vihar, Raibareli Road, Lucknow, 226025, India

ARTICLE INFO

Keywords:
Distillery wastewater
Toxicity
Physico-chemical
Biological treatment
Value-added products
Sustainability

ABSTRACT

Ethanol distillation generates a huge volume of unwanted chemical liquid known as distillery wastewater. Distillery wastewater is acidic, dark brown having high biological oxygen demand, chemical oxygen demand, contains various salt contents, and heavy metals. Inadequate and indiscriminate disposal of distillery wastewater deteriorates the quality of the soil, water, and ultimately groundwater. Its direct exposure via food web shows toxic, carcinogenic, and mutagenic effects on aquatic-terrestrial organisms including humans. So, there is an urgent need for its proper management. For this purpose, a group of researchers applied distillery wastewater for fertigation while others focused on its physico-chemical, biological treatment approaches. But until now no cutting-edge technology has been proposed for its effective management. So, it becomes imperative to comprehend its toxicity, treatment methods, and implication for environmental sustainability. This paper reviews the last decade's research data on advanced physico-chemical, biological, and combined (physico-chemical and biological) methods to treat distillery wastewater and its reuse aspects. Finally, it revealed that the combined methods along with the production of value-added products are one of the best options for distillery wastewater management.

1. Introduction

The increased hydrocarbonaceous fuel demand and concern for greenhouse gases (GHGs) emission worldwide gave a boost to clean fuels like ethanol which is expected to reach 137 billion (B) L by 2026. Various countries like the United States of America (11.3%), Brazil (27%), China (4%), Canada (5%), and Indonesia (13%) have targeted blending of ethanol with gasoline by 2026–2028 (OECD-FAO, 2017). Similarly, the Government of India mandates the use of 'indigenous ethanol only' for ethanol-blended petrol to achieve sustainable development goals (SDGs) and estimated that the ethanol supply will rise to 20% by 2028 (MOP&NG, 2018a; OECD-FAO, 2017; SDGs, 2018). Distillery industries are the second-most wastewater generating agro-processing industries next to paper-pulp and produces about amount (12–15 L) wastewater per liter of ethanol production (Wagha and Nemadeb, 2018). Aqueous waste generated during ethanol production is known as distillery wastewater (DWW)/stillage/vinasse/distillery slop or spent wash (SW) (Oosterkamp et al., 2019; Cooper et al.,

Abbreviations: ACC, 1-amino cyclopropane-1-carboxylic acid; AD, anaerobic digestion; AMF, arbuscular mycorrhizal fungi; AOPs, advanced oxidation process; ASPs, aluminosilicate particles; BI, biodegradability index; BOD, biological oxygen demand; BS, biosurfactants; CAC, commercial activated carbon; COD, chemical oxygen demand; CTA, cellulose triacetate; CW, constructed wetland; DE, distillery effluents; DOM, dissolved organic matter; DSW, distillery spent wash; DWW, distillery wastewater; EC, electrical conductivity; ECSB, external circulation sludge bed; EDCs, endocrine-disrupting chemicals; EF, electro-Fenton; EO, electro-oxidation; EPSs, extracellular polymeric substances; FO, forward osmosis; GAC, granular activated carbons; GHGs, greenhouse gases; HMs, heavy metals; HRT, hydraulic retention time; HTI-TFC, hydration technology innovations-thin film composite; kDa, kilodaltons; LC, lethal concentrations; LiP, lignin peroxidase; MBRs, membrane bioreactors; MCCAC, microbial coated commercially activated carbon; MF, microfiltration; MFC, microbial fuel cell; MnP, manganese peroxidase; MOSE, Moringa oleifera seed extract; MT, membrane technology; MW, molecular; NF, nano-filtration; OLR, organic loading rate; PAC, powdered activated carbon; PD, power density; PE, phenyl ethanol; PEA, phenyethylatacetate; PES, polyethersulfone; PGPM, plant growth-promoting microbes; PHAs, polyhydroxyalkanoates; PHB, polyhydroxy butyrate; PHB, polyhydroxybutyrate; PMDE, post methanated distillery effluent; PSB, photosynthetic bacteria; RO, reverse osmosis; SCP, single-cell protein; SDGs, sustainable development goals; SP, sodium persulphates; SW, Spent wash; TDS, total dissolved solids; TKN, total Kjeldahl nitrogen; TN, total nitrogen; TOC, total organic carbon; TP, total phosphate; UF, ultrafiltration; VFA, volatile fatty acid; WAO, wet air oxidation; WHO, world health organization.

* Corresponding author.
E-mail addresses: sheelratna222@gmail.com, sratna.rs@bbau.ac.in (S. Ratna).

https://doi.org/10.1016/j.jenvman.2021.112544
Received 1 May 2020; Received in revised form 16 March 2021; Accepted 1 April 2021

Chapter 6
Physiological and Molecular Aspects of Retrieving Environmental Stress in Plants by Microbial Interactions

Swati Rastogi, Sheel Ratna, Olfa Ben Said, and Rajesh Kumar

Abstract Environmental stress is the foremost limiting factor for agricultural productivity. It is essential to alleviate the distress caused by environmental and edaphic conditions in plants, failing to which would affect their growth, development, and productivity. Microorganisms have enormous metabolic capabilities to lessen the environmental stress and their interactions with plants provide a local and systemic defense under various biotic and abiotic stresses. Due to an increase in adverse external conditions, it is imperative to study plant–microbe relationships at the physiological and molecular level to provide deeper insights into the stress-mitigating mechanisms.

6.1 Introduction

Decline in crop yield and ultimately agricultural productivity has resulted from extreme climatic conditions which burden the land with environmental stress. The geographical land area that is unaffected by any biotic or abiotic constraint is diminishing with the advent of industrialization, pollution, and moderation in the environment. Drought, salinity, acidity, alkalinity, low/high temperature, and nutrient deprivation are some of the paramount abiotic stresses along with biotic stress which includes pest and diseases and show a huge impact on world's agriculture (Latef et al. 2016; Meena et al. 2017). Plants being sessile are generally exposed to these environmental stresses that cause morphological, physiological, biochemical, and molecular alterations in them and may lead to diminution in average yields by 50%. To *fi*ght back such constraints, plants have excogitated and developed several intricate speci*fi*c mechanisms that provide them resistance and minimize damage

S. Rastogi · S. Ratna · R. Kumar (✉)
Rhizosphere Biology Laboratory, Department of Microbiology, Babasaheb Bhimrao Ambedkar University (A Central University), Lucknow, India

O. B. Said
Laboratory of Environment Biomonitoring, Coastal Ecology and Ecotoxicology Unit, Faculty of Sciences of Bizerte, University of Carthage, Zarzouna, Tunisia

A. Sharma (ed.), *Microbes and Signaling Biomolecules Against Plant Stress*,
Rhizosphere Biology, https://doi.org/10.1007/978-981-15-7094-0_6

Chapter 11
Phytoremediation: A Synergistic Interaction Between Plants and Microbes for Removal of Unwanted Chemicals/ Contaminants

Sheel Ratna, Swati Rastogi, and Rajesh Kumar

Abstract Environmental pollution with obnoxious contaminants is detrimental to plant growth and poses health hazards to humans and other life forms. Thus, remediation of such antagonistic environment has become a key issue for environmentalists all around the world. Phytoremediation, a cooperative association between plants and microbes, is an emerging in situ cost-effective technology and provides a viable option in the treatment of such contaminated environments. Present chapter emphasizes on plant–microbes interactions during phytoremediation and how such beneficial interactions lead to improved plant growth and contamination free environment.

11.1 Introduction

Environmental contamination is one of the most intractable concerns worldwide to ensure the safest and healthiest environment. The source of pollution is natural and anthropogenic activities. Key anthropogenic sources of pollution are related to the burning of fossil fuels, mining and untreated or partially treated disposal of municipal solid wastes and wastewater discharges or use for irrigation and excessive utilization of fertilizers and pesticides (Pinto et al. 2016, 2018). Continuous and consistent increase in a variety of organic and inorganic pollutants has been reported to cause environmental pollution which results in severe health hazards in living beings. Inorganic contaminants are salts of nitrate, ammonia, sulfate, phosphate, cyanide, heavy metals (HMs), while alkanes, antibiotics, dioxins, phenols, polychlorinated biphenyls (PCBs), polycyclic aromatic hydrocarbons (PAHs), Persistent Organic Pollutants (POPs), pesticides, synthetic azo dyes, polyaromatic, chlorinated, and nitro-aromatic compounds constitute organic contaminants.

S. Ratna · S. Rastogi · R. Kumar (✉)
Rhizosphere Biology Laboratory, Department of Microbiology, Babasaheb Bhimrao Ambedkar University (A Central University), Lucknow, India

A. Sharma (ed.), *Microbes and Signaling Biomolecules Against Plant Stress*, Rhizosphere Biology, https://doi.org/10.1007/978-981-15-7094-0_11

In: Environmental Degradation: Causes and Remediation Strategies
DOI: 10.26832/aesa-2020-edcrs-010

CHAPTER
[10]

Remediation of heavy metals using non-conventional adsorbents and biosurfactant-producing bacteria

Swati Rastogi* and Rajesh Kumar

Rhizosphere Biology Laboratory, Department of Microbiology, Babasaheb Bhimrao Ambedkar University (A Central University), Vidya Vihar Raebareli Road, Lucknow, India

ABSTRACT

Heavy metal pollution in the ecosystem has attracted worldwide attention due to the persistent non-biodegradable toxic nature that affects not only human beings but also animals and vegetation. Instead of using available conventional techniques, the focus has been shifted to utilize eco-friendly, cost-effective, integrated remediation approaches that are simple, non-conventional with design flexibility and does not harm the prevailing surroundings. The main approaches utilized for remediation of heavy metal contaminated soils are sand capping or land filling, phytoremediation, bioremediation, washing, electro-chemical remediation, stabilization, soil replacement, phytoextraction, phytovoltalization, etc., but again they have their own merits and demerits. Many treatment technologies are employed at industrial scale for HM removal from wastewater effluents such as chemical precipitation, flocculation, coagulation, solvent extraction, adsorption, complexation, electro-kinetics, membrane filtration, etc. Therefore, the present chapter critically highlights the role of non-conventional adsorbents and bacterial surfactants as the best alternative technique for heavy metal remediation from contaminated soil and water systems.

KEYWORDS

Adsorbents, Bio-surfactants, Environmental sustainability, Heavy metals

✉ Swati Rastogi, Email: sswatirrastogi73@gmail.com